The Pennsylvania State University

The Graduate School

Intercollege Graduate Degree Program in Ecology

POTENTIAL USE OF N_2-FIXING CYANOBACTERIA FOR ESTABLISHING RENEWABLE BIOLOGICAL SOIL CRUSTS AND MODULATING SOIL NITROGEN IN AGROECOSYSTEMS

A Dissertation in

Ecology

by

Xin Peng

Submitted in Partial Fulfillment
of the Requirements
for the Degree of

Doctor of Philosophy

August 2016

The dissertation of Xin Peng was reviewed and approved* by the following:

Mary Ann Bruns
Associate Professor of Soil Science/Microbial Ecology
Dissertation Advisor
Chair of Committee

Katriona Shea
Alumni Professor of Biology

Armen R. Kemanian
Associate Professor of Production Systems and Modeling

Zhibiao Zhao
Associate Professor of Statistics

David Eissenstat
Professor of Woody Plant Physiology
Chair of Ecology Intercollege Graduate Degree Program

*Signatures are on file in the Graduate School

ABSTRACT

Large amounts of synthetic nitrogen (N) fertilizer are used in modern agriculture to increase crop yields, but N use efficiency is low due to high N losses and poor soil N retention. Biological N fixation by free-living cyanobacteria has been utilized extensively in flooded rice paddy systems, but rarely in agriculture of temperate regions like the United States. The objective of this dissertation research was to develop a renewable means of delivering N to soils that will be environmentally sustainable and economically beneficial through reducing the need for commercial fertilizer and increasing soil stability. The approach involves the establishment of renewable biological soil crusts (BSCs) using filamentous N_2-fixing cyanobacteria, which takes advantage of their capabilities to photosynthesize, fix atmospheric N_2, and stabilize soil surfaces. The overarching hypothesis of this research is that cyanobacteria will survive and promote BSC succession after being applied to agricultural soils, as they increase soil carbon and N content.

Cyanobacteria were enriched from naturally formed BSCs on agricultural soils and their growth was compared to commercial strains in soil microcosm tests under N-limited conditions. Selected cyanobacteria were further evaluated for potential N_2 fixation and soil N retention at different N concentrations, using $^{15}N_2$ isotope labeling of cells and simulated rainfall experiments, respectively. A succession model was developed to simulate the microbial dynamics and N contributions of BSCs following the artificial application of N_2-fixing cyanobacteria to soil. The model simulation results were compared with one year of observations of naturally occurring BSCs in agricultural fields. Additional cyanobacterial properties, including cyanotoxin content, drought resistance and large-scale biomass production in photobioreactors (PBRs) were also evaluated in consideration of future field applications.

First, these results showed that artificial BSCs formed by DG1 - a cyanobacterial enrichment obtained from local agricultural soil - exhibit high biomass density and stability on N-

limited soils (both sandy soil and silt loam soil). Second, DG1 could fix 0.1 mg N g^{-1} dry biomass day^{-1} from atmospheric N_2 in N-free medium, but fixed less N_2 in the presence of inorganic N. In addition, when soil nitrate was at adequate levels, application to soils of a small amount of living DG1 biomass (0.88 g dry biomass m^{-2}) resulted in more soil nitrate retention under simulated rainfall than non-inoculated controls. Thus DG1 has potential to reduce N loss from soil. Third, based on the dynamics of cyanobacteria, green algae, and moss compartments of BSCs in model simulations and field observations, application of cyanobacteria (i.e. DG1) could accelerate the growth and succession of BSCs, and improve N retention in soil, especially when the inoculum is added to soils with high available inorganic N. Finally, DG1 has several additional properties that are favorable for field application, including negative cyanotoxin test results, rapid recovery after eight weeks under air-dry conditions, preliminary evidence of UV protection, and capability for growth in large-scale PBRs.

In conclusion, this study demonstrates the feasibility of developing high-performance cyanobacterial enrichments for future applications in temperate agriculture. The results showed that the selected cyanobacterial enrichment DG1 has potential to be used as an agricultural soil amendment to accelerate BSC formation, improve soil stability and reduce application rates of synthetic N fertilizer.

TABLE OF CONTENTS

LIST OF FIGURES

LIST OF TABLES

ACKNOWLEDGEMENTS

I sincerely thank my advisor Mary Ann Bruns, for her great advice, support and encouragement. She is also my role model as a female scientist from whom I have learned a lot of good leadership and personality skills. The 5-year Ph.D. experience with Dr. Bruns is a precious treasure in my life, and I will always carry her good qualities with me in future.

I thank my committee members Katriona Shea, Armen Kemanian, Zhibiao Zhao, and my former committee member Enid Martinez, for their inspirational ideas and help during my thesis research. I thank Mark Signs and Kim Martin at the Penn State Shared Fermentation Facility, Todd Sowers at the Penn State Earth and Environmental Systems Institute, and Louis S Saporito at the USDA Agricultural Research Service, for their helpful support and suggestions in my experiments. I also thank Gail L. Rosen, Yemin Lan, Don Bryant, Zhongkui Li, Richard Macur, Mark Allen, and Rocco Fiato for their help and comments. I thank Chengxi Lu for his great help during my fourth year's field and lab work, as well as my previous lab mates Rosemary Gutierrez, Claudia Rojas-Alvarado, Clarissa A. Lehman, Beatrice Aren Ajeng Laing, Tania Galindo-Castañeda for their companion and support.

I thank my parents Bing Xu and Gengsheng Peng for their love and encouragement. I also thank Qing Xu, for his support and understanding. Finally, I appreciate all my family members and friends.

This work was funded by the Research Applications for Innovation (RAIN) grant from the College of Agricultural Sciences of the Pennsylvania State University. I have received my graduate assistantship and travel funds from the College of Agricultural Sciences and the Huck Institutes of the Life Sciences. I also have received some travel funds from the Accelergy Corporation.

Chapter 1

Biological Nitrogen Fixation by Cyanobacteria and Their Potential Use as Surface Soil Amendments in Agriculture

1.1 Current problems in agricultural soil fertility

Soil fertility is crucial for crop productivity. In modern agricultural systems, high crop yield is ensured by the use of large amounts of synthetic nitrogen (N) fertilizer. In 2011, for example, 12.8 Tg of N fertilizer were used in the United States alone (Figure 1-1) (USDA-ERS, 2013). However, it has been determined that crops take up only 40%-50% of applied fertilizer N (also defined as fertilizer N use efficiency) (Canfield et al., 2010; Chien et al., 2009; Dhar et al., 2015). Excessive application of N fertilizers causes several environmental problems, including water eutrophication (Schindler and Hecky, 2009), soil acidification (Barak et al., 1997), and greenhouse gas emission (Gruber and Galloway, 2008). In addition, abundance and functional diversity of soil microbial communities can decline when synthetic N fertilizers are used without replacing soil organic matter lost through crop cultivation (Marschner et al., 2003; Tilman et al., 2001; Zhong et al., 2010). The N_2-fixing bacteria are especially sensitive to soil N content, and they become less active in ecosystems with high soil N content (Compton et al., 2004). Such decline in N_2-fixing bacteria may in turn have a detrimental positive feedback so that the agroecosystem becomes even more reliant on N fertilizer additions.

1.2 Biological N fixation

Increased use of biological N fixation (BNF) has been proposed as a means to improve soil N retention in sustainable crop production systems (Cassman et al., 2002; Peoples et al., 1995; Vance, 2001). BNF is carried out by prokaryotic organisms having nitrogenase enzymes that reduce atmospheric N_2 to NH_3. The overall reaction stoichiometry of BNF is summarized as follows (Howard and Rees, 1996): $N_2 + 8H^+ + 8e^- + 16\ ATP \rightarrow 2NH_3 + H_2 + 16ADP + 16Pi$.

Nitrogenase enzymes are highly sensitive to inactivation by O_2 and therefore require a nearly anoxic environment to function (Fay, 1992). BNF consumes little energy, has a very high catalytic efficiency, and occurs at ambient temperature and pressure (Rees and Howard, 2000). In contrast, industrial N_2 fixation by the Haber-Bosch process requires high temperatures (650-750 K) and extreme pressures (50-200 bar) (Vojvodic et al., 2014). Globally, the total N input from BNF is about 90-130 Tg N yr^{-1} in terrestrial ecosystems with no human intervention, which is higher than industrial N fixation though fertilizer production (about 80 Tg N yr^{-1}) (Galloway et al., 1995). Moreover, biologically fixed N is coupled to cellular carbon (C) when it enters the soil, so that it is nitrified less rapidly and subjected to slower conversion to the highly mobile form of nitrate-N in soil (Gardner and Drinkwater, 2009).

BNF is carried out by three different groups of prokaryotes based on their relationships with other organisms. First, symbiotic N fixation occurs in partnership between N_2-fixing prokaryotes and their specific hosts. The most commonly studied symbioses take place between rhizobia and legumes, cyanobacteria and aquatic ferns, cyanobacteria and lichen fungi and *Frankia spp.* with some non-legume plants (McNeill and Unkovich, 2007). Second, endophytic and associative N_2 fixers, such as *Azotobacter, Beijerinckia* and *Azospirillum spp.*, live in close contact with certain tropical grasses, including sugar cane (*Saccharum spp.*), Kallar grass (*Leptochloa fusca* (L.) Kunth), and some cereal crops. These N_2 fixers reside on or in plant roots

and/or within intracellular spaces in plant tissues (Elmerich and Newton, 2010; James, 2000). The third group of N_2 fixers is free-living bacteria that do not require specific hosts. These include a large variety of cyanobacteria (for example, *Anabaena, Nostoc, Gloeothece, Cyanothece, Lyngbya, Trichodesmium, Katagnymene*, etc.), and members of other bacterial phyla, such as free living *Azotobacter, Thiobacillus*, and *Clostridium* (Issa et al., 2014; Stacey et al., 1992).

Such free-living N_2 fixers have the potential to be widely used in agriculture, because they are not constrained to associations with specific host plants. It has been estimated that BNF by free-living bacteria, mostly cyanobacteria, contributes 0.1-25 kg N ha^{-1} yr^{-1}, while the typical fertilization rates in crop production ranges between 50-200 kg N ha^{-1} yr^{-1} (Sylvia et al., 2005). Therefore, free-living cyanobacteria are a potential source of renewable N to reduce synthetic N fertilizer requirements in sustainable agriculture.

1.3 Cyanobacteria in biological soil crusts (BSCs)

Cyanobacteria, formerly known as blue-green algae, are a large phylum of gram-negative photosynthetic (mostly oxygenic) bacteria that are widely distributed in aquatic and terrestrial ecosystems. Based on the microfossil record, cyanobacteria have existed on Earth for 3.3-3.5 billion years (Schopf and Packer, 1987). Cyanobacteria have several characteristics that enhance its environmental adaptability. First, as mentioned above, many cyanobacteria can fix atmospheric N_2. Some filamentous cyanobacteria form specialized cells called heterocysts, which cannot produce O_2 (due to lack of photosystem II) and provide cellular environments for high activity of nitrogenase. Heterocysts' thick cell walls also protect nitrogenase by slowing O_2 diffusion into the cells (Adams, 2000). In addition, cyanobacteria have evolved a highly efficient C-concentrating mechanism (CCM), which significantly promotes photosynthesis under low CO_2

conditions (Cohen and Gurevitz, 2006; Price et al., 1998). Finally, although cyanobacteria are phototrophic, some can carry out facultative heterotrophic metabolism, enabling them to survive in the dark (Mannan and Pakrasi, 1993; Summers et al., 1995).

Cyanobacterial members of biological soil crusts (BSCs) have been studied intensively in arid and semiarid areas. BSCs are complex communities of cyanobacteria, bacteria, algae, lichens, moss (bryophytes) and fungi which are intimately bound to soil particles to form cohesive surface biofilms or mats (Belnap and Lange, 2001). The presence of photosynthesizing and N_2-fixing organisms allows BSCs to become established on bare soils and rock surfaces in the early stages of terrestrial ecosystem succession (Sancho et al., 2014). Especially in arid and semiarid areas, BSCs facilitate soil formation, improve soil quality and facilitate the eventual establishment of vascular plants (Langhans et al., 2009a). As the only organisms that fix both atmospheric CO_2 and N_2, cyanobacteria are crucial first colonizers on terrestrial surfaces. Growth and activity of cyanobacteria lead to increased crust stability and higher microbial and bryophyte diversity during BSC development (Langhans et al., 2009b).

BSCs have high potential to fix atmospheric CO_2 and N_2. Globally, cryptogamic covers are estimated to take up 3.9 Pg C per year (7% of total net plant primary production) and 49 Tg N per year (46% of all biological N_2 fixations) (Elbert et al., 2012). Of these totals, BSCs (mainly by cyanobacteria) contribute about 26 Tg N per year through N_2 fixation (Weber et al., 2015). It has also been estimated that BSC-associated net C deposition could range from 7-51 kg C ha^{-1} yr^{-1} (Wilske et al., 2009). Although BSCs have high potential to fix C and N in a wide variety of ecosystems, they have received little attention in humid climates, especially in row crop agricultural systems of North America.

1.4 Applications of cyanobacteria in agriculture

Field applications of cyanobacteria have been mostly studied in flooded rice paddy systems, where cyanobacteria are either free-living or in symbiotic association with aquatic ferns (mostly *Azolla spp*.) (Vaishampayan et al., 2001). The free-living heterocystous cyanobacteria, which either have been applied and/or observed to supply fixed N in rice cultivation, are mostly members of the genera *Anabaena, Nostoc, Aulosira* and *Tolypothrix* (Mishra and Pabbi, 2004; Pereira et al., 2009; Prasanna et al., 2009; Prasanna and Nayak, 2007). It has been reported in multiple rice cultivation studies that N_2 fixation by cyanobacteria could reduce synthetic N fertilizer usage by 25-50 kg N ha^{-1} crop $season^{-1}$, which is equivalent to 30-50% of the typical fertilizer N application rate in rice production (Choudhury and Kennedy, 2004; Hashem, 2001; Roger and Ladha, 1992; Saadatnia and Riahi, 2009; Singh, 1961; Venkataraman, 1975).

Besides rice, free-living, N_2-fixing cyanobacteria have been explored as biofertilizer amendments in several recent studies, for instance, wheat, corn, common bean, tomato, etc. (Hegazi et al., 2010; Karthikeyan et al., 2007; Maqubela et al., 2009; Prasanna et al., 2013; Swarnalakshmi et al., 2013). The observed effects of cyanobacterial biofertilization in these studies (in field or greenhouse) include increasing crop yields, reducing inorganic N fertilizer requirement by up to 50%-67%, improving plant growth, enhancing seed germination, and decreasing pathogen susceptibility. Based on these studies, the application of cyanobacteria could have great benefits in row crop agriculture in North America.

Every year for the past 15 years, cyanobacterial and algal BSCs have been observed on soil surfaces in diverse agricultural fields at the Russell E. Larson Agronomy Research Farm (GPS coordinates 40.72 -77.93) of the Pennsylvania State University. Microscopic observations and molecular analyses of *16S rRNA genes* of BSCs sampled in 2001 indicated the presence of *Nostoc spp.* in maize plots of the Hunter Rotation Experiment (Castillo and Bruns, 2001). More

recent photographs of BSCs on soil surfaces (Figure 1-2) clearly showed the presence of cyanobacteria, green algae, and moss in diverse fields. As a consequence of their diversity and stability, BSCs provide conditions that enhance survival and functioning of their constituents in contrast to individual populations (Pointing and Belnap, 2012). Thus, the application of biofilm-forming, N_2-fixing cyanobacteria to establish BSCs on arable soils could provide renewable supplements of biologically fixed N_2 in temperate agriculture.

1.5 Objective, hypothesis, and rationale for this research

The dissertation study aims to evaluate the potential application of N_2-fixing cyanobacteria to agriculture soil surfaces as a means to promote development of BSC that fix N_2, enhance soil stability, and reduce nutrient losses. The overall hypothesis of my dissertation is depicted in a diagram of a conceptual model in Figure 1-3. After colonization during the initial stage of BSC development, cyanobacteria subsequently fix C and N, which initiates microbial succession to form stable BSCs that characterized by cyanobacteria, green algae, bryophytes, and other microorganisms living together. In addition, BSC production of microbial biomass and extracellular polymeric substances (EPS) will have a feedback effect on soil properties and create more favorable conditions for maintenance of BSCs. As summarized in Table 1-1, my dissertation research investigated several different aspects of the potential application of cyanobacterial soil amendments, including modeling, lab experiments, and field observations.

This study provides proof of concept that stable BSCs can be established using N_2-fixing, biofilm-forming cyanobacteria on arable soils. It also provides suitable cyanobacterial enrichments and sufficient references that could be utilized directly in developing commercial cyanobacterial soil amendments for agricultural application. Finally, this study improves our understanding of cyanobacterial contributions to BSC succession and soil N cycling in

agricultural systems. Stable BSCs could be self-renewable after their establishment. Therefore, artificial BSCs formed by soil cyanobacterial amendments could provide long-term ecosystem service provision in agroecosystems. These services include improvement of soil nutrient and properties, remediation of greenhouse gas emissions, enhancing soil stability and resilience, and reducing the risk of using large amounts of synthetic N fertilizer.

1.6 References

Adams, D.G., 2000. Heterocyst formation in cyanobacteria. Current opinion in microbiology 3, 618-624.

Barak, P., Jobe, B., Krueger, A., Peterson, L., Laird, D., 1997. Effects of long-term soil acidification due to nitrogen fertilizer inputs in Wisconsin. Plant and Soil 197, 61-69.

Belnap J, Lange LE, 2001. Biological soil crusts: structure, function and management. Springer, New York.

Belnap, J., Lange, O., 2001. Biological soil crusts: structure, function and management. Springer, New York.

Canfield, D.E., Glazer, A.N., Falkowski, P.G., 2010. The Evolution and Future of Earth's Nitrogen Cycle. Science 330, 192-196.

Cassman, K.G., Dobermann, A., Walters, D.T., 2002. Agroecosystems, nitrogen-use efficiency, and nitrogen management. AMBIO: A Journal of the Human Environment 31, 132-140.

Castillo, H., Bruns, M.A., 2001. Cyanobacterial diversity in agricultural soils, Ninth International Symposium in Microbial Ecology, Amsterdam, The Netherlands.

Chien, S.H., Prochnow, L.I., Cantarella, H., 2009. Chapter 8 Recent Developments of Fertilizer Production and Use to Improve Nutrient Efficiency and Minimize Environmental Impacts, in: Donald, L.S. (Ed.), Advances in Agronomy. Academic Press, pp. 267-322.

Choudhury, A.T.M.A., Kennedy, I.R., 2004. Prospects and potentials for systems of biological nitrogen fixation in sustainable rice production. Biology and Fertility of Soils 39, 219-227.

Cohen, Y., Gurevitz, M., 2006. The cyanobacteria - ecology, physiology, and molecular genetics, Prokaryotes, pp. 1074-1098.

Compton, J.E., Watrud, L.S., Porteous, L.A., DeGrood, S., 2004. Response of soil microbial biomass and community composition to chronic nitrogen additions at Harvard forest. Forest Ecology and Management 196, 143-158.

Dhar, D., Prasanna, R., Pabbi, S., Vishwakarma, R., 2015. Significance of Cyanobacteria as Inoculants in Agriculture, in: Das, D. (Ed.), Algal Biorefinery: An Integrated Approach. Springer International Publishing, pp. 339-374.

Elbert, W., Weber, B., Burrows, S., Steinkamp, J., Budel, B., Andreae, M.O., Poschl, U., 2012. Contribution of cryptogamic covers to the global cycles of carbon and nitrogen. Nature Geoscience 5, 459-462.

Elmerich, C., Newton, W.E., 2010. Associative and endophytic nitrogen-fixing bacteria and Cyanobacterial associations. Springer Dordrecht, Netherlands.

Fay, P., 1992. Oxygen relations of nitrogen fixation in cyanobacteria. Microbiological reviews 56, 340-373.

Galloway, J.N., Schlesinger, W.H., Levy, H., Michaels, A., Schnoor, J.L., 1995. Nitrogen fixation: Anthropogenic enhancement - environmental response. Global Biogeochemical Cycles 9, 235-252.

Gardner, J.B., Drinkwater, L.E., 2009. The fate of nitrogen in grain cropping systems: a meta-analysis of ^{15}N field experiments. Ecological Applications 19, 2167-2184.

Gruber, N., Galloway, J.N., 2008. An Earth-system perspective of the global nitrogen cycle. Nature 451, 293-296.

Hashem, M.A., 2001. Problems and prospects of cyanobacterial biofertilizer for rice cultivation. Functional Plant Biology 28, 881-888.

Hegazi, A.Z., Mostafa, S.S.M., Ahmed, H.M.I., 2010. Influence of different cyanobacterial application methods on growth and seed production of common bean under various levels of mineral nitrogen fertilization. Nature and Science 8, 183-194.

Howard, J.B., Rees, D.C., 1996. Structural basis of biological nitrogen fixation. Chemical Reviews 96, 2965-2982.

Issa, A.A., Abd-Alla, M.H., Ohyama, T., 2014. Nitrogen Fixing Cyanobacteria: Future Prospect, in: Ohyama, T. (Ed.), Advances in Biology and Ecology of Nitrogen Fixation. inTech, Rijeka, Croatia, pp. 23-48.

James, E., 2000. Nitrogen fixation in endophytic and associative symbiosis. Field crops research 65, 197-209.

Karthikeyan, N., Prasanna, R., Nain, L., Kaushik, B.D., 2007. Evaluating the potential of plant growth promoting cyanobacteria as inoculants for wheat. European journal of soil biology 43, 23-30.

Langhans, T.M., Storm, C., Schwabe, A., 2009a. Biological soil crusts and their microenvironment: impact on emergence, survival and establishment of seedlings. Flora-Morphology, Distribution, Functional Ecology of Plants 204, 157-168.

Langhans, T.M., Storm, C., Schwabe, A., 2009b. Community assembly of biological soil crusts of different successional stages in a temperate sand ecosystem, as assessed by direct determination and enrichment techniques. Microbial Ecology 58, 394-407.

Mannan, R.M., Pakrasi, H.B., 1993. Dark heterotrophic growth conditions result in an increase in the content of photosystem II units in the filamentous cyanobacterium *Anabaena variabilis* ATCC 29413. Plant physiology 103, 971-977.

Maqubela, M., Mnkeni, P., Issa, O.M., Pardo, M., D'Acqui, L., 2009. *Nostoc* cyanobacterial inoculation in South African agricultural soils enhances soil structure, fertility, and maize growth. Plant and Soil 315, 79-92.

Marschner, P., Kandeler, E., Marschner, B., 2003. Structure and function of the soil microbial community in a long-term fertilizer experiment. Soil Biology and Biochemistry 35, 453-461.

McNeill, A., Unkovich, M., 2007. The nitrogen cycle in terrestrial ecosystems, Nutrient cycling in terrestrial ecosystems. Springer, pp. 37-64.

Mishra, U., Pabbi, S., 2004. Cyanobacteria: a potential biofertilizer for rice. Resonance 9, 6-10.

Peoples, M., Herridge, D., Ladha, J., 1995. Biological nitrogen fixation: an efficient source of nitrogen for sustainable agricultural production? Plant and Soil 174, 3-28.

Pereira, I., Ortega, R., Barrientos, L., Moya, M., Reyes, G., Kramm, V., 2009. Development of a biofertilizer based on filamentous nitrogen-fixing cyanobacteria for rice crops in Chile. Journal of Applied Phycology 21, 135-144.

Pointing, S.B., Belnap, J., 2012. Microbial colonization and controls in dryland systems. Nature Reviews Microbiology 10, 551-562.

Prasanna, R., Chaudhary, V., Gupta, V., Babu, S., Kumar, A., Singh, R., Shivay, Y.S., Nain, L., 2013. Cyanobacteria mediated plant growth promotion and bioprotection against Fusarium wilt in tomato. European Journal of Plant Pathology 136, 337-353.

Prasanna, R., Jaiswal, P., Nayak, S., Sood, A., Kaushik, B.D., 2009. Cyanobacterial diversity in the rhizosphere of rice and its ecological significance. Indian Journal of Microbiology 49, 89-97.

Prasanna, R., Nayak, S., 2007. Influence of diverse rice soil ecologies on cyanobacterial diversity and abundance. Wetlands Ecology and Management 15, 127-134.

Price, G.D., Sültemeyer, D., Klughammer, B., Ludwig, M., Badger, M.R., 1998. The functioning of the CO_2 concentrating mechanism in several cyanobacterial strains: a review of general physiological characteristics, genes, proteins, and recent advances. Canadian Journal of Botany 76, 973-1002.

Rees, D.C., Howard, J.B., 2000. Nitrogenase: standing at the crossroads. Current opinion in chemical biology 4, 559-566.

Roger, P.A., Ladha, J.K., 1992. Biological N_2 Fixation in wetland rice fields: Estimation and contribution to nitrogen balance. Plant and Soil 141, 41-55.

Saadatnia, H., Riahi, H., 2009. Cyanobacteria from paddy fields in Iran as a biofertilizer in rice plants. Plant Soil Environ 55, 207-212.

Sancho, L.G., Maestre, F.T., Büdel, B., 2014. Biological soil crusts in a changing world: introduction to the special issue. Biodiversity and Conservation 23, 1611-1617.

Schindler, D., Hecky, R., 2009. Eutrophication: more nitrogen data needed. Science 324, 721-722.

Schopf, J.W., Packer, B.M., 1987. Early Archean (3.3-billion to 3.5-billion-year-old) microfossils from Warrawoona Group, Australia. Science 237, 70-73.

Singh, R.N., 1961. Role of blue-green algae in nitrogen economy of Indian agriculture. Indian Council of Agricultural Research, New Delhi.

Stacey, G., Burris, R.H., Evans, H.J., 1992. Biological nitrogen fixation. Springer Science & Business Media.

Summers, M.L., Wallis, J.G., Campbell, E.L., Meeks, J.C., 1995. Genetic evidence of a major role for glucose-6-phosphate dehydrogenase in nitrogen fixation and dark growth of the cyanobacterium *Nostoc sp*. strain ATCC 29133. Journal of bacteriology 177, 6184-6194.

Swarnalakshmi, K., Prasanna, R., Kumar, A., Pattnaik, S., Chakravarty, K., Shivay, Y.S., Singh, R., Saxena, A.K., 2013. Evaluating the influence of novel cyanobacterial biofilmed biofertilizers on soil fertility and plant nutrition in wheat. European journal of soil biology 55, 107-116.

Sylvia, D.M., Fuhrmann, J.J., Hartel, P., Zuberer, D.A., 2005. Principles and applications of soil microbiology. Pearson Prentice Hall, Upper Saddle River, NJ.

Tilman, D., Fargione, J., Wolff, B., D'Antonio, C., Dobson, A., Howarth, R., Schindler, D., Schlesinger, W.H., Simberloff, D., Swackhamer, D., 2001. Forecasting agriculturally driven global environmental change. Science 292, 281-284.

USDA-ERS, 2013. Fertilizer Use and Price.

Vaishampayan, A., Sinha, R., Hader, D.-P., Dey, T., Gupta, A., Bhan, U., Rao, A., 2001. Cyanobacterial biofertilizers in rice agriculture. The Botanical Review 67, 453-516.

Vance, C.P., 2001. Symbiotic nitrogen fixation and phosphorus acquisition. Plant nutrition in a world of declining renewable resources. Plant physiology 127, 390-397.

Venkataraman, G.S., 1975. The role of cyanobacteria in tropical rice cultivation, in: Stewart, W.D.P. (Ed.), Nitrogen fixation by free living microorganisms. Cambridge University Press, Cambridge, pp. 207-218.

Vojvodic, A., Medford, A.J., Studt, F., Abild-Pedersen, F., Khan, T.S., Bligaard, T., Nørskov, J., 2014. Exploring the limits: A low-pressure, low-temperature Haber–Bosch process. Chemical Physics Letters 598, 108-112.

Weber, B., Wu, D., Tamm, A., Ruckteschler, N., Rodríguez-Caballero, E., Steinkamp, J., Meusel, H., Elbert, W., Behrendt, T., Sörgel, M., 2015. Biological soil crusts accelerate the

nitrogen cycle through large NO and HONO emissions in drylands. Proceedings of the National Academy of Sciences 112, 15384-15389.

Wilske, B., Burgheimer, J., Maseyk, K., Karnieli, A., Zaady, E., Andreae, M.O., Yakir, D., Kesselmeier, J., 2009. Modeling the variability in annual carbon fluxes related to biological soil crusts in a Mediterranean shrubland. Biogeosciences Discuss. 6, 7295-7324.

Zhong, W., Gu, T., Wang, W., Zhang, B., Lin, X., Huang, Q., Shen, W., 2010. The effects of mineral fertilizer and organic manure on soil microbial community and diversity. Plant and Soil 326, 511-522.

1.7 Figures and tables

Figure 1-1. Annual consumptions of nitrogen fertilizer in the United States 1960-2011. This chart was plotted based on the data reported by the United States Department of Agriculture - Economic Research Service (USDA-ERS, 2013).

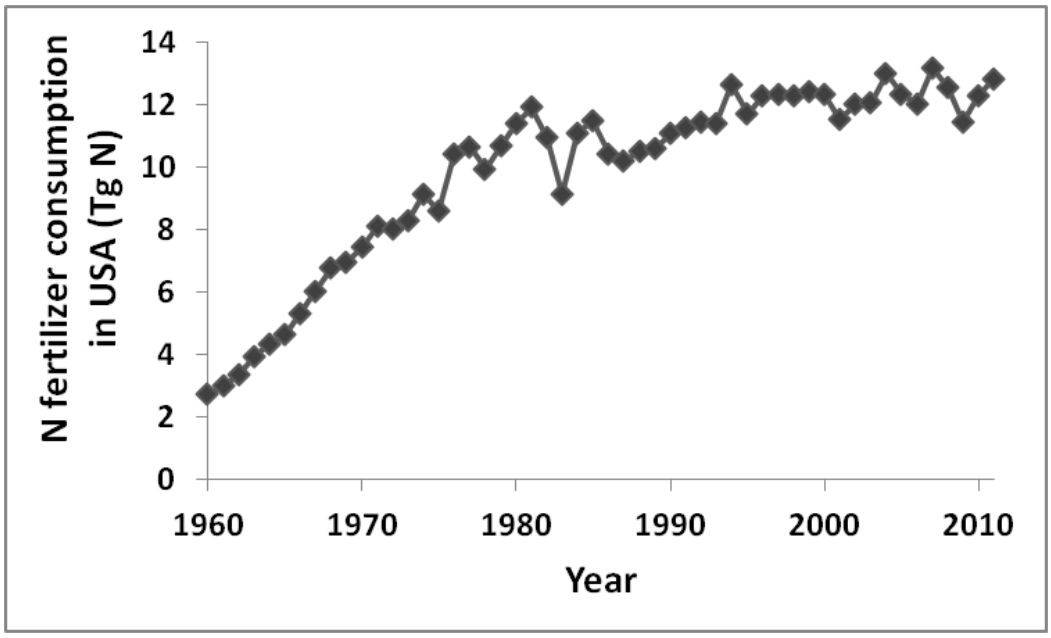

Figure 1-2. Naturally developed BSCs in a no-till corn plot at the Russell E. Larson Agronomy Research Farm of the Pennsylvania State University. This photo was taken in September, 2011.

Figure 1-3. Conceptual model of BSCs succession. Black arrows indicate the transition through states, while gray arrows indicate the direct and indirect effects.

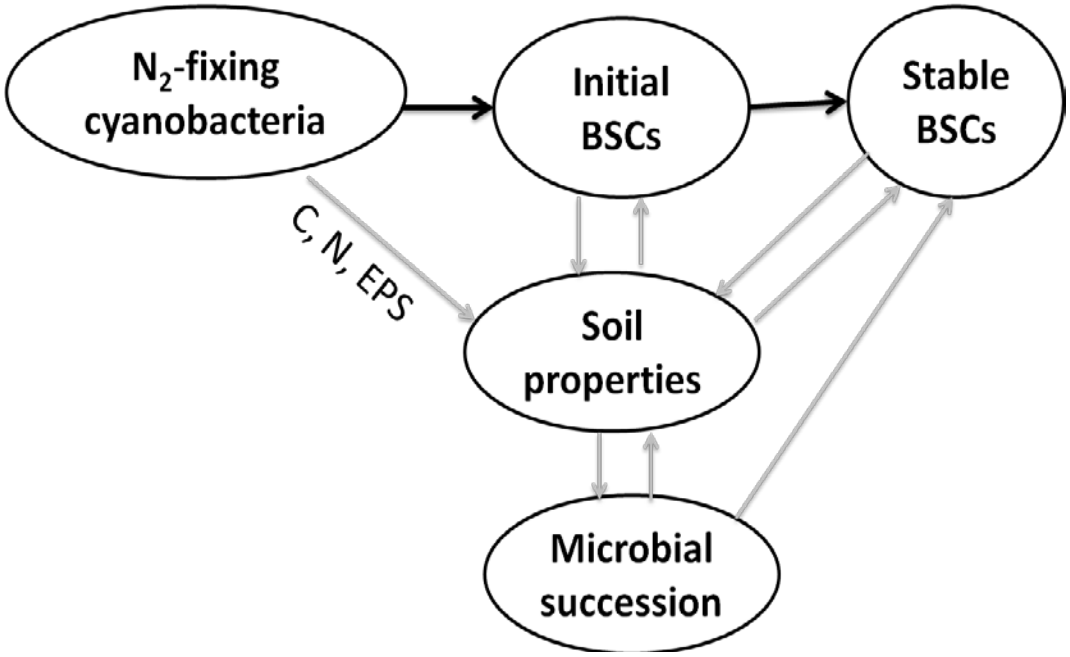

Table 1-1. Summary of topics studied in this dissertation.

Study content	Chapter
Local cyanobacterial enrichment isolation	Chapter 2
Strain selection	Chapter 2
Metagenomic DNA analysis	Chapter 2
N_2 fixation	Chapter 3
Cyanotoxin production	Chapter 3
Cyanobacterial growth and artificial BSC formation on soil surface	Chapter 2 & 4
Soil N retention by BSCs	Chapter 4
Cyanobacterial BSC stability	Chapter 2 & 4
Influence of BSCs on water infiltration	Chapter 4
BSC succession model	Chapter 5
Simulating BSC dynamics in agricultural fields	Chapter 5
Large scale cultivation of filamentous cyanobacteria	Appendix A
Resistance to drought	Appendix B
Preliminary evidence for UV protection	Appendix C

Chapter 2

Selecting N_2-Fixing Cyanobacteria for Agricultural Soil Amendment and Biological Soil Crust Formation

2.1 Introduction

In agroecosystems worldwide, crops take up only 50% or less of applied fertilizer nitrogen (N) (Chien et al., 2009; Galloway et al., 2008). Such low N use efficiency leads to several environmental problems, including water eutrophication, soil acidification, and greenhouse gas emission (Barak et al., 1997; Gruber and Galloway, 2008; Schindler and Hecky, 2009). Organic N sources, such as N_2-fixing legumes in cover crops or rotations, can significantly increase soil N retention (30-42% on average) and improve soil N use efficiency (Gardner and Drinkwater, 2009). In contrast to industrial N fertilizer, biologically fixed N enters soil in a form that is coupled to carbon (C) in plant residues and must undergo multiple transformations before becoming susceptible to loss as nitrate. Another source of organic N is represented by free-living or symbiotic N_2-fixing cyanobacteria, which are used mainly in rice paddy agriculture (Vaishampayan et al., 2001). In several rice cultivation studies, biofertilization with N_2-fixing cyanobacteria contributed between 25 to 50 kg N ha^{-1} and reduced synthetic N fertilizer use by 30-50% (Choudhury and Kennedy, 2004; Pereira et al., 2008; Roger and Ladha, 1992; Saadatnia and Riahi, 2009; Singh, 1961). Biological N fixation by cyanobacteria in open-field or row crop agriculture in North America, however, has received little attention by agronomists (Metting, 1996).

Cyanobacteria, also known as blue-green algae, comprise a large phylum of bacteria capable of photosynthesis, many of which also fix atmospheric N_2, especially those with specialized, chlorophyll-free heterocysts (Adams, 2000; Cohen and Gurevitz, 2006). Because they fix both CO_2 and N_2, cyanobacteria are pioneer colonizers during the formation of biological

soil crusts (BSCs) in widespread terrestrial ecosystems (Starks et al., 1981; Langhans et al., 2009). BSCs are complex communities of microorganisms intimately bound to soil particles to form cohesive surface biofilms or mats, and they have been studied most intensively in natural arid and semi-arid ecosystems (Belnap and Lange, 2001). It has been estimated that cryptogamic covers in natural ecosystems fix about 49 Tg N per year globally from atmospheric N_2, which represents 46% of all biological N fixation (Elbert et al., 2012). Naturally occurring BSCs contribute about 26 Tg N per year worldwide, and cyanobacteria are the main organisms responsible (Weber et al., 2015). The study of N contributions by BSCs in agroecosystems, on the other hand, is limited, despite long-term recognition that BSCs establish readily on disturbed soils (Starks and Shubert, 1982). Observations at the Pennsylvania State University Agronomy Research Farm, for example, indicate that BSCs are common and reappear every spring on soils of diverse cropping systems (Castillo and Bruns, 2001).

Recently, use of cyanobacteria has been proposed as an approach to increase nutrient availability and soil stability for sustainable agriculture (Singh et al., 2011). Besides rice, agricultural use of free-living, N_2-fixing cyanobacteria has been explored in Asia as a biofertilizer for row crop production of wheat, corn, common bean, and tomato (Hegazi et al., 2010; Karthikeyan et al., 2007; Maqubela et al., 2009; Prasanna et al., 2013). Reported benefits include higher crop yields, reduced inorganic N fertilizer use (up to 50%-67%), improved plant growth, increased soil organic C, better seed germination, and reduced pathogen susceptibility. Two cyanobacterial genera, *Anabaena* and *Nostoc,* members of the Nostocaceae family, have been used most in these studies. These genera also have been observed to predominate in naturally formed BSCs in rice fields (Prasanna et al., 2009; Prasanna and Nayak, 2007).

Recent developments in inoculation technology have recognized the importance of biofilms to increase the survival rate of microorganisms compared to inocula composed of free-living cells (Dhar et al., 2015). Applications of cyanobacterial biofilms as wheat seed coatings

were reported to enhance rhizosphere colonization and soil fertility (Swarnalakshmi et al., 2013). The extracellular mucilage/polysaccharide produced by cyanobacteria can accelerate the formation of BSCs on the soil surface (Mager and Thomas, 2011). BSCs have high microbial diversity and stability, which are vital for their microbial functions and survival under harsh environmental conditions (Pointing and Belnap, 2012). Cyanobacteria on soil surfaces add C to soils through photosynthesis, in contrast to heterotrophic growth of cyanobacteria inoculated with seeds and planted underground. Thus, application of biofilm-forming, N_2-fixing cyanobacteria on soil surfaces to form BSCs could provide renewable supplements of biologically fixed N to serve as "micro-cover crops" in diverse agroecosystems.

The objectives of the present study were to cultivate and select biofilm-forming cyanobacteria that form stable BSCs on agricultural soils to provide biologically fixed N and increase soil stability. Three criteria were used to evaluate cyanobacterial potential for soil applications: reliability of serial transfers in N-free culture media; robust growth on soil surfaces; and resistance to detachment from soil particles by water flushing. We hypothesized that contrasting growth characteristics of filamentous, heterocyst-forming cyanobacteria would influence their efficacy in forming BSCs for agricultural purposes.

2.2 Materials and methods

2.2.1 Commercial cultures

Eight commercially available strains of cyanobacteria were obtained from American Type Culture Collection (ATCC) and the Culture Collection of Algae at the University of Texas at Austin (UTEX), based on culture collection descriptions stating that strains either originated from soils or could grow under N-limited conditions. Strains evaluated were: *Anabaena variabilis*

(ATCC 29413); *A. cylindrica* (UTEX B1611); *A. verrucosa* (UTEX B1619); *A. subcylindrica* (UTEX B1617); *Nostoc punctiforme* (ATCC 29133); *N. muscorum* (UTEX 1037); *N. commune* (UTEX B1621); and *N. parmeloides* (UTEX B1627) (Table S2-1).

2.2.2 Cultivation conditions

A modified BG11(N-) medium (MBG11(N-)) was used for culture maintenance. MBG11(N-) was prepared according to UTEX directions for BG11(N-) (UTEX, 2016) except for the following changes to eliminate some sources of C and N: no citric acid was added; $FeCl_3 \cdot 6H_2O$ was substituted for ammonium iron (III) citrate to achieve the same Fe concentration; and $CoSO_4 \cdot 4H_2O$in trace mineral solution was substituted for $Co(NO_3)_2 \cdot 6H_2O$ to achieve the same Co concentration (Table S2-2). All reagents were ACS-certified. The liquid medium was adjusted to pH 7.1-7.3 with 2M HCl and sterilized by autoclaving. Solid MBG11(N-) was prepared by adding 1.5% Bacto-Agar (Difco) before autoclaving and used for strain maintenance and streak-plate purification.

Cultures were initially grown on solid MBG11(N-) in petri dishes at 22-23°C under continuous fluorescent illumination ('natural light') with an average intensity of 250 Lux. They were then cultured in liquid medium in Erlenmeyer flasks (1/5 flask volume) under the same conditions with rotary shaking at 90 revolutions per minute (RPM). Cyanobacterial biomass was harvested or transferred to new media (fivefold dilution) after 30-day growth periods.

Concentrated cell suspensions (final density of 1-3 mg dry biomass per ml) were obtained from liquid cultures by one of the two following methods. Uniformly suspended cyanobacteria were harvested by centrifuging at 6000 g for five minutes, and resuspended in the remaining medium. Flocculated growth was harvested by gravitational settling for 30 min with removal of supernatant liquid by pipetting. Dry biomass densities of liquid culture condensates were

determined by weighing after drying at 60 °C for three days until no further weight change was observed.

2.2.3 Isolation of cyanobacteria from local soil

Observations since 2000 at the Pennsylvania State University Agronomy Research Farm (GPS coordinates 40.72 -77.93) indicated that BSCs were common on the surfaces of diverse research fields. Soils at this location are Hagerstown silt loams classified as typic Hapludalfs (Soil Survey Staff, 2010). Bulk surface soils were collected for placement in pots and kept moist in a greenhouse environment to allow development of BSCs for one month. Crust samples (about 0.25 cm^2, with some attached soil particles) were aseptically removed from soil surfaces, washed with sterile water, and transferred to 25 ml of liquid MBG11(N-) medium as described above. After two weeks, visible new growth was evident as new biomass attached to original BSC particulates and was removed with a small inoculating loop for streaking onto the surfaces of solid MBG11(N-) medium in petri dishes. Up to 20 plates were prepared from each of six flasks inoculated with BSCs. After 2-4 weeks incubation, growth was serially transferred by further streaking on solid medium until the macroscopic appearance was consistent and microscopic observation appeared reproducible at 400x magnification.

After serial streaking transfers on solid medium, small amounts of uniform growth were removed with needle tips and transferred to 1 ml liquid MBG11(N-) for additional disruptive treatments (vortexing at 3200 RPM or ultrasonication at 42 kHz, with 35 W power supply) before and after incubation. Liquid suspensions were spread across the surfaces of solid MBG11(N-) to attempt colony separation. Cultures that persisted as confluent growth were expected to have heterogeneous composition.

2.2.4 Quantifying growth and crust formation on soils

Growth and crust formation of cyanobacteria on soil were monitored using artificial soil microcosms prepared in standard petri dishes (diameter = 8.5 cm) containing 45 ml autoclaved N-limited sandy soil (soil properties given in Table S2-3) and 12 ml liquid MBG11(N-). To inoculate the soil, 3 ml of condensed fresh cyanobacterial biomass (about 1-2 mg dry biomass ml^{-1}) was distributed evenly by pipetting onto the soil surface. Petri dish edges were wrapped with Parafilm M® (Bemis Company, Neenah, WI) and soil microcosms were incubated under the same conditions described above with observations for up to 80 days. Triplicate microcosms were randomly selected for sacrificial harvesting of surface soil (upper 3 mm).

The biomass density of cyanobacteria from microcosm samples was estimated by measuring chlorophyll a content. Chlorophylls in crust samples from soil microcosms were extracted with a 1:1 ratio DMSO: acetone solution based on Nayak's method (Nayak et al., 2004). Mixtures containing 4 ml extraction solution per gram fresh crust were vortexed (3200 RPM) for 30 seconds and then kept in the dark at room temperature for 72 hr. Chlorophyll a concentration (Chl a) was calculated using the following equation:

$$\text{Chl a } (\mu g\ ml^{-1}) = 11.64 \times (A_{663} - A_{750}) - 2.16 \times (A_{645} - A_{750}) + 0.1 \times (A_{630} - A_{750})$$

where A_{750}, A_{663}, A_{645}, and A_{630} were absorbance readings of the cleared extracts at 750, 663, 645, and 630 nm (UNESCO, 1966).

Increases in cyanobacterial biomass during soil microcosm incubations were determined by measuring chlorophyll a contents of crust samples and comparing them to standard curve values. For each strain or cyanobacterial enrichment, a standard curve was prepared by plotting chlorophyll a concentrations extracted from known amounts of dry biomass (determined by direct weighing) added to 10 g soil and measured using the procedure described above. Duplicates of negative controls with 10 g soil and no biomass, which provided the soil background absorbance readings, were used to adjust the absorbances of inoculated samples. The relationships between

chlorophyll a and cyanobacterial dry biomass contents were determined by simple linear regressions.

2.2.5 Biomass recovery from soil

Cyanobacterial biomass was quantified after application and growth on soil surfaces by using a water flush treatment, as shown in Figure 2-1. To permit water drainage during the treatment, five 3-mm holes in the bottom of each microcosm were made with the tip of a soldering iron. Four replicates of soil microcosms (either with freshly applied biomass or after 80-day growth) were placed on the top of a Hirsch funnel connected to a vacuum flask. A total volume of 100 ml H_2O was poured carefully onto the surface of the soil microcosm (20 ml poured within 15 sec for a total of five times).Water was allowed to drain by gravity until no free water could be observed on the soil surface before adding the next 20 ml water. The entire surface area of each treated plate was harvested after 24 h to a depth of 3 mm for biomass determination from chlorophyll a. Biomass recovery was calculated as the percentage of biomass initially applied to soil that remained in the soil after the water treatment.

Freshly applied individual strains and mixtures of *A. cylindrica* and *N. muscorum* were also evaluated for recovery from soil after the water-flush treatment. To prepare mixtures for testing, the two strains were inoculated at 1:1 volume ratio (about 0.2 mg ml^{-1} for each strain) in liquid MBG11(N-). The flasks were firstly shaken at 90 RPM for one week to mix strains well, and then were left unshaken for three weeks to allow strains to form biofilms together on the liquid surface without disturbance. The mixed culture was condensed to 2 mg dry biomass ml^{-1} prior to soil application.

2.2.6 Data analysis

All test results were analyzed by one-way ANOVA and Tukey's multiple comparisons ($p < 0.05$). Cyanobacterial growth response after the water flush treatment was tested by one-tailed t-test (H_0: $\mu = 100\%$, right tailed). A 'BSC competence score' was devised to rank the ability of cyanobacterial strains and enrichment to become established on soil surfaces. This score was calculated based on two properties: the biomass density established in soil microcosms after 35-45 day cultivation, and the percent soil recovery of freshly applied biomass following the water flush treatment. Both mean (scored based on Tukey's multiple comparison result) and coefficient of variation (CV, positively scored if a CV was lower than the average) were evaluated. The 'BSC competence score' of each cyanobacterial strains/enrichment was calculated as the sum of all individual scores.

2.2.7 DNA analysis of selected cyanobacterial enrichment

Condensed biomass from 30-day liquid cultures of the selected cyanobacterial enrichment (three replicates) was used for metagenomic DNA extraction. For each replicate, four DNA extracts (each from 2 mg biomass) obtained with the MoBio PowerBiofilm DNA Isolation kit (MoBio, Solano Beach, CA) were pooled and quantified using a Qubit system. Three DNA samples were subjected to paired-end sequencing with an Illumina MiSeq at the Genomics Core Facility of The Huck Institutes of the Life Sciences at Penn State University. Sequences were processed and assembled with the IDBA-UD program (Peng et al., 2012). Contig scoring and assembly was performed with BWA mean and MaxBin methods (Wu et al., 2014). Sequences have been submitted to GenBank as BioSample accession SAMN04488150. Taxonomic

information was obtained from sequencing data using the PhyloPhlAn method (Segata et al., 2013).

2.3 Results

2.3.1 Cultivation in N-free medium

Five of eight commercial cultures grew on solid MBG11(N-) medium with no N supplementation: *A. variabilis, A. cylindrica, N. punctiforme, N. muscorum and N. commune* (Table S2-1). Three robust cyanobacterial enrichments from local soils were selected for further study: Dark Green (designated 'DG1'), Pinpoint Green (designated 'PG1'), and Medium Brown (designated 'MB1'). The enrichments were subjected to cell disruption treatments in liquid medium and streaked on solid MBG11(N-) medium at least ten times to verify consistent microscopic appearance (Figure S2-1). The PG1 and MB1 enrichments formed discrete colonies upon streaking for isolation, while DG1 produced confluent growth on solid medium. These three enrichments could not be further separated by sonication or vortexing treatments as assessed by microscopy.

Several cultures (*N. commune,* PG1 and MB1) that grew well on solid medium showed inconsistent growth in liquid medium (Table S1). In contrast, *A. variabilis, A. cylindrica, N. muscorum, N. punctiforme,* and the DG1 enrichment showed robust growth but varied degrees of flocculation in liquid MBG11(N-) medium. Growth in liquid cultures of *Anabaena spp.* appeared uniform and non-aggregated, while *Nostoc spp.* and DG1 formed flocculated and/or biofilm structures (Figure 2-2). These five cyanobacterial cultures were used in subsequent soil microcosm experiments since they exhibited highest potential for large-scale cultivation in liquid medium.

2.3.2 Cyanobacterial growth and surface BSC development in soil microcosms

The four most robust cyanobacterial strains and the DG1 enrichment exhibited good growth in N-limited soil microcosms during the 80-day incubation periods. As shown in Figure 2-3, cyanobacterial growth on surfaces of soil microcosms was biphasic following inoculation. In the first phase, biomass densities of all strains and DG1 enrichment increased significantly during the first month. Especially, *A. variabilis* had the highest growth rate (6.9 fold increase in 14 days) followed by DG1 enrichment (3.7 fold increase in 14 days).

The four pure cultures and the DG1 enrichment reached the second phase after one month's growth, during which the biomass increased much slower through the following cultivation time. *A. variabilis* had the highest biomass density on the soil surface (1145.2 ± 62.8 μg cm^{-2}) after 35-45 day cultivation, which was significantly higher than the biomass densities of *A. cylindrica* (307.9 ± 7.7 μg cm^{-2}) and the DG1 enrichment (394.5 ± 24.7 μg cm^{-2}). The biomass densities of *N. muscorum* (176.7 ± 31.2 μg cm^{-2}) and *N. punctiforme* (134.9 ± 16.4 μg cm^{-2}) were significantly lower compared to other strains after 35-45 day cultivation. No significant difference was observed between the biomass densities of *A. cylindrica* and the DG1 enrichment, as well as the two *Nostoc spp*.. In addition, after being cultivated for a month, the two *Nostoc spp.* and DG1 formed coherent BSCs that could be picked up with a glass slide (Figure S2-2). None of *Anabaena spp*. formed cohesive BSCs in the soil microcosms.

2.3.3 Stability under water flush treatment

Biomass recoveries of all cyanobacterial strains/mixtures after the water flush treatment are summarized in Figure 2-4. The final biomass recovery was the result of both the coherence of biomass on soil surface and the growth of cyanobacteria during the 24-hour treatment period.

The two *Nostoc spp.* and the DG1 enrichment were resistant to flushing treatments. Freshly applied DG1 enrichment also showed the most rapid growth response after the application (increased 68.4 ± 17.6%, $p = 0.002$), followed by freshly applied *N. muscorum* (increased 27.4 ± 15.7%, $p = 0.020$) and the mixture of *A. cylindrica* and *N. muscorum* (increased 26.2 ± 13.6%, $p = 0.015$). The two *Nostoc spp.* after 80-day cultivation and the freshly applied *N. punctiforme* were also stable on the soil surface after the flush treatment, with about 100% recovery but no significant increase. The DG1 enrichment had a slightly lower recovery rate (87.0 ± 9.3% remained) after being cultured in soil microcosms for 80 days.

The two *Anabaena spp.* were not as resistant to the flush treatment compared to *Nostoc spp.* or the DG1 enrichment. Freshly applied *A. variabilis* (27.3 ± 7.1% recovered) and *A. cylindrical* (42.3 ± 9.8% recovered) had the lowest recovery rates. The retention rates of *Anabaena spp.* (35.3 ± 5.6% recovered for *A. variabilis*; 63.2 ± 11.3% recovered for *A. cylindrica*) increased slightly after 80 days cultivation. However, such retention rates were still lower than *Nostoc spp.* and the DG1 enrichment.

2.3.4 BSC competence

As summarized in Table 2-1, the DG1 enrichment had the highest BSC competence score (= 5) for future field applications based on both high biomass density and high fresh biomass recovery on the soil surface. *A. variabilis* had moderate competence score (= 3) as a result of its

high biomass density on soil surface after 35-45 day cultivation. Finally, *A. cylindrica, N. muscorum and N. punctiforme* had the lowest competence scores (= 2), indicating that they might not be suitable for field applications.

2.3.5 Metagenomic characterization of DG1 enrichment

Cyanobacterial enrichment DG1 was selected for its robust growth both in liquid and on solid media after screening dozens of enrichment cultures. Paired-end Illumina sequences of the DG1 metagenome were assembled with the IDBA-UD program (Peng et al., 2012) into 5295 contigs between 1000-669000 bp. As shown in Table 2-2, after scoring and binning assembled contigs (using BWAmean and MaxBin), about 90% of the sequences were assignable to Nostocaceae genomes from eight strains belonging to three genera (*Nostoc, Anabaena*, and *Cylindrospermopsis*) and seven plasmids associated with these strains. Genome nucleotide similarities ranged from 79-90%. The phylogenetic analysis of the cyanobacterial bin in DG1 is shown in Figure S2-4. The remaining sequences were assigned to six bacterial bins, including four were *alphaproteobacteria* (*Acetobacteraceae, Rhizobiaceae, Methylobacteraceae, Sphingomonadales*), one *gammaproteobacteria* (*Xanthomonadaceae*), and one member of *Cytophagales*. Three of the alphaproteobacterial families identified (Rhizobiaceae, Methylobacteriaceae, and Acetobacteriaceae) contain representatives recognized as having N_2-fixing capabilities.

2.4 Discussion

Filamentous cyanobacteria have attracted the most attention in biofilmed biofertilizer applications (Swarnalakshmi et al., 2013; Toledo et al., 1995). However, our results showed that

not all filamentous cyanobacteria could form stable biofilms that were resistant to water flow. Besides filamentous cell morphology, the flocculation of cells in liquid cultures could be a good indicator of biofilm competence and BSC stability. Similar morphological traits were also observed in another study suggesting the importance of the ability to form supracellular cyanobacterial ropes for BSC colonization and stability (Garcia-Pichel and Wojciechowski, 2009). In addition, most developmental studies of cyanobacterial biofertilizers have focused on the rapid growth of cyanobacteria during mass production in liquid media and provision of N to crops (Hashem, 2001; Jha and Prasad, 2006; Mishra and Pabbi, 2004; Silva and Silva, 2013). Our protocol for evaluating for N_2-fixing cyanobacteria as agricultural amendments, on the other hand, also took into account the importance of biocrust-formation potential.

Although very few field studies of artificial cyanobacterial crust formation have been conducted under humid soil conditions, our results were consistent with research conducted in semiarid regions. In our soil microcosm studies, biomass of the four most robust cyanobacterial strains (*A. variabilis*, *A. cylindrica*, *N. muscorum*, and *N. punctiforme*) and the DG1 enrichment increased 1.1-6.0 fold after 7-10 day cultivation; while coherent BSCs, which could be picked up with a glass slide, were formed by DG1 and *Nostoc spp.* in a month. Chen and coworkers established artificial crusts on desert soil by inoculating *Microcoleus vaginatus* and irrigating 20 mm day^{-1} by automatic sprinkling, during which they reported a 0.8-4 fold decrease/increase after 7-10 day cultivation and stable crusts were observed after 22-day growth (Chen et al., 2006). In addition, cyanobacterial biomass densities varied from 0.13-1.32 mg cm^{-2} (*Nostoc spp.* 0.13-0.18 mg cm^{-2}) in slow growth phases of soil microcosm studies. This is in the same range as that of Pankratova, who reported naturally formed *Nostoc commune* crust densities (0.14-0.29 and 0.47-0.74 mg cm^{-2}) in different meadow ecosystems (Pankratova, 2006). Based on these comparisons, we propose that the soil microcosms in our study are good representatives for modeling cyanobacterial growth on field soils.

The establishment of preliminary cyanobacterial crusts is a crucial initial event in the formation of BSCs in desert ecosystems. Once formed, cyanobacterial crusts provide nutrients and diverse niches for microbial growth, thus triggering subsequent microbial colonization and growth during BSC succession (Lan et al., 2012). Moss species, which are indicators of some mature BSCs, appeared a year after the application of *Microcoleus vaginatus* in desert reclamation (Wang et al., 2009). This was significantly faster than natural BSC formation rates that typically took 5-20 years (Langhans et al., 2009). In our studies, the local enrichment DG1 grew fast after inoculation and formed stable initial biocrusts in soil microcosms that had both high biomass densities and good resistance to water forces. Therefore, we propose that inoculation of the DG1 enrichment may accelerate the formation of mature BSCs, especially under soil conditions of humid, temperate agricultural ecosystems.

Although cyanobacteria could not be separated from associated bacteria in the DG1 enrichment, the mixture showed equivalent or better performance based on our three screening criteria compared to commercial pure cultures. In addition, DG1 retained consistent composition and macroscopic growth appearance throughout monthly transfers to fresh liquid MBG11(N-) medium for more than three years. These characteristics indicated that the bacterial associates did not interfere with the ability of the Nostoc sp. to form BSCs. Cyanobacteria, particularly heterocystous strains, have long been known to have close associations with other bacteria in freshwater and marine systems (Nausch, 1996; Paerl et al., 1989; Salomon et al., 2003). The presence of associated bacteria has also been proposed to promote the growth and N_2-fixation of *Anabaena spp. (*Lupton and Marshall, 1981; Paerl, 1977). In considering the potential use of applying the DG1 enrichment to soil, which itself harbors highly diverse microbial populations, it would be uneconomic or even unrealistic to use purified strains for these purposes.

Application of cyanobacteria to soil surfaces for BSC formation may be more economically and environmentally sustainable than applying cyanobacteria as seed treatments or

fertilizer. Cyanobacteria used in seed surface treatments become introduced more deeply into the soil, where photosynthetic organisms are less adapted to thrive. Moreover, to realize significant N contributions to soil, direct use of cyanobacterial biomass as fertilizer requires large quantities that are not economically feasible. Instead, the small quantities of cyanobacteria (0.1-0.5 mg cm^{-2} based on our study) inoculated on surface soil can form self-renewable BSCs. In addition to fixing atmospheric N_2, BSCs could also act to immobilize and retain inorganic N when soil N concentrations are high. Nutrient capture by stable BSCs can therefore help reduce N runoff and increase N use efficiency.

The sandy soil used in our microcosms provided less favorable colonization surfaces compared to most agricultural soils with finer soil textures. This soil provided suboptimal conditions for cyanobacterial growth and BSC formation as the result of its lower surface area and low organic matter content. Additional observations also indicated that DG1 survived desiccation for periods of at least eight weeks (described in Appendix B). Therefore, it is reasonable to expect that the selected cyanobacteria would perform better under less harsh soil conditions in typical agroecosystems. Finally, the selected high-performance cyanobacteria need to be evaluated using more varied agricultural soils in future studies.

2.5 Conclusion

This study established a cost effective system for selecting N_2-fixing cyanobacteria as BSC- forming soil amendments on agricultural soils. Cyanobacterial strains with distinct morphological types had different growth potentials and binding capabilities to soil particles. Compared to other individual cyanobacterial strains available commercially, the preliminary artificial BSCs formed by the DG1 enrichment had both high biomass density and crust stability.

Therefore, this high-performance candidate, DG1, has good potential for future cyanobacterial applications.

2.6 Acknowledgement

We thank Drs. Gail Rosen and Yemin Lan, Drexel University, for assistance with metagenome analysis. We thank Dr. Don Bryant, Penn State Dept of Biochemistry and Molecular Biology, for providing *A. variabilis* and *N. punctiforme;* and Dr. Richard Macur, Center for Biofilm Engineering at Montana State University, for his insightful comments. This research was funded by the Research Applications for Innovation (RAIN) grant from the College of Agricultural Sciences of The Pennsylvania State University.

2.7 References

Adams, D.G., 2000. Heterocyst formation in cyanobacteria. Current opinion in microbiology 3, 618-624.

Barak, P., Jobe, B., Krueger, A., Peterson, L., Laird, D., 1997. Effects of long-term soil acidification due to nitrogen fertilizer inputs in Wisconsin. Plant and Soil 197, 61-69.

Belnap, J., Lange, O., 2001. Biological soil crusts: structure, function and management. Springer, New York.

Castillo, H., Bruns, M.A., 2001. Cyanobacterial diversity in agricultural soils, Ninth International Symposium in Microbial Ecology, Amsterdam, The Netherlands.

Chen, L., Xie, Z., Hu, C., Li, D., Wang, G., Liu, Y., 2006. Man-made desert algal crusts as affected by environmental factors in Inner Mongolia, China. Journal of Arid Environments 67, 521-527.

Chien, S.H., Prochnow, L.I., Cantarella, H. 2009. Chapter 8 Recent developments of fertilizer production and use to improve nutrient efficiency and minimize environmental impacts, in: Donald, L.S. (Ed.), Advances in Agronomy. Academic Press, pp. 267-322.

Choudhury, A.T.M.A., Kennedy, I.R., 2004. Prospects and potentials for systems of biological nitrogen fixation in sustainable rice production. Biology and Fertility of Soils 39, 219-227.

Cohen, Y., Gurevitz, M. 2006. The cyanobacteria—ecology, physiology, and molecular genetics, pp. 1074-1098, In M. Dworkin et al. (eds.), The Prokaryotes: An Evolving Electronic Resource for the Microbiological Community, 3rd ed., [1st online ed.] Vol. 4, Springer-Verlag, New York.

Dhar, D.W., Prasanna, R., Pabbi, S., Vishwakarma, R. 2015. Significance of cyanobacteria as inoculants in agriculture, algal biorefinery: an integrated Approach. Springer, pp. 339-374.

Elbert, W., Weber, B., Burrows, S., Steinkamp, J., Budel, B., Andreae, M.O., Poschl, U. 2012. Contribution of cryptogamic covers to the global cycles of carbon and nitrogen. Nature Geoscience 5, 459-462.

Galloway, J.N., Townsend, A.R., Erisman, J.W., Bekunda, M., Cai, Z., Freney, J.R., Martinelli, L.A., Seitzinger, S.P., Sutton, M.A. 2008. Transformation of the nitrogen cycle: recent trends, questions, and potential solutions. Science 320, 889-892.

Garcia-Pichel, F., Wojciechowski, M.F. 2009. The Evolution of a Capacity to Build Supra-Cellular Ropes Enabled Filamentous Cyanobacteria to Colonize Highly Erodible Substrates. PloS one 4, e7801.

Gardner, J.B., Drinkwater, L.E., 2009. The fate of nitrogen in grain cropping systems: a meta-analysis of ^{15}N field experiments. Ecological Applications 19, 2167-2184.

Gruber, N., Galloway, J.N., 2008. An Earth-system perspective of the global nitrogen cycle. Nature 451, 293-296.

Hashem, M.A., 2001. Problems and prospects of cyanobacterial biofertilizer for rice cultivation. Functional Plant Biology 28, 881-888.

Hegazi, A.Z., Mostafa, S.S.M., Ahmed, H.M.I., 2010. Influence of different cyanobacterial application methods on growth and seed production of common bean under various levels of mineral nitrogen fertilization. Nature and Science 8, 183-194.

Jha, M.N., Prasad, A.N., 2006. Efficacy of new inexpensive cyanobacterial biofertilizer including its shelf-life. World Journal of Microbiology and Biotechnology 22, 73-79.

Karthikeyan, N., Prasanna, R., Nain, L., Kaushik, B.D., 2007. Evaluating the potential of plant growth promoting cyanobacteria as inoculants for wheat. European journal of soil biology 43, 23-30.

Lan, S., Wu, L., Zhang, D., Hu, C., 2012. Successional stages of biological soil crusts and their microstructure variability in Shapotou region (China). Environmental Earth Sciences 65, 77-88.

Langhans, T.M., Storm, C., Schwabe, A., 2009. Community assembly of biological soil crusts of different successional stages in a temperate sand ecosystem, as assessed by direct determination and enrichment techniques. Microb Ecol 58, 394-407.

Mager, D., Thomas, A., 2011. Extracellular polysaccharides from cyanobacterial soil crusts: a review of their role in dryland soil processes. Journal of Arid Environments 75, 91-97.

Maqubela, M., Mnkeni, P., Issa, O.M., Pardo, M., D'Acqui, L., 2009. *Nostoc* cyanobacterial inoculation in South African agricultural soils enhances soil structure, fertility, and maize growth. Plant and Soil 315, 79-92.

Metting, F.B., Jr. 1996. Biodiversity and application of microalgae. J. Indus. Microbiol. 17:477-489.

Mishra, U., Pabbi, S., 2004. Cyanobacteria: A potential biofertilizer for rice. Resonance 9, 6-10.

Nayak, S., Prasanna, R., Pabby, A., Dominic, T.K., Singh, P.K., 2004. Effect of urea, blue green algae and *Azolla* on nitrogen fixation and chlorophyll accumulation in soil under rice. Biology and Fertility of Soils 40, 67-72.

Pankratova, E., 2006. Functioning of cyanobacteria in soil ecosystems. Eurasian Soil Science 39, S118-S127.

Peng, Y., Leung, H.C., Yiu, S.-M., Chin, F.Y., 2012. IDBA-UD: a de novo assembler for single-cell and metagenomic sequencing data with highly uneven depth. Bioinformatics 28, 1420-1428.

Pereira, I., Ortega, R., Barrientos, L., Moya, M., Reyes, G., Kramm, V., 2008. Development of a biofertilizer based on filamentous nitrogen-fixing cyanobacteria for rice crops in Chile. Journal of Applied Phycology 21, 135-144.

Pointing, S.B., Belnap, J., 2012. Microbial colonization and controls in dryland systems. Nat Rev Micro 10, 551-562.

Prasanna, R., Chaudhary, V., Gupta, V., Babu, S., Kumar, A., Singh, R., Shivay, Y.S., Nain, L., 2013. Cyanobacteria mediated plant growth promotion and bioprotection against Fusarium wilt in tomato. European Journal of Plant Pathology 136, 337-353.

Prasanna, R., Jaiswal, P., Nayak, S., Sood, A., Kaushik, B.D., 2009. Cyanobacterial diversity in the rhizosphere of rice and its ecological significance. Indian Journal of Microbiology 49, 89-97.

Prasanna, R., Nayak, S., 2007. Influence of diverse rice soil ecologies on cyanobacterial diversity and abundance. Wetlands Ecology and Management 15, 127-134.

Roger, P.A., Ladha, J.K., 1992. Biological N_2 Fixation in wetland rice fields: Estimation and contribution to nitrogen balance. Plant and Soil 141, 41-55.

Saadatnia, H., Riahi, H., 2009. Cyanobacteria from paddy fields in Iran as a biofertilizer in rice plants. Plant Soil Environ 55, 207-212.

Schindler, D., Hecky, R., 2009. Eutrophication: more nitrogen data needed. Science 324, 721-722.

Segata, N., Börnigen, D., Morgan, X.C., Huttenhower, C., 2013. PhyloPhlAn is a new method for improved phylogenetic and taxonomic placement of microbes. Nature communications 4, 1-11.

Silva, P.G., Silva, d.J.H., 2013. Biomass production of Tolypothrix tenuis as a basic component of a cyanobacterial biofertilizer. Journal of Applied Phycology 25, 1729-1736.

Singh, J.S., Pandey, V.C., Singh, D., 2011. Efficient soil microorganisms: a new dimension for sustainable agriculture and environmental development. Agriculture, Ecosystems & Environment 140, 339-353.

Singh, R.N., 1961. Role of blue-green algae in nitrogen economy of Indian agriculture. Indian Council of Agricultural Research, New Delhi.

Soil Survey Staff, 2010. Keys to soil taxonomy, 11th ed. USDA-Natural Resources Conservation Service, Washington,DC.

Starks, T.L., Shubert, L.E., F.R. Trainor. 1981. Ecology of soil algae: a review. Phycologia 20:65-80.

Starks, T.L, Shubert, L.E. 1982. Colonization and succession of algae and soil-algal interactions associated with disturbed areas. J. Phycol. 18:99-107.

Swarnalakshmi, K., Prasanna, R., Kumar, A., Pattnaik, S., Chakravarty, K., Shivay, Y.S., Singh, R., Saxena, A.K., 2013. Evaluating the influence of novel cyanobacterial biofilmed biofertilizers on soil fertility and plant nutrition in wheat. European journal of soil biology 55, 107-116.

Toledo, G., Bashan, Y., Soeldner, A., 1995. In vitro colonization and increase in nitrogen fixation of seedling roots of black mangrove inoculated by a filamentous cyanobacteria. Canadian Journal of Microbiology 41, 1012-1020.

UNESCO, 1966. Determination of photosynthetic pigments in seawater, Monographs on oceanographic methodology. United Nations Educational, Scientific and Cultural Organization, Place de Fontenoy, pp. 15-16.

UTEX, 2016. BG-11(-N) Medium The Culture Collection of Algae.

Vaishampayan, A., Sinha, R., Hader, D.-P., Dey, T., Gupta, A., Bhan, U., Rao, A., 2001. Cyanobacterial biofertilizers in rice agriculture. The Botanical Review 67, 453-516.

Wang, W., Liu, Y., Li, D., Hu, C., Rao, B., 2009. Feasibility of cyanobacterial inoculation for biological soil crusts formation in desert area. Soil Biology and Biochemistry 41, 926-929.

Weber, B., Wu, D., Tamm, A., Ruckteschler, N., Rodríguez-Caballero, E., Steinkamp, J., Meusel, H., Elbert, W., Behrendt, T., Sörgel, M., 2015. Biological soil crusts accelerate the nitrogen cycle through large NO and HONO emissions in drylands. Proceedings of the National Academy of Sciences 112, 15384-15389.

Wu, Y.-W., Tang, Y.-H., Tringe, S.G., Simmons, B.A., Singer, S.W., 2014. MaxBin: an automated binning method to recover individual genomes from metagenomes using an expectation-maximization algorithm. Microbiome 2, 1.

2.8 Figures and tables

Figure 2-1. Experimental setup for the cyanobacterial soil retention test. (A) A microcosm plate supported by the Hirsch funnel inserted into suction flask; (B) perforations on bottom of microcosm plate (diameter = 5 mm).

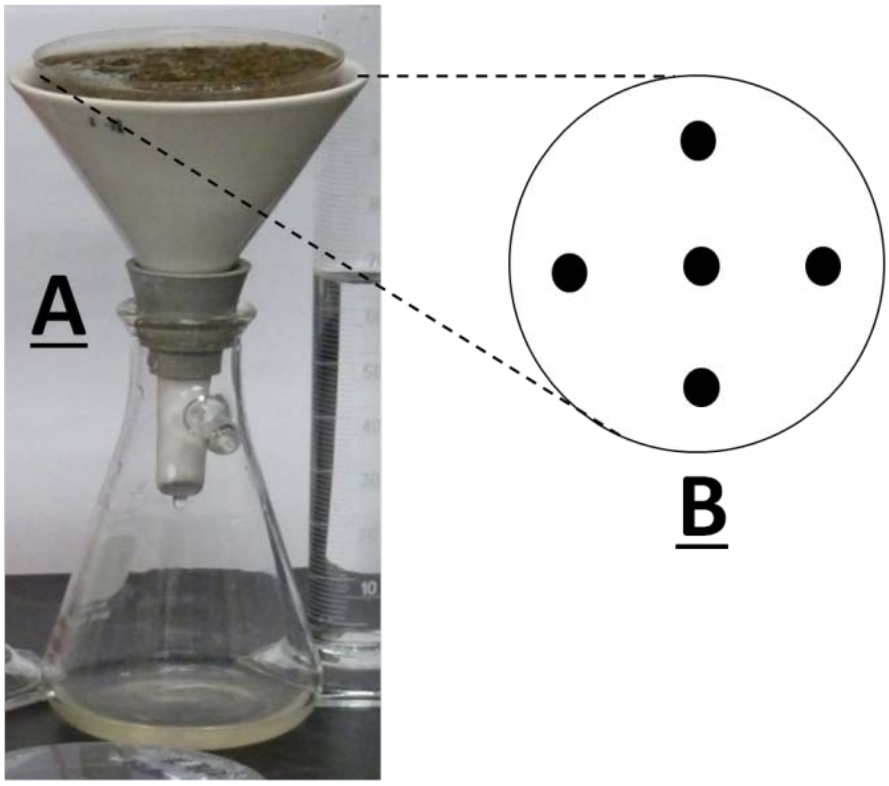

Figure 2-2. Varied degrees of flocculation exhibited by five cyanobacterial cultures right after being inoculated to MBG11(N-) liquid medium in 125-ml flasks. From left to right are *Anabaena variabilis* (ATCC 29413), *Anabaena cylindrica* (UTEX B1611), *Nostoc muscorum* (UTEX 1037), *Nostoc punctiforme* (ATCC 29133), and the DG1 enrichment.

Figure 2-3. Chlorophyll-based biomass measurements of cyanobacterial growth on surfaces of soil microcosms. Error bars show standard deviations.

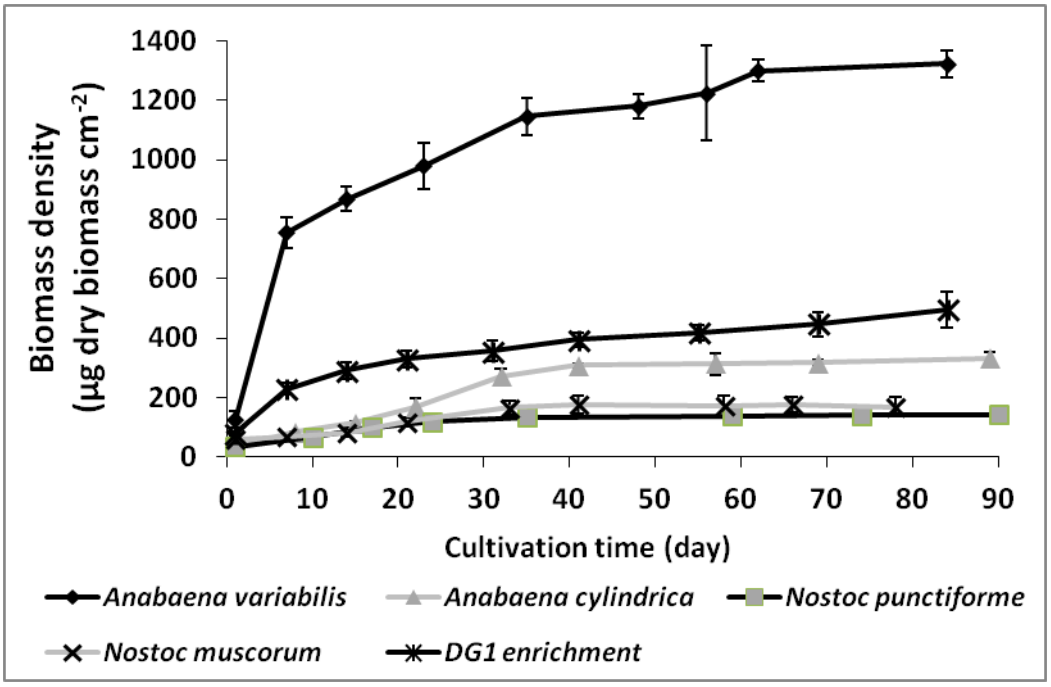

Figure 2-4. Percent biomass retention on soil surfaces after a 24-hour water flush treatment of freshly applied cyanobacteria (F) and surface biofilms after 80-day incubation (S). Error bars are standard deviations. Different letters show the result of Tukey's multiple comparison tests ($p < 0.05$).

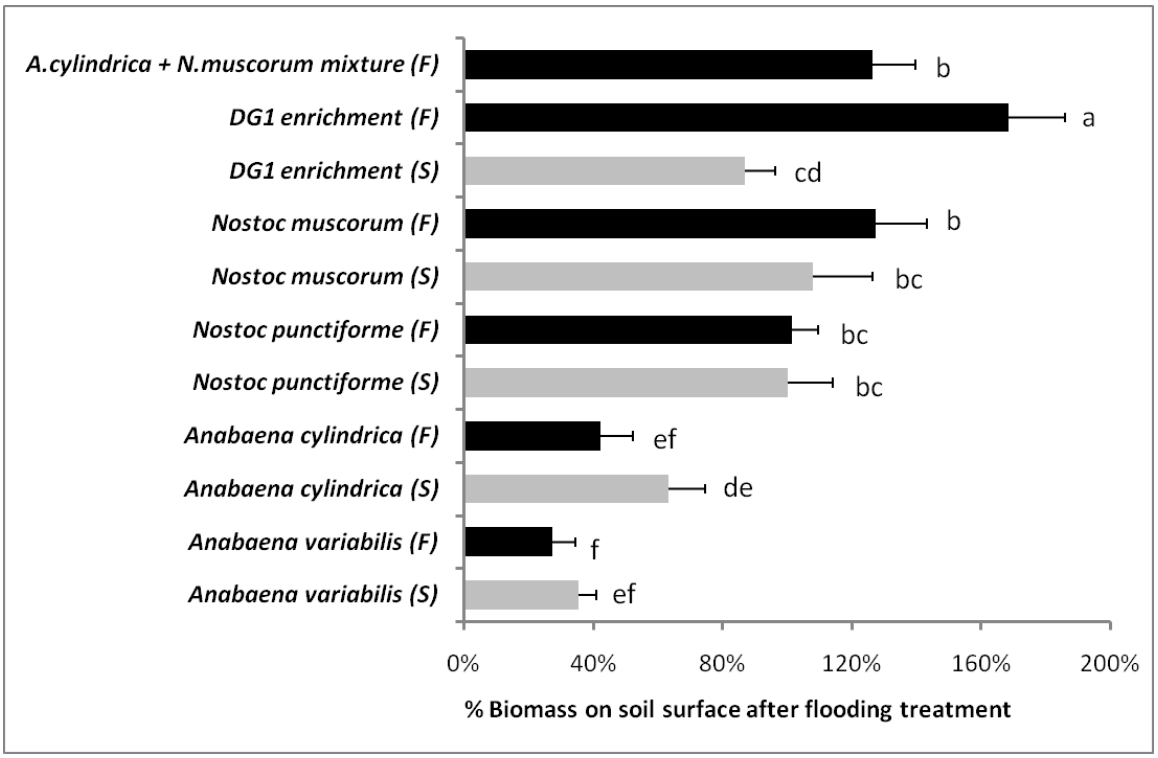

Table 2-1. BSC competence characteristics of cyanobacterial cultures and mixtures. 'Higher numbers of '+' symbols in the columns of means indicate higher statistical significance levels in Tukey's multiple comparisons of means. A '+' symbol in columns of coefficients of variation (CV) indicates that the CV is smaller than the average CV of that property determined for all cultures and mixtures.

	Biomass density on soil surface after 35-45 day cultivation		Recovery of freshly applied biomass after water flush treatment		BSC competence scores (N of '+')
	Mean	Coefficient of variation	Mean	Coefficient of variation	
Anabaena variabilis	+ +	+	-	-	3
Anabaena cylindrica	+	+	-	-	2
Nostoc punctiforme	-	-	+	+	2
Nostoc muscorum	-	-	+	+	2
DG1 enrichment	+	+	++	+	5
A. cylindrica + *N. muscorum* mixture	Not applicable		+	+	Not applicable

Table 2-2. Taxonomic summary of bins from Illumina Mi-Seq paired-end reads of metagenomics DNA of the DG1 enrichment. Bins represent results for all sequences combined from three replicate samples. The 'p_, c_, o_, f_ , g_, s_' stand for phylum, class, order, family, genus and species.

Bin ID	Length (bp)	Completeness	Bacterial taxonomy
1	7,852,759	100.00%	p_Cyanobacteria. c_Nostocophycidae. o_Nostocales. f_Nostocaceae.
2	6,657,127	92.50%	p_Proteobacteria. c_Alphaproteobacteria. o_Sphingomonadales.
3	6,623,980	96.30%	p_Proteobacteria. c_Alphaproteobacteria. o_Rhizobiales. f_Rhizobiaceae.
4	6,545,365	75.70%	p_Proteobacteria. c_Alphaproteobacteria. o_Rhizobiales. f_Methylobacteriaceae. g_Methylobacterium.
5	5,613,185	99.10%	p_Proteobacteria. c_Alphaproteobacteria. o_Rhodospirillales. f_Acetobacteraceae.
6	5,049,553	99.10%	p_Proteobacteria. c_Gammaproteobacteria. o_Xanthomonadales. f_Xanthomonadaceae. g_Stenotrophomonas. s_maltophilia.
7	296,899	10.30%	p_Bacteroidetes. c_Cytophagia. o_Cytophagales.

2.9 Supplementary materials

Figure S2-1. Three cyanobacterial enrichments (designated DG1, MB1, and PG1) obtained from local BSCs showing reliable transfers and robust growth on solid MBG11(N-) medium (first row) and consistent microscopic appearance under 400x magnification (second row).)

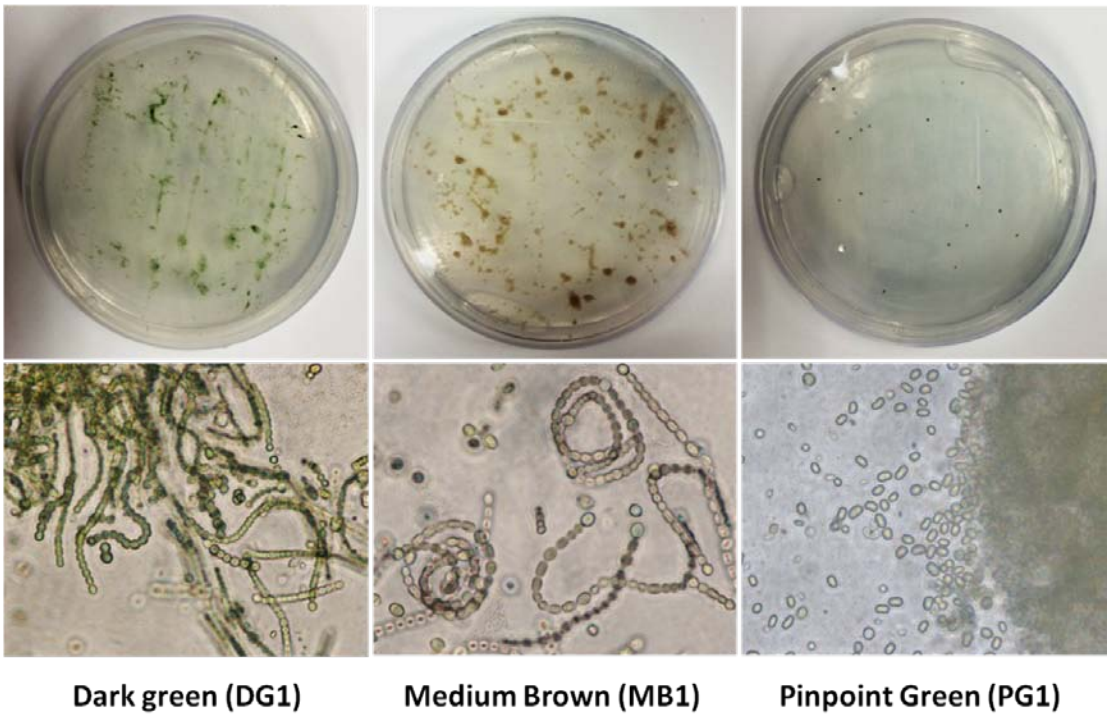

Figure S2-2. Cohesive BSCs formed by the DG1 enrichment after one month of growth on sandy soil. (A) Intact biocrusts could be lifted from the soil surfaces with a glass slide after addition of water to the microcosm. (B) Filamentous DG1 biocrust coatings of sand particles (brown areas) under 80x magnification. Two non-associated white quartz particles are included in the image for contrast. (C) Filamentous structure of DG1 crust under 400x magnification.

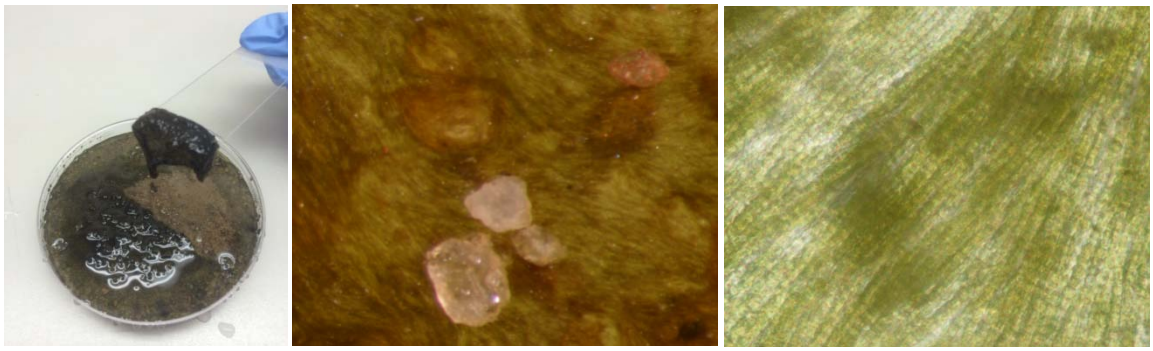

(A) (B) (C)

Figure S2-3. Standard curves showing relationships between biomass and chlorophyll a for four pure cyanobacterial cultures and the DG1 enrichment on soil surfaces. Equations of best fit lines and R-squares are listed for all linear regressions.

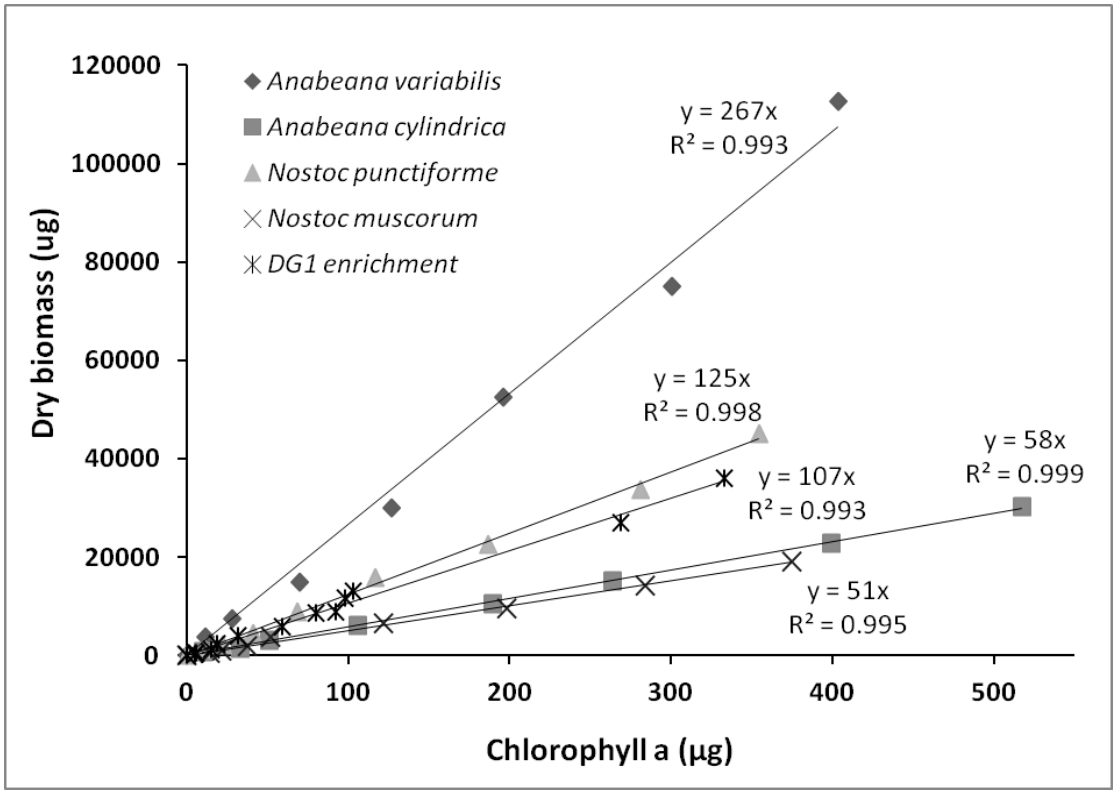

Figure S2-4. The phylogenetic tree of the cyanobacterial bin (marked as sampleCo.001) from the DG1 enrichment.

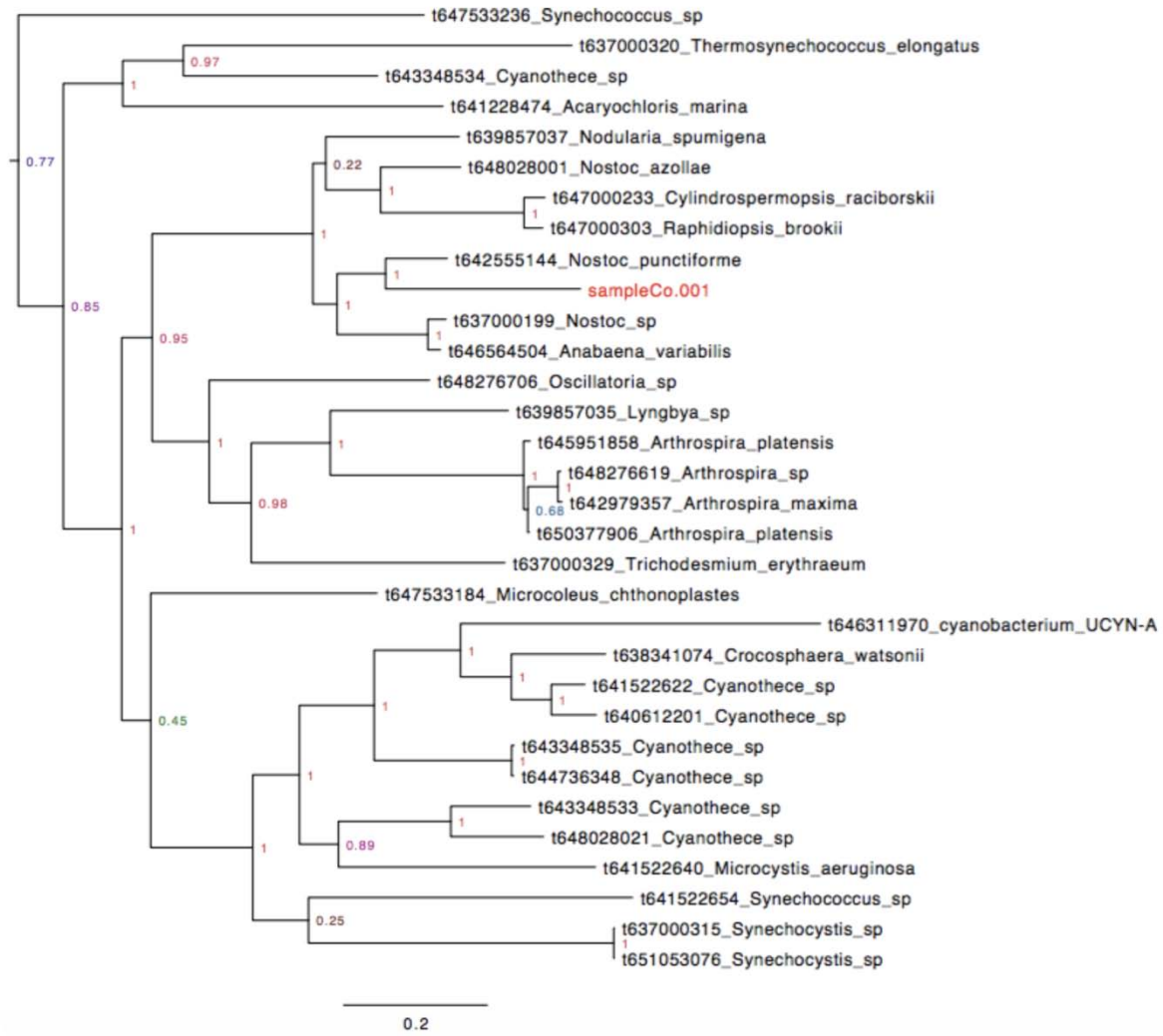

Table S2-1. Information on strains obtained from American Type Culture Collection (ATCC) and the Culture Collection of Algae at the University of Texas at Austin (UTEX). '+' indicates stable growth of cyanobacteria after ten serial transfers. '-' indicates unstable growth and/or strain crashes.

Cyanobacterial strains and enrichments	ID number	Source	Growth in MBG11(N-) medium	
			Solid surface	Liquid
Anabaena variabilis	29413	ATCC, Fresh water	+	+
Anabaena cylindrica	B1611†	UTEX, pond water	+	+
Anabaena verrucosa	B1619‡	UTEX, serpentine soils	-	-
Anabaena subcylindrica	B1617	UTEX, soil	-	-
Nostoc punctiforme	29133	ATCC, *Macrozamia sp.* root	+	+
Nostoc muscorum	1037	UTEX, arid soils	+	+
Nostoc commune	B1621	UTEX, soil	+	-
Nostoc parmeloides	B1627	UTEX, serpentine soils	-	-
DG1 enrichment	NA	Agricultural soil in central PA	+	+
GP1 enrichment	NA	Agricultural soil in central PA	+	-
MB1 enrichment	NA	Agricultural soil in central PA	+	-

†ID changed to 1611.

‡ No longer available in UTEX.

Table S2-2. Modified BG11(N-) medium (MBG11(N-)).

Compounds	Weight (g)	FW (g mol^{-1})	Final concentration in MNB medium (mmol L^{-1})
Major compounds	(100x) 0.1 L stock		
$Na_2S_2O_3$	1.480	158.11	0.936
$MgSO_4 \cdot 7H_2O$	0.750	246.47	0.304
K_2HPO_4	0.400	174.18	0.229
$CaCl_2 \cdot 2H_2O$	0.360	147.01	0.245
Na_2CO_3	0.200	105.99	0.189
$FeCl_3 \cdot 6H_2O$	0.051	270.3	0.019
$Na_2EDTA \cdot 2H_2O$	0.010	523.79	0.0019
Trace compounds	(1000x) 1 L stock		
H_3BO_3	2.860	61.83	0.0463
$MnCl_2 \cdot 4H_2O$	1.810	197.91	0.00915
$ZnSO_4 \cdot 7H_2O$	0.220	287.54	0.000765
$Na_2MoO_4 \cdot 2H_2O$	0.390	241.95	0.00161
$CuSO_4 \cdot 5H_2O$	0.079	249.68	0.00032
$CoSO_4 \cdot 4H_2O$	0.048	281.1	0.00017

Table S2-3. Properties of the sandy soil used in soil microcosms. Values for bulk density, ammonium-N, and nitrate-N are given as means ± standard deviations.

Soil properties		Sandy soil (94% sand, 4% clay, 2% silt)	
		Before autoclaving	After autoclaving
Soil pH		8.3	8.3
N%		0.02	0.02
C%		0.42	0.43
Bulk density (g cm^{-3})		1.524 ± 0.002	ND
Soil nutrient levels (ppm)	Ammonium-N	0.77 ± 0.06	1.33 ± 0.42
	Nitrate-N	6.78 ± 0.96	6.89 ± 0.25
	Phosphorus	23	20
	Potassium	55	48
	Magnesium	74	62
	Calcium	3173	2909

Chapter 3

Functional Properties of a Biofilm-Forming Cyanobacterial Enrichment Culture Grown with and without Nitrate

3.1 Introduction

Cyanobacteria (formerly blue-green algae) comprise a large phylum of oxygenic photosynthetic bacteria found in both aquatic and terrestrial ecosystems. Many cyanobacteria fix atmospheric N_2 with nitrogenase enzymes, which require near-absence of O_2 to function effectively. Because photosynthesis generates O_2, some filamentous cyanobacteria restrict N_2 fixation to specialized, thick-walled heterocysts that do not photosynthesize. The nitrogenase in heterocysts is thereby physically separated and protected from the O_2 produced by photosynthetic vegetative cells (Berman-Frank et al., 2007). Such morphological differentiation enables heterocystous cyanobacteria like *Anabaena*, *Nostoc*, *Aulosira* and *Tolypothrix spp.* to be used for supplying nitrogen (N) in rice cultivation (Mishra and Pabbi, 2004; Pereira et al., 2009; Prasanna and Nayak, 2007). The application of N_2-fixing cyanobacteria in rice paddy systems has been reported to contribute 25-50 kg N ha^{-1} cropping $season^{-1}$, which is equivalent to 30-50% of synthetic fertilizer N typically applied in rice production (Choudhury and Kennedy, 2004; Dhar et al., 2015; Hashem, 2001; Venkataraman, 1975

Cyanobacteria also are the main N_2-fixing organisms in cryptogamic covers worldwide, contributing an estimated 49 Tg N_2 $year^{-1}$, or 46% of all biological nitrogen fixation in natural ecosystems (Elbert et al., 2012). Despite their long-known ability to fix atmospheric N_2, the intentional use of cyanobacteria as N sources in temperate agriculture has gained little interest, most likely due to the ready availability of synthetic fertilizers (Reynaud and Metting, 1988). In agricultural systems, the N_2-fixing ability of naturally occurring cyanobacteria is likely suppressed by high levels of soil mineral N resulting from fertilizer use, as is the case for

biological N fixation by leguminous crops (McNeill and Unkovich, 2007). In studies of both laboratory cultures and natural biological soil crusts (BSCs), N_2 fixation by cyanobacteria was reduced and/or completely inhibited in the presence of environmental NH_4^+ and NO_3^- (Delwiche and Wijler, 1956; Klubek and Skujiņš, 1980; Sprőber et al., 2003).

After 15 years of observing surface growth of cyanobacterial BSCs on local agricultural soils, we isolated a robust, N_2-fixing cyanobacterial enrichment (designated DG1, for Dark Green 1) from soils collected from the Pennsylvania State University (Penn State) Agronomy Research Farm (GPS coordinates 40.72 -77.93) (Castillo and Bruns, 2001). The DG1 enrichment culture has shown consistently robust growth in N-free liquid media and forms stable BSCs on soil surfaces, suggesting that DG1 has high potential to be developed as a soil surface amendment for temperate agriculture. In considering use of DG1 as a soil amendment, however, it is important to recognize that some cyanobacteria produce cyanotoxins in the environment, particularly in eutrophic waters. Although toxin production associated with aquatic cyanobacterial blooms has been studied extensively (Bláha et al., 2009; Codd et al., 2005), toxicity of cyanobacteria growing on soil surfaces has not been documented. Furthermore, it is not clear how soil inorganic N concentrations might affect cyanotoxin production.

Several cyanotoxins have been detected in drinking water supplies, and the U.S. Environmental Protection Agency has recently published numerical safety thresholds for some of the most commonly detected toxins. These include two neurotoxins, anatoxin-a and saxitoxin; one hepatotoxin, microcystin; and one cytotoxin, cylindrospermopsin (Kasich et al., 2015). Although no safety standard exists for another neurotoxin, Beta-Methylamino-L-alanine (BMAA), this compound has been studied extensively because of its possible association with Parkinson's, Alzheimer's, and Amyotrophic Lateral Sclerosis (ALS) diseases (Holtcamp, 2012). Reports of toxins produced by harmful algal blooms in lakes and estuaries suggest that high levels of

available inorganic N favor growth of toxic over non-toxic cyanobacterial strains of *Microcystis spp*. (Davis et al., 2010; Vézie et al., 2002).

In this study, we assessed the effect of inorganic N concentrations on N_2 fixation by DG1. We also tested for the presence of toxins in DG1 biomass grown with and without nitrate N. For N_2 fixation measurements, we used the $^{15}N_2$ labeling technique (Bei et al., 2013; Montoya et al., 1996), because it is more sensitive and precise than the acetylene reduction assay (Belnap, 2002; Millineaux et al., 1981; Witty, 1979). We hypothesized that N_2 fixation by DG1 would decrease as environmental nitrate concentration increase. In addition, we evaluated DG1 cultures for the presence of detectable cyanotoxins after growth in media with or without nitrate-N.

3.2 Materials and methods

3.2.1 Cyanobacterial material

The cyanobacterial enrichment DG1 was obtained from a naturally formed BSC growing on Hagerstown silt loam, which is classified as a Typic Hapludalfs (Soil Survey Staff, 2010). This soil had been collected from field surfaces at the Penn State Agronomy Research Farm (GPS coordinates 40.72 -77.93) (Peng, Chapter 2).

3.2.2 Cultivation conditions

The most widely used medium for cultivating microalgae is known as BG11, which contains about 250 ppm nitrate-N (UTEX, 2016). A modified BG11 (N-) medium, MBG11(N-), was prepared according to UTEX directions, but with the following substitutions to eliminate sources of carbon (C) and N: no citric acid was added; $FeCl_3 \cdot 6H_2O$ was substituted for

ammonium Fe (III) citrate to achieve the same Fe concentration; and $CoSO_4 \cdot 4H_2O$ in trace mineral solution was substituted for $Co(NO_3)_2 \cdot 6H_2O$ to achieve the same Co concentration. To prepare culture media with different N levels, MBG11(N-) was combined with another medium containing $NaNO_3$ (MBG11) at different ratios (Table S3-1). In MBG11 medium, the $NaNO_3$ was substituted for $Na_2S_2O_3$. Four culture media with different N concentrations (0, 62, 124, and 274 ppm) were prepared by mixing BG11(N-) and MBG11 media based on the volume ratios shown in Table S3-1. The final culture media were adjusted to pH 7.1-7.3 with 2 M HCl and sterilized by autoclaving.

The DG1 enrichment was routinely maintained in MBG11(N-) at 22-23°C and 250 Lux by inoculating one-month-old, condensed cells (40-50 mg dry biomass L^{-1} of inoculum) to fresh medium. For the isotope labeling experiment, DG1 was cultured in 1-L baffled flasks with rotary shaking at 90 revolutions per minute (RPM), with each flask containing 200 ml media with 0, 62, 124, or 247 ppm nitrate-N. We selected these nitrate-N concentrations to assess their effect on N_2 fixation by DG1 because they represented observed variation in mineral N observed in field soils. At the Penn State Agronomy Research Farm, for example, soil nitrate-N concentrations in the upper 1-cm layers of multiple corn plots (under either no-till or conventional tillage) varied from 1.2 to 413 ppm N, with a mean of 90.7 ppm (Peng, Chapter 5).

Continuous fluorescent illumination ('natural light') was used for growing cyanobacterial cultures. To accommodate increasing cell density during growth, light intensities were increased from 180 Lux (day 0-13) to 210 Lux (day 14-20) to 250 Lux (day 21-25). To obtain cells for cyanotoxin testing, DG1 was inoculated into 500-ml Erlenmeyer flasks containing 90-ml amounts of media containing 0 or 124 ppm nitrate-N.

3.2.3 Biomass harvesting, preparation, and quantification

After being cultivated for 25 days in baffled flasks or 14 days in photo bioreactors, DG1 biomass was transferred to sterile conical tubes for gravitational settling for 30 minutes. After removing cleared supernatant from the tubes, each flask contained 12-15 ml concentrated cells having an average dry biomass density of 2.5 mg ml^{-1}. A 1.5-ml subsample of concentrated cells was used for biomass quantification (see below), while 10 ml of concentrated cells were pipetted into one petri dish (5-cm diameter) for subsequent placement in the growth chamber (described below). Petri dishes were wrapped carefully with Parafilm M® (Bemis Company, Neenah, WI) so that all plate edges were covered uniformly with one layer of film.

To quantify starting biomass densities, the 1.5-ml subsample of condensed culture was centrifuged at 9000 RPM for two minutes. Then, cells were washed with distilled water three times to remove inorganic salts. Each wash entailed resuspending the centrifuged cells in 1.5-ml distilled water, centrifuging again for two min, and then removing supernatant liquid. Finally, dry biomass densities of the cell condensates were determined gravimetrically after drying at 60℃.

3.2.4 Growth chamber design

A test chamber was built for $^{15}N_2$ isotope labeling based on Holst's method (Holst et al., 2009). We used a glass desiccator (21-L volume) as the growth chamber, which was connected to a gas gauge custom-calibrated to read between -0.1 - 0.6 bar (Swagelok, Pittsburgh, PA), a gas tight septum, and a vacuum pump through vacuum fittings (Swagelok Ultra-Torr, Pittsburgh, PA) (Figure 3-1and Figure S3-1). A LED light ring, constructed from “natural light” strips (HitLites, Baton Rouge, LA), was fitted around the exterior of the desiccator to produce a uniform light

intensity (210 Lux) following a 14/10 h light - dark cycle. The test chamber was confirmed to be gas-tight before each experiment by observing a constant reading (at -0.1 bar) on the gas gauge for a period of two hr after evacuating the desiccator. Headspace gas samples were collected through the septum using 140-ml syringes and 25-gauge needles with Luer-Lock fittings. These also were used to inject $^{15}N_2$ and O_2 into the growth chamber.

3.2.5 Estimating N_2 fixation rate through $^{15}N_2$ labeling

A complete randomized experiment was designed with four replicates of four liquid medium N concentrations (0, 62, 124, and 247 ppm nitrate-N) when culturing the DG1 enrichment in baffled flasks. To check for the potential of $^{15}N_2$ gas adsorption to biomass surfaces (de Jonge and Mittelmeijer-Hazeleger, 1996), four replicates of dead cell controls were also placed in the growth chamber for $^{15}N_2$ labeling. Dead cell controls were prepared by heating the fresh DG1 enrichment at 95ºC for an hour and then adding treatments, non-exposure controls of DG1 enrichment cell samples (four replicates x four medium N concentrations) were prepared for a separate incubation without $^{15}N_2$ under identical experimental conditions.

All treatment microcosms and dead cell controls were placed randomly in the growth chamber without overlap, which included sixteen petri dishes containing liquid suspensions of DG1 enrichment cultures and four petri dishes of dead cell controls. A total volume of 300 ml $^{15}N_2$ gas (chemical purity > 99.9%, isotopic enrichment > 98%, Cambridge Isotope Laboratories, Inc.) was injected into the growth chamber, which elevated the headspace Atom %^{15}N to 1.77%. The DG1 cell suspensions in petri dishes were incubated for seven days. Every other day, a 60-ml sample of headspace air was withdrawn from the test chamber and analyzed with an oxygen analyzer (Quantek Model 901). If the O_2% declined in the growth chamber, additional O_2 gas

(99.8% purity, Medipure) was injected so that the headspace O_2 concentration remained at atmospheric level.

Biomass and liquid medium from each petri dish were quantitatively transferred to centrifuge tubes after the incubation. The biomass in each tube was first concentrated by centrifuging at 6000 g for five minutes. After the removal of supernatant liquid, the condensed DG1 biomass (volume < 2 ml) was resuspended in 10 ml distilled water and centrifuged (6000 g, 5 min, and supernatant liquid removed) four times to remove dissolved nitrate-N from the samples. This washing procedure was confirmed to have no observable effect on cell integrity by microscopic examination. Condensed and washed biomass samples were transferred to 5-ml polystyrene grinding vials for drying in the dark at 60°C for seven days. Finally, the dry biomass samples were ground with polystyrene grinding balls (one ball in each vial) for 3 minutes using a SPEX Sample Prep 8000D Mixer/Mill.

3.2.6 Isotopic analysis and calculations

The $\delta^{15}N$, weight %N, and weight %C of all dried and ground DG1 biomass samples were analyzed by elemental analysis - isotope ratio mass spectrometry (EA-IRMS) at the Penn State Laboratory for Isotopes and Metals in the Environment (LIME). The ^{15}N atom % excess, biomass-based N_2 fixation rate, and amount of N_2-N fixed in each petri dish were calculated for each ^{15}N labeled sample to evaluate N_2 fixation by living DG1 biomass.

First, given that:

$$\delta^{15}\mathrm{N}\ (‰) = \left[\frac{(^{15}\mathrm{N}/^{14}\mathrm{N})_{\mathrm{sample}}}{(^{15}\mathrm{N}/^{14}\mathrm{N})_{\mathrm{atmosphere}}} - 1\right] \times 1000‰$$

where the $(^{15}\mathrm{N}/^{14}\mathrm{N})_{\mathrm{atmosphere}}$ is 0.003676 (Junk and Svec, 1958). The atom percentage of ^{15}N can be calculated as:

$$\text{Atom\%}^{15}\text{N} = \left[\frac{(10^{-3} \times \delta^{15}\text{N} + 1) \times (^{15}\text{N}/^{14}\text{N})_{\text{atmosphere}}}{1 + (10^{-3} \times \delta^{15}\text{N} + 1) \times (^{15}\text{N}/^{14}\text{N})_{\text{atmosphere}}}\right] \times 100\%$$

and ^{15}N atom % excess as:

$$^{15}\text{N atom \% excess} = (\text{Atom\%}^{15}\text{N})_{\text{T}} - \overline{(\text{Atom\%}^{15}\text{N})_{\text{C}}}$$

where $(\text{Atom\%}^{15}\text{N})_{\text{T}}$ is the ^{15}N atom % of samples that have been labeled with ^{15}N, and $\overline{(\text{Atom\%}^{15}\text{N})_{\text{C}}}$ is the mean ^{15}N atom % of the corresponding non-exposure control samples with the same medium N concentrations.

Second, the ^{15}N weight percentage of the total N was calculated as:

$$\text{Wt\%}^{15}\text{N} = \frac{\text{Atom\%}^{15}\text{N} \times 15}{\text{Atom\%}^{15}\text{N} \times 15 + (100\% - \text{Atom\%}^{15}\text{N}) \times 14} \times 100\%$$

Therefore, the weight of ^{15}N fixed per unit dry DG1 biomass was:

$$\text{Wt}^{15}\text{N (mg N} \cdot \text{mg}^{-1} \text{ dry biomass)} = 1 \times \text{Wt\%N} \times \left[(\text{Wt\%}^{15}\text{N})_{\text{T}} - \overline{(\text{Wt\%}^{15}\text{N})_{\text{C}}}\right]$$

where $(\text{Wt\%}^{15}\text{N})_{\text{T}}$ is the ^{15}N weight percentage of samples that have been labeled with ^{15}N, and $\overline{(\text{Wt\%}^{15}\text{N})_{\text{C}}}$ is the mean ^{15}N weight percentage of the corresponding non-exposure control samples in liquid medium with the same N concentration. Given that the atom percentage of ^{15}N in the headspace $[(\text{Atom\%}^{15}\text{N})_{\text{Headspace}}]$ of the test chamber was 1.77%, the weight of ^{14}N fixed per unit dry DG1 biomass was:

$$\text{Wt}^{14}\text{N (mg N} \cdot \text{mg}^{-1} \text{ dry biomass)} = \frac{\text{Wt}^{15}\text{N} \times \left[1 - (\text{Atom\%}^{15}\text{N})_{\text{Headspace}}\right] \times 14}{15 \times (\text{Atom\%}^{15}\text{N})_{\text{Headspace}}}$$

Then the biomass based N_2 fixation rate was estimated as:

$$N_2 \text{ fixation rate/biomass } (\mu\text{g N} \cdot \text{g}^{-1}\text{dry biomass} \cdot \text{day}^{-1}) = 10^6 \times \frac{(\text{Wt}^{15}\text{N} + \text{Wt}^{14}\text{N})}{\text{t}}$$

where t is the incubation time (seven days). Finally, total N_2 fixed in one petri dish was estimated as:

$$N_2 \text{ fixed amount } (\mu\text{g N} \cdot \text{petri dish}^{-1}) = 10^3 \times (\text{Wt}^{15}\text{N} + \text{Wt}^{14}\text{N}) \times \text{V} \times \text{BD}$$

where V is the loading volume (10 ml) and BD is the biomass density (mg dry biomass ml^{-1}) of the concentrated DG1 cell suspension.

3.2.7 Cyanotoxin testing

One-month-old DG1 cultures grown with or without nitrate-N (124 ppm) were pooled and mixed before transferring three 30-ml subsamples into appropriate containers. Subsamples were shipped to BSA Environmental Services, Inc. (Beachwood, OH) for testing saxitoxin, beta-methylamino-L-alanine (BMAA), anatoxin-a, microcystin, and cylindrospermopsin using ELISA kits (Abraxis, Warminster, PA). Meanwhile, three 15-ml subsamples from each pooled liquid sample were transferred to pre-weighed, 15-ml centrifuge tubes for quantification. The cyanobacterial biomass was harvested by centrifuging at 6000 g for five min and washing (four times) as described previously, and then weighed after being dried at 60℃.

3.2.8 Data analysis

All data were analyzed by SPSS 16.0 (Norusis, 2008) and shown as mean ± standard error. The results of the isotope labeling experiment were analyzed by one-way ANOVA and Tukey's multiple comparisons ($p < 0.05$), while the ^{15}N atom % excess of the dead cell controls were analyzed by a one-tailed t-test (H_0: $\mu = 0$, right tailed). The natural log data transformation was performed on response data in the ANOVA analysis if their residuals did not follow a normal distribution. The biomass densities from flasks with different N concentrations for toxin testing were compared by two-sample t tests (H_0: $\mu_1 = \mu_2$).

3.3 Results and discussion

3.3.1 Biofilm formation and cell C/N balance

All DG1 suspensions, except for dead cell controls, remained active during incubation in the growth chamber, as demonstrated by continuous O_2 consumption and formation of coherent biofilms in petri dish containers (Figure 3-2). The DG1 biomass exhibited no differences in cellular N content or C:N ratio after being cultured for 25 days and incubated in the growth chamber for seven days in liquid media of varied nitrate-N concentrations (0, 62, 124, or 247 ppm nitrate-N). These results indicated that DG1 effectively maintained cellular C and N balance. The coherent biofilms generated by DG1 suggested significant extracellular polymeric substances (EPS) production, although no visible differences in biofilm thickness or consistency could be observed.

3.3.2 N_2 fixation at different nitrate-N concentrations in growth media

Possible association of ^{15}N-label with biomass during incubation was assessed by measuring the ^{15}N atom % excess of dead cell controls. Because this value was not larger than zero ($p = 0.995$), we concluded there was no significant association of ^{15}N on cell surfaces. Enriched ^{15}N was found in all biomass samples, indicating that DG1 was actively fixing N_2 from the headspace atmosphere. As shown in Table 3-1, N_2 fixation by DG1 was expressed as ^{15}N atom % excess or as N_2 fixation rate ($\mu g\ N\ g^{-1}$ dry biomass day^{-1}). The N_2 fixation by DG1 in N-free medium was significantly higher ($p < 0.0001$) than that of DG1 at all three levels of nitrate-N. The mean ^{15}N atom % excess of labeled DG1 biomass grown in N-free medium was 0.0143%, which was 4.9, 3.9 and 3.8 times higher than means observed in media with 62, 124, and 247 ppm nitrate-N, respectively. The mean N_2 fixation rate of DG1 in N-free medium was

101.3 μg N g^{-1} dry biomass day^{-1}, which was correspondingly 5.4, 4.0, and 3.8 times greater, respectively, than rates in the presence of increasingly higher N.

In addition to the large difference in overall means for N_2 fixation by DG1 in N-free and N-supplemented media, N_2 fixation by DG1 in medium with 247 ppm N (26.6 μg N g^{-1} dry biomass day^{-1}) was significantly higher than N_2 fixation at 62 ppm N (18.9 μg N g^{-1} dry biomass day^{-1}) (Table 3-1). One possible explanation for this observation was that the cyanobacteria maintained consistent C:N ratios in their biomass by modulating the production of EPS. On one hand, previously generated EPS could serve as a C source for fixed N assimilation when environmental N is abundant. On the other hand, EPS could serve as a sink of fixed C when N is limited (Liang et al., 2014; Mager and Thomas, 2011; Otero and Vincenzini, 2003). No significant difference was observed in ^{15}N atom % excess among DG1 samples incubated with 62, 124, or 247 ppm nitrate-N (Table 3-1). Therefore, the difference in biomass-based N_2 fixation rates by DG1 at 62 and 247 ppm nitrate-N could be attributable to less EPS production as the nitrate-N increased, thus resulting in less dry biomass per cell.

The N_2 fixation rates by the DG1 enrichment in our study were comparable to rates reported for cyanobacterial biomass in previous ^{15}N labeling studies performed under moist conditions. For example, the mean N_2 fixation rate of DG1 in N-free medium, expressed as 4.22 mg N kg^{-1} dry biomass h^{-1}, was similar to a rate of 6.05 mg N kg^{-1} dry biomass h^{-1} reported for naturally occurring cyanobacterial BSCs (Holst et al., 2009). In another study using 70-d pot incubation of rice paddy soil containing 1.5 g N kg^{-1}, an estimated 0.0235 μg N cm^{-2} soil surface day^{-1} was fixed by indigenous cyanobacteria applied to soil in unplanted pots (Bei et al., 2013). In our experiment, the N_2 fixation rate of DG1 ranged from 0.0225-0.0347 μg N cm^{-2} day^{-1} when nitrate-N present was in the medium. When the N_2 fixation rate was determined on the basis of cell C, the rate showed a decrease from 209.6 μg N mg^{-1} C day^{-1} (at 0 ppm N) to 40.6 μg N mg^{-1} C day^{-1} (at 62 ppm N). A similar decrease in N_2 fixation rate from 110 to 25 μg N mg^{-1} C day^{-1}

was observed by Spröber et al. with the cyanobacterium *Cylindrospermopsis raciborskii* when they replaced N-free liquid culture medium with one containing 0.3 ppm nitrate-N in a continuous culture reactor (Sprőber et al., 2003).

Spröber and coworkers also found that N_2 fixation of *C. raciborskii* ceased at ammonium-N concentrations above 0.3 ppm (testing up to 3 ppm ammonium-N). In our experiment, DG1 was pre-cultured in N-containing media for 25 days, so that the lower ^{15}N atom % excess observed in N-grown biomass could not have been due to cessation of N_2 fixation upon addition of mineral N. Therefore, we concluded that DG1 continued to fix atmospheric N_2, but at lower rates in the presence of available inorganic N. In both studies, there was no relationship between medium N concentration and cyanobacterial N_2 fixation. Instead, availability of mineral N appeared to function as a switch to either decrease or stop N_2 fixation. The present study demonstrates that DG1 application in the field could result in its fixing N_2 under varied environmental N conditions.

3.3.3 Potential N input in agriculture

Widely varying ranges for N_2 fixation rates by cyanobacteria in agroecosystems have been reported. Based on the Acetylene Reduction Assay (ARA), estimates for cyanobacterial N_2 fixation in rice fields have varied from a few to 80 kg N ha^{-1} $crop^{-1}$ with a mean of 27 kg ha^{-1} (Roger and Ladha, 1992). For wheat crops, cyanobacteria have been estimated to fix 13-28 kg N ha^{-1} crop $season^{-1}$ (Witty et al., 1979). Compared to $^{15}N_2$ labeling, the ARA method of measuring N_2 fixation involves greater uncertainty due to reported differences in the conversion ratio (moles of C_2H_2 reduced per mole of N_2 fixed). In a review of 39 studies, these ratios ranged from 3.2-9.3, with an average ratio of 4.7 (Montoya et al., 1996). Assuming a typical growing season of 160 days for cyanobacteria in agriculture field (Peng, Chapter 5), DG1 was estimated to fix 0.36-2.2

kg N ha^{-1} $crop^{-1}$, which was considerably lower than values reported in previous field studies. DG1 biomass was incubated in liquid medium during exposure to $^{15}N_2$. Because such aqueous conditions could have constrained gas exchange in this experiment, DG1 may have exhibited greater N_2 fixation rates if it had been growing on soil surfaces.

We propose to apply DG1 as a means to promote BSC formation on agricultural soils. In addition to fixing atmospheric N_2, BSCs have been reported to reduce N losses from soil by assimilating and immobilizing inorganic N, thereby making it less prone to leaching and denitrification (Castillo-Monroy et al., 2010; Delgado-Baquerizo et al., 2010; Delgado-Baquerizo et al., 2013). The N assimilated by BSCs is stored for subsequent remineralization, which extends the period during which inorganic N can be taken up by crops. The observed rapid growth of naturally occurring BSCs in the field after spring fertilization (Peng, Chapter 5) also supported their role in assimilating N. Therefore, the persistence of DG1 in BSCs following soil application could serve multiple N functions and account for greater net soil N delivery to crops beyond our study's measurements of $^{15}N_2$ fixation.

Besides soil N concentration, several other factors reportedly influence N_2 fixation by cyanobacteria in arid and semiarid regions, including soil C content, moisture, temperature, pH, and light intensities (Belnap and Lange, 2001). In our study of N_2 fixation potential of DG1, we focused on its ability to fix N_2 under varied inorganic N concentrations, because moisture, temperature, and C content in agroecosystems are more favorable for BSC growth than in arid and semi-arid ecosystems. More field studies will be needed for fuller understanding of N contributions by DG1 in different agricultural systems.

3.3.4 Cyanotoxin test results

After one month cultivation, no significant difference was found in DG1 biomass densities grown in liquid media containing 0 and 124 ppm N (p-value = 0.426), At a culture density of 0.272 mg dry biomass ml^{-1}, none of the toxins (anatoxin-a, microcystin, saxitoxin, cylindrospermopsin and BMAA) were detected at their respective sensitivity limits (Table 3-2). As a rule, detection limits for toxins are lower than the lowest existing drinking water safety levels, except that there is currently no guidance for BMAA. The negative results we observed do not completely exclude the possibilities that DG1 may produce even lower amounts of the tested cyanotoxins or that DG1 produces other toxins yet to be identified.

Besides environmental N, other factors may also influence toxin production. Among these are phosphorus concentration, light intensity, and temperature (Chorus and Bartram, 1999; Kaebernick and Neilan, 2001; Vézie et al., 2002; Watanabe and Oishi, 1985). In most studies, toxin production is enhanced under conditions that favor rapid growth. Because the DG1 enrichment comprises a mixture of cyanobacterial strains and other bacteria (Peng, Chapter 2), individual populations could respond differently to environmental conditions. While it is possible that DG1 does not produce these toxins, the potential for toxin production by inoculated or natural BSCs growing on humid, temperate soils warrants further study.

3.4 Conclusions

This study assessed N_2 fixation and toxin production by a novel cyanobacterial enrichment DG1 that represents a potential agricultural soil amendment. Our findings support our hypothesis that N_2 fixation by DG1 would decrease as environmental nitrate concentration increased. We observed that DG1 fixed $^{15}N_2$ in the presence of 0, 64, 124, or 245 ppm nitrate-N,

but that the N_2 fixation rate was significantly higher in N-free than in any of the N-supplemented media. In addition, we determined that no cyanotoxins were detected in DG1 liquid cultures grown with either 0 or 124 ppm nitrate-N at the sensitivity levels of test assays. The results indicated that DG1 has good potential to be used as an agricultural soil amendment. However, additional research is needed to evaluate N contributions and toxin production by DG1 under the varied soil and weather conditions occurring at field scales.

3.5 Acknowledgement

We thank Dr. Todd Sowers, Director of the Laboratory for Isotopes and Metals in the Environment at Penn State, for his helpful advice on constructing the $^{15}N_2$ labeling growth chamber. Funding for this research was provided by a Research Applications for Innovation grant from the Penn State University College of Agricultural Sciences.

3.6 References

Bei, Q., Liu, G., Tang, H., Cadisch, G., Rasche, F., Xie, Z., 2013. Heterotrophic and phototrophic $^{15}N_2$ fixation and distribution of fixed ^{15}N in a flooded rice–soil system. Soil Biology and Biochemistry 59, 25-31.

Belnap, J., 2002. Nitrogen fixation in biological soil crusts from southeast Utah, USA. Biology and Fertility of Soils 35, 128-135.

Belnap, J., Lange, O., 2001. Biological soil crusts: structure, function and management. Springer, New York.

Berman-Frank, I., Quigg, A., Finkel, Z.V., Irwin, A.J., Haramaty, L., 2007. Nitrogen-fixation strategies and Fe requirements in cyanobacteria. Limnology and Oceanography 52, 2260-2269.

Bláha, L., Babica, P., Maršálek, B., 2009. Toxins produced in cyanobacterial water blooms-toxicity and risks. Interdisciplinary toxicology 2, 36-41.

Castillo, H., Bruns, M.A., 2001. Cyanobacterial diversity in agricultural soils, Ninth International Symposium in Microbial Ecology, Amsterdam, The Netherlands.

Castillo-Monroy, A.P., Maestre, F.T., Delgado-Baquerizo, M., Gallardo, A., 2010. Biological soil crusts modulate nitrogen availability in semi-arid ecosystems: insights from a Mediterranean grassland. Plant and Soil 333, 21-34.

Chorus, I., Bartram, J., 1999. Toxic cyanobacteria in water: A guide to their public health consequences, monitoring and management. Spon Press, London and New York.

Choudhury, A.T.M.A., Kennedy, I.R., 2004. Prospects and potentials for systems of biological nitrogen fixation in sustainable rice production. Biology and Fertility of Soils 39, 219-227.

Codd, G.A., Morrison, L.F., Metcalf, J.S., 2005. Cyanobacterial toxins: risk management for health protection. Toxicology and applied pharmacology 203, 264-272.

Davis, T.W., Harke, M.J., Marcoval, M., Goleski, J., Orano-Dawson, C., Berry, D.L., Gobler, C.J., 2010. Effects of nitrogenous compounds and phosphorus on the growth of toxic and non-toxic strains of *Microcystis* during cyanobacterial blooms. Aquatic Microbial Ecology 61, 149.

De Jonge, H., Mittelmeijer-Hazeleger, M.C. 1996. Adsorption of CO_2 and N_2 on soil organic matter: nature of porosity, surface area, and diffusion mechanisms. Environmental Science & Technology 30, 408-413.

Delgado-Baquerizo, M., Castillo-Monroy, A.P., Maestre, F.T., Gallardo, A., 2010. Plants and biological soil crusts modulate the dominance of N forms in a semi-arid grassland. Soil Biology and Biochemistry 42, 376-378.

Delgado-Baquerizo, M., Maestre, F.T., Gallardo, A., 2013. Biological soil crusts increase the resistance of soil nitrogen dynamics to changes in temperatures in a semi-arid ecosystem. Plant and Soil 366, 35-47.

Delwiche, C., Wijler, J., 1956. Non-symbiotic nitrogen fixation in soil. Plant and Soil 7, 113-129.

Dhar, D.W., Prasanna, R., Pabbi, S., Vishwakarma, R., 2015. Significance of Cyanobacteria as Inoculants in Agriculture, Algal Biorefinery: An Integrated Approach. Springer, pp. 339-374.

Elbert, W., Weber, B., Burrows, S., Steinkamp, J., Budel, B., Andreae, M.O., Poschl, U., 2012. Contribution of cryptogamic covers to the global cycles of carbon and nitrogen. Nature Geoscience 5, 459-462.

Hashem, M.A., 2001. Problems and prospects of cyanobacterial biofertilizer for rice cultivation. Functional Plant Biology 28, 881-888.

Holst, J., Butterbach-Bahl, K., Liu, C., Zheng, X., Kaiser, A.J., Schnitzler, J.-P., Zechmeister-Boltenstern, S., Brüggemann, N., 2009. Dinitrogen fixation by biological soil crusts in an Inner Mongolian steppe. Biology and Fertility of Soils 45, 679-690.

Holtcamp, W., 2012. The Emerging Science of BMAA: Do Cyanobacteria Contribute to Neurodegenerative Disease? Environmental Health Perspectives 120, 110-116.

Junk, G., Svec, H.J., 1958. The absolute abundance of the nitrogen isotopes in the atmosphere and compressed gas from various sources. Geochimica et Cosmochimica Acta 14, 234-243.

Kaebernick, M., Neilan, B.A., 2001. Ecological and molecular investigations of cyanotoxin production. FEMS Microbiology Ecology 35, 1-9.

Kasich, J.R., Taylor, G.M., Butler, G.W., 2015. Public Water System Harmful Algal Bloom Response Strategy. Ohio Environmental Protection Agency.

Klubek, B., Skujiņš, J., 1980. Heterotrophic N_2-fixation in arid soil crusts. Soil Biology and Biochemistry 12, 229-236.

Liang, B., Wu, T.-D., Sun, H.-J., Vali, H., Guerquin-Kern, J.-L., Wang, C.-H., Bosak, T., 2014. Cyanophycin mediates the accumulation and storage of fixed carbon in non-heterocystous filamentous cyanobacteria from coniform mats. PloS one 9, e88142.

Mager, D., Thomas, A., 2011. Extracellular polysaccharides from cyanobacterial soil crusts: a review of their role in dryland soil processes. Journal of Arid Environments 75, 91-97.

McNeill, A., Unkovich, M., 2007. The nitrogen cycle in terrestrial ecosystems, Nutrient cycling in terrestrial ecosystems. Springer, pp. 37-64.

Millineaux, P.M., Gallon, J.R., Chaplin, A.E., 1981. Acetylene reduction (nitrogen fixation) by cyanobacteria grown under alternating light-dark cycles. FEMS Microbiology Letters 10, 245-247.

Mishra, U., Pabbi, S., 2004. Cyanobacteria: a potential biofertilizer for rice. Resonance 9, 6-10.

Montoya, J.P., Voss, M., Kahler, P., Capone, D.G., 1996. A Simple, High-Precision, High-Sensitivity Tracer Assay for N (inf2) Fixation. Applied and environmental microbiology 62, 986-993.

Norusis, M., 2008. SPSS 16.0 statistical procedures companion. Prentice Hall Press, Upper Saddle River.

Otero, A., Vincenzini, M., 2003. Extracellular polysaccharide synthesis by *Nostoc* strains as affected by N source and light intensity. Journal of Biotechnology 102, 143-152.

Pereira, I., Ortega, R., Barrientos, L., Moya, M., Reyes, G., Kramm, V., 2009. Development of a biofertilizer based on filamentous nitrogen-fixing cyanobacteria for rice crops in Chile. Journal of Applied Phycology 21, 135-144.

Prasanna, R., Nayak, S., 2007. Influence of diverse rice soil ecologies on cyanobacterial diversity and abundance. Wetlands Ecology and Management 15, 127-134.

Reynaud, P.A., Metting, B., 1988. Colonization potential of cyanobacteria on temperate irrigated soils in Washington State, USA. Biological Agriculture & Horticulture 5, 197-208.

Roger, P.A., Ladha, J.K., 1992. Biological N_2 Fixation in wetland rice fields: Estimation and contribution to nitrogen balance. Plant and Soil 141, 41-55.

Soil Survey Staff, 2010. Keys to soil taxonomy, 11th ed. USDA-Natural Resources Conservation Service, Washington, DC.

Sprőber, P., Shafik, H.M., Présing, M., Kovács, A.W., Herodek, S., 2003. Nitrogen uptake and fixation in the cyanobacterium *Cylindrospermopsis raciborskii* under different nitrogen conditions. Hydrobiologia 506, 169-174.

Venkataraman, G.S., 1975. The role of cyanobacteria in tropical rice cultivation, in: Stewart, W.D.P. (Ed.), Nitrogen fixation by free living microorganisms. Cambridge University Press, Cambridge, pp. 207-218.

Vézie, C., Rapala, J., Vaitomaa, J., Seitsonen, J., Sivonen, K., 2002. Effect of nitrogen and phosphorus on growth of toxic and nontoxic Microcystis strains and on intracellular microcystin concentrations. Microb Ecol 43, 443-454.

Watanabe, M.F., Oishi, S., 1985. Effects of environmental factors on toxicity of a cyanobacterium (*Microcystis aeruginosa*) under culture conditions. Applied and environmental microbiology 49, 1342-1344.

Witty, J.F., 1979. Algal nitrogen fixation on temperate arable fields. Plant and Soil 52, 165-183.

Witty, J.F., Keay, P.J., Frogatt, P.J., Dart, P.J., 1979. Algal nitrogen fixation on temperate arable fields. Plant and Soil 52, 151-164.

3.7 Figures and tables

Figure 3-1. Diagram of the growth chamber used for $^{15}N_2$ labeling.

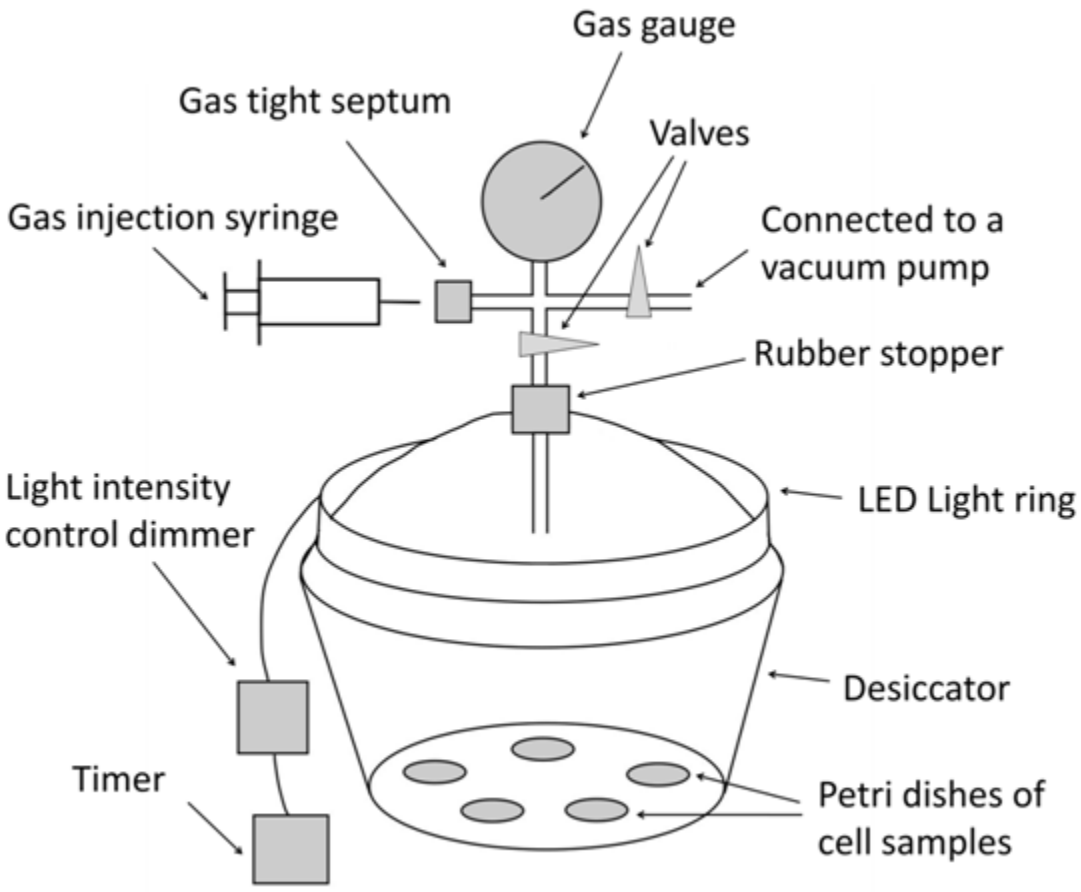

Figure 3-2. Photo of a typical biofilm formed by the DG1 enrichment after incubation for seven days in the growth chamber. The petri dish was placed at an angle for photographing to show how the cohesive biofilm moved toward the lower left with the liquid medium.

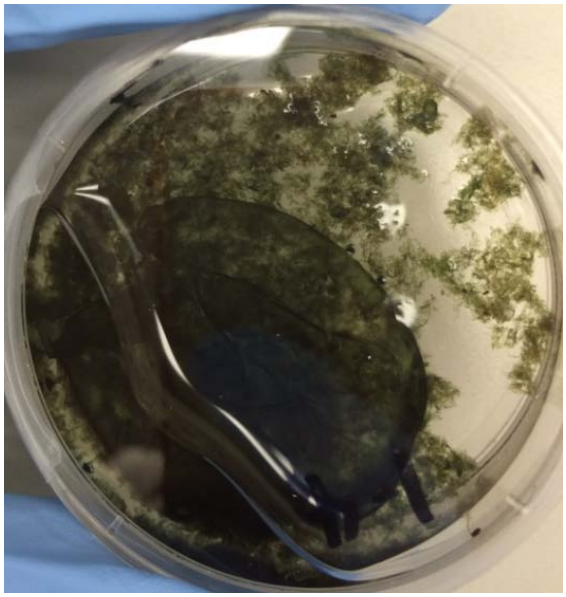

Table 3-1. N_2 fixation by DG1, which was grown in liquid media containing varied nitrate-N concentrations and incubated for seven days in the $^{15}N_2$ labeled chamber. Values are shown as mean ± standard error of the mean (n = 4). Different letters show results of Tukey's multiple comparison tests ($p < 0.05$).

Medium N Concentration (ppm)	Weight %N	C/N ratio	^{15}N atom % excess † ‡	N_2 fixation rate/ biomass † (μg N · g^{-1} dry biomass · day^{-1})
0	8.78 ± 0.19	5.51 ± 0.05	0.0143 ± 0.0014 a	101.3 ± 9.7 a
62	8.49 ± 0.19	5.48 ± 0.06	0.0029 ± 0.0000 b	18.9 ± 0.5 c
124	8.57 ± 0.19	5.52 ± 0.08	0.0037 ± 0.0003 b	25.6 ± 2.4 bc
247	8.55 ± 0.02	5.53 ± 0.05	0.0038 ± 0.0002 b	26.6 ± 1.4 b

† The natural log data transformation was applied before the ANOVA analysis.

‡ Values are relative to unexposed DG1 samples.

Table 3-2. Summary of cyanotoxin tests of liquid cultures of DG1. 'ND' indicates that toxin was not detected by the ELISA kits.

	Cyanotoxin concentration (µg L^{-1})				
	Anatoxin-a	Microcystin	Saxitoxin	Cylindrospermopsin	Beta-Methylamino-L-alanine (BMAA)
DG1 liquid culture (Medium N concentration = 0 ppm)	ND	ND	ND	ND	ND
DG1 liquid culture (Medium N concentration = 124 ppm)	ND	ND	ND	ND	ND
Detection limit (µg/L)	10	0.15	0.02	0.05	5
EPA drinking water guidance level (µg L^{-1}) †	< 20	< 0.3	< 0.2	< 0.7	Unknown

† The safety levels are for children under six and sensitive populations (Kasich et al., 2015).

3.8 Supplementary materials

Figure S3-1. Photo of the growth chamber used for $^{15}N_2$ labeling.

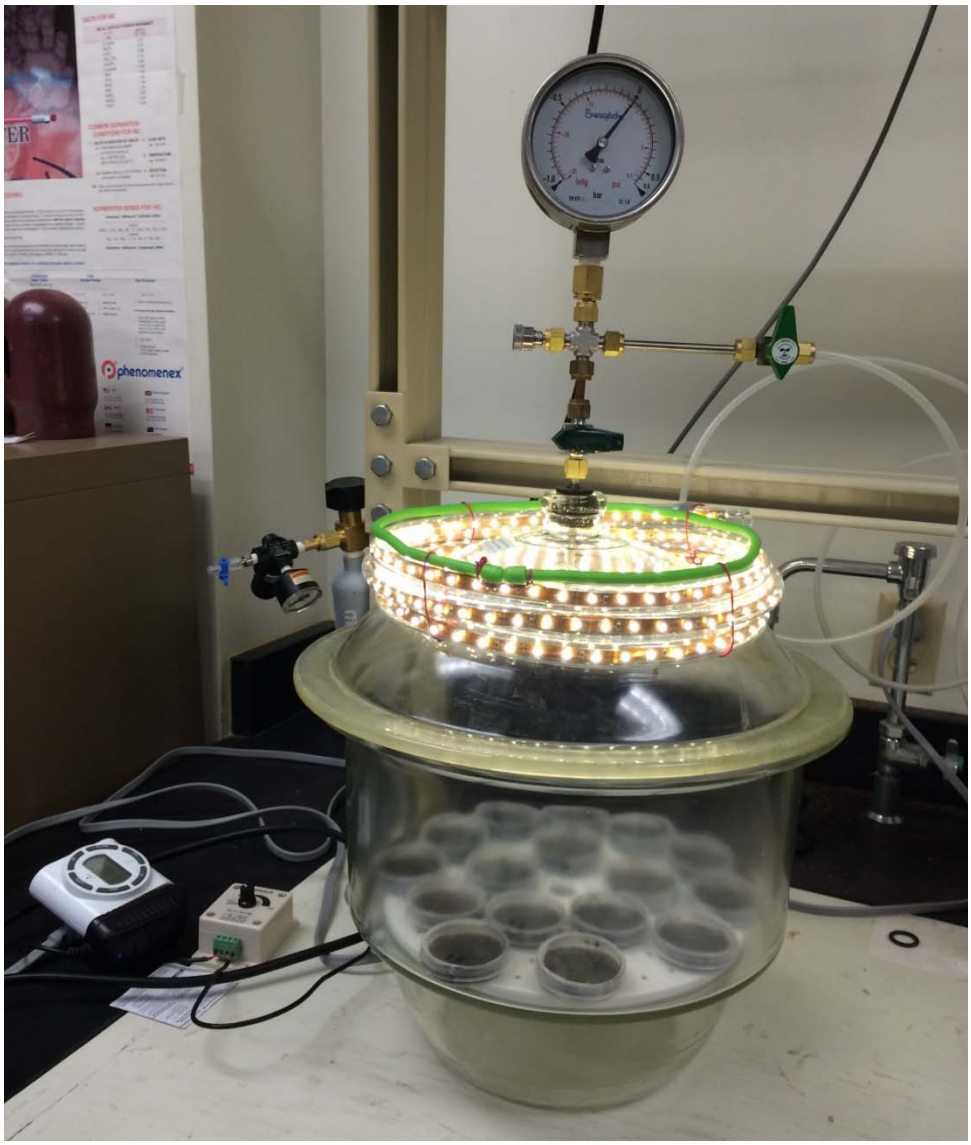

Table S3-1. (A) Modified BG11(N-) medium (MBG11(N-)) and modified BG11 medium (MBG11) recipes. (B) Volume mixing ratios of MBG11(N-) and MBG11 in preparing media with different nitrate-N concentrations.

(A)

Compounds	Weight (g)	FW(g mol^{-1})	Final concentration in MBG11(N-) medium (mmol L^{-1})
Major components of (MBG11(N-))	(100x) 0.1 L stock		
$Na_2S_2O_3$	1.480	158.11	0.936
$MgSO_4 \cdot 7H_2O$	0.750	246.47	0.304
K_2HPO_4	0.400	174.18	0.229
$CaCl_2 \cdot 2H_2O$	0.360	147.01	0.245
Na_2CO_3	0.200	105.99	0.189
$FeCl_3 \cdot 6H_2O$	0.051	270.3	0.019
$Na_2EDTA \cdot 2H_2O$	0.010	523.79	0.0019
Major compounds (MBG11)	(100x) 0.1 L stock		
$NaNO_3$	15.000	84.99	17.6
$MgSO_4 \cdot 7H_2O$	0.750	246.47	0.304
K_2HPO_4	0.400	174.18	0.229
$CaCl_2 \cdot 2H_2O$	0.360	147.01	0.245
Na_2CO_3	0.200	105.99	0.189
$FeCl_3 \cdot 6H_2O$	0.051	270.3	0.019
$Na_2EDTA \cdot 2H_2O$	0.010	523.79	0.0019
Trace compounds	(1000x) 1 L stock		
H_3BO_3	2.860	61.83	0.0463
$MnCl_2 \cdot 4H_2O$	1.810	197.91	0.00915
$ZnSO_4 \cdot 7H_2O$	0.220	287.54	0.000765
$Na_2MoO_4 \cdot 2H_2O$	0.390	241.95	0.00161
$CuSO_4 \cdot 5H_2O$	0.079	249.68	0.00032
$CoSO_4 \cdot 4H_2O$	0.048	281.1	0.00017

Table S3-1. (Continued)

(B)

Medium N content (ppm)	Mix ratio of volume	
	MBG11(N-)	MBG11
0	1	0
62	1	3
124	1	1
247	0	1

Chapter 4

Effects of Cyanobacterial Inoculum Size and Biocrust Establishment Time on Nitrate Leaching from Arable Soils under Simulated Rainfall

4.1 Introduction

Cyanobacteria have been studied extensively as photosynthetic members of biological soil crusts (BSCs), which are communities of prokaryotic and eukaryotic microorganisms that become established on soil surfaces (Belnap and Lange, 2001). As the main N_2-fixing components of BSCs, cyanobacteria act as pioneer colonizers during BSC establishment and succession (Langhans et al., 2009). BSCs have been studied mostly in arid and semi-arid ecosystems because of their importance in contributing fixed carbon (C) and nitrogen (N) to these nutrient-poor systems and producing extracellular polymeric substances that enhance soil stability (Belnap, 2006; Strauss et al., 2012).

In addition to fixing atmospheric N_2, BSCs in arid and semiarid regions have been shown to influence soil N cycling by increasing N retention and dampening fluctuations in nutrient concentrations (Castillo-Monroy et al., 2010; Delgado-Baquerizo et al., 2013). Naturally occurring BSCs can modulate soil NO_3^- and NH_4^+ availability by immobilizing soil mineral N and releasing it gradually for subsequent plant uptake (Hawkes, 2003). Some cyanobacteria in aquatic and wastewater systems have also shown high N uptake potential, such as *Cylindrospermopsis raciborskii* (Sprőber et al., 2003) and *Synechococcus elongatus* (Aguilar-May and del Pilar Sánchez-Saavedra, 2009). Despite these wide-ranging observations, cyanobacterial N immobilization in agricultural ecosystems of temperate regions has received little attention.

On a global level, agricultural crops take up only 50% or less of applied fertilizer N (Chien et al., 2009; Galloway et al., 2008). Low N use efficiency results in large N losses due to

runoff and leaching, off-site N pollution, and eutrophication (Schindler and Hecky, 2009). The present investigation of the potential for BSCs to mitigate N losses from agricultural soils is based on 15 years of observations of BSCs in diverse crop fields at the Pennsylvania State University Agronomy Research Farm (Castillo and Bruns, 2001). To investigate cyanobacteria from these agroecosystems more fully, we cultured and selected a robust cyanobacterial enrichment (named 'DG1') from the naturally formed BSCs. Our previous study indicated that the DG1 enrichment could be applied as a surface soil amendment to facilitate the formation of BSCs on agricultural soils. Although cyanobacteria have been used as biofertilizers in rice paddy cultivation (Mishra and Pabbi, 2004; Sinha and Häder, 1996; Vaishampayan et al., 2001), they have been rarely studied in temperate agricultural systems growing row crops, forages, or small grains. Despite the global importance of natural C and N fixation by cryptogamic crusts worldwide (Elbert et al., 2012), very little literature exists on cyanobacterial crusts or BSCs on agricultural soil surfaces (Pankratova, 2006).

Unlike the nutrient-limited soils in most arid and semi-arid ecosystems, agricultural soils typically receive large amounts of synthetic N fertilizers, and soil mineral N content can vary dramatically during crop growth. It has been shown that cyanobacteria grown in liquid cultures exhibit distinct growth responses to different N sources and concentrations (Costa et al., 2001), and that high mineral N content can suppress cyanobacterial N_2 fixation (Sprőber et al., 2003). Due to higher soil N contents, BSCs in agroecosystems may therefore perform differently from commonly studied BSCs of arid and semi-arid areas. In a previous study, the DG1 enrichment grew well in liquid cultures with concentrations ranging from zero to 247 ppm nitrate-N (Peng, Chapter 3), indicating their potential to take up excessive mineral N and increase its retention time in agricultural soils.

Another difference between humid agricultural soils and those in arid/semi-arid areas is higher frequency and volume of precipitation, which is a major driver of N leaching from soils

(Lehmann and Schroth, 2003). Since most agricultural soil particles are negatively charged, NO_3^- is more susceptible to leaching than NH_4^+ and organic N species during water infiltration. As a major pathway of N loss from modern cropping systems, leaching is mainly determined by soil NO_3^- concentrations and by the characteristics of water flow (volume, residence time, path, etc.) as water moves through the soil (McNeill and Unkovich, 2007). As the result of EPS production (Mager and Thomas, 2011), cyanobacterial crusts also can increase soil aggregation, pore formation, and surface stability (Belnap, 2006). Our previous study demonstrated that DG1 formed coherent BSCs on soil (Peng, Chapter 2), thus the application of the DG1 enrichment may also improve N use efficiency by reducing N leaching.

In this study, we used soil microcosms and simulated rainfall to address the following four questions. (1) Does soil nitrate content result in different growth responses of DG1 after application to soil? (2) Do inoculum size and establishment time on soil affect the stability of cyanobacterial biomass exposed to rainfall? (3) Do inoculum size and establishment time influence soil N retention? (4) Are there interaction effects between soil nitrate content, inoculum size, and establishment time? Our objectives were to assess these practical considerations related to application and early growth of the DG1 enrichment on soil surfaces and DG1's potential for increasing N retention in agricultural soils.

4.2. Materials and methods

4.2.1. Cultivation, harvesting, and biomass quantification

The cyanobacterial enrichment DG1 had been obtained from naturally formed BSCs growing on Hagerstown silt loam soil. The DG1 enrichment was maintained and transferred monthly in modified BG11 medium (N-free, designated 'MBG11(N-)') (Peng, Chapter 2). To

produce sufficient biomass for our experiments, DG1 was cultured in 1.5-L photo bioreactors (description in Appendix A) containing 1.2 L of MBG11(N-) medium. After 14 days' growth, cyanobacterial biomass from each reactor was concentrated by gravitational settling, after which most of the cleared supernatant was removed.

The condensed biomass was pooled to obtain at least 200 ml concentrated DG1 cell suspension for each experimental block as described below. Half of the suspension was used for the growth experiments in section 4.2.2, which also served as no-rainfall positive controls in section 4.2.3. The other half was used for the treatments in the rainfall simulation experiments in section 4.2.3. For each batch of pooled biomass, four 1.5-ml subsamples were oven dried for gravimetric quantification of biomass prior to soil inoculation (Peng, Chapter 2).

4.2.2 Monitoring cyanobacterial growth on moist arable soils (no rainfall)

4.2.2.1 Preparation of soil microcosms

Artificial soil microcosms were prepared in small petri dishes (diameter = 8.5 cm) containing 15 cm^3 (bulk density = 1.04 g cm^{-2}) autoclaved soil. This soil, which was classified as Hagerstown silt loam (Typic Hapludalfs) (Soil Survey Staff, 2010), had been collected at the Pennsylvania State University Agronomy Research Farm (GPS coordinates 40.72 -77.93) from a mixture of Ap/B1 horizon soils (30-cm depth) in a location that had no history of N fertilization. The soil was well-mixed, air-dried and passed through a 2-mm sieve prior to autoclaving. Soil chemical analyses are reported in Table S4-1. To prepare soil microcosms with different nitrate-N concentrations, MBG11 (N-) liquid medium was mixed with varied volumes of modified BG11 medium (MBG11) to prepare culture media with nitrate-N concentrations of 0, 62, and 124 ppm

(Peng, Chapter 3). This range of N contents is typically observed in surface field soils at the Pennsylvania State University Agronomy Farm (Williams et al., 2011).

To inoculate the surfaces of soil microcosms, 1, 2 or 4 ml of the concentrated DG1 cell suspensions (average dry biomass density of 1.7 mg ml^{-1}) were further condensed to a volume of less than 0.5 ml by centrifuging at 6000 g for five minutes and removal of supernatant liquid. Biomass amounts of 1, 2 and 4 ml thus corresponded to initial inoculum densities of 0.88, 1.75 and 3.51 g dry biomass m^{-2} in soil microcosms. Then, the highly condensed cells were resuspended in 6 ml fresh liquid culture medium (nitrate-N concentrations of 0, 62 or 124 ppm N) and evenly pipetted onto soil surfaces. The edges of the petri dishes were sealed with Parafilm M® (Bemis Company, Neenah, WI) and incubated at 22-23 °C under continuous fluorescent illumination ('natural light') with an average light intensity of 250 Lux.

4.2.2.2 Experimental design and sample collection for growth experiments

A randomized complete block design (RCBD) was applied in growth experiments testing the effects of growth medium N concentration and inoculum amount. Each of three replicated blocks consisted of all combinations of the following two factors with three levels per factor. Factor one was the biomass amount added to soil surfaces (1, 2 or 4 ml of condensed DG1), while factor two was the culture medium N concentration in microcosms (0, 62 or 124 ppm). Combinations of the two factors were randomly applied to soil microcosms in each block.

A total of 27 soil microcosms were set up in every block using half of the concentrated DG1 suspensions, which contained three replicate microcosms for every factor level combination comprising three biomass amounts by three medium N concentrations. After inoculating DG1 onto soils on day 1, one replicate microcosm was randomly selected for sacrificial harvesting on day 2, day 4, and day 8 (collection of upper 3-mm soil for chlorophyll analysis). These harvesting

dates corresponded to one, three, and seven days of soil contact time for biofilm establishment following DG1 inoculation.

4.2.2.3 Chlorophyll analysis and growth evaluation

Chlorophylls in surface soil samples from each microcosm were extracted with a total 20 ml of 1:1 ratio DMSO: acetone solution based on Nayak's method (Nayak et al., 2004). Absorbances of cleared extracts were measured at 750, 663, 645, and 630 nm (A_{750}, A_{663}, A_{645}, and A_{630}). Replicates of negative control samples per block were included in chlorophyll extractions and measurements to adjust for soil background absorbances. These samples were collected from the upper 3-mm soils of microcosms that had not been inoculated with DG1, but incubated in the same way as inoculated microcosms.

Chlorophyll a concentration in each extract (Chl a) was calculated as (UNESCO, 1966):

$$\text{Chl a } (\mu\text{g ml}^{-1}) = 11.64 \times (A_{663} - A_{750}) - 2.16 \times (A_{645} - A_{750}) + 0.1 \times (A_{630} - A_{750})$$

The growth of DG1 during incubation from day 2 to day 8 was determined from the percentage increase in chlorophyll a content (% Chl a increase) and adjusted by subtracting absorbances of negative controls. The % Chl a increase was calculated as:

$$\%\ \text{Chl a increase} = \frac{(\text{Chl a})_{\text{day 8}} - (\text{Chl a})_{\text{day 2}}}{(\text{Chl a})_{\text{day 8}} - (\text{Chl a})_{\text{NC}}} \times 100\%$$

where $(\text{Chl a})_{\text{day 8}}$ and $(\text{Chl a})_{\text{day 2}}$ were chlorophyll a concentrations of the samples at day 8 and day 2, and $(\text{Chl a})_{\text{NC}}$ was the average chlorophyll a concentration of four negative control samples.

4.2.3 Evaluation of biomass recovery and soil nitrate-N retention after simulated rainfall

4.2.3.1 Rainfall simulator and calibration

We used a portable rainfall simulator meeting standard design specifications at the USDA Agricultural Research Service at Penn State University (Humphry et al., 2002). This simulator was designed to deliver a uniform rainfall volume over a 1-m^2 area at a distance of 3 m below the rain-producing nozzle. For the present study, the simulator was adjusted to deliver an average rainfall rate of 3.3 cm hr^{-1} over 30 min, representative of a typical natural precipitation event in central Pennsylvania.

Prior to each treatment block, the rainfall rate was calibrated by adjusting the water pressure at the rain-producing nozzle (Kibet et al., 2014). Rainfall rate was validated before every rainfall treatment by confirming that a 10-sec total water flow from the nozzle using a collection pipe was consistent over three trials (nozzle size = 24 wsq full jet 3/8 HH, precipitation intensity = 3.3 cm hr^{-1}, 10 second flow = 1140 ml). Water-collecting cylinders (10-cm height with the same 5-cm diameter as petri dish microcosms) were arranged in a three by six matrix (about 16 cm between columns and rows) to support the microcosms within the uniform rainfall area. The uniformity of rainfall was pre-tested and validated by measuring water volumes across a complete set of cylinders after a 30-minute rainfall event (CV < 5%).

4.2.3.2 Preparation of the sample collection device

For rainfall trials, soil microcosms were fixed onto the tops of collection cylinders as shown in Figure S4-1. To enable water infiltration and downward flow through the soils in the microcosms, the bottoms of the petri dishes were pre-perforated with five drainage holes (diameter = 5 mm) and covered with a piece of waterproof duct tape during incubation. Before

each rainfall treatment, the tape was removed from the petri dish bottom, and the microcosm was securely attached to the top of the cylinder with duct tape. In addition, as shown in Figure S4-1, a duct tape 'canopy' was placed above a small, circular opening near the top of the cylinder. The canopy prevented water from entering the opening, which was designed to help maintain atmospheric pressure in the cylinder during water collection. Immediately prior to rainfall application, the petri dish lids were removed from the microcosms.

4.2.3.3 Experimental design and sample collection for rainfall simulations

Three factors, each of which had three levels, were studied for their effect on biomass recovery and N retention after application of the DG1 enrichment to soils under simulated rainfall: establishment time after inoculation (1, 3 and 7 day); biomass amount inoculated on the soil surface (1, 2, and 4 ml of 1.7 mg dry biomass ml^{-1} cell condensates); and medium N concentration in soil microcosms (0, 62, and 124 ppm nitrate-N). We designed a split plot experiment containing three replicated blocks, using establishment time as the whole plot factor that divided each block into three subplots. All combinations of biomass amount and medium N content (three by three) were completely randomly arranged in each subplot (array of microcosms receiving simulated rainfall). Here we applied the earlier described soil microcosms for monitoring cyanobacterial growth as no-rainfall positive controls. In each block, triplicates of negative controls (microcosms with no inoculum) were also prepared with media having 0, 62, and 124 ppm nitrate-N, and they were incubated and sampled in the same manner as inoculated microcosms. Therefore, each block in the rainfall simulation experiment contained a total of 81 soil microcosms: three sets of nine microcosms (27 microcosms comprising two factors at three levels) for each establishment time (1, 3, and 7 days); 27 negative (non-inoculated) controls; and 27 positive (no-rainfall) controls.

Rainfall simulations were carried out three times in each block, with the three sub-plots comprising the three different biocrust establishment times. Besides the no-rain positive controls, sub-plot samples were selected randomly from one of the three microcosms (with the same biomass amount and medium N concentration) in each treatment, as well as three of the nine microcosms with the same medium N concentration in each set of negative controls with no biomass inoculated. Therefore, nine treatments and nine negative control microcosms were treated under each simulated rainfall event. The soil microcosms were allowed to stand for 1-2 hr following rainfall application until no free water above the soil surface could be observed and until no water drops formed at the bottom drainage holes within 20 sec. Surface soil samples (0-3 mm) in treatment microcosms were collected and analyzed as described earlier to quantify their chlorophyll a contents. Water that had flowed through the microcosms into collecting cylinders was transferred to sterile 50-ml centrifuge tubes for volumetric measurements. Nitrate N concentrations for each liquid sample were analyzed by the Agricultural Analytical Services Laboratory at the Pennsylvania State University.

4.2.3.4 Calculations

Three properties of each DG1 treatment were evaluated after rainfall events: the adjusted infiltrated water volume, DG1 biomass recovered on the soil surface, and N retained in soil microcosms. First, in order to minimize systematic bias, volume readings of infiltrated water were standardized between different blocks using the following equation:

$$adV_{ij} = \frac{V_{ij} \times \overline{V_{I\,(biomass=0)}}}{\overline{V_{(biomass=0)}}}$$

where adV_{ij} and V_{ij} are the adjusted and original infiltrated water volume of sample j in block i , while $\overline{V_{i\,(biomass=0)}}$ and $\overline{V_{(biomass=0)}}$ are the average water volumes of non-inoculated negative controls in block i and in all blocks.

Then, the percent biomass recovered of the DG1 enrichment (Biomass %) was estimated at:

$$\text{Biomass\%} = \frac{(\text{Chl a})}{(\text{Chl a})_{\text{no rain}}} \times 100\%$$

where (Chl a) and $(\text{Chl a})_{\text{no rain}}$ are the chlorophyll a contents in the treatment soil samples and its corresponding positive controls.

Finally, nitrate-N leached (mg N microcosm^{-1}) was estimated by multiplying the infiltrated water volume by its nitrate N concentration, assuming that the infiltrated water contained all leached soil nitrate. For each rainfall treatment sub-plot, a background nitrate N content in soil was calculated as the average N leached from negative controls containing N-free medium. N retained in soil microcosms ($N_{retained}$) was estimated at:

$$N_{retained}(\text{mg N microcosm}^{-1}) = N_{medium} + N_{background} - N_{leached}$$

while the percent N retained in microcosms (N%) was calculated as:

$$N\% = \frac{N_{retained}}{N_{medium} + N_{background}} \times 100\%$$

where $N_{leached}$, N_{medium}, and $N_{background}$ are nitrate N contents in the infiltrated water, the culture medium, and the soil background. Based on the medium preparation protocols, the nitrate-N contents in the microcosms with medium N concentrations at 62 and 124 ppm N were 0.37 and 0.74 mg N microcosm^{-1} respectively.

4.2.4 Data analysis

All data were analyzed by SPSS 16.0 (Norusis, 2008) and shown as mean ± standard error. General linear models (GLM) were used to analyze the results of soil microcosm experiments, in which replicate was a random factor and other factors were fixed. The models were simplified by pooling some non-significant interaction effects as error terms, including the two-way interactions of replicate × biomass amount and replicate × medium N concentration, as well as all three- and four-way interactions. ANOVA analysis and Tukey's multiple comparisons ($p < 0.05$) were applied to these GLM models. The natural log data transformation was performed on response data in the ANOVA analysis if their residuals did not follow a normal distribution.

4.3 Results

4.3.1 Cyanobacterial growth in soil microcosms

DG1 biomass increased during seven days' incubation in soil microcosms at all inoculum amounts and N concentration levels, as measured by chlorophyll a contents (Figure S4-2). Inoculum size had a significant effect on growth ($p = 0.013$, Table 4-1). The smallest inoculum size (1 ml) yielded the largest percentage increase in chlorophyll a from day 2-8 (61.3 ± 8.6%), while larger inoculum sizes (2 and 4 ml) resulted in smaller increases of (46.1 ± 0.04%) and (30.0 ± 9.1%), respectively (Figure 4-1). The percentage increase in chlorophyll a observed with 1-ml inoculum was significantly greater than for the 4-ml inoculum, but not for the 2-ml inoculum (Figure 4-1).

As shown in table 4-1, the nitrate-N concentration of the medium added to soil microcosms before incubation had no significant effect on growth of DG1. However, a highly significant interaction was observed between N concentration and inoculum size ($p = 0.005$). At

the medium N concentration of zero, the average percentage increase in chlorophyll a from days 2-8 was highest in microcosms inoculated with 1-ml DG1 (77.1 ± 0.1%), followed by chlorophyll a increases from 2-ml and 4-ml inocula of (38.9 ± 6.0%) and (22.0 ± 8.7%), respectively. As medium N concentration increased from 0 to 124 ppm, however, such differences were reduced and even reversed. In addition, for soil microcosms receiving 4-ml inocula, the percentage increase of chlorophyll a increased significantly as medium N concentration increased. Such significant differences were not observed as the medium N concentration changed for either the 1-ml or 2-ml inoculum levels.

4.3.2 The effect of cyanobacterial inoculum on soil water infiltration under simulated rainfall

The volume of infiltrated water was highly variable among different samples after application of simulated rainfall (Figure S4-3). As shown in Table 4-2A, no significant effect or interaction effect was detected on the infiltrated water volume, indicating that the application of DG1 on soil surface had no significant influence on soil water infiltration under different inoculum sizes and establishment times. After being standardized by the non-inoculated negative controls, the average infiltrated water of the 162 samples was 18.9 ± 0.5 ml, which was about 58% of the total precipitation.

4.3.3 Stability of cyanobacterial BSCs under simulated rainfall

DG1 biomass remaining in soil microcosms following simulated rainfall was measured from the chlorophyll a content. As shown in Table 4-2B, the establishment time of cyanobacteria had a highly significant effect ($p = 0.001$) on biomass recovery after simulated rain. The average percent recoveries of biomass were slightly but significantly higher after the one-day (86.8 ±

2.9%) and seven-day (87.7 ± 2.7%) establishment times than at the three-day establishment time (76.5 ± 2.4%) (Figure 4-3). Lower recovery after the three-day establishment time could have been due to variability in cell acclimation and cohesion to soil particles during the establishment period. In some cases, the biomass percentages recovered from the microcosms were greater than 100%, which could be due to experimental error or a rapid growth response of DG1 upon exposure to air for the rainfall application (Figure S4-4).

4.3.4 The contribution of DG1 to soil N retention

The effect of the presence of DG1 biomass in reducing soil N loss was evaluated based on the amount of nitrate N retained in soil after the simulated rain. The nitrate-N in the water from the rainfall simulation nozzle was not detectable (test detection limit was 0.5 ppm). The background soil nitrate N contents in microcosms varied from 0.01 to 0.08 mg N microcosm^{-1}, with an average at 0.06 ± 0.01 mg N microcosm^{-1}. All soil microcosms, with or without the cyanobacterial inoculum, retained a fraction of N when the medium N concentration was 62 or 124 ppm N, corresponding to 0.37 or 0.74 mg N microcosm^{-1} (Figure S4-5).

All variables, except for replication, had significant or highly significant effects on soil N retention after the simulated rain, including the establishment time ($p = 0.043$), biomass amounts of DG1 inoculum ($p < 0.001$) and medium N concentration in soil microcosms ($p < 0.001$) (Table 4-2C). First, N retained after rainfall by soil microcosms having one-day establishment time (0.18 ± 0.02 mg N microcosm^{-1}) was significantly lower than N retained by microcosms after three-day (0.23 ± 0.02 mg N microcosm^{-1}) and seven-day (0.24 ± 0.03 mg N microcosm^{-1}) establishment times (Figure 4-4A). No significant difference in N retention was observed between microcosms after three-day and seven-day establishment times. Second, compared to the non-inoculated negative controls (0.16 ± 0.01 mg N microcosm^{-1}), the average N retained in inoculated

microcosms increased by 52% to 76% (Figure 4-4B). With respect to inoculum size, mean N contents retained in soil microcosms were not significantly different. For 1, 2, and 4 ml inocula, N contents were 0.25 ± 0.02, 0.28 ± 0.03, and 0.27 ± 0.02 mg N microcosm^{-1}, respectively. Finally, after the rainfall treatment, inoculated soil microcosms prepared with 124 ppm nitrate-N contained significantly higher amounts of soil N (0.26 ± 0.01 mg N microcosm^{-1}), compared to the microcosms prepared with 62 ppm nitrate-N (0.17 ± 0.01 mg N microcosm^{-1}) (Figure 4-4C).

The percent and the amount of N retained in soil microcosms had similar trends in the main effect plots of establishment time and biomass amount, as well as in their interaction plots (Figure S4-6A, B, and D). However, because the amount of N retained in soil microcosms only increased 51.5 % as medium N concentration doubled, the percent N retained in microcosms with 124 ppm nitrate-N (32.7 ± 1.9%) was actually significantly lower than results from microcosms with 62 ppm nitrate-N (40.2 ± 2.7%) (Figure S4-6C).

In addition to the main factor effects, a significant interaction effect was detected between inoculum size and establishment time ($p = 0.04996$, Table 4-2C). As shown in Figure 4-5, soil microcosms inoculated with 1, 2 or 4 ml all retained significantly more nitrate-N after three-day establishment time. After being treated with rainfall, nitrate-N retained in soil microcosms was 99% to 137% greater in inoculated microcosms than in non-inoculated negative controls (0.15 ± 0.02 mg N microcosm^{-1}) after being cultivated on soil surface for three days. A similar trend was observed in soil microcosms after the seven-day establishment time, where nitrate-N contents were 48%-63% greater than in non-inoculated controls, although these differences were not statistically significant. Soil microcosms after only one-day establishment time before rainfall did not show such differences.

4.4 Discussion

In the present study, growth rates of the DG1 enrichment did not differ in soil microcosms amended with sodium nitrate at concentrations of 0, 62, and 124 ppm, even though more nitrate -N was retained in the soil as the medium N concentration increased (Table 4-2). Similar growth responses of DG1 in the presence or absence of soil mineral N suggest that DG1 was able to use N from de novo biological N_2 fixation as readily as soil inorganic N in satisfying N requirements of growth. In addition, physical immobilization of the DG1 enrichment on soil particles could potentially limit access by DG1 to all soil N despite high overall N concentrations. Such growth constraints of immobilized cyanobacteria have been shown previously in waste water treatment systems using *Synechococcus elongatus* (Aguilar-May and del Pilar Sánchez-Saavedra, 2009).

In arid and semi-arid areas, natural formation of stable BSCs requires several years or decades of undisturbed conditions (Langhans et al., 2009; Read et al., 2016). However, such periods may be significantly shorter when soils have more available moisture, particularly at levels close to field capacity (ca. volumetric water content = 30% for silt loam soil). Previous studies have demonstrated that cyanobacterial soil crusts can become established within one month when additional water is applied. These studies include field trials using *Microcoleus vaginatus* (Chen et al., 2006) and growth of *Nostoc spp.* in soil microcosms (Peng, Chapter 2). In the present study, we evaluated BSC formation by DG1 after relatively short periods of one, three, and seven days, because these are realistic intervals in humid regions where rainfall events may occur soon after field application of cyanobacteria. Three days after inoculation, DG1 showed significant increases in biomass and N retention, and stable BSCs were observed after one week. While it is possible that longer periods of crust development would result in different patterns of water infiltration, biomass increase, and N retention, extended observation periods were beyond

the scope of this study. Later stages of BSC development in many agricultural fields in Central Pennsylvania, for example, are characterized by abundant growth of green algae and mosses that can alter soil properties further.

To our knowledge, retention of mineral N by cyanobacteria on agricultural soils has not been reported previously. To date, the most comparable research studies have investigated the use of cyanobacteria for N uptake from wastewaters. For example, the cyanobacterium *Synechococcus elongatus* removed a total of 7.7-12.9 mg N L^{-1} after being cultivated in wastewater containing 5.2 ppm nitrate-N and 17.9 ppm ammonium-N (Aguilar-May and del Pilar Sánchez-Saavedra, 2009). Applying this concept to our soil microcosms after one week of DG1 growth, we calculated average N retentions of 16.8 ± 2.5 and 21.6 ± 3.3 mg N L^{-1}, respectively, in media with 62 and 124 ppm nitrate-N, based on total microcosm volumes of 15 ml of soil and water. Accordingly, the average NO_3^- retention during the first three days of DG1 growth could be expressed as 0.017 ± 0.004 and 0.025 ± 0.006 mM h^{-1} at medium concentrations of 62 and 124 ppm N. This result was consistent with the nitrate uptake rate of 0.02-0.05 mM h^{-1} by *Synechococcus sp.* strain PCC 7942 during the first two days of ground water treatment (Hu et al., 2000). In that study, nitrate removal by cyanobacteria increased significantly as the nitrate concentration increased from 4.5 to 33.0 ppm N, which is similar to what we observed when increasing medium N from 62 to 124 ppm.

In microcosms subjected to rainfall, the inoculum size of DG1 (1, 2 and 4 ml) did not affect nitrate-N retention (Figure 4-4B), even though the chlorophyll a contents of soil samples from the positive controls (microcosms that did not receive rainfall) increased significantly as the initial DG1 biomass amount increased from 1 to 4 ml (data not shown). In a previous study, we demonstrated that the DG1 enrichment maintained a consistent cell N content of 8.7% after being cultured for one month, regardless of the N concentration in the growth medium (ranged from 0 to 247 ppm) (Peng, Chapter 3). Based on our biomass measurements, it was not possible for DG1

to have immobilized all nitrate-N that had been retained in the soil. Since no significant changes had been observed in water infiltration rates after the application of different biomass amounts, we inferred that DG1 not only immobilized intracellular N but also produced extracellular polymeric substances that adsorbed N and contributed to N retention.

In the present study, the 1-ml inoculum corresponded to a field application rate of 0.88 g dry biomass m^{-2}. Because the 1-ml inoculum performed as well or better than the 2- or 4-ml inocula, this application rate would be more economical and effective for future field applications. The lowest application rate in our study was considerably lower than rates used in other studies of N_2-fixing cyanobacterial soil amendments (*Nostoc* and *Anabeana spp.*). Assuming a typical cell water content of 80% (Bratbak and Dundas, 1984), reported rates have varied from 10 g fresh biomass per pot (equivalent to 113 g dry biomass m^{-2}) for greenhouse wheat cultivation (Gheda and Ahmed, 2015) to 6 g dry biomass m^{-2} for corn under field conditions (Maqubela et al., 2009). On the other hand, it has been reported that cyanobacteria (mixture of *Nostoc* and *Anabaena spp.*) compensated for 50% urea-N upon use of a small application rate at 6 mg dry biomass m^{-2} in rice paddy systems (Pereira et al., 2009), indicating the potential feasibility of using lower application rates.

In our previous studies, the densest biomass coverage by the DG1 enrichment on N-limited sandy soil surfaces was estimated at 4.96 g m^{-2} after 84 day cultivation in microcosms (Peng, Chapter 2). We consider this biomass density to be a good estimate of the environmental carrying capacity of DG1 on the sandy soil used in our previous experiments, so that the 1-ml application rate of DG1 would represent about 18% of the observed maximum biomass density on coarse-textured soils. The carrying capacities of DG1 on finer-textured agricultural soils are likely to be higher with additional N and greater soil particle surface areas. The difference between this maximum biomass density and the field application rate based on the 1-ml inoculum suggests good potential for growth and N uptake in agricultural systems.

4.5 Conclusion

This study evaluated the growth of a novel cyanobacteria soil amendment DG1 on agricultural soil surfaces and its potential contribution to modulating soil mineral N in agroecosystems. DG1 performed well across a range of soil mineral N concentrations and retained a significant amount of soil nitrate. Table 4-3 summarizes the effects of soil nitrate concentration, cyanobacterial application rate and establishment time on three response variables. Cyanobacterial growth was affected by cyanobacterial application rate; biomass recovery was affected by establishment time; and N retention was affected by all three independent variables. After integrating all results in our studies, we concluded that lower application rates (ca. 0.9 g dry biomass m^{-2}) and a period of establishment time (ca. 7 days without significant rain) will be efficient and cost-effective in future agricultural applications.

4.6 Acknowledgement

We thank Mark Signs, Director of Shared Fermentation Facility at the Pennsylvania State University, for his assistance with the establishment of photobioreactors; and Louis S Saporito, United States Department of Agriculture (USDA) Agricultural Research Service, for the guidance on rainfall simulator. This research was funded by the Research Applications for Innovation (RAIN) grant from the College of Agricultural Sciences of the Pennsylvania State University.

4.7 References

Aguilar-May, B., del Pilar Sánchez-Saavedra, M., 2009. Growth and removal of nitrogen and phosphorus by free-living and chitosan-immobilized cells of the marine cyanobacterium *Synechococcus elongatus*. Journal of Applied Phycology 21, 353-360.

Barak, P., Jobe, B., Krueger, A., Peterson, L., Laird, D., 1997. Effects of long-term soil acidification due to nitrogen fertilizer inputs in Wisconsin. Plant and Soil 197, 61-69.

Belnap, J., 2006. The potential roles of biological soil crusts in dryland hydrologic cycles. Hydrological processes 20, 3159-3178.

Belnap, J., Lange, O., 2001. Biological soil crusts: structure, function and management. Springer, New York.

Bratbak, G., Dundas, I., 1984. Bacterial dry matter content and biomass estimations. Applied and environmental microbiology 48, 755-757.

Castillo, H., Bruns, M.A., 2001. Cyanobacterial diversity in agricultural soils, Ninth International Symposium in Microbial Ecology, Amsterdam, The Netherlands.

Castillo-Monroy, A.P., Maestre, F.T., Delgado-Baquerizo, M., Gallardo, A., 2010. Biological soil crusts modulate nitrogen availability in semi-arid ecosystems: insights from a Mediterranean grassland. Plant and Soil 333, 21-34.

Chen, L., Xie, Z., Hu, C., Li, D., Wang, G., Liu, Y., 2006. Man-made desert algal crusts as affected by environmental factors in Inner Mongolia, China. Journal of Arid Environments 67, 521-527.

Chien, S.H., Prochnow, L.I., Cantarella, H., 2009. Chapter 8 Recent developments of fertilizer production and use to improve nutrient efficiency and minimize environmental impacts, in: Donald, L.S. (Ed.), Advances in Agronomy. Academic Press, pp. 267-322.

Costa, J.A.V., Cozza, K.L., Oliveira, L., Magagnin, G., 2001. Different nitrogen sources and growth responses of *Spirulina platensis* in microenvironments. World Journal of Microbiology and Biotechnology 17, 439-442.

Delgado-Baquerizo, M., Morillas, L., Maestre, F.T., Gallardo, A., 2013. Biocrusts control the nitrogen dynamics and microbial functional diversity of semi-arid soils in response to nutrient additions. Plant and Soil 372, 643-654.

Elbert, W., Weber, B., Burrows, S., Steinkamp, J., Budel, B., Andreae, M.O., Poschl, U., 2012. Contribution of cryptogamic covers to the global cycles of carbon and nitrogen. Nature Geoscience 5, 459-462.

Galloway, J.N., Townsend, A.R., Erisman, J.W., Bekunda, M., Cai, Z., Freney, J.R., Martinelli, L.A., Seitzinger, S.P., Sutton, M.A., 2008. Transformation of the nitrogen cycle: recent trends, questions, and potential solutions. Science 320, 889-892.

Gheda, S.F., Ahmed, D.A., 2015. Improved soil characteristics and wheat germination as influenced by inoculation of *Nostoc kihlmani* and *Anabaena cylindrica*. Rendiconti Lincei 26, 121-131.

Hawkes, C.V., 2003. Nitrogen cycling mediated by biological soil crusts and arbuscular mycorrhizal fungi. Ecology 84, 1553-1562.

Hu, Q., Westerhoff, P., Vermaas, W., 2000. Removal of nitrate from groundwater by cyanobacteria: quantitative assessment of factors influencing nitrate uptake. Applied and environmental microbiology 66, 133-139.

Humphry, J., Daniel, T., Edwards, D., Sharpley, A., 2002. A portable rainfall simulator for plot–scale runoff studies. Applied Engineering in Agriculture 18, 199.

Kibet, L.C., Saporito, L.S., Allen, A.L., May, E.B., Kleinman, P.J., Hashem, F.M., Bryant, R.B., 2014. A protocol for conducting rainfall simulation to study soil runoff. Journal of visualized experiments 86, e51664.

Langhans, T.M., Storm, C., Schwabe, A., 2009. Community assembly of biological soil crusts of different successional stages in a temperate sand ecosystem, as assessed by direct determination and enrichment techniques. Microbial Ecology 58, 394-407.

Lehmann, J., Schroth, G., 2003. Nutrient leaching. Trees, crops and soil fertility. CABI Publishing, Wallingford, 151-166.

Mager, D., Thomas, A., 2011. Extracellular polysaccharides from cyanobacterial soil crusts: a review of their role in dryland soil processes. Journal of Arid Environments 75, 91-97.

Maqubela, M., Mnkeni, P., Issa, O.M., Pardo, M., D'Acqui, L., 2009. *Nostoc* cyanobacterial inoculation in South African agricultural soils enhances soil structure, fertility, and maize growth. Plant and Soil 315, 79-92.

McNeill, A., Unkovich, M., 2007. The nitrogen cycle in terrestrial ecosystems, Nutrient cycling in terrestrial ecosystems. Springer, pp. 37-64.

Mishra, U., Pabbi, S., 2004. Cyanobacteria: a potential biofertilizer for rice. Resonance 9, 6-10.

Nayak, S., Prasanna, R., Pabby, A., Dominic, T.K., Singh, P.K., 2004. Effect of urea, blue green algae and *Azolla* on nitrogen fixation and chlorophyll accumulation in soil under rice. Biology and Fertility of Soils 40, 67-72.

Norusis, M., 2008. SPSS 16.0 statistical procedures companion. Prentice Hall Press. Upper Saddle River, NJ.

Pankratova, E., 2006. Functioning of cyanobacteria in soil ecosystems. Eurasian Soil Science 39, S118-S127.

Pereira, I., Ortega, R., Barrientos, L., Moya, M., Reyes, G., Kramm, V., 2009. Development of a biofertilizer based on filamentous nitrogen-fixing cyanobacteria for rice crops in Chile. Journal of Applied Phycology 21, 135-144.

Read, C.F., Elith, J., Vesk, P.A., 2016. Testing a model of biological soil crust succession. Journal of Vegetation Science 27, 176-186.

Schindler, D., Hecky, R., 2009. Eutrophication: more nitrogen data needed. Science 324, 721-722.

Sinha, R.P., Häder, D.P., 1996. Photobiology and ecophysiology of rice field cyanobacteria. Photochemistry and Photobiology 64, 887-896.

Soil Survey Staff, 2010. Keys to soil taxonomy, 11th ed. USDA-Natural Resources Conservation Service, Washington, DC.

Sprőber, P., Shafik, H.M., Présing, M., Kovács, A.W., Herodek, S., 2003. Nitrogen uptake and fixation in the cyanobacterium *Cylindrospermopsis raciborskii* under different nitrogen conditions. Hydrobiologia 506, 169-174.

Strauss, S.L., Day, T.A., Garcia-Pichel, F., 2012. Nitrogen cycling in desert biological soil crusts across biogeographic regions in the Southwestern United States. Biogeochemistry 108, 171-182.

UNESCO, 1966. Determination of photosynthetic pigments in seawater, Monographs on oceanographic methodology. United Nations Educational, Scientific and Cultural Organization, Place de Fontenoy, pp. 15-16.

Vaishampayan, A., Sinha, R., Hader, D.P., Dey, T., Gupta, A., Bhan, U., Rao, A., 2001. Cyanobacterial biofertilizers in rice agriculture. The Botanical Review 67, 453-516.

Williams, M.R., Feyereisen, G.W., Beegle, D.B., Shannon, R.D., Folmar, G.J., Bryant, R.B., 2011. Manure application under winter conditions: Nutrient runoff and leaching losses. Transactions of the ASABE 54, 891-899.

4.8 Figures and tables

Figure 4-1. The main effect plot for % increase of chlorophyll a in soil microcosms from day 2-8 under different biomass amounts of the DG1 enrichment inoculum. The three DG1 inoculum sizes applied to soil microcosms (1, 2, and 4 ml) corresponded to initial biomass densities of 0.88, 1.75 and 3.51 g dry biomass m^{-2} on soil surfaces, respectively. Error bars are standard error of the mean. Different letters show the result of Tukey's multiple comparison tests (after the natural log data transformation, $p < 0.05$).

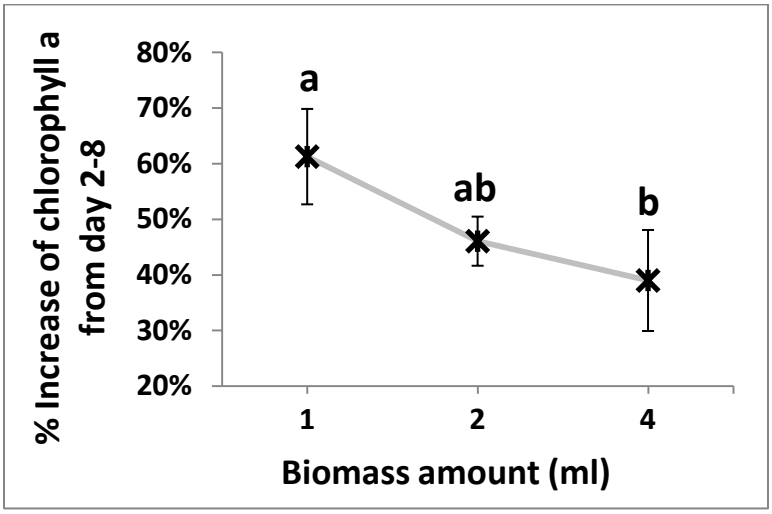

Figure 4-2. Interaction plot for the percent increase of chlorophyll a in soil microcosms from day 2-8. The two interacting variables are biomass amount of the DG1 enrichment inoculum and medium N concentration in soil microcosms. The three DG1 inoculum sizes applied to soil microcosms (1, 2, and 4 ml) corresponded to initial biomass densities of 0.88, 1.75 and 3.51 g dry biomass m^{-2} on soil surfaces, respectively. Error bars are standard error of the mean. The '*' shows a significant difference within the column based on the Tukey's multiple comparison tests (after the natural log data transformation, $p < 0.05$).

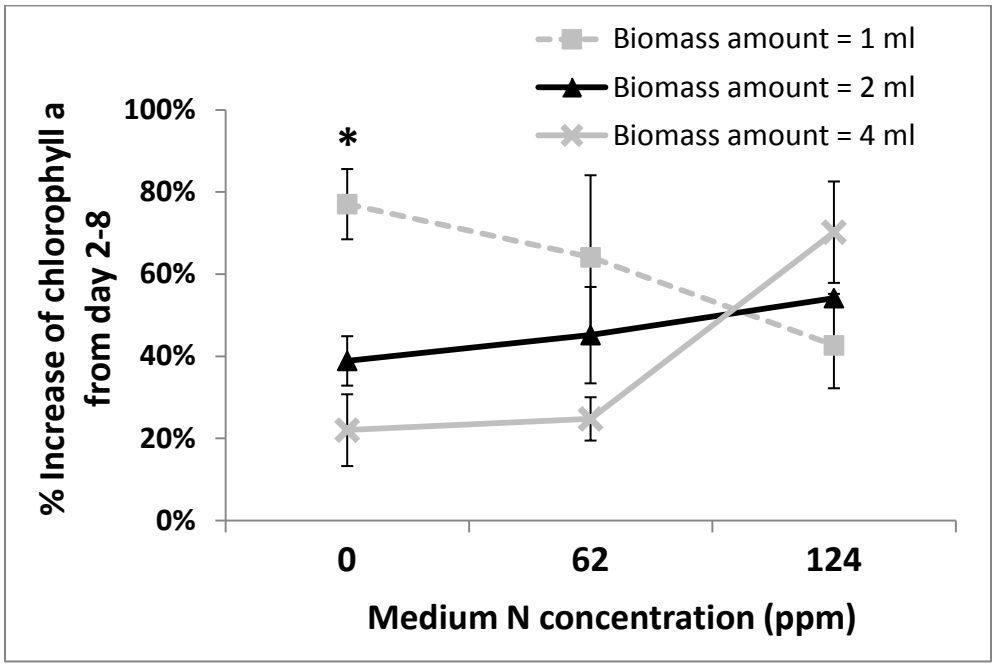

Figure 4-3. Main effect plot for % biomass recovered of the DG1 enrichment on soil surface after different establishment times followed by rainfall. Error bars are standard error of the mean. Different letters show the result of Tukey's multiple comparison tests ($p < 0.05$).

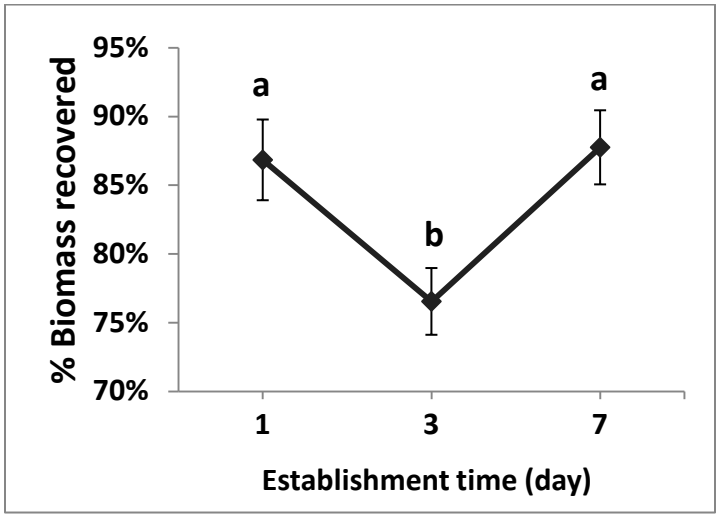

Figure 4-4. Main effect plots for N retained in soil microcosms after the rainfall. Variables include: (A) the establishment time, (B) biomass amounts of DG1 inoculum, and (C) medium N concentration in soil microcosms. The three DG1 inoculum sizes applied to soil microcosms (1, 2, and 4 ml) corresponded to initial biomass densities of 0.88, 1.75 and 3.51 g dry biomass m^{-2} on soil surfaces, respectively. Error bars are standard error of the mean. Different letters or '*' show the result of Tukey's multiple comparison tests ($p < 0.05$).

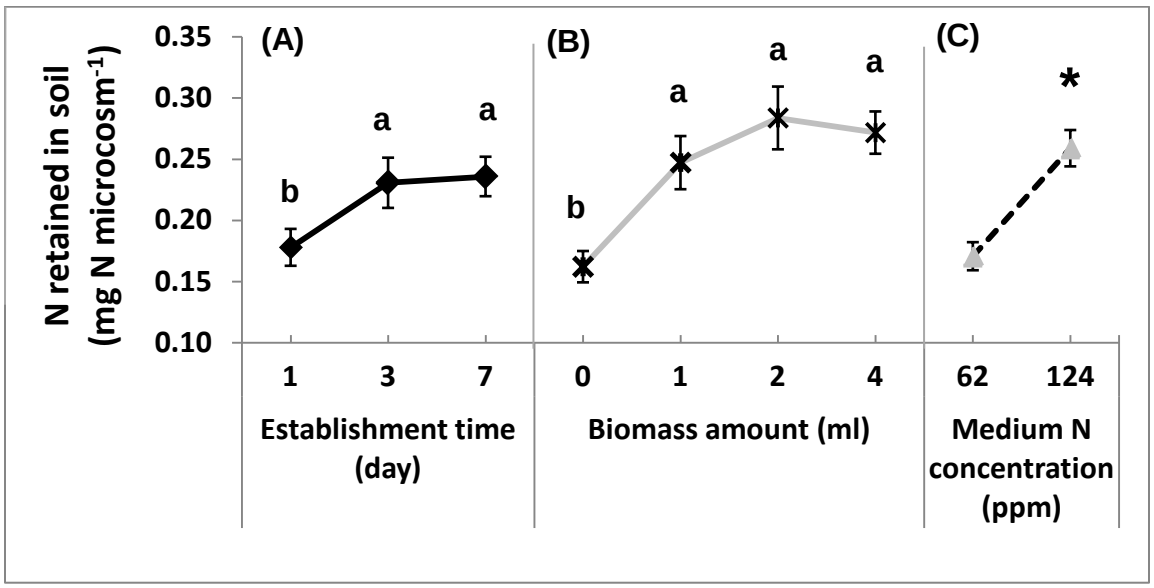

Figure 4-5. Interaction plot for N retained in soil microcosms after the rainfall. The two interacting variables are biomass amount of the DG1 enrichment inoculum and their establishment time. The three DG1 inoculum sizes applied to soil microcosms (1, 2, and 4 ml) corresponded to initial biomass densities of 0.88, 1.75 and 3.51 g dry biomass m^{-2} on soil surfaces, respectively. Error bars are standard error of the mean. The '*' shows a significant difference within the column based on the Tukey's multiple comparison tests ($p < 0.05$).

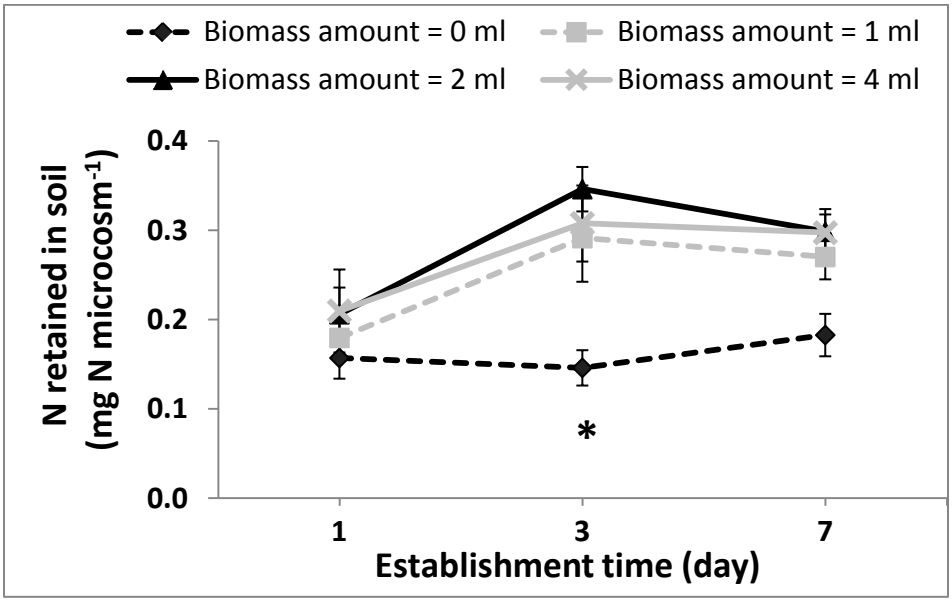

Table 4-1. ANOVA analysis for % increase of chlorophyll a in soil microcosms from day 2-8 after the natural log data transformation. The '*' and '**' show significant ($p < 0.05$) and highly significant effects ($p < 0.01$) respectively, based on their F-tests.

% Increase of chlorophyll a from day 2-8 (after natural log transformation)			
Independent variable	F-statistics (numDF, denDF)	p-value	Significance
Replication	2.927 (2,16)	0.083	
Biomass amount	5.809 (2,16)	0.013	*
Medium N concentration	2.251 (2,16)	0.138	
Biomass amount x Medium N concentration	5.587 (4,16)	0.005	**

Table 4-2. ANOVA analyses for the observations of different responses after the simulated rain: (A) unified infiltrated water volume, (B) % biomass recovered of the DG1 enrichment on the soil surface, and (C) N retained in soil microcosms. The '*' and '**' show significant ($p < 0.05$) and highly significant effects ($p < 0.01$) respectively, based on their F-tests.

(A) Infiltrated water volume (adjusted by no-biomass controls)			
Independent variable	F-statistics (numDF, denDF)	p-value	Significance
Replication	0.310 (2,4)	0.750	
Establishment time	1.300 (2,4)	0.367	
Replication x Establishment time	0.729 (4,132)	0.574	
Biomass amount	2.425 (3,132)	0.069	
Medium N concentration	1.027 (2,132)	0.361	
Biomass amount x Medium N concentration	1.532 (6,132)	0.172	
Biomass amount x Establishment time	0.314 (6,132)	0.929	
Medium N concentration x Establishment time	0.866 (4,132)	0.486	
(B) % Biomass recovered			
Independent variable	F-statistics (numDF, denDF)	p-value	Significance
Replication	5.278 (2,4)	0.076	
Establishment time	52.278 (2,4)	0.001	**
Replication x Establishment time	0.099 (4,56)	0.982	
Biomass amount	0.320 (2,56)	0.727	
Medium N concentration	0.618 (2,56)	0.543	
Biomass amount x Medium N concentration	2.332 (4,56)	0.067	
Biomass amount x Establishment time	1.172 (4,56)	0.333	
Medium N concentration x Establishment time	0.522 (4,56)	0.720	
(C) N retained in soil			
Independent variable	F-statistics (numDF, denDF)	p-value	Significance
Replication	0.522 (2,4)	0.629	
Establishment time	7.471 (2,4)	0.045	*
Replication x Establishment time	1.522(4,84)	0.203	
Biomass amount	18.007 (3,84)	<0.000	**
Medium N concentration	28.717 (1,84)	<0.000	**
Biomass amount x Medium N concentration	0.770 (3,84)	0.514	
Biomass amount x Establishment time	2.209 (6,84)	0.050†	*
Medium N concentration x Establishment time	0.176 (2,84)	0.839	

† p - value = 0.04996

Table 4-3. Summarized effects of different independent factors on the distinct responses investigated in our study. '——' Indicates no significant effect has been observed. The inequalities are expressed based on the Tukey's multiple comparisons ($p < 0.05$).

Responses	Independent factors		
	Medium N concentration (ppm)	Biomass amount (ml)	Establishment time (day)
% Increase of chlorophyll a	——	1 ≥ 2 ≥ 4	Not applicable
Infiltrated water volume	——	——	——
% Biomass recovered	——	——	3 < 1 ≈ 7
N retained in soil	124 > 62	0 < 1 ≈ 2 ≈ 4	1 < 3 ≈ 7

4.9 Supplementary materials

Figure S4-1. Diagram of a sample collection device for the simulated rainfall treatment.

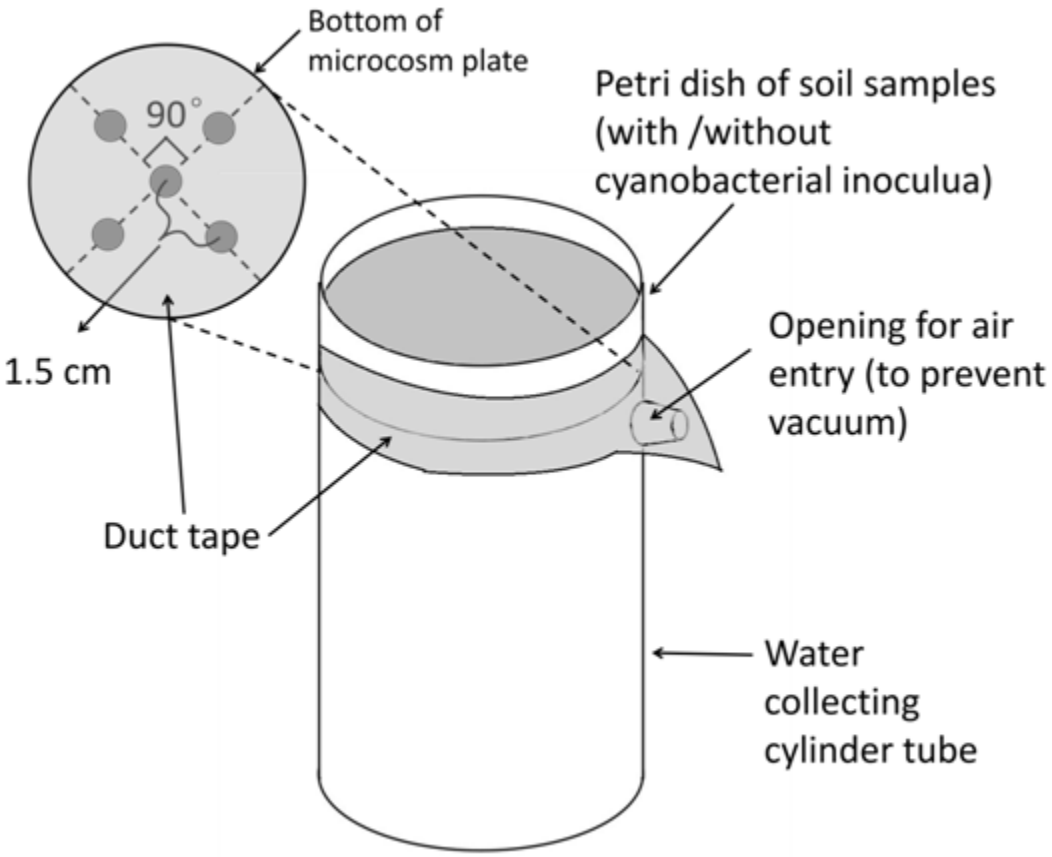

Figure S4-2. Box plot of % increase of chlorophyll a in soil microcosms from day 2-8. Each box represents a treatment combination (n = 3). The three DG1 inoculum sizes applied to soil microcosms (1, 2, and 4 ml) corresponded to initial biomass densities of 0.88, 1.75 and 3.51 g dry biomass m^{-2} on soil surfaces, respectively.

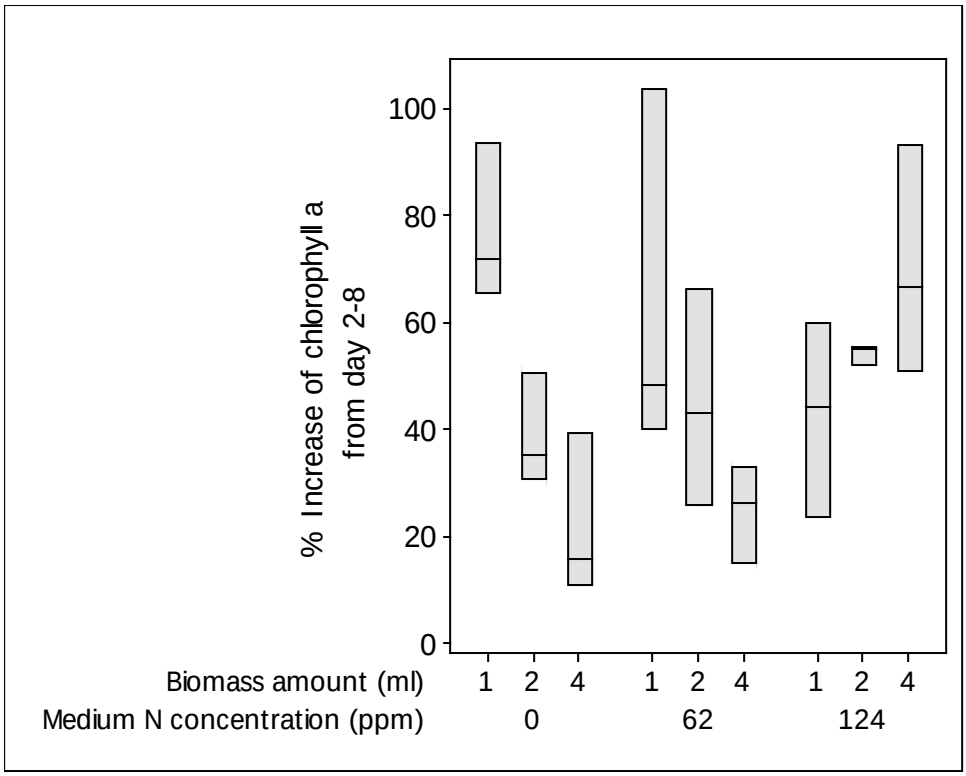

Figure S4-3. Box plot of adjusted infiltrated water volume collected after the rainfall. Each box represents a treatment combination (n = 3 for biomass amount ≠ 0, n = 9 for biomass amount = 0). The three DG1 inoculum sizes applied to soil microcosms (1, 2, and 4 ml) corresponded to initial biomass densities of 0.88, 1.75 and 3.51 g dry biomass m^{-2} on soil surfaces, respectively.

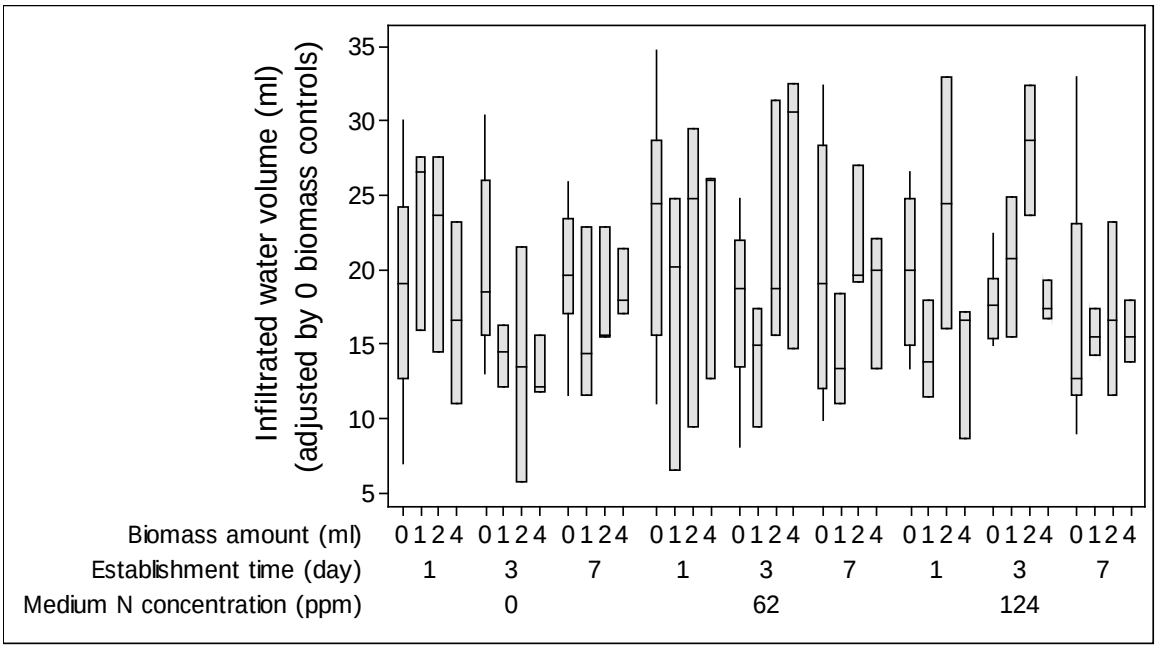

Figure S4-4. Box plot of % biomass recovered of the DG1 enrichment on soil surface after the rainfall. Each box represents a treatment combination (n = 3). The three DG1 inoculum sizes applied to soil microcosms (1, 2, and 4 ml) corresponded to initial biomass densities of 0.88, 1.75 and 3.51 g dry biomass m^{-2} on soil surfaces, respectively.

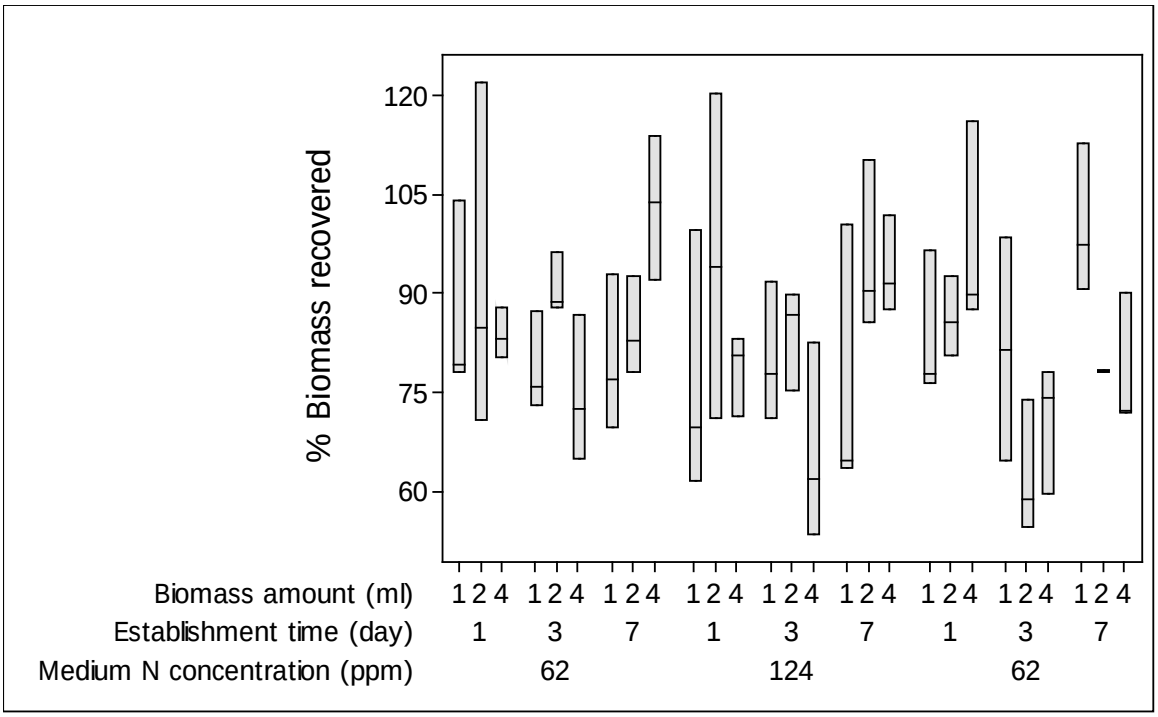

Figure S4-5. Box plot of N retained in soil microcosms after the rainfall. Each box represents a treatment combination (n = 3 for biomass amount ≠ 0, n = 9 for biomass amount = 0). The three DG1 inoculum sizes applied to soil microcosms (1, 2, and 4 ml) corresponded to initial biomass densities of 0.88, 1.75 and 3.51 g dry biomass m^{-2} on soil surfaces, respectively.

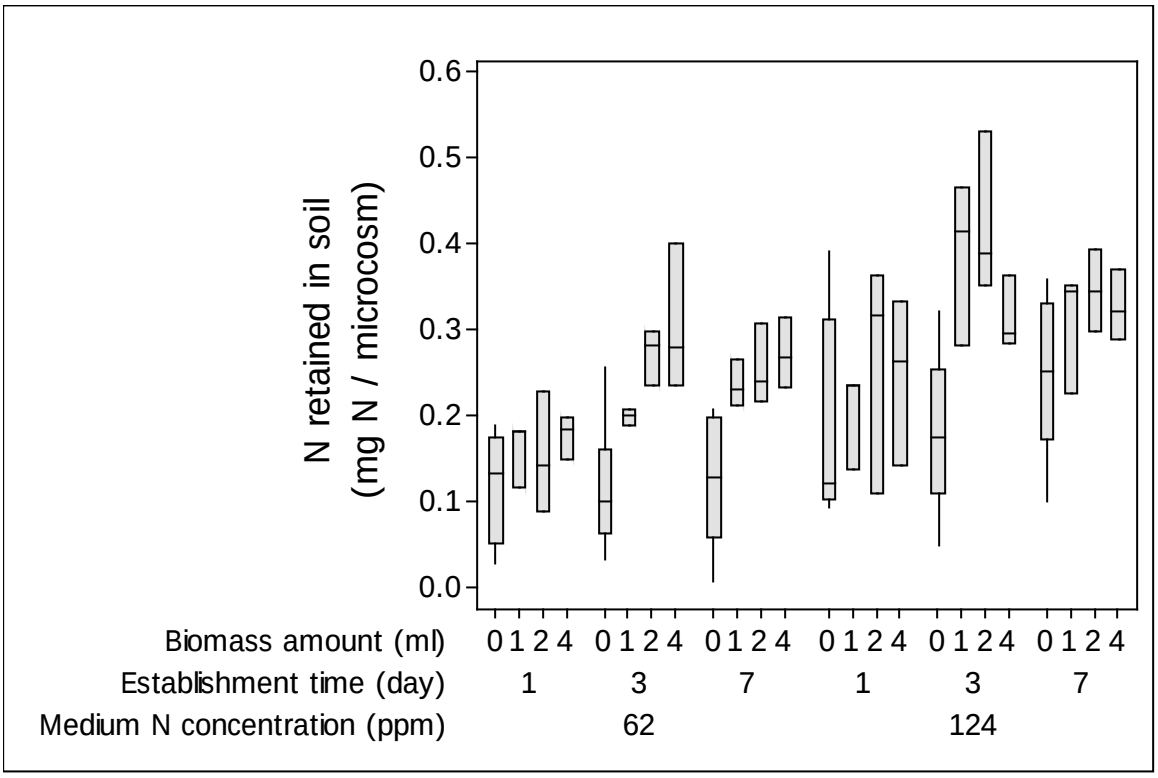

Figure S4-6. Main effect plot of (A) the establishment time, (B) biomass amounts of DG1 inoculum, and (C) medium N concentration in soil microcosms for % N retained in soil microcosms after the rainfall treatment. (D)The interaction plot of the biomass amount and the establishment time for %N retained in soil microcosms. The three DG1 inoculum sizes applied to soil microcosms (1, 2, and 4 ml) corresponded to initial biomass densities of 0.88, 1.75 and 3.51 g dry biomass m^{-2} on soil surfaces, respectively. Error bars are standard error of the mean. Different letters or '*' show the result of Tukey's multiple comparison tests ($p < 0.05$).

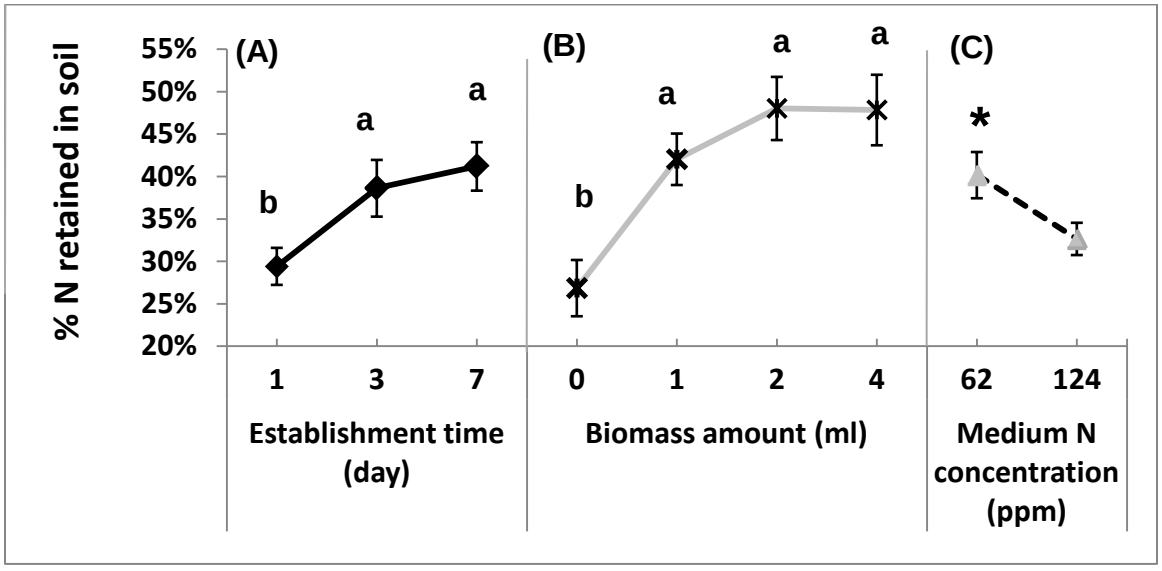

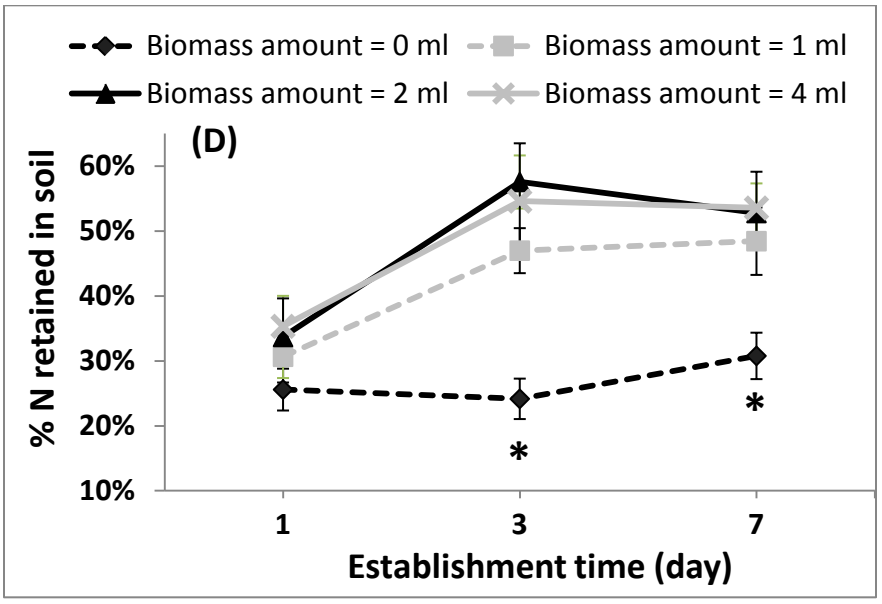

Table S4-1. Element contents of the soil used in soil microcosms. Values are shown as mean ± standard deviation.

Elements		Content
C%		1.17 ± 0.02
N%		0.17 ± 0.00
Ammonium N (ppm)	Before autoclaving	0.77 ± 0.06
	After autoclaving	1.33 ± 0.42
Nitrate N (ppm)	Before autoclaving	6.78 ± 0.96
	After autoclaving	6.89 ± 0.25
Phosphorus (ppm)		372.5 ± 13.9
Metal elements (ppm)		
Aluminum		24139.7 ± 597.3
Iron		27263.3 ± 999.8
Potassium		3376.2 ± 209.9
Magnesium		2044.1 ± 31.0
Calcium		3424.9 ± 119.4
Chromium		57.37 ± 8.71
Copper		17.72 ± 0.39
Lead		19.16 ± 0.78
Nickel		25.21 ± 0.60
Zinc		51.41 ± 0.54
Barium		121.77 ± 2.26
Cobalt		14.57 ± 0.28
Manganese		839.89 ± 27.45
Sodium		42.89 ± 3.49
Strontium		16.19 ± 0.34

Chapter 5

Succession of Biological Soil Crusts and Their Potential Nitrogen Contributions in Agroecosystems - Theoretical Modeling and Field Observations

5.1 Introduction

Biological soil crusts (BSCs) are formed by complex microbial communities in association with soil particles (Belnap and Lange, 2001). BSCs have been studied mostly in arid and semiarid ecosystems because of their roles in adding organic carbon (C) and nitrogen (N) to soil through photosynthesis and N_2 fixation (Belnap, 2002; Housman et al., 2006b; Strauss et al., 2012; Yoshitake et al., 2010). As drivers of the early stages of terrestrial ecosystem succession, BSCs can improve soil quality and thus facilitate colonization by vascular plants (Breen and Levesque, 2006; Langhans et al., 2009a; Li et al., 2002). BSCs occur in a wide variety of ecosystems, and they have been estimated to contribute about 26 Tg N yr^{-1} globally (Elbert et al., 2012; Weber et al., 2015). However, the study of BSCs in temperate, humid regions is very limited. Notably, very few studies of BSCs in temperate agroecosystems have been reported (Reynaud and Metting, 1986).

Cyanobacteria are the main BSC members capable of fixing atmospheric N_2. In addition, photosynthesis by cyanobacteria involves a highly efficient C-concentrating mechanism (CCM), which enables them to maintain high rates of photosynthesis and accelerates organic C accumulation in the soil (Price et al., 1998). Cyanobacteria are the true pioneers in BSC succession, and they play a key role in the establishment and self-sustenance of BSCs on soils (Langhans et al., 2009b). After colonization by free-living cyanobacteria, microbial diversity and richness increase due to colonization by other organisms, including green algae, lichens (cyanobacterial symbiosis with fungi), and moss (usually last to appear) during BSC succession

(Lan et al., 2012, 2013; Schmidt et al., 2008; Zhang et al., 2009). Therefore, initial colonization by cyanobacteria results in formation of self-sustaining BSCs under suitable environmental conditions.

We have observed annual growth of naturally occurring BSCs containing cyanobacteria, green algae and moss in diverse agricultural fields at the Pennsylvania State University (Penn State) Agronomy Research Farm since 2001 (Castillo and Bruns, 2001). In our previous work, we obtained from local soil an N_2-fixing cyanobacterial enrichment culture (named DG1) with good potential to be applied as an agricultural soil amendment to enable BSC formation and serve as a source of biologically fixed N (Peng, Chapter 2, 3, and 4). Although considerable research on using cyanobacteria as biofertilizers has been conducted in Asian countries (Choudhury and Kennedy, 2004; Dhar et al., 2015; Hashem, 2001), the roles of cyanobacteria in North American agroecosystems have been virtually ignored. Because so little information is available about BSCs on temperate arable soils, model simulations would be useful prior to undertaking field studies on cyanobacterial applications. Information obtained from model simulations can provide insights into expected/projected dynamics of BSC formation and succession, so that field experiments can be designed and performed more efficiently.

Recently, BSCs have been proposed as good model systems for exploring community ecology questions related to biodiversity, environmental stress, species interactions, and succession (Bowker et al., 2014; Bowker et al., 2010). Community succession models can be classified as descriptive, linear/non-linear simulation, population dynamic, or Markov models, among which Markov models have the most predictive ability (Usher, 1981). Community succession has been studied and modeled widely in different ecosystems using Markov models (Zhang, 2014; Gotelli, 1995; Horn et al., 1975; Usher, 1979). However, models describing microbial successions in soils are rare and mostly conceptual (Belnap and Eldridge, 2001;

Bowker, 2007). To date, the only published mathematical BSC succession model has been based on hierarchical regression simulation (Read et al., 2016).

Here, based on density-dependent logistic growth modeling of the three main photosynthetic components in BSCs: cyanobacteria, green algae and moss, we established a stochastic Markov succession model in a theoretical study of BSC dynamics that could occur following artificial application of cyanobacteria to soil. In addition, we collected data on naturally occurring BSCs and associated soil properties for one year in agricultural fields. We applied modeling and field observations to investigate: (1) BSC succession under contrasting environmental conditions; (2) the relationship between cyanobacterial N contributions and the initial soil N and/or cyanobacterial inoculum size; (3) the dynamics of naturally formed BSCs in actual agricultural fields; (4) the congruence between our field observations and model predictions.

5.2 Materials and methods

5.2.1 Simulation model of BSC succession

5.2.1.1 System and assumptions

The initial system to be modeled is 1 m^2 of non-vegetated surface area (upper 1-cm soil) in an agricultural field that has not been colonized by any BSC communities. We suppose that an inoculum of living cyanobacterial biomass is applied to this area to enable surface colonization. Establishment and growth of cyanobacteria result in sequential colonization by green algae, followed by moss (bryophytes). During BSC succession, natural colonization of soil by airborne

or waterborne cyanobacterisa/green algae/moss from other fields with BSCs can also occur when conditions are favorable.

In the model, we make several assumptions for simplification and clarity. First, we assume that optimum soil conditions for microbial growth are maintained, with surface soil temperature at 22-23℃, soil moisture content at field capacity, and pH at 7.1-7.3. Therefore, soil N availability is assumed to be the only environmental factor affecting growth and transfers of BSC compartments. Our second assumption is that growth rates and local extinction rates for each biotic compartment in the model do not change during the modeled period. Third, we assume moss is ten times less competitive for soil N than green algae, which will be reflected in the carrying capacities and inter-compartment transition rates. Fourth, N and biomass are uniformly distributed across the homogeneous 1-m^2 soil area.

5.2.1.2 Community matrix analysis

As shown in the loop diagram in Figure 5-1, the BSC succession model is represented as four different compartments, three of which consist of living biomass (cyanobacteria, green algae, and moss) and one consisting of uncolonized soil or soil with dead biomass. In this model the time step is one day. Each compartment has its own stasis rate (Pcc, Paa, Pmm, Puu), which is the percentage of biomass that remains within that compartment on the succeeding day. Each compartment is assigned a local extinction rate, which is the density-independent proportion of biomass that dies each day (Dc, Da, and Dm). In addition, several stochastic transition rates describe the proportion of biomass in each compartment that is transferred to another compartment each day (Pca, Pam, Puc, Pua, Pum). Thus, a matrix showing the relationships among the four compartments in the loop diagram is:

$$\begin{array}{c} \\ U \\ C \\ A \\ M \end{array} \begin{array}{c} \begin{array}{cccc} U & C & A & M \end{array} \\ \begin{pmatrix} P_{uu} & D_c & D_a & D_m \\ P_{uc} & P_{cc} & 0 & 0 \\ P_{ua} & P_{ca} & P_{aa} & 0 \\ P_{um} & 0 & P_{am} & P_{mm} \end{pmatrix} \end{array}$$

where $P_{uu} + P_{uc} + P_{ua} + P_{um} = 1$; $P_{cc} + D_c + P_{ca} = 1$; $P_{aa} + D_a + P_{am} = 1$; and $P_{mm} + D_m = 1$.

5.2.1.3 Simulation of available soil N and BSC community dynamics

The community matrix was used to establish a discrete model with daily time-steps. Parameters and variables are summarized in Table 5-1, along with their sources, which include experimental data, literature values, and reasonable estimates based on preliminary experiments (Mišurcová et al., 2010; Piorreck et al., 1984; Shaffer et al., 2010; Zechmeister et al., 2008). We assumed that all N from dead cells was available immediately for uptake as labile N or for escape from the upper layer of soil. N(t) is defined as available N at time t. At each time step, N(t) was estimated as N(t-1) plus N input from dead cells and biomass transitions from one compartment to another minus N assimilated by all live biomass and daily N loss from the soil surface. Therefore, N(t+1) was expressed as (Code S5-1):

$$N(t+1) = N(t) + (Dc + Pca) \times C(t) \times Nc + (Da + Pam) \times A(t) \times Na + Dm \times M(t) \times Nm$$
$$- [A(t+1) - A(t)] \times Na - [M(t+1) - M(t)] \times Nm - [C(t+1) - C(t)] \times Nc \times R - k \times N(t)$$

where Nc, Na and Nm are the cell N contents of cyanobacteria, green algae and moss; C(t), A(t) and M(t) are the biomass amounts of cyanobacteria, green algae and moss at time t; R is the proportion of cyanobacterial N assimilated from the surface soil available N; and k is the average daily soil N loss rate from the 1-m^2 surface area.

Estimates for R were obtained from direct measurements during $^{15}N_2$ fixation experiments (Peng, Chapter 3). When N (t) > 10 mg N m^{-2} (1 ppm in soil at 1 cm depth), R = 0.77; when N (t) ≤ 10 mg N m^{-2}, R = 0, which is the case when cyanobacteria obtain all cellular N from atmospheric N_2. If soil available N is insufficient to fulfill growth requirements, cyanobacteria will take up as much available N as possible and meet the remaining demand through N_2 fixation. We also assumed that leaching was the main pathway for N loss from 0-1 cm surface soils and that denitrification losses were insignificant. We used the annual precipitation of 100 cm, which is typical in central Pennsylvania, for estimating the average daily percentage of N loss from leaching (Shaffer et al., 2010).

Biomass densities of BSC components at time (t + 1) were estimated using the equations below. Proportions of C(t + 1), A(t + 1), and M(t + 1) remaining from the previous day were assumed to maintain density-dependent logistic growth, during which the carrying capacity of green algae and moss were determined by the soil N content of the previous time step. The carrying capacity of green algae was calculated to be N(t) / Na, since green algae were assumed to take up all available soil N for growth. The carrying capacity for moss, on the other hand, was calculated to be [N(t) / (10 × Nm)], based on our assumption that moss is less competitive for N than green algae. Therefore, the daily biomass densities of the three BSC components were calculated as (Code S5-2):

$$C(t+1) = P_{uc} + P_{cc} \times \left[C(t) + r_c \times C(t) \times \left(1 - \frac{C(t)}{K_c} \right) \right]$$

$$A(t+1) = P_{ua} + P_{ca} \times C(t) + P_{aa} \times \left[A(t) + r_a \times A(t) \times \left(1 - \frac{A(t)}{\left(\frac{N(t)}{Na}\right)} \right) \right]$$

$$M(t+1) = P_{um} + P_{am} \times A(t) + P_{mm} \times \left[M(t) + r_m \times M(t) \times \left(1 - \frac{M(t)}{\left(\frac{N(t)}{Nm \times 10}\right)} \right) \right]$$

where r_c, r_a and r_m are the growth rates of cyanobacteria, green algae and moss, respectively; K_c is the environmental carrying capacity of cyanobacteria; and $P_{cc} = 1 - D_c - P_{ca}(t)$, $P_{aa} = 1 - D_a - P_{am}(t)$, $P_{mm} = 1 - D_m$.

The daily transition rates at time t were defined as stochastic parameters influenced by the real-time available N in the surface soil. The probability functions of these transition rates are summarized in Table 5-2 (Code S5-3). The model was run 5000 times to simulate the average densities of BSC components during succession and their available N contributions to the system (Code S5-4). One same response scale (RS, ranging from 0.01 to 2) was multiplied by all transition rates for model sensitivity evaluation. In order to evaluate the sensitivity of model responses to daily transition rates, elasticity analyses were performed on the natural spontaneous BSC colonization rate, transition proportion, and the transition rate response scale using the equation:

$$\text{Elasticity } (E_i) = \frac{\partial R}{\partial V_i} \times \frac{V_i}{R}$$

where R is the response and V is the variable (Code S5-5).

5.2.1.4 Simulation of the effects of environmental restrictions and inoculum size

In order to describe BSC succession under non-optimal conditions, we carried out another series of simulations of biomass densities by applying decreased growth rates and increased local extinction rates to all BSC compartments. For a given simulation, the same percentage (designated as the environmental restriction factor, ERF) of increase and decrease was applied as a specific level of environmental restriction (Code S5-6). We also simulated the natural colonization and succession of BSCs without cyanobacterial inoculation at different levels of available N in surface soils (Code S5-7). In addition, BSC successions with a wide range of

average daily surface soil N loss rates were simulated to indicate distinct soil N dynamics under different environmental conditions (Code S5-8). These simulations were run for 1000 days to enable equilibrium-state characterization of BSC successions.

Finally, the net soil available N contribution ($N_{contribution}$) and the effectiveness of inoculated cyanobacteria in contributing soil N (N_{effect}) were evaluated for a 100-day period (typical crop growth duration) as (Code S5-9):

$$N_{contribution} = \sum_{i=1}^{100} N(i) - \sum_{i=1}^{100} N_0(i)$$

$$N_{effect} = N_{contribution} \div C(0)$$

where $\sum_{i=1}^{100} N(i)$ is the sum of daily available N in surface soil with cyanobacteria applied, and $\sum_{i=1}^{100} N_0(i)$ is the sum of daily available N with no initial cyanobacterial inoculum, with C(0) as the initial cyanobacterial inoculum size.

5.2.2 Observation of naturally occurring BSCs in agricultural fields

5.2.2.1 Study area

Our study site was located at the Pennsylvania State University Agronomy Research Farm (GPS coordinates 40.7 -77.9), which has a typical humid temperate continental climate, classified as Dfb in the Köppen-Geiger climate classification (Kottek et al., 2006). During our field observations from September 2014 to August 2015, the weather was coldest in February with an average minimum air temperature of -13.1℃. The weather was warmest in July with an average maximum air temperature of 26.4℃ (Figure S5-1). The total annual precipitation from 9/1/2014 to 8/31/2015 was 958.4 mm.

BSCs were observed in corn fields managed with either no-till or conventional tillage. Both types of tillage were considered because although conventional tillage is most common in United States, more and more farmers are adopting no-till management practiced to reduce soil erosion and increase C sequestration (Alvarez, R., 2005). Soils in all fields are classified as Hagerstown silt loam (fine, loamy, mixed mesic Typic Hapludalfs (Soil Survey Staff, 2010). These fields had been in continuous corn cultivation for at least ten years prior to the observation year. All fields had two fertilizer applications in May and June in every crop season. Therefore, no-till plots received 185 kg N ha^{-1} in 2014 and 130 kg N ha^{-1} in 2015, while conventionally tilled plots received 112 kg N ha^{-1} in 2014 and 130 kg N ha^{-1} in 2015. During our observational period, corn was harvested on November in 2014 and planted in May in 2015.

5.2.2.2 Quantification of areal coverage by BSCs

Three no-till and three conventionally tilled fields were selected and systematically sampled for BSC observation. In each field, three locations at 6, 9 and 12 m along one selected inter row (row was 15 m from the field corner) were chosen for GPS coordinates (Table S5-1), quadrat placement, and photography. For data collection at each location, a 50 cm by 50 cm white PVC frame was placed on the ground at the exact site marked on the ground. Data collection on BSC coverage was obtained biweekly within the same time period (100-400 pm) for one year from 9/10/2014 to 8/21/2015. All photos were taken with a Canon EOS REBEL T2i digital camera with EF-S 18-55 mm lens. Shutter and aperture were adjusted based on light conditions.

Photographs were color-balanced by using the brightest area of the white frame as the white color internal standard. The area inside the frame was selected and standardized to a 1000 × 1000 pixel bitmap image (using Photoshop 7.0). The RGB (red, green, blue) coordinates of all pixels in each bitmap image were obtained and converted to HSV (hue, saturation, brightness)

coordinates (Code S5-10) (Agoston, 2005; Joblove and Greenberg, 1978). Pixels corresponding to the areas covered by any BSC component (cyanobacteria, algae, or moss) were selected when the HSV coordinates were as follows: $55 \leq H \leq 195$, $S \geq 0.15$ and $0.15 < V < 0.7$. Pixels corresponding to areas dominated by cyanobacterial biomass were distinguished by the coordinates $85 \leq H \leq 195$, $S \geq 0.15$ and $0.15 < V < 0.7$. These boundaries were carefully determined and confirmed with 20 randomly selected photographs. This was achieved by first manually changing the colors of the pixels identified as 'BSC pixels' based on their HSV values and confirming that these colored areas corresponded to BSCs in the original photographs (Code S5-11). Finally, the percentages of BSC and cyanobacterial coverage in each quadrat were determined by dividing the number of qualified pixels by 1000000, which was the total pixel number in each bitmap image (Code S5-10). The average coverage of BSCs in three quadrats in each field was used as the sample observation value.

5.2.2.3 Monitoring other surface soil properties

The surface soil temperature at 0-5 cm was measured next to each quadrat as it was being photographed. The average of three measurements was calculated as the field temperature at each time point. During the period of observation, soil samples were collected from the surface 0-1 cm near the quadrats. Samples were collected by pressing a sterile petri dish lid (5-cm diameter) and lifting it off with a spatula. Soil samples from each field were pooled for measurement of soil gravimetric water content (ASTM D2216, 1998).

Additional soil samples, either with no distinguishable BSCs or full coverage by cyanobacterial/algal BSCs were collected and pooled as described above on 10/8/2014, 4/2/2015, and 8/4/2015. These time points corresponded to the time after crop maturity while plants remained standing in the field; after soil thawing and before application of fertilizer; and a late

stage of corn growth, respectively. Soil samples were air dried and analyzed for total N content, ammonium-N and nitrate-N by the Agricultural Analytical Services Laboratory at the Pennsylvania State University. The latter two soil properties were measured only for samples collected on 4/2/2015, and 8/4/2015.

5.2.2.4 Data analysis

All results were analyzed by SPSS 16.0 (Norusis, 2008). Observations from no-till and conventionally tilled fields were compared with two sample t-comparisons (H_0: $\mu_1 = \mu_2$, $p < 0.05$).

5.3 Results

5.3.1 Simulated BSC and available N dynamics under optimum conditions

Starting with a cyanobacterial inoculum of 1000 mg m^{-2} in a 1000-day simulation, the three BSC compartments - cyanobacteria, green algae, and moss - reached equilibrium densities of 3.9 g m^{-2}, 2.8 g m^{-2}, and 1.5 g m^{-2}, respectively. These equilibrium densities were achieved under both initial N conditions (0 or 2000 mg m^{-2}) (Figure 5-2). Meanwhile, the available soil N content at the equilibrium state was 0.2 g m^{-2} whether the initial N availability was 0 or 2000 mg m^{-2}.

Under both initial N conditions, cyanobacterial biomass increased quickly, reaching equilibrium at about 30 days. In contrast, the pre-equilibrium dynamics of green algae and moss differed markedly (Figure 5-2A and B). At an initial soil N content of 0 mg m^{-2}, the biomass of green algae and moss increased slowly before reaching their equilibrium densities, with the day of moss appearance typically exceeding 70 days. In contrast, at an initial soil N content of 2000

mg m^{-2}, significant increases of green algae and moss occurred in the early stages of growth (Figure 5-2C and D). In the presence of soil N, green algae and moss appeared soon after cyanobacterial inoculation and grew rapidly during the first 49 (for green algae) or 99 (for moss) days, then they declined slowly to equilibrium density. The biomass density of green algae was highest at 10.4 g m^{-2} on day 49, while the biomass density of moss was highest at 3.6 g m^{-2} on day 99.

Based on elasticity analyses initiated with a cyanobacterial inoculum of 1000 mg m^{-2}, the equilibrium density and succession of each BSC biotic compartment were not sensitive to changes in any of the three variables tested which corresponded to the stochastic BSC transition rates (Table 5-3). These variables were the natural BSC colonization rate due to wind or water; the daily transition proportion; and the response scale of transition probability. Linear relationships were observed between all pairs of variables and responses (data not shown). Although all elasticity values were lower than 0.003, the simulated BSC dynamics were more sensitive to changes in the daily transition proportions (Tca and Tam). These daily transition proportions had positive correlations with the equilibrium densities of green algae and moss, but a negative correlation with the day of moss appearance.

5.3.2 Simulated environmental effects on BSC succession and available N

BSC succession under environmental restrictions was simulated under different ERFs, which lower growth rates and higher local extinction rates at the same percentage (Figure 5-3A). Under initial conditions of 0 mg m^{-2} available N and 1000 mg m^{-2} cyanobacterial inoculum, the days of appearance for both green algae and moss increased slowly at first and then more rapidly as environmental restrictions increased. The equilibrium biomass densities of each BSC compartment decreased as the environmental restriction percentages increased from 0% to 64%.

When the environmental restriction percentages were equal to or larger than 65%, the equilibrium densities for each compartment were less than 0.05 mg m^{-2}, which meant that self-sustaining BSC communities would not be formed.

This observed threshold (65%) for formation of self-sustaining BSC communities can also be estimated mathematically from the cyanobacterial equilibrium biomass density (here designated as C^*) as:

$$C^* = P_{uc} + (1 - D_C - P_{ca}) \times \left[C^* + r_c \times C^* \times (1 - \frac{C^*}{K_c})\right]$$

Here, Puc and Pca are close to zero under the threshold environmental restriction conditions, because soil available N is comparatively low. Therefore, after omitting Puc and Pca, we can calculate C^* as:

$$C^* \approx (1 + \frac{1}{r_c} + \frac{1}{r_c \times (1 - D_C)}) \times K_c$$

where C^* should be larger than zero if the BSC communities are self-sustaining. Therefore, the relationship between cyanobacterial growth rate (r) and local extinction rate (D) for self-sustaining BSCs can be simplified as: $r_c > D_C / (1 - D_C)$. This reflects the fact that cyanobacteria are the only BSC components that fix N_2 and they are the key drivers of BSC succession and self-sustenance.

In the simulation model, the initial available soil N content exerted a marked effect on natural colonization and succession of BSCs, i.e., without initial inoculum (Figure 5-3B). As the initial available soil N increased, the first appearance of BSC components became earlier, indicating acceleration of BSC succession. The sequential order of natural colonization on soil with 0-110 mg m^{-2} available N was cyanobacteria → green algae → moss. However, this sequence changed to green algae → cyanobacteria → moss when soil available N was equal to or larger than 120 mg m^{-2}. As shown in Figure 5-3B, the biomass densities at the end of the 1000-day simulation increased as soil initial available N increased from zero to 1000 mg m^{-2}, especially

when the initial available N increased from 0-500 mg m^{-2}. This was because BSC compartments did not reach their equilibrium densities by the day 1000 under such initial conditions (an example is shown in Figure S5-2A). If initial soil available N was higher than 1000 mg m^{-2}, the biomass densities of BSC components at the end of the simulation were the same as their corresponding equilibrium biomass densities (as mentioned in section 5.3.1).

Based on our 1000-day simulation initiated with 1 g m^{-2} cyanobacterial inoculum, the average daily soil N loss rate had no significant effect on the cyanobacterial equilibrium biomass density (Figure 5-3C). However, if the average soil N loss rate increased from 0.001 to 0.01 g N loss g^{-1} total available N day^{-1}, the equilibrium biomass densities of green algae and moss decreased dramatically (~78%). On the other hand, the equilibrium biomass densities of green algae and moss decreased more slowly when the average daily soil N loss rate was increased from 0.01 to 0.1 g N loss g^{-1} total available N day^{-1}. This two-stage relationship was also observed for soil available N at the equilibrium state. Finally, our simulation also indicated that the increase of surface soil N loss could decrease the rate of BSC succession, especially by delaying the appearance of moss.

5.3.3 Potential N contribution under different model initializations

Model simulations were run for 100 days to evaluate the net N contributions of inoculated cyanobacteria during one growing season under varying conditions of initial available N in surface soil and cyanobacterial application rate. These ranges were 0.1-10 g N m^{-2} (equivalent to 10-1000 ppm N on soil surface) and 0.05-5 g dry biomass m^{-2}, respectively. Across all combinations, the net N contributions during the 100-day simulation ranged from 1.5-22.4 g m^{-2} (Figure 5-4A). More specifically, at a typical inoculum size of 1 g m^{-2}, net N contributions ranged from 3.6-12.5 g N m^{-2}. When initial soil available N was high (ca. 6-10 g m^{-2}), the net N

contribution of cyanobacteria increased significantly as the inoculum size increased. However, this effect was moderated as the initial soil available N decreased. As shown in Figure 5-4B, the simulated effectiveness of the cyanobacterial net N contribution (i.e., N_2 fixation combined with N retention by assimilation) ranged from 1.5-66.1 mg N mg^{-1} of cyanobacterial biomass. The N contribution effectiveness decreased very quickly at first and then more slowly as the cyanobacterial inoculum size increased. The curvatures of such responsive relationships decreased as the initial soil available N increased. The model simulations here were all conducted under optimum conditions sustained for the entire 100-day period. Under actual field conditions, however, the N contributions by cyanobacteria after application would be lower than these simulated estimates due to non-optimum and more varying conditions.

5.3.4 Dynamics of naturally formed BSCs in agricultural fields

Our system of processing and color coding BSC images from field surfaces could differentiate soil areas of cyanobacteria (colorized blue) and green algae/moss (colorized red) (Figure S5-3). Biweekly analysis of images from September 2014 to August 2015 showed that total coverage of BSCs (combined red and blue) ranged from 0.0%-97.4% of the 2500-cm^2 quadrat area across all photographs (Figure 5-5). Quadrat coverage dominated by cyanobacteria (blue only) ranged from 0.0%-57.1%. At all sampling times, cyanobacteria comprised 20-30% of the BSC area within the quadrat in both no-till and conventionally tilled fields. BSC coverage persisted into November 2014, when coverage began to decline, after which BSCs sporadically presented through December until full snow cover. Then, BSCs re-appeared in next June, reaching highest coverage in August. Overall, the coverages of total BSCs and cyanobacteria dominated BSCs were higher in conventionally tilled fields than in no-till fields during periods of crop growth.

5.3.5 Soil temperature, moisture and N conditions for BSCs in agricultural fields

Mean gravimetric water contents of surface soils ranged from 0.18-0.69 g water g^{-1} soil in no-till fields and from 0.03-0.55 g water g^{-1} soil in conventionally tilled fields (Figure 5-6A). During the year of observations, no-till fields had higher surface soil water content than conventionally tilled fields most of the time. In addition, the average surface soil temperatures ranged from 0.2-24.5℃ in no-till fields and from 0.1-27.4℃ in conventionally tilled fields (Figure 5-6B). During most of the year, surface soil temperatures in tilled fields were slightly higher (by 0.5℃ or less) than in no-till fields, except in late May and June 2015, when soil temperatures in conventionally tilled fields were 3-4℃ higher.

Soils in the no-till and conventionally tilled fields had marked differences in background soil N due to previous management histories. Mean total N contents of non-BSC-covered surface soils in no-till fields were 0.30%, 0.34%, and 0.31% at the three sampling times (Figure 5-7A). These values were 1.6, 1.9 and 2 times higher than the total N contents in surface soils of conventionally tilled fields (Figure 5-7B). In regard to soil nitrate-N and ammonium-N, no significant differences were observed between BSC-free soil in no-till and conventionally tilled fields on 4/2/2015 and 8/4/2015 (Figure 5-7 C and D). Also, no significant difference was observed between the non-BSC and cyanobacterially dominated BSCs in total N, ammonium-N and nitrate-N contents (Table S5-2).

5.4 Discussion

5.4.1 BSC succession under nutrient limited conditions

Patterns of natural BSC colonization and succession obtained with our simulation model are similar to previous studies describing BSCs in ecosystems with low soil nutrient contents. In a survey of dryland BSCs, Bowker and coworkers found a significant correlation between the abundance of N_2-fixing cyanobacteria and soil Mn and Zn, when these micronutrients were limited (Bowker et al., 2005). Assuming that no micronutrients were limited, we observed a similar linear correlation between biomass density and soil N in our model simulations (R^2 = 0.98, $p < 0.000$), when soil available N was ≤ 20 ppm and no cyanobacteria were inoculated (Figure 5-3B). In another study of BSC succession on soils recently exposed by glacial retreat, it was observed that N_2-fixing cyanobacteria colonized first when the initial soil ammonium and nitrate N concentrations were less than 1 ppm (Schmidt et al., 2008). Moreover, chlorophyll a levels increased about 4.4 times (0.5 to 2.2 μg g^{-1} dry soil) during the first four years of BSC succession. This increase is consistent with simulated results obtained with our model under conditions of no initial biomass or available soil N and the assumption that BSC succession is three times faster under optimum conditions (ca. biomass density increased from 0.31 g m^{-2} to 1.36 g m^{-2} from day 122 to day 487) (Figure S5-2).

5.4.2 Model insights for BSC succession on agricultural soil

Unlike resource-limited soils in dryland regions, agricultural soils offer more favorable conditions for cyanobacerial growth, including more moderate temperatures, greater moisture, and more nutrients, especially when they receive large amounts of N from fertilizers. Accordingly, our model offers several new insights on BSC dynamics in temperate

agroecosystems in more humid regions. The first insight relates to BSC response to soil N. In arid and semiarid ecosystems around the world, the average biomass of BSCs is about 224 mg m^{-2} (Büdel, 2002). In our model, however, the simulated equilibrium biomass density of BSCs was much higher (3.2 g m^{-2}) under conditions of sufficient available soil N (ca. > 10 ppm) and an environmental restriction factor corresponding to increased optimum local extinction rates and decreased optimum growth rates for all BSC components by 50%. BSC biomass densities are therefore increased when soil N is available.

The second insight relates to BSC development rate. Natural formations of BSCs typically take 5-20 years in arid and semiarid ecosystems (Langhans et al., 2009). Nevertheless, it has been confirmed in multiple dryland studies that BSC succession can be accelerated by increased soil moisture (from irrigation or rain) and/or additional cyanobacterial application (Chen et al., 2006; Dojani et al., 2011; Wang et al., 2009). Similarly, in our model, the cyanobacterial component reached its equilibrium biomass density after 30 days following a 1 g m^{-2} inoculum size on soil under optimum conditions (Figure 5-2 B and D).

The third insight is the role of cyanobacteria in modulating soil N. When soil available N is high, cyanobacteria reduce their N_2 fixation, (Peng, Chapter 3), but they still contribute to improved soil N retention by assimilating excess soil N and retaining inorganic N in extracellular polysaccharides (Peng, Chapter 4). Such N immobilization processes by BSCs following fertilization events can reduce N losses from soil and release N gradually for later crop uptake. Based on our model simulation, inoculated cyanobacteria can contribute significantly to N use efficiency, especially in soils receiving high amounts of fertilizer.

5.4.3 Potential feasibility and benefits of cyanobacteria application in agroecosystems

Soils of agroecosystems are highly disturbed by human activities. Agricultural practices can result in scraping and displacement of soil surfaces by tillage or mowing equipment, compression by wheel tracks, and exposure to herbicides, all of which could adversely affect BSC succession and regeneration (Zaady et al., 2013). Our field observations confirmed that BSCs exposed to adverse conditions can regrow on agricultural soils. The higher percentages of BSC coverage in conventionally tilled fields than in no-till fields during the crop growing season was probably due to the fact that heavy crop residues in the no-till fields could restrict the exposure of BSCs to sunlight.

During our yearlong field observation period, we also saw a 50-day lag time between the start of favorable environmental condition (5/26/2015, when fields were fertilized and soil temperature was > 20ºC), and the appearance of significant BSCs on soil (7/8/2015, total BSC coverage > 7%). As the result of this lag, the naturally colonized BSCs would contribute little to soil N retention in the first 50 days of corn growth, which is a period of severe soil N loss during the growing season (Jaynes et al., 2001). Based on our model simulation, the application of small amounts of cyanobacteria with N fertilizer could dramatically accelerate early BSC succession. For example, with 200 ppm initial available N and 1g m^{-2} cyanobacteria inoculum, the simulated total BSC biomass density after two weeks' growth under optimum conditions was 3639 mg m^{-2} (2761 mg m^{-2} cyanobacteria + 861 g m^{-2} green algae + 16 mg m^{-2} moss) (Figure 5-2D). This is about 20 times the density of of naturally colonized BSC biomass, which was simulated as 185 mg m^{-2} (71 mg m^{-2} cyanobacteria + 105 mg m^{-2} green algae + 9 mg m^{-2} moss) under the same conditions (Figure S5-2B). Therefore, we propose that cyanobacterial applications to agricultural soil (with or soon after fertilizer application) can significantly increase N use efficiency by

effectively boosting the establishment of BSCs and eliminating the lag time for BSC establishment.

5.4.4 Comparisons of model simulations and field observations

The BSC succession order (green algae → cyanobacteria → moss) simulated by the model under high initial soil available N content was well supported by our BSC observations in the field as well as by natural BSC development in greenhouse soil pot studies (unpublished results, Figure S5-4). We also compared our model simulation results to changes in biomass densities observed in no-till and conventionally tilled fields. As shown in Figure 5-8, we performed model simulations over 71-days for both no-till and conventionally tilled fields by applying fitted environmental restriction factors (ERF) and incorporating soil N contents calculated from fertilization events that occurred during the observation year. The model simulations were consistent with BSC biomass and coverage observed in both no-till and conventionally tilled field conditions. Based on the two simulations, an initial 1g m^{-2} inoculum of cyanobacteria could contribute 8.1 kg ha^{-1} net available N and store 2.8 kg ha^{-1} N in BSC biomass in the no-till field. In the conventionally tilled field, this inoculum could contribute 3.3 kg ha^{-1} net available N and store 9.2 kg ha^{-1} N in BSC biomass. As cells die, the N stored in BSC biomass could be further mineralized, thereby contributing additional N during the remaining portion of the growing season and after crop harvest. This model was developed and parameterized using data from DG1 growth experiments described in Chapters 2, 3, and 4. Our results supported our hypothesis that the model would be capable of predicting BSC responses and their potential N contributions following DG1 application in agricultural fields.

Our simulation model consolidated the effects of several potentially restrictive environmental factors into a single factor, which was applied uniformly to all three BSC

components. However, in reality, moss, green algae, and cyanobacteria may have different adaptive characteristics in response to environmental constraints and successional stages (Housman et al., 2006a). Moreover, most of the estimated transition parameters used in our model and their relationships with soil N have not been validated by experiments. Therefore, in order to complete model parameterization, more greenhouse and field studies manipulating different environmental factors and cyanobacterial treatments are needed.

5.5 Conclusions

In this study, BSC succession by cyanobacteria, green algae, and moss in an agricultural system was investigated through modeling and field observations. Our stochastic Markov succession model showed that the inoculation of cyanobacteria could significantly accelerate the growth and succession of BSCs on agricultural soil. Based on this model, environmental restrictions on growth rate and local extinction rate are crucial for predicting long-term BSC self-sustenance; while soil initial available N influences BSC succession rate and sequence. Our observations of natural BSCs during a one-year period in agricultural fields provided evidence for renewable cyanobacterial growth on agricultural soils, and they supported our model simulations. Integrating field observations with model simulations showed that cyanobacterial inoculation, either at the same time or soon after soil N fertilization, could make significant net N contributions and increase soil N use efficiency in temperate agroecosystems.

5.6 Acknowledgement

The author thanks Dr. Armen Kemanian, Penn State Dept of Plant Science and Dr. Katriona Shea, Penn State Dept of Biology, for their helpful advice on model development; and

Dr. Qing Xu, Beijing Institute of Biotechnology, for his help in coloring the specific pixels of selected BSC photographs.

5.7 References

Agoston, M.K., 2005. Computer graphics and geometric modeling. Springer, Curpertino, CA.

Alvarez, R., 2005. A review of nitrogen fertilizer and conservation tillage effects on soil organic carbon storage. Soil Use and Management 21, 38-52.

ASTM D2216, 1998. Standard Test Method for Laboratory Determination of Water (Moisture) Content of Soil and Rock by Mass. American Society for Testing and Materials, Philadelphia, PA.

Belnap, J., 2002. Nitrogen fixation in biological soil crusts from southeast Utah, USA. Biology and Fertility of Soils 35, 128-135.

Belnap, J., Eldridge, D., 2001. Disturbance and recovery of biological soil crusts, Biological soil crusts: structure, function, and management. Springer, pp. 363-383.

Belnap, J., Lange, O., 2001. Biological soil crusts: structure, function and management. Springer, New York.

Bowker, M.A., 2007. Biological soil crust rehabilitation in theory and practice: an under exploited opportunity. Restoration Ecology 15, 13-23.

Bowker, M.A., Belnap, J., Davidson, D.W., Phillips, S.L., 2005. Evidence for micronutrient limitation of biological soil crusts: importance to arid-lands restoration. Ecological Applications 15, 1941-1951.

Bowker, M.A., Maestre, F.T., Eldridge, D., Belnap, J., Castillo-Monroy, A., Escolar, C., Soliveres, S., 2014. Biological soil crusts (biocrusts) as a model system in community, landscape and ecosystem ecology. Biodiversity and Conservation 23, 1619-1637.

Bowker, M.A., Maestre, F.T., Escolar, C., 2010. Biological crusts as a model system for examining the biodiversity–ecosystem function relationship in soils. Soil Biology and Biochemistry 42, 405-417.

Breen, K., Levesque, E., 2006. Proglacial succession of biological soil crusts and vascular plants: biotic interactions in the High Arctic. Botany 84, 1714-1731.

Büdel, B., 2002. Diversity and ecology of biological crusts, Progress in Botany. Springer, pp. 386-404.

Castillo, H., Bruns, M.A., 2001. Cyanobacterial diversity in agricultural soils, Ninth International Symposium in Microbial Ecology, Amsterdam, The Netherlands.

Chen, L., Xie, Z., Hu, C., Li, D., Wang, G., Liu, Y., 2006. Man-made desert algal crusts as affected by environmental factors in Inner Mongolia, China. Journal of Arid Environments 67, 521-527.

Choudhury, A.T.M.A., Kennedy, I.R., 2004. Prospects and potentials for systems of biological nitrogen fixation in sustainable rice production. Biology and Fertility of Soils 39, 219-227.

Dhar, D., Prasanna, R., Pabbi, S., Vishwakarma, R., 2015. Significance of Cyanobacteria as Inoculants in Agriculture, in: Das, D. (Ed.), Algal Biorefinery: An Integrated Approach. Springer International Publishing, pp. 339-374.

Dojani, S., Büdel, B., Deutschewitz, K., Weber, B., 2011. Rapid succession of biological soil crusts after experimental disturbance in the Succulent Karoo, South Africa. Applied Soil Ecology 48, 263-269.

Elbert, W., Weber, B., Burrows, S., Steinkamp, J., Budel, B., Andreae, M.O., Poschl, U., 2012. Contribution of cryptogamic covers to the global cycles of carbon and nitrogen. Nature Geoscience 5, 459-462.

Gotelli, N.J., 1995. A primer of ecology. Sinauer Associates Incorporated, Sunderland, MA.

Hashem, M.A., 2001. Problems and prospects of cyanobacterial biofertilizer for rice cultivation. Functional Plant Biology 28, 881-888.

Horn, H.S., Cody, M.L., Diamond, J.M., 1975. Markovian properties of forest succession, Harvard University Press, Cambridge, MA, 196-211.

Housman, D., Powers, H., Collins, A., Belnap, J., 2006a. Carbon and nitrogen fixation differ between successional stages of biological soil crusts in the Colorado Plateau and Chihuahuan Desert. Journal of Arid Environments 66, 620-634.

Housman, D.C., Powers, H.H., Collins, A.D., Belnap, J., 2006b. Carbon and Nitrogen fixation differ between successional stages of biological soil crusts in the Colorado Plateau and Chihuahuan Desert. Journal of Arid Environments 66, 620-634.

Jaynes, D., Colvin, T., Karlen, D., Cambardella, C., Meek, D., 2001. Nitrate loss in subsurface drainage as affected by nitrogen fertilizer rate. Journal of Environmental Quality 30, 1305-1314.

Joblove, G.H., Greenberg, D., 1978. Color spaces for computer graphics, ACM siggraph computer graphics. ACM, pp. 20-25.

Kottek, M., Grieser, J., Beck, C., Rudolf, B., Rubel, F., 2006. World map of the Köppen-Geiger climate classification updated. Meteorologische Zeitschrift 15, 259-263.

Lan, S., Wu, L., Zhang, D., Hu, C., 2012. Successional stages of biological soil crusts and their microstructure variability in Shapotou region (China). Environmental Earth Sciences 65, 77-88.

Lan, S., Wu, L., Zhang, D., Hu, C., 2013. Assessing level of development and successional stages in biological soil crusts with biological indicators. Microb Ecol 66, 394-403.

Langhans, T.M., Storm, C., Schwabe, A., 2009a. Biological soil crusts and their microenvironment: impact on emergence, survival and establishment of seedlings. Flora-Morphology, Distribution, Functional Ecology of Plants 204, 157-168.

Langhans, T.M., Storm, C., Schwabe, A., 2009b. Community assembly of biological soil crusts of different successional stages in a temperate sand ecosystem, as assessed by direct determination and enrichment techniques. Microbial Ecology 58, 394-407.

Li, X.-R., Wang, X.-P., Li, T., Zhang, J.-G., 2002. Microbiotic soil crust and its effect on vegetation and habitat on artificially stabilized desert dunes in Tengger Desert, North China. Biology and Fertility of Soils 35, 147-154.

Mišurcová, L., Kráčmar, S., Klejdus, B., Vacek, J., 2010. Nitrogen content, dietary fiber, and digestibility in algal food products. Czech J. Food Sci 28, 27-35.

Norusis, M., 2008. SPSS 16.0 statistical procedures companion. Prentice Hall Press, Upper Saddle River, NJ.

Piorreck, M., Baasch, K.-H., Pohl, P., 1984. Biomass production, total protein, chlorophylls, lipids and fatty acids of freshwater green and blue-green algae under different nitrogen regimes. Phytochemistry 23, 207-216.

Price, G.D., Sültemeyer, D., Klughammer, B., Ludwig, M., Badger, M.R., 1998. The functioning of the CO2 concentrating mechanism in several cyanobacterial strains: a review of general physiological characteristics, genes, proteins, and recent advances. Canadian Journal of Botany 76, 973-1002.

Read, C.F., Elith, J., Vesk, P.A., 2016. Testing a model of biological soil crust succession. Journal of Vegetation Science 27, 176-186.

Schmidt, S.K., Reed, S.C., Nemergut, D.R., Stuart Grandy, A., Cleveland, C.C., Weintraub, M.N., Hill, A.W., Costello, E.K., Meyer, A.F., Neff, J.C., Martin, A.M., 2008. The earliest stages of ecosystem succession in high-elevation (5000 metres above sea level), recently deglaciated soils. Proceedings of the Royal Society of London B: Biological Sciences 275, 2793-2802.

Shaffer, M.J., Delgado, J.A., Gross, C., Follett, R.F., Gagliardi, P., 2010. Simulation processes for the nitrogen loss and environmental assessment package. Advances in nitrogen management for water quality. SWCS, Ankeny, IA, 362-373.

Soil Survey Staff, 2010. Keys to soil taxonomy, 11th ed. USDA-Natural Resources Conservation Service, Washington,DC.

Strauss, S.L., Day, T.A., Garcia-Pichel, F., 2012. Nitrogen cycling in desert biological soil crusts across biogeographic regions in the Southwestern United States. Biogeochemistry 108, 171-182.

Usher, M., 1981. Modelling ecological succession, with particular reference to Markovian models, Vegetation dynamics in grasslans, healthlands and mediterranean ligneous formations. Springer, pp. 11-18.

Usher, M.B., 1979. Markovian approaches to ecological succession. The Journal of Animal Ecology, 413-426.

Wang, W., Liu, Y., Li, D., Hu, C., Rao, B., 2009. Feasibility of cyanobacterial inoculation for biological soil crusts formation in desert area. Soil Biology and Biochemistry 41, 926-929.

Weber, B., Wu, D., Tamm, A., Ruckteschler, N., Rodríguez-Caballero, E., Steinkamp, J., Meusel, H., Elbert, W., Behrendt, T., Sörgel, M., 2015. Biological soil crusts accelerate the nitrogen cycle through large NO and HONO emissions in drylands. Proceedings of the National Academy of Sciences 112, 15384-15389.

Yoshitake, S., Uchida, M., Koizumi, H., Kanda, H., Nakatsubo, T., 2010. Production of biological soil crusts in the early stage of primary succession on a High Arctic glacier foreland. New Phytologist 186, 451-460.

Zaady, E., Arbel, S., Barkai, D., Sarig, S., 2013. Long-term impact of agricultural practices on biological soil crusts and their hydrological processes in a semiarid landscape. Journal of Arid Environments 90, 5-11.

Zechmeister, H.G., Richter, A., Smidt, S., Hohenwallner, D., Roder, I., Maringer, S., Wanek, W., 2008. Total Nitrogen Content and delta (15)N Signatures in Moss Tissue: Indicative Value for Nitrogen Deposition Patterns and Source Allocation on a Nationwide Scale. Environmental Science & Technology 42, 8661.

Zhang, B., Zhang, Y., Zhao, J., Wu, N., Chen, R., Zhang, J., 2009. Microalgal species variation at different successional stages in biological soil crusts of the Gurbantunggut Desert, Northwestern China. Biology and Fertility of Soils 45, 539-547.

Zhang, W., 2014. Research advances in theories and methods of community assembly and succession. Environmental Skeptics and Critics 3, 52-60.

5.8 Figures and tables

Figure 5-1. Simplified loop diagram for BSC succession model. Pcc, Paa, Pmm and Puu are stasis rates; Puc, Pua, Pum, Pca and Pam are transition rates; Dc, Dm and Da are local extinction rates. (C = cyanobacteria; A = green algae; M = moss; U = uncolonized soil with or without dead necromass.)

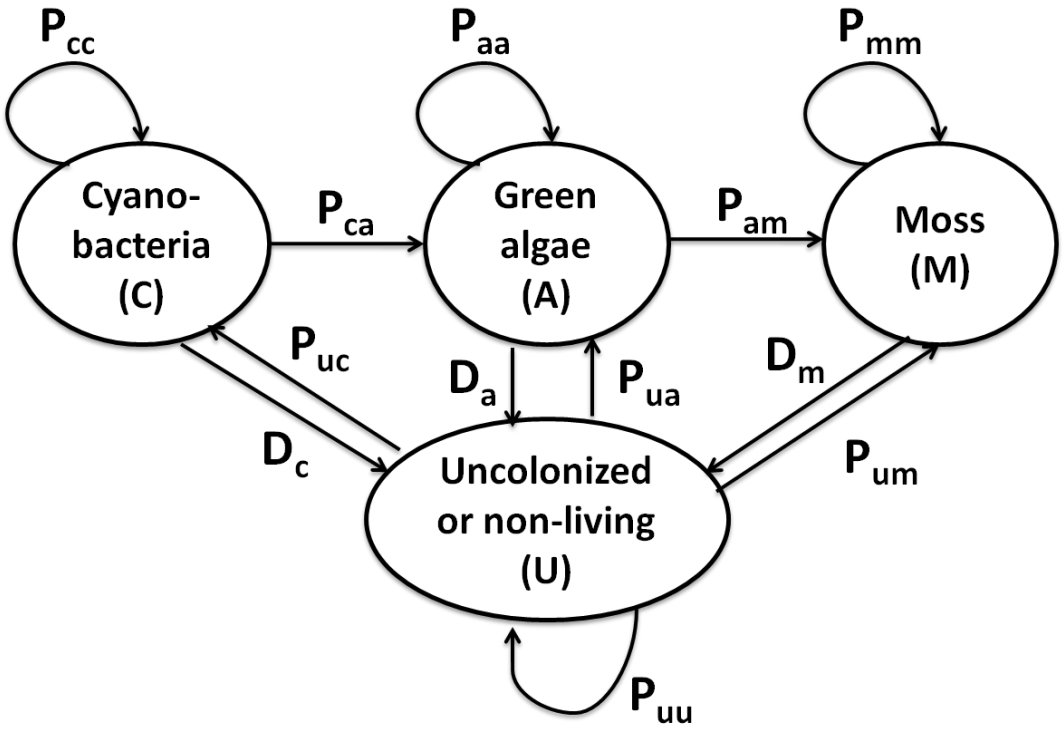

Figure 5-2. Simulated BSC community dynamics under optimum conditions. (A) Initial condition of 1000 mg m^{-2} inoculated cyanobacteria and no available surface soil N, 1000-day simulation. (B) Initial condition of 1000 mg m^{-2} inoculated cyanobacteria and no available surface soil N, 100-day simulation. (C) Initial condition of 1000 mg m^{-2} inoculated cyanobacteria and 2000 mg m^{-2} available surface soil N (equivalent to 200 ppm), 1000-day simulation. (D) Initial condition of 1000 mg m^{-2} inoculated cyanobacteria and 2000 mg m^{-2} available surface soil N, 100-day simulation.

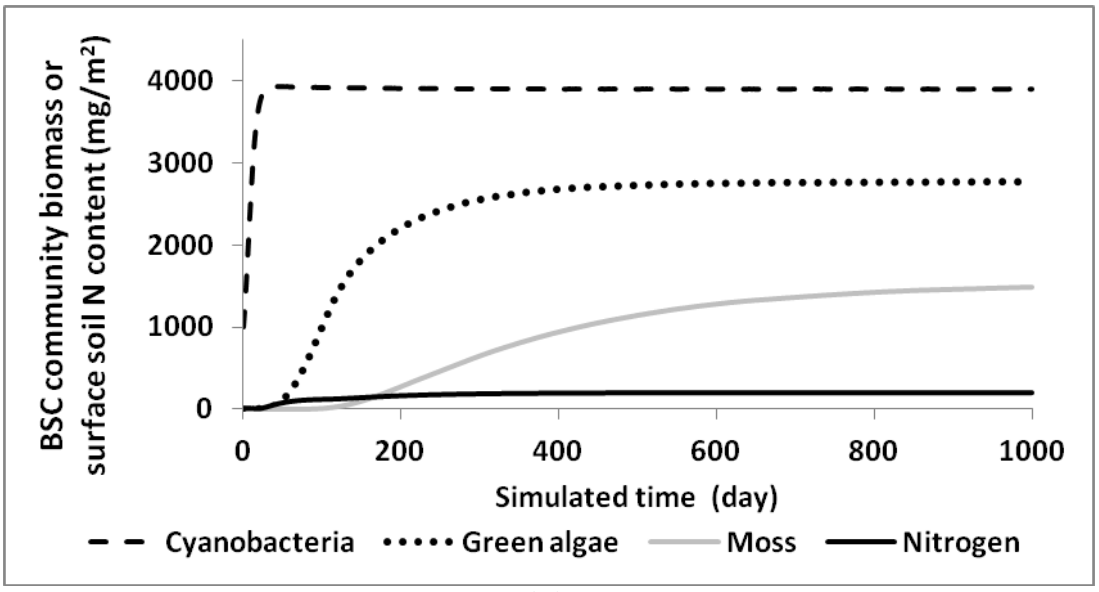

(A)

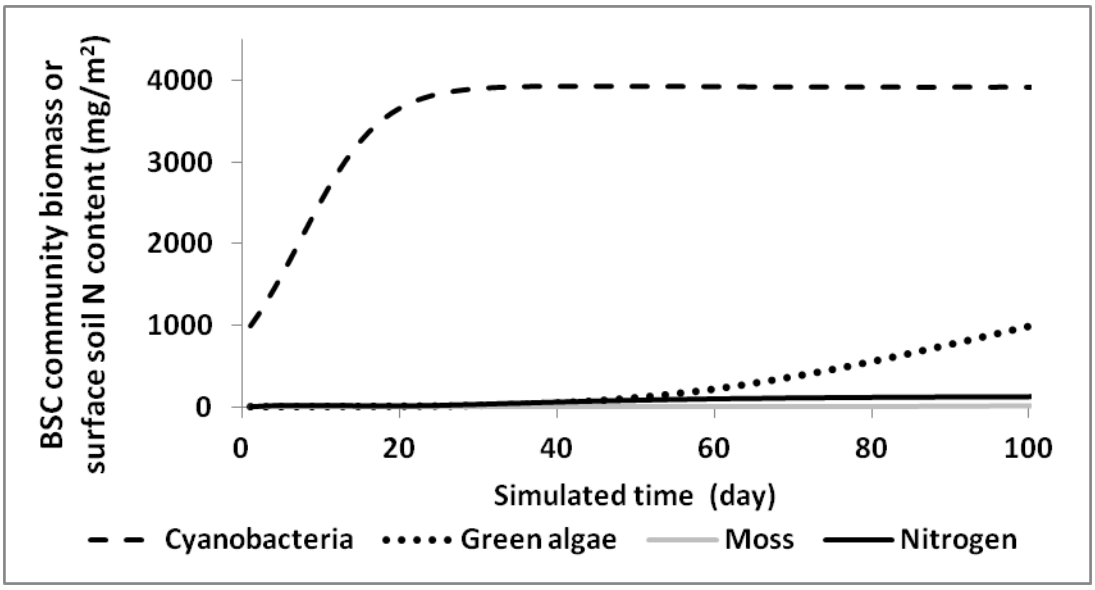

(B)

Figure 5-2. (Continued)

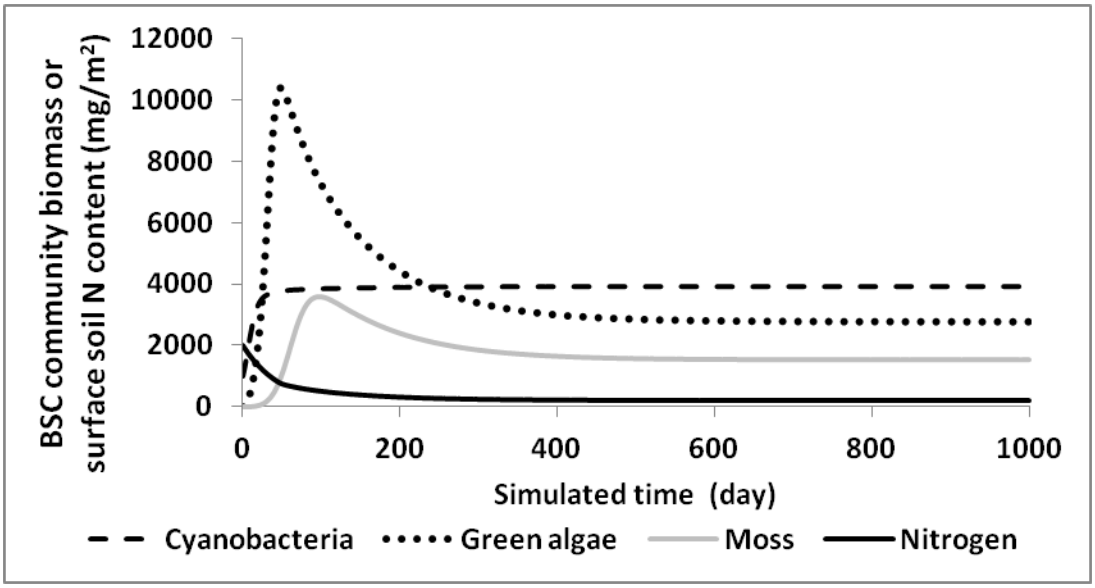

(C)

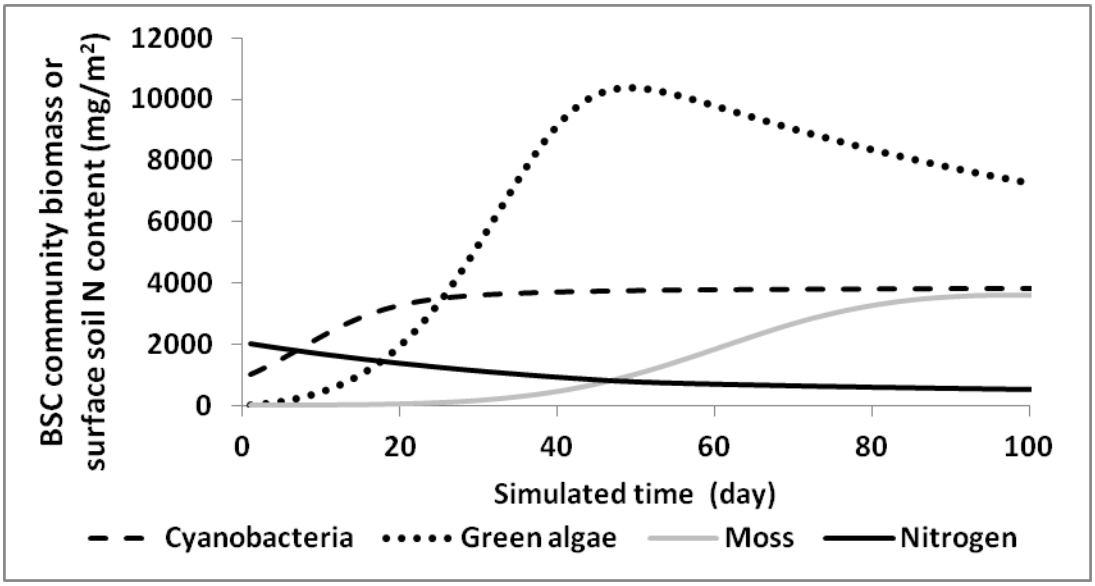

(D)

Figure 5-3. Final biomass densities of different BSC components and available N content in surface soil (refer to the y-axis on left) after the 1000-day simulation, and initial appearance days of distinct BSC components during the succession (refer to the y-axis on right). (A) Initial condition of 1000 mg m^{-2} cyanobacterial inoculum and no available surface soil N under varied intensities of combined environmental stresses. (B) Initial condition of no cyanobacterial inoculum and varied available N contents in surface soil under the optimum condition. (C) Initial condition of 1000 mg m^{-2} cyanobacterial inoculum and no available surface soil N under varied daily soil N loss rate in surface soil.

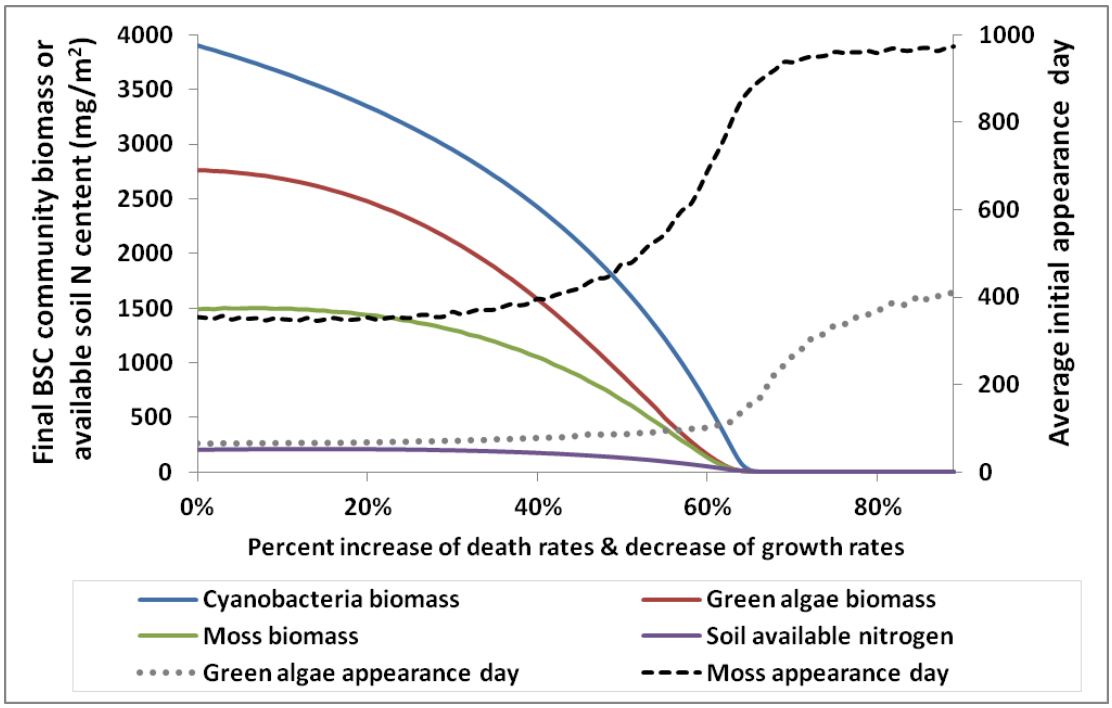

(A)

Figure 5-3. (Continued)

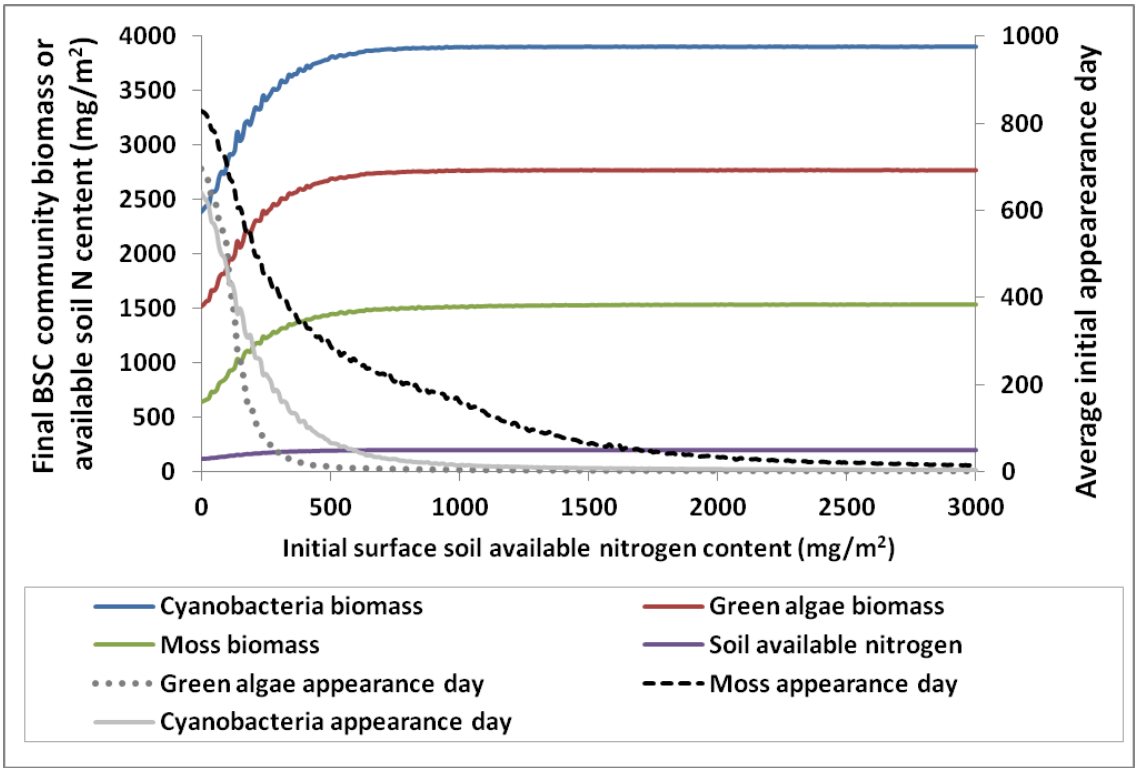

(B)

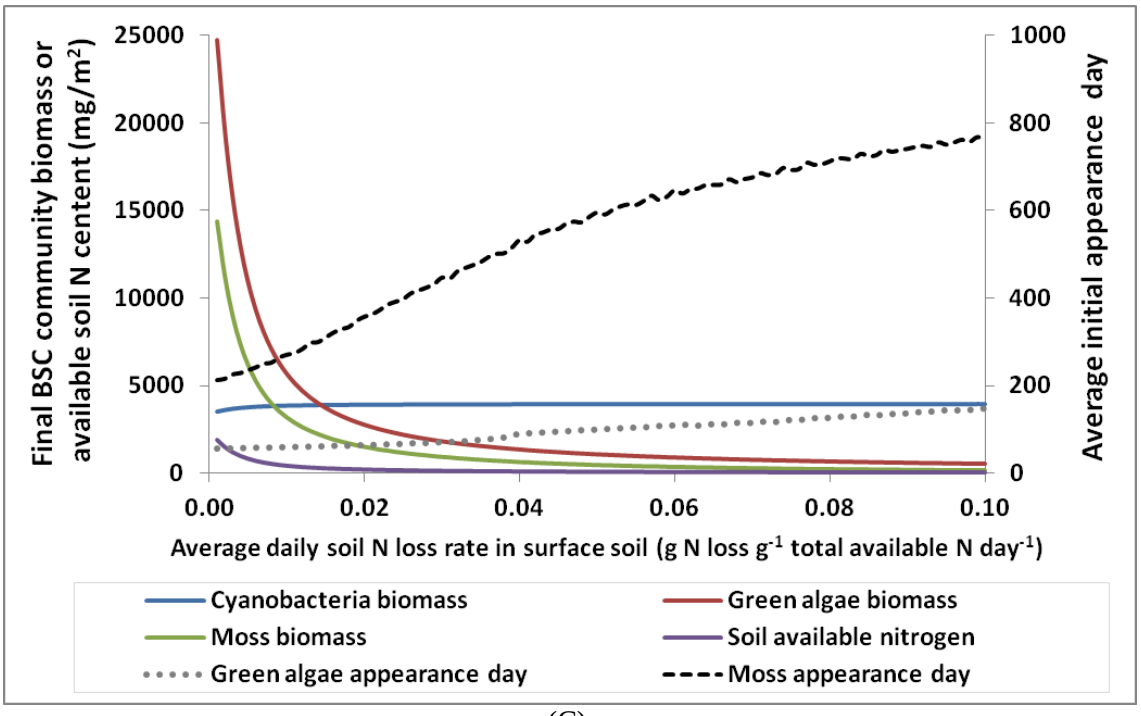

(C)

Figure 5-4. Surface plots of (A) net soil available N contribution of inoculated cyanobacteria, and (B) effectiveness in contributing soil N (mg net N contribution per mg inoculated cyanobacteria) after the 100-day simulation under optimum condition and varied initial conditions (available N contents in surface soil and cyanobacterial inoculum sizes). The surface plots are also projected onto the top XY plane with the same color mapping. In both plots, the 100-10000 mg m^{-2} initial surface soil available N was equivalent to 10-1000 ppm N on soil surface.

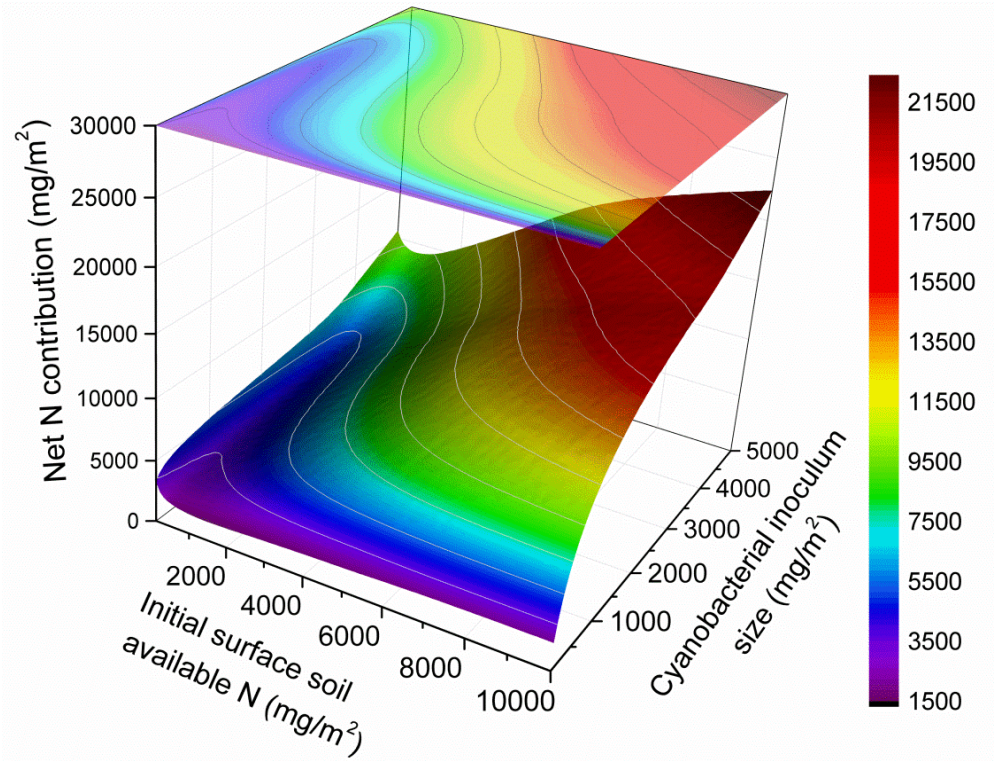

(A)

Figure 5-4. (Continued)

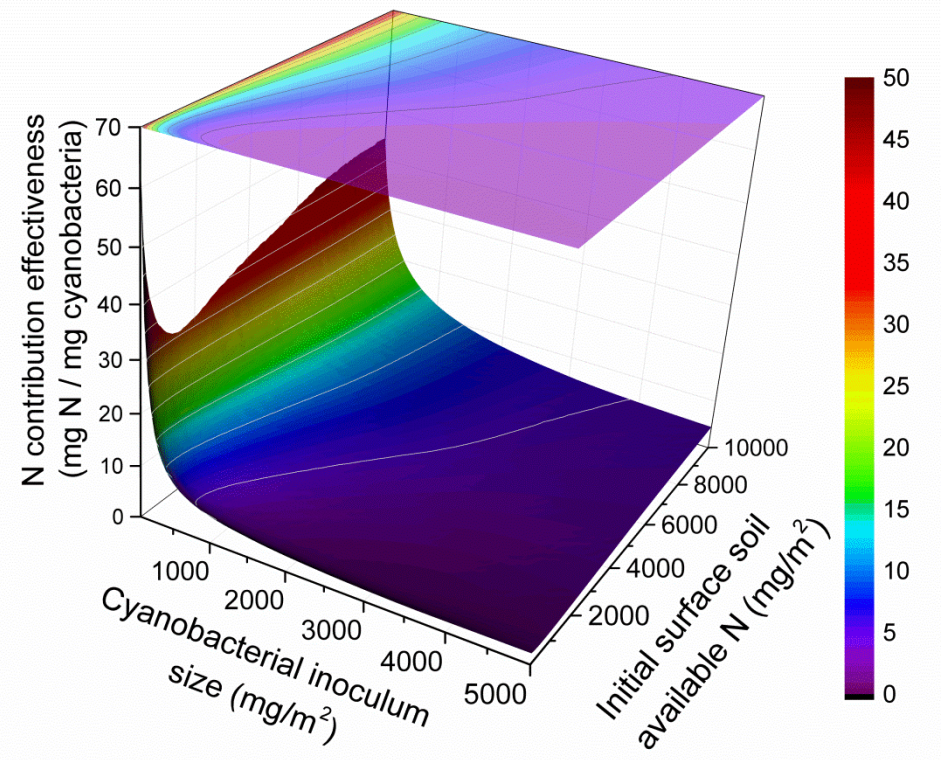

(B)

Figure 5-5. Observed dynamics of BSC coverage of no-till and conventionally tilled corn fields. Error bars are standard error (n = 3). '*' indicates a significant difference in total BSC coverage between the tillage treatments ($p < 0.05$).

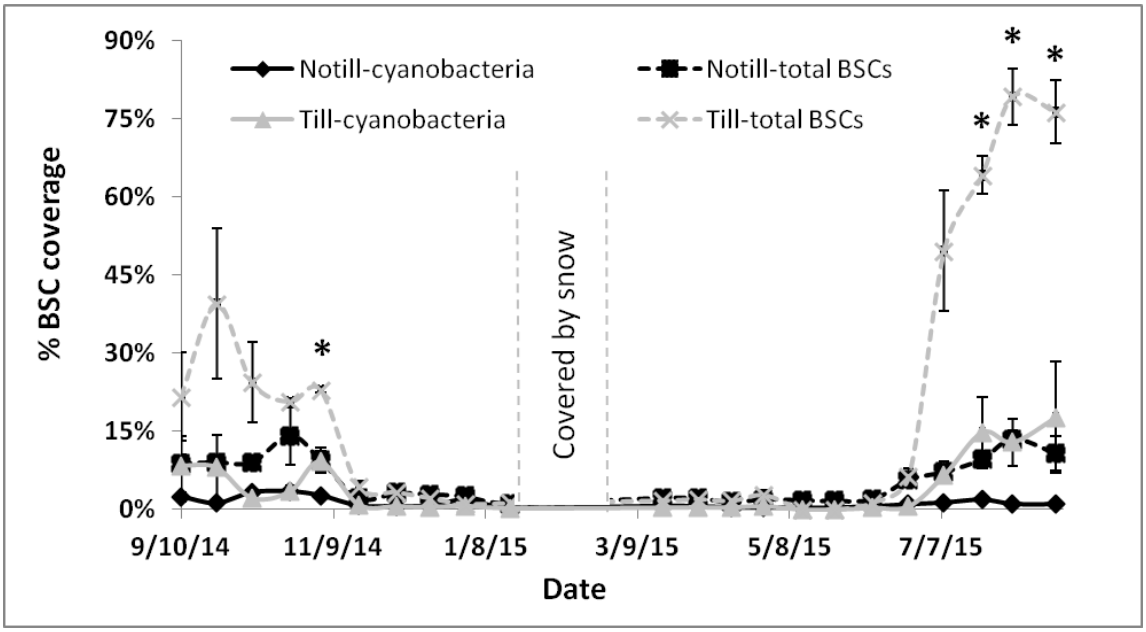

Figure 5-6. Dynamics of (A) surface soil gravimetric water content (0-1 cm) and (B) surface soil temperature in no-till and conventionally tilled corn fields. Error bars are standard error (n = 3).

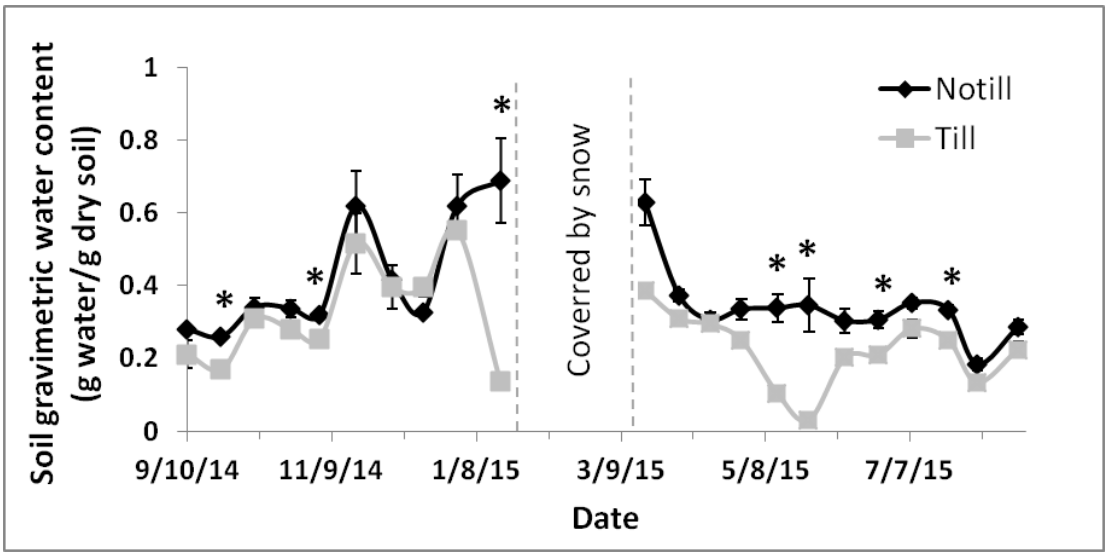

(A)

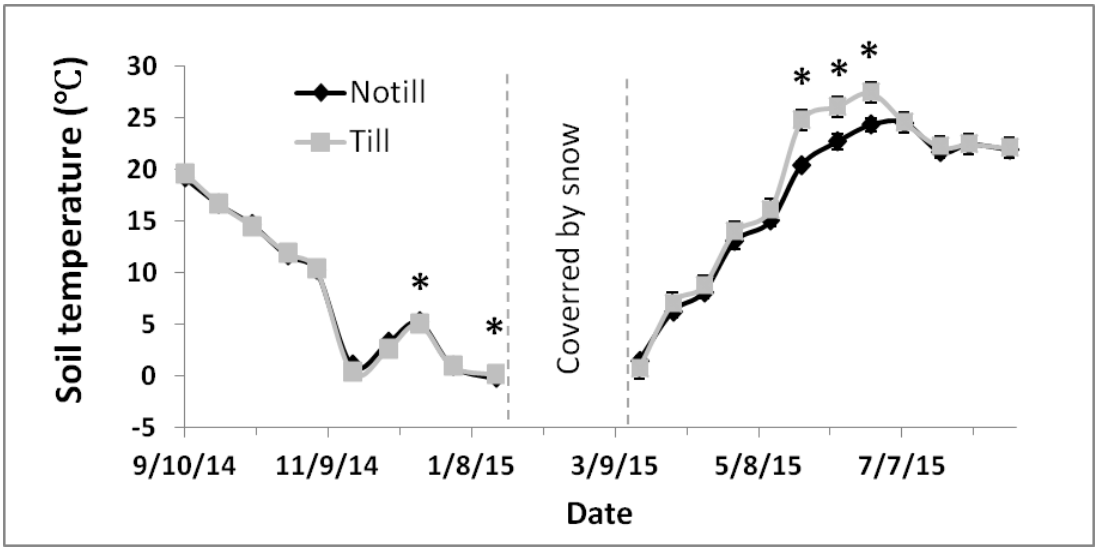

(B)

Figure 5-7. Surface soil N contents in no-till and conventionally tilled corn fields (from areas without visible BSCs), including (A) total N% in no-till fields, (B) total N% in conventional tilled fields, (C) ammonium-N, and (D) nitrate-N. Error bars are standard error (n = 3).

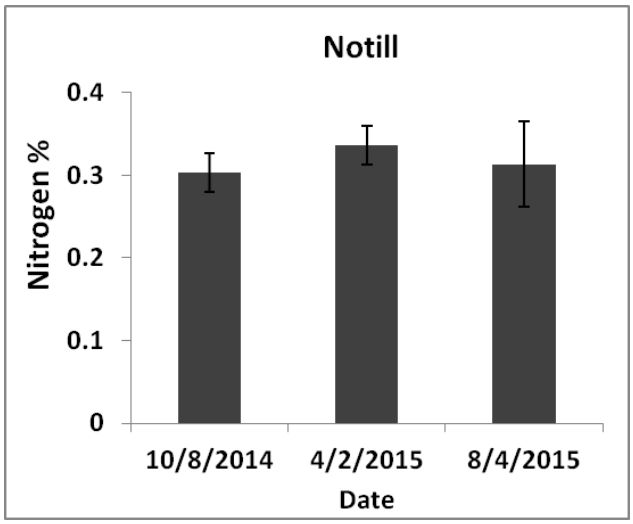

(A)

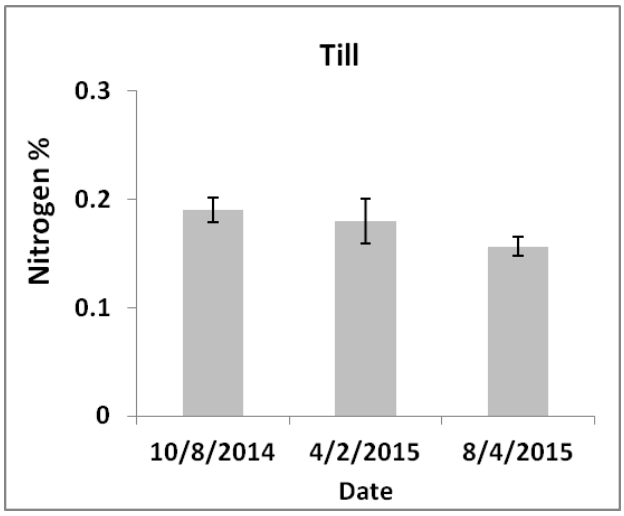

(B)

Figure 5-7.(Continued)

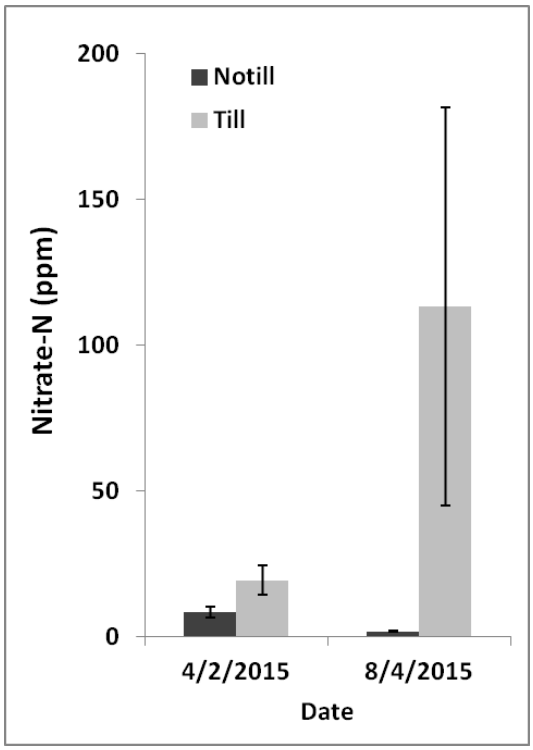

(C)

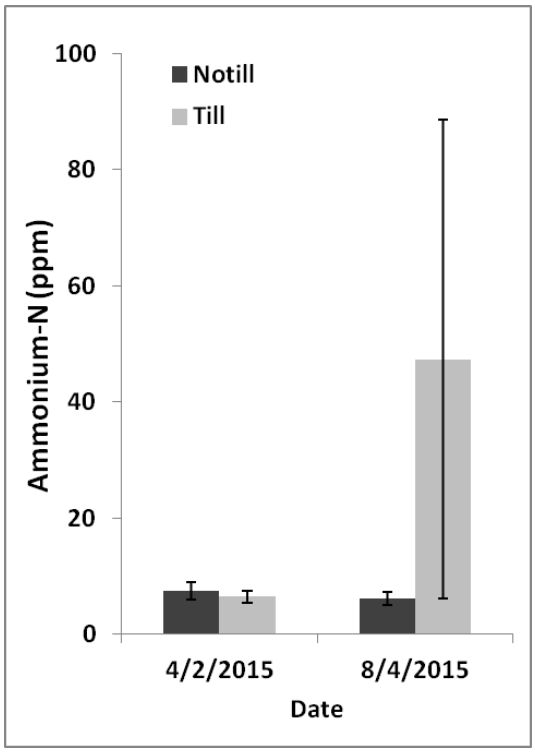

(D)

Figure 5-8. Comparisons of model simulation results with field observations of BSCs in (A) no-till and (B) conventionally tilled corn fields. BSC biomass densities were obtained by assuming that image pixels corresponding to BSCs had biomass densities of 5000 mg m^{-2} (Peng, Chapter 2). Model conditions were: (1) initial soil inorganic N content of 20 kg N ha^{-1}; (2) additional inorganic N content due to 106 kg N ha^{-1} application on 06/17/15 (no-till) and on 06/24/15 (conventionally tilled); (3) the environmental restriction factors (ERF) was zero at the beginning of the simulation, followed by application of ERF of 48% after 7/8/15 (no-till) and of 20% after 6/24/15 (conventionally tilled). The higher ERF applied for BSCs in no-till fields was chosen because of higher crop residue coverage and lower soil temperatures measured in these fields during the year of observation.

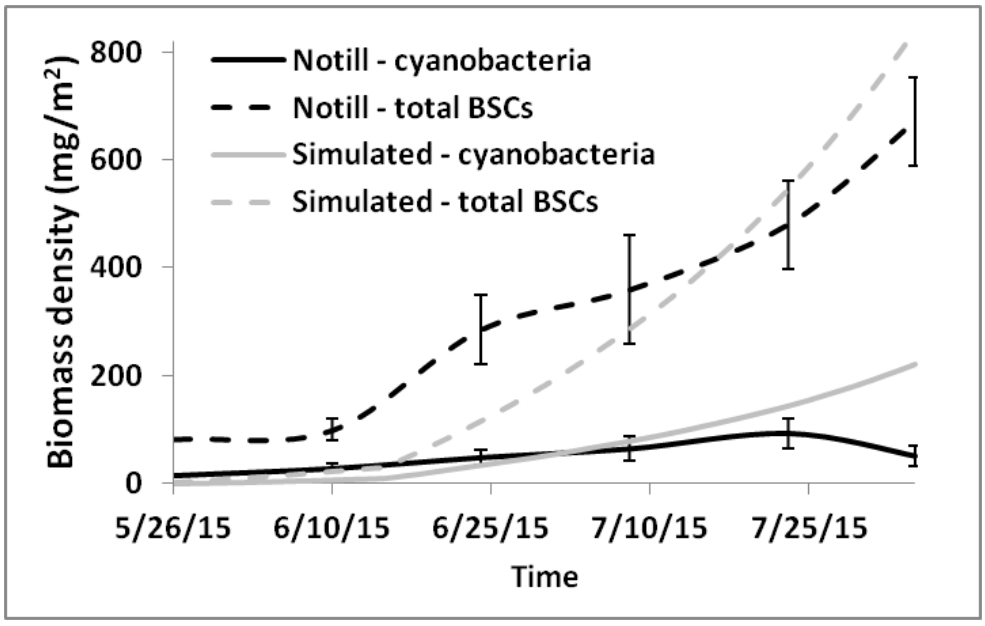

(A)

Figure 5-8. (Continued)

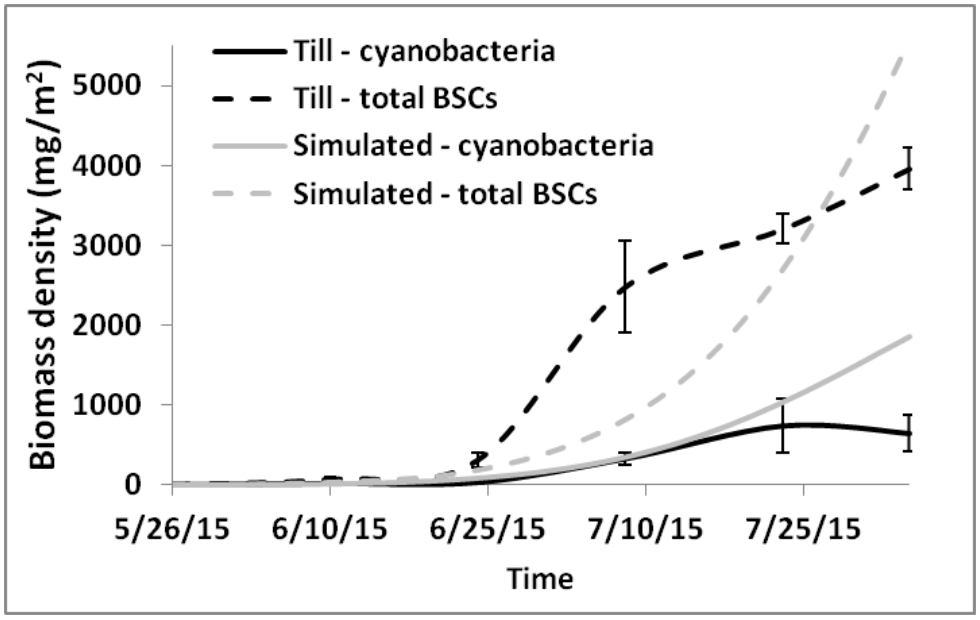

(B)

Table 5-1. Parameters and variables applied in the BSC community dynamics model.

Reference 1 (Mišurcová et al., 2010; Piorreck et al., 1984); reference 2 (Zechmeister et al., 2008); reference 3 (Shaffer et al., 2010).

Parameters and variables	Symbol	Unit	Typical value	Source
Cyanobacterial N content	Nc	g N g^{-1} dry biomass	0.087	Chapter 3
Green algae N content	Na	g N g^{-1} dry biomass	0.06	Reference 1
Moss N content	Nm	g N g^{-1} dry biomass	0.012	Reference 2
Initial inoculum size of cyanobacteria	C(0)	mg m^{-2}	1000	Chapter 4
Initial amount of green algae	A(0)	mg m^{-2}	0	Assumption
Initial amount of moss	M(0)	mg m^{-2}	0	Assumption
Cyanobacterial maximum carrying capacity under optimum condition	Kc max	mg m^{-2}	5000	Chapter 2
Cyanobacterial maximum growth rate	rC max	g new cell g^{-1} old cell day^{-1}	0.25	Chapter 2
Green algae maximum growth rate	rA max	g new cell g^{-1} old cell day^{-1}	0.15	Estimate
Moss maximum growth rate	rM max	g new cell g^{-1} old cell day^{-1}	0.1	Estimate
Cyanobacterial minimum local extinction rate	Dc min	g dead cell g^{-1} old cell day^{-1}	0.05	Estimate
Algae minimum daily local extinction rate	Da min	g dead cell g^{-1} old cell day^{-1}	0.03	Estimate
Moss minimum daily local extinction rate	Dm min	g dead cell g^{-1} old cell day^{-1}	0.01	Estimate
Daily transition proportion from cyanobacteria to green algae	Tca	g green algae g^{-1} cyanobacteria	0.05	Estimate
Daily transition proportion from green algae to moss	Tam	g moss g^{-1} green algae	0.05	Estimate
Natural spontaneous BSC colonization rate	Q	mg dry biomass m^{-2} soil day^{-1}	10	Estimate
Soil nitrogen saturation in surface soil	Nmax	mg N m^{-2} soil	10000 †	Estimate
Average daily soil nitrogen loss rate in surface soil	k	g N loss g^{-1} total available N day^{-1}	0.02	Reference 3

† Equivalent to 1000 ppm in surface 0-1cm soil. Estimated based on observations of rare high N concentrations.

Table 5-2. Summary of daily transition rates in BSC community dynamics model.

Daily transition rates	Symbol	Probability function	Constrain
Uncolonized soil → cyanobacteria	Puc	P[Puc(t) = Q] = N(t)/Nmax	N(t) ≥ 10 mg N m^{-2}
		P[Puc(t) = Q] = 10/Nmax	N(t) < 10 mg N m^{-2}
Uncolonized soil → green algae	Pua	P[Pua(t) = Q] = 2*N(t)/Nmax	N(t) ≥ 100 mg N m^{-2}
	Pum	P[Pum (t) = Q] = N(t)/(5×Nmax)	N(t) ≥ 1000 mg N m^{-2}
Cyanobacteria → green algae	Pca	P[Pca(t) = Tca] = 2*N(t)/Nmax	None
Green algae → moss	Pam	P[Pam(t) = Tam] = N(t)/(5×Nmax)	None

Table 5-3. Elasticity analysis of estimated stochastic transition rates in model with (A) 0 ppm and (B) 200 ppm initial soil surface available N.

(A) Soil initial available N = 0 ppm.

Elasticity		Responses				
		Equilibrium density of cyanobacteria	Equilibrium density of green algae	Equilibrium density of moss	Green algae appearance day	Moss appearance day
Variables	Natural spontaneous BSC colonization rate ($1 \le Q \le 100$)	2.05×10^{-5}	9.44×10^{-4}	9.10×10^{-4}	1.63×10^{-5}	-4.10×10^{-4}
	Daily transition proportion (Tca & Tam) ($0.002 \le T \le 0.2$)	-5.69×10^{-4}	2.13×10^{-3}	1.68×10^{-3}	2.44×10^{-5}	-8.4×10^{-4}
	Response scale of transition probability ($0.01 \le RS \le 2$)	-1.23×10^{-4}	5.95×10^{-4}	4.87×10^{-4}	-3.11×10^{-6}	-2.13×10^{-4}

(B) Soil initial available N = 2000 mg m^{-2} (equivalent to 200 ppm).

Elasticity		Responses				
		Equilibrium density of cyanobacteria	Equilibrium density of green algae	Equilibrium density of moss	Green algae appearance day	Moss appearance day
Variables	Natural spontaneous BSC colonization rate ($1 \le Q \le 100$)	2.05×10^{-5}	9.46×10^{-4}	8.25×10^{-4}	-7.70×10^{-6}	-6.40×10^{-4}
	Daily transition proportion (Tca $ Tam) ($0.002 \le T \le 0.2$)	-5.70×10^{-4}	2.12×10^{-3}	1.48×10^{-3}	-1.70×10^{-5}	-1.24×10^{-3}
	Response scale of transition probability ($0.01 \le RS \le 2$)	-1.23×10^{-4}	5.95×10^{-4}	4.03×10^{-4}	-1.16×10^{-5}	-6.13×10^{-4}

5.9 Supplementary materials

Figure S5-1. Weather record of the field study site (station ID:USC00368449).

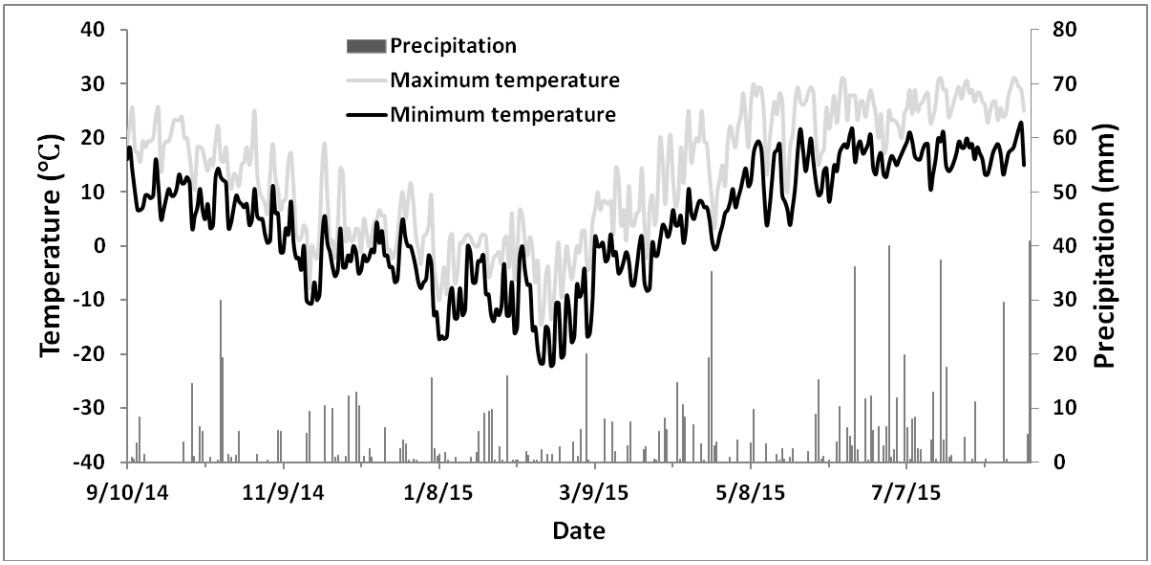

Figure S5-2. Simulated BSC succession starting with no cyanobacterial inoculum under the optimum condition. (A) A 1000-day simulation starting with zero available soil N. (B) A 100-day simulation initiated with 200 ppm surface soil available N.

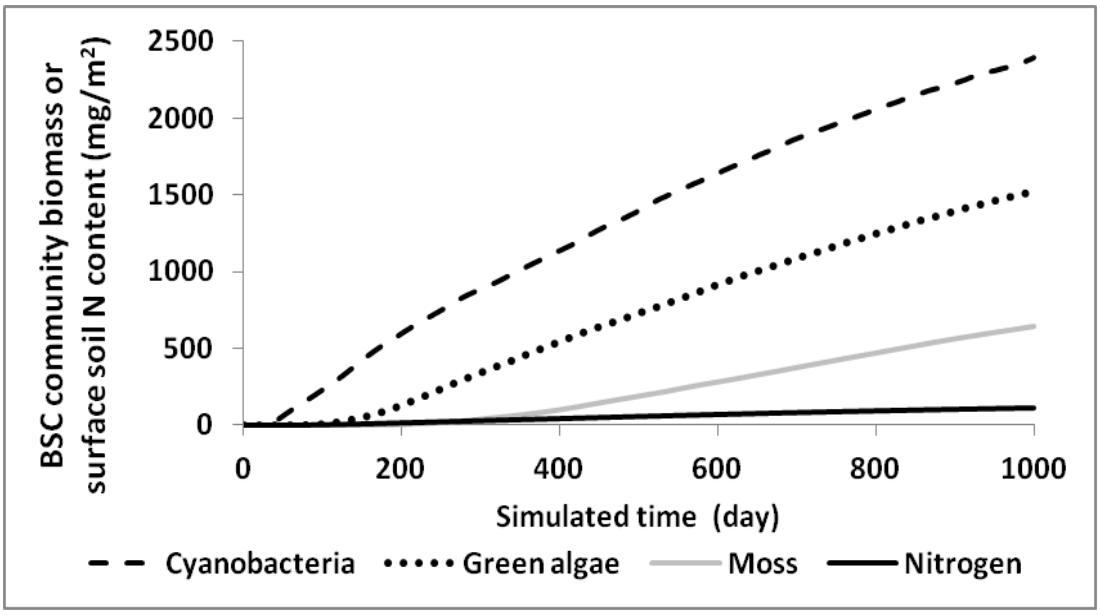

(A)

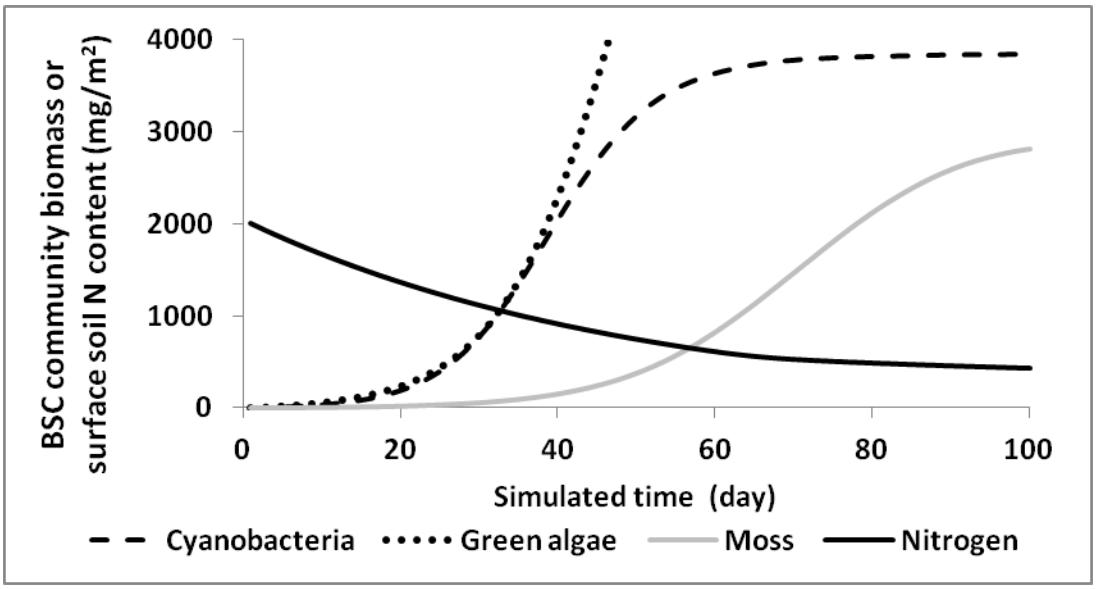

(B)

Figure S5-3. Examples of conditional coloring based on empirically determined thresholds in standardized BSC photographs after digitalization (see method description in text). From left to right are percentages of total BSC coverage; the corresponding standardized photographs; and the conditional colored graphs based on thresholds. BSCs dominated by green algae or moss are shown in red in the conditional colored graphs, while the blue colored areas indicate BSCs dominated by cyanobacteria.

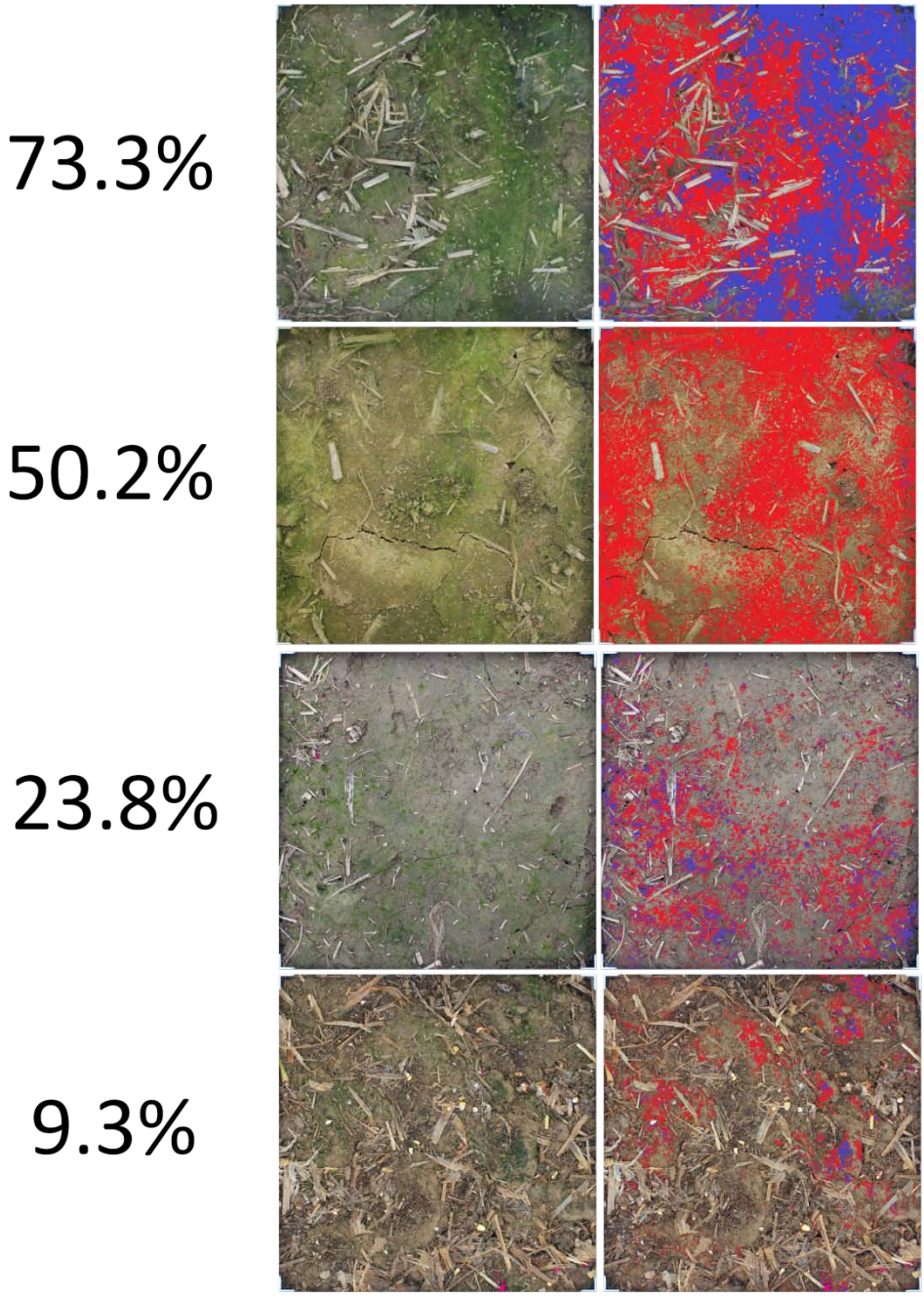

Figure S5-4. An observation of natural colonization and succession of BSC communities on soil surface. The pot (diameter = 18 cm) was filled with the Hagerstown soils collected from the Penn State Agronomy Research farm (soil total N ~ 0.2%) and placed in a glass-roofed greenhouse from October to January without additional light source. Additional distilled water was added daily to keep the water content close to its field capacity.

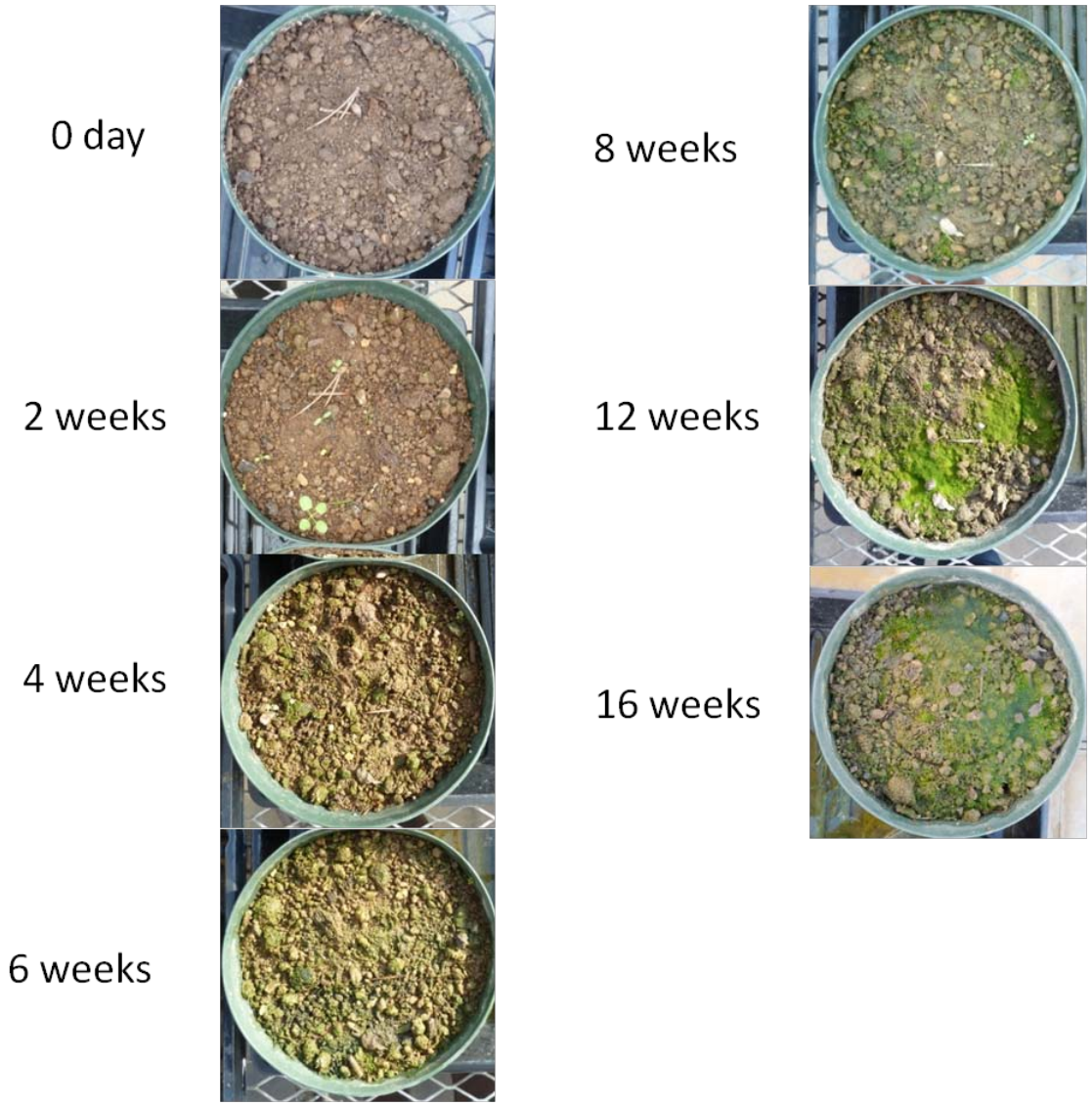

Table S5-1. GPS coordinates of sampling subplots.

Plot	Subplot	GPS coordinates	
		No-till	Till
1	1-1	40.7164 -77.9273	40.7218 -77.9320
	1-2	40.7722 -78.0061	40.7200 -77.9332
	1-3	40.7463 -77.9033	40.7200 -77.9333
2	2-1	40.7168 -77.9230	40.7193 -77.9347
	2-2	40.7167 -77.9261	40.7195 -77.9344
	2-3	40.7168 -77.9277	40.7194 -77.9343
3	3-1	40.7220 -77.9222	40.7201 -77.9350
	3-2	40.7222 -77.9323	40.7197 -77.9347
	3-3	40.7221 -77.9322	40.7197 -77.9347

Table S5-2. Additional N testing results for soil surface samples covered with observable BSCs. Values are shown as mean ± standard error of the mean (n = 3). '*' indicates significant difference between no-till and conventionally tilled plots ($p < 0.05$).

Time	Tillage	N%	Ammonium -N (ppm)	Nitrate-N (ppm)
10/8/2014	No-till	0.33 ± 0.04	NA	NA
	Conventional Till	0.20 ± 0.02	NA	NA
4/2/2015	No-till	0.30 †	4.10 †	9.51 †
	Conventional Till	0.19 †	3.90 †	10.50 †
8/4/2015	No-till	0.30 ± 0.02 *	5.87 ± 0.98	145.3 ± 133.8
	Conventional Till	0.16 ± 0.01	5.00 ± 0.10	102.7 ± 42.3

'NA' indicates the sample was not analyzed.
† The three soil samples from the three different plots were pooled for N analysis.

Code S5-1. Calculate soil available N content [operated in Visual Basic for Applications (VBA)].

```
Function nitrogen(bcyano, balgae, bmoss, rc, ra, rm, kc, ka, km, dc, da, dm, Puc, Pca, Pam, preN
As Double) As Double
Dim newalgae, newmoss, newcyano, paa, pmm, pcc, R As Double
paa = 1 - da - Pam
pmm = 1 - dm
pcc = 1 - dc - Pca
newcyano = Puc + pcc * rc * bcyano * (1 - bcyano / kc)

If ka > 0 Then
newalgae = Pca * bcyano + paa * ra * balgae * (1 - balgae / ka)
Else: newalgae = 0
End If

If km > 0 Then
newmoss = Pam * balgae + pmm * rm * bmoss * (1 - bmoss / km)
Else: newmoss = 0
End If

If preN > 10 Then
R = 0.77
Else: R = 0
End If

nitrogen = preN + (dc + Pca) * bcyano * 0.087 + (da + Pam) * balgae * 0.06 + dm * bmoss * 0.012
- newalgae * 0.06 - newmoss * 0.012 - newcyano * R * 0.087 - 0.02 * preN

If nitrogen < preN * 0.98 Then   'pure N loss no uptake
nitrogen = preN * 0.98
End If
End Function
```

Code S5-2. Calculate microbial biomass density (operated in VBA).

```
'Calculate the biomass of cyanobacteria
Function bcyano(prebcyano, rc, kc, Pca, Puc, dc As Double) As Double
Dim pcc As Double
pcc = 1 - Pca - dc
If kc > 0 Then
bcyano = Puc + pcc * (prebcyano + rc * prebcyano * (1 - prebcyano / kc))
Else: bcyano = 0
End If
If bcyano < 0 Then
bcyano = 0
End If
End Function

'calculate green algae biomass
Function balgae(prebalgae, prebcyano, ra, ka, Pua, Pca, Pam, da As Double) As Double
Dim paa As Double
paa = 1 - Pam - da
If ka > 0 Then
balgae = prebcyano * Pca + Pua + paa * (prebalgae + ra * prebalgae * (1 - prebalgae / ka))
Else: balgae = 0
End If
If balgae < 0 Then
balgae = 0
End If
End Function

'calculate moss biomass
Function bmoss(prebmoss As Double, prebalgae As Double, rm As Double, km As Double, Pum
As Double, Pam As Double, dm As Double) As Double
Dim pmm As Double
pmm = 1 - dm
If km > 0 Then
bmoss = prebalgae * Pam + Pum + pmm * (prebmoss + rm * prebmoss * (1 - prebmoss / km))
Else: bmoss = 0
End If
If bmoss < 0 Then
bmoss = 0
End If
End Function
```

Code S5-3. Calculation of daily transition rates in the BSC dynamics model (operated in VBA).

```
'Calculate Puc
Function Puc(preN As Double) As Double
Dim rand As Double
rand = Rnd()
If preN >= 10 And rand > preN / 10000 Then
  Puc = 0
  ElseIf preN >= 10 And rand <= preN / 10000 Then
  Puc = 10
  ElseIf preN < 10 And rand > 10 / 10000 Then
  Puc = 0
  Else: Puc = 10
End If
End Function

'calculate Pua
Function Pua(preN As Double) As Double
Dim rand As Double
rand = Rnd()
If preN >= 100 And rand <= preN / 5000 Then
  Pua = 10
  Else: Pua = 0
End If
End Function

'calculate Pum
Function Pum(preN As Double) As Double
Dim rand As Double
rand = Rnd()
If preN >= 1000 And rand <= preN / 50000 Then
  Pum = 10
  Else: Pum = 0
End If
End Function

'calculate Pca
Function Pca(preN, ra As Double) As Double
Dim rand As Double
rand = Rnd()
If rand > preN / 5000 Then
Pca = 0
Else: Pca = 0.05
End If
End Function
```

```
'calculate Pam
Function Pam(preN, rm As Double) As Double
Dim rand As Double
rand = Rnd()
If rand > preN / 50000 Then
Pam = 0
Else: Pam = 0.05
End If
End Function
```

Code S5-4. Simulation of BSC succession (operated in VBA).

```
Sub Macro1() ' basic growth model
Dim soilN(999, 4999) As Double, cyanoB(999, 4999) As Double, algaeB(999, 4999) As Double,
mossB(999, 4999) As Double 'mg/m2
Dim rc As Double, ra As Double, rm As Double, dc As Double, da As Double, dm As Double
Dim kc As Double, ka As Double, km As Double, PucR As Double, PuaR As Double, PumR As
Double, PcaR As Double, PamR As Double
Dim i As Long, j As Long

'initial state
rc = Cells(9, 4)
ra = Cells(10, 4)
rm = Cells(11, 4)
dc = Cells(12, 4)
da = Cells(13, 4)
dm = Cells(14, 4)
kc = Cells(8, 4)

For i = 0 To 4999
soilN(0, i) = Cells(20, 4)
cyanoB(0, i) = Cells(5, 4)
algaeB(0, i) = Cells(6, 4)
mossB(0, i) = Cells(7, 4)
Next i

For j = 0 To 4999
    For i = 1 To 999            '1000days
    'calculate parameters
      PucR = Puc(soilN(i - 1, j))
      PuaR = Pua(soilN(i - 1, j))
      PumR = Pum(soilN(i - 1, j))
      PcaR = Pca(soilN(i - 1, j), ra)
      PamR = Pam(soilN(i - 1, j), rm)
      ka = soilN(i - 1, j) / 0.06
      km = soilN(i - 1, j) / 0.12
    'calculate amounts
    'bcyano , balgae, bmoss, rc, ra, rm, kc, ka, km, dc, da, dm, Puc, Pca, Pam, preN
    'prebcyano, rc, kc, Pca, Puc, dc
    soilN(i, j) = nitrogen(cyanoB(i - 1, j), algaeB(i - 1, j), mossB(i - 1, j), rc, ra, rm, kc, ka, km, dc,
da, dm, PucR, PcaR, PamR, soilN(i - 1, j))
    cyanoB(i, j) = bcyano(cyanoB(i - 1, j), rc, kc, PcaR, PucR, dc)
    algaeB(i, j) = balgae(algaeB(i - 1, j), cyanoB(i - 1, j), ra, ka, PuaR, PcaR, PamR, da)
    mossB(i, j) = bmoss(mossB(i - 1, j), algaeB(i - 1, j), rm, km, PumR, PamR, dm)
    Next i
```

```
Next j

For i = 1 To 1000      'print results

   Cells(i + 1, 8) = i
   Cells(i + 1, 9) = WorksheetFunction.Average(WorksheetFunction.Index(cyanoB, i, 0))
   Cells(i + 1, 10) = WorksheetFunction.StDev(WorksheetFunction.Index(cyanoB, i, 0))
   Cells(i + 1, 11) = WorksheetFunction.Average(WorksheetFunction.Index(algaeB, i, 0))
   Cells(i + 1, 12) = WorksheetFunction.StDev(WorksheetFunction.Index(algaeB, i, 0))
   Cells(i + 1, 13) = WorksheetFunction.Average(WorksheetFunction.Index(mossB, i, 0))
   Cells(i + 1, 14) = WorksheetFunction.StDev(WorksheetFunction.Index(mossB, i, 0))
   Cells(i + 1, 15) = WorksheetFunction.Average(WorksheetFunction.Index(soilN, i, 0))
   Cells(i + 1, 16) = WorksheetFunction.StDev(WorksheetFunction.Index(soilN, i, 0))
Next i
End Sub
```

Code S5-5. Elasticity analyses (operated in VBA).

```
'Functions for Q (as k)
'calculate Puc
Function Puc(k, preN As Double) As Double
Dim rand As Double
rand = Rnd()
If preN >= 10 And rand > preN / 10000 Then
Puc = 0
ElseIf preN >= 10 And rand <= preN / 10000 Then
Puc = k
ElseIf preN < 10 And rand > 10 / 10000 Then
Puc = 0
Else: Puc = k
End If
End Function

'calculate Pua
Function Pua(k, preN As Double) As Double
Dim rand As Double
rand = Rnd()
If preN >= 100 And rand <= preN / 5000 Then
Pua = k
Else: Pua = 0
End If
End Function

'calculate Pum
Function Pum(k, preN As Double) As Double
Dim rand As Double
rand = Rnd()
If preN >= 1000 And rand <= preN / 50000 Then
Pum = k
Else: Pum = 0
End If
End Function

'Function for T (as k)
'calculate Pca
Function Pca(k, preN, ra As Double) As Double
Dim rand As Double
rand = Rnd()
If rand > preN / 5000 Then
Pca = 0
```

```
Else: Pca = 0.002 + 0.002 * k
End If
End Function

'calculate Pam
Function Pam(k, preN, rm As Double) As Double
Dim rand As Double
rand = Rnd()
If rand > preN / 50000 Then
Pam = 0
Else: Pam = 0.002 + 0.002 * k
End If
End Function

'Sub for RS
Sub Macro1()
Dim soilN(999) As Double, cyanoB(999) As Double, algaeB(999) As Double, mossB(999) As
Double 'mg/m2
Dim EndN(199, 4999) As Double, Endcyano(199, 4999) As Double, Endalgae(199, 4999) As
Double, Endmoss(199, 4999) As Double 'equilibrium density
Dim Comealgae(199, 4999) As Double, Comemoss(199, 4999) As Double
Dim rc As Double, ra As Double, rm As Double, dc As Double, da As Double, dm As Double
Dim kc As Double, ka As Double, km As Double, PucR As Double, PuaR As Double, PumR As
Double, PcaR As Double, PamR As Double
Dim i As Long, j As Long, k As Long
'initial state
kc = Cells(8, 4)
For k = 0 To 199
  For j = 0 To 4999
   Comealgae(k, j) = 2
   Comemoss(k, j) = 2
  Next j
Next k
For k = 0 To 199
  'initial state
  rc = Cells(9, 4)
  ra = Cells(10, 4)
  rm = Cells(11, 4)
  dc = Cells(12, 4)
  da = Cells(13, 4)
  dm = Cells(14, 4)

  soilN(0) = Cells(20, 4)
  cyanoB(0) = Cells(5, 4)
  algaeB(0) = Cells(6, 4)
  mossB(0) = Cells(7, 4)
```

```
  For i = 1 To 999
    soilN(i) = 0
    cyanoB(i) = 0
    algaeB(i) = 0
    mossB(i) = 0
  Next i
For j = 0 To 4999
    For i = 1 To 999                '1000days
    'calculate parameters
       PucR = Puc(soilN(i - 1)) * (1 + k) / 100
       PuaR = Pua(soilN(i - 1)) * (1 + k) / 100
       PumR = Pum(soilN(i - 1)) * (1 + k) / 100
       PcaR = Pca(soilN(i - 1), ra) * (1 + k) / 100
       PamR = Pam(soilN(i - 1), rm) * (1 + k) / 100
       ka = soilN(i - 1) / 0.06
       km = soilN(i - 1) / 0.12
    'calculate amounts
    soilN(i) = nitrogen(cyanoB(i - 1), algaeB(i - 1), mossB(i - 1), rc, ra, rm, kc, ka, km, dc, da, dm,
PucR, PcaR, PamR, soilN(i - 1))
    cyanoB(i) = bcyano(cyanoB(i - 1), rc, kc, PcaR, PucR, dc)
    algaeB(i) = balgae(algaeB(i - 1), cyanoB(i - 1), ra, ka, PuaR, PcaR, PamR, da)
    If algaeB(i) = 0 Then
    Comealgae(k, j) = Comealgae(k, j) + 1
    End If
    mossB(i) = bmoss(mossB(i - 1), algaeB(i - 1), rm, km, PumR, PamR, dm)
    If mossB(i) = 0 Then
    Comemoss(k, j) = Comemoss(k, j) + 1
    End If
    Next i
    'calculate equiliburium density
    EndN(k, j) = (soilN(990) + soilN(991) + soilN(992) + soilN(993) + soilN(994) + soilN(995) +
soilN(996) + soilN(997) + soilN(998) + soilN(999)) / 10
    Endcyano(k, j) = (cyanoB(990) + cyanoB(991) + cyanoB(992) + cyanoB(993) + cyanoB(994) +
cyanoB(995) + cyanoB(996) + cyanoB(997) + cyanoB(998) + cyanoB(999)) / 10
    Endalgae(k, j) = (algaeB(990) + algaeB(991) + algaeB(992) + algaeB(993) + algaeB(994) +
algaeB(995) + algaeB(996) + algaeB(997) + algaeB(998) + algaeB(999)) / 10
    Endmoss(k, j) = (mossB(990) + mossB(991) + mossB(992) + mossB(993) + mossB(994) +
mossB(995) + mossB(996) + mossB(997) + mossB(998) + mossB(999)) / 10
Next j
Next k
'print results
For k = 1 To 200
    Cells(k + 1, 19) = WorksheetFunction.Average(WorksheetFunction.Index(Endcyano, k, 0))
    Cells(k + 1, 20) = WorksheetFunction.StDev(WorksheetFunction.Index(Endcyano, k, 0))
    Cells(k + 1, 21) = WorksheetFunction.Average(WorksheetFunction.Index(Endalgae, k, 0))
    Cells(k + 1, 22) = WorksheetFunction.StDev(WorksheetFunction.Index(Endalgae, k, 0))
```

```
    Cells(k + 1, 23) = WorksheetFunction.Average(WorksheetFunction.Index(Endmoss, k, 0))
    Cells(k + 1, 24) = WorksheetFunction.StDev(WorksheetFunction.Index(Endmoss, k, 0))

    Cells(k + 1, 25) = WorksheetFunction.Average(WorksheetFunction.Index(EndN, k, 0))
    Cells(k + 1, 26) = WorksheetFunction.StDev(WorksheetFunction.Index(EndN, k, 0))
    Cells(k + 1, 27) = WorksheetFunction.Average(WorksheetFunction.Index(Comealgae, k, 0))
    Cells(k + 1, 28) = WorksheetFunction.StDev(WorksheetFunction.Index(Comealgae, k, 0))
    Cells(k + 1, 29) = WorksheetFunction.Average(WorksheetFunction.Index(Comemoss, k, 0))
    Cells(k + 1, 30) = WorksheetFunction.StDev(WorksheetFunction.Index(Comemoss, k, 0))
Next k

End Sub
```

Code S5-6. BSC succession under environmental pressures (operated in VBA).

```
Sub Macro1()
Dim soilN(999) As Double, cyanoB(999) As Double, algaeB(999) As Double, mossB(999) As
Double 'mg/m2
Dim EndN(89, 4999) As Double, Endcyano(89, 4999) As Double, Endalgae(89, 4999) As Double,
Endmoss(89, 4999) As Double 'equilibrium density
Dim Comealgae(89, 4999) As Double, Comemoss(89, 4999) As Double
Dim rc As Double, ra As Double, rm As Double, dc As Double, da As Double, dm As Double
Dim kc As Double, ka As Double, km As Double, PucR As Double, PuaR As Double, PumR As
Double, PcaR As Double, PamR As Double
Dim i As Long, j As Long, k As Long

kc = Cells(8, 4)   'initial state
For k = 0 To 89
  For j = 0 To 4999
   Comealgae(k, j) = 2
   Comemoss(k, j) = 2
  Next j
Next k
For k = 0 To 89
  'initial state
  rc = Cells(9, 4) * (1 - k / 100)
  ra = Cells(10, 4) * (1 - k / 100)
  rm = Cells(11, 4) * (1 - k / 100)
  dc = Cells(12, 4) * (1 + k / 100)
  da = Cells(13, 4) * (1 + k / 100)
  dm = Cells(14, 4) * (1 + k / 100)
  soilN(0) = Cells(20, 4)
  cyanoB(0) = Cells(5, 4)
  algaeB(0) = Cells(6, 4)
  mossB(0) = Cells(7, 4)
  For i = 1 To 999
   soilN(i) = 0
   cyanoB(i) = 0
   algaeB(i) = 0
   mossB(i) = 0
  Next i
For j = 0 To 4999
   For i = 1 To 999              '1000days
      PucR = Puc(soilN(i - 1))       'calculate parameters
      PuaR = Pua(soilN(i - 1))
      PumR = Pum(soilN(i - 1))
      PcaR = Pca(soilN(i - 1), ra)
      PamR = Pam(soilN(i - 1), rm)
```

```
      ka = soilN(i - 1) / 0.06
      km = soilN(i - 1) / 0.12

   'calculate amounts
   soilN(i) = nitrogen(cyanoB(i - 1), algaeB(i - 1), mossB(i - 1), rc, ra, rm, kc, ka, km, dc, da, dm,
PucR, PcaR, PamR, soilN(i - 1))
   cyanoB(i) = bcyano(cyanoB(i - 1), rc, kc, PcaR, PucR, dc)
   algaeB(i) = balgae(algaeB(i - 1), cyanoB(i - 1), ra, ka, PuaR, PcaR, PamR, da)

  If algaeB(i) = 0 Then
   Comealgae(k, j) = Comealgae(k, j) + 1
   End If
   mossB(i) = bmoss(mossB(i - 1), algaeB(i - 1), rm, km, PumR, PamR, dm)

  If mossB(i) = 0 Then
   Comemoss(k, j) = Comemoss(k, j) + 1
   End If
   Next i

  'calculate equilibrium/end density
   EndN(k, j) = (soilN(990) + soilN(991) + soilN(992) + soilN(993) + soilN(994) + soilN(995) +
soilN(996) + soilN(997) + soilN(998) + soilN(999)) / 10
   Endcyano(k, j) = (cyanoB(990) + cyanoB(991) + cyanoB(992) + cyanoB(993) + cyanoB(994) +
cyanoB(995) + cyanoB(996) + cyanoB(997) + cyanoB(998) + cyanoB(999)) / 10
   Endalgae(k, j) = (algaeB(990) + algaeB(991) + algaeB(992) + algaeB(993) + algaeB(994) +
algaeB(995) + algaeB(996) + algaeB(997) + algaeB(998) + algaeB(999)) / 10
   Endmoss(k, j) = (mossB(990) + mossB(991) + mossB(992) + mossB(993) + mossB(994) +
mossB(995) + mossB(996) + mossB(997) + mossB(998) + mossB(999)) / 10
Next j
Next k

For k = 1 To 90    'print results
   Cells(k + 1, 19) = WorksheetFunction.Average(WorksheetFunction.Index(Endcyano, k, 0))
   Cells(k + 1, 20) = WorksheetFunction.StDev(WorksheetFunction.Index(Endcyano, k, 0))
   Cells(k + 1, 21) = WorksheetFunction.Average(WorksheetFunction.Index(Endalgae, k, 0))
   Cells(k + 1, 22) = WorksheetFunction.StDev(WorksheetFunction.Index(Endalgae, k, 0))
   Cells(k + 1, 23) = WorksheetFunction.Average(WorksheetFunction.Index(Endmoss, k, 0))
   Cells(k + 1, 24) = WorksheetFunction.StDev(WorksheetFunction.Index(Endmoss, k, 0))
   Cells(k + 1, 25) = WorksheetFunction.Average(WorksheetFunction.Index(EndN, k, 0))
   Cells(k + 1, 26) = WorksheetFunction.StDev(WorksheetFunction.Index(EndN, k, 0))
   Cells(k + 1, 27) = WorksheetFunction.Average(WorksheetFunction.Index(Comealgae, k, 0))
   Cells(k + 1, 28) = WorksheetFunction.StDev(WorksheetFunction.Index(Comealgae, k, 0))
   Cells(k + 1, 29) = WorksheetFunction.Average(WorksheetFunction.Index(Comemoss, k, 0))
   Cells(k + 1, 30) = WorksheetFunction.StDev(WorksheetFunction.Index(Comemoss, k, 0))
Next k
End Sub
```

Code S5-7. Natural succession of BSCs without initial available N and cyanobacterial inoculum (operated in VBA).

```
Sub Macro1() ' N vs succession

Dim soilN(999) As Double, cyanoB(999) As Double, algaeB(999) As Double, mossB(999) As Double 'mg/m2
Dim EndN(300, 4999) As Double, Endcyano(300, 4999) As Double, Endalgae(300, 4999) As Double, Endmoss(300, 4999) As Double 'equilibrium density
Dim Comealgae(300, 4999) As Double, Comemoss(300, 4999) As Double, Comecyano(300, 4999) As Double
Dim rc As Double, ra As Double, rm As Double, dc As Double, da As Double, dm As Double
Dim kc As Double, ka As Double, km As Double, PucR As Double, PuaR As Double, PumR As Double, PcaR As Double, PamR As Double
Dim i As Long, j As Long, k As Long

'initial state
rc = Cells(9, 4)
ra = Cells(10, 4)
rm = Cells(11, 4)
dc = Cells(12, 4)
da = Cells(13, 4)
dm = Cells(14, 4)
kc = Cells(8, 4)
cyanoB(0) = Cells(5, 4)
algaeB(0) = Cells(6, 4)
mossB(0) = Cells(7, 4)

For k = 0 To 300
  For j = 0 To 4999
   Comealgae(k, j) = 2
   Comemoss(k, j) = 2
   Comecyano(k, j) = 2
  Next j
Next k

For k = 0 To 300
    soilN(0) = 10 * k
 For i = 1 To 999
    soilN(i) = 0
    cyanoB(i) = 0
    algaeB(i) = 0
    mossB(i) = 0
  Next i
For j = 0 To 4999
  For i = 1 To 999              '1000days
```

```
    'calculate parameters
       PucR = Puc(soilN(i - 1))
       PuaR = Pua(soilN(i - 1))
       PumR = Pum(soilN(i - 1))
       PcaR = Pca(soilN(i - 1), ra)
       PamR = Pam(soilN(i - 1), rm)
       ka = soilN(i - 1) / 0.06
       km = soilN(i - 1) / 0.12

    'calculate amounts
    soilN(i) = nitrogen(cyanoB(i - 1), algaeB(i - 1), mossB(i - 1), rc, ra, rm, kc, ka, km, dc, da, dm,
PucR, PcaR, PamR, soilN(i - 1))

    cyanoB(i) = bcyano(cyanoB(i - 1), rc, kc, PcaR, PucR, dc)
     If cyanoB(i) = 0 Then
    Comecyano(k, j) = Comecyano(k, j) + 1
    End If

    algaeB(i) = balgae(algaeB(i - 1), cyanoB(i - 1), ra, ka, PuaR, PcaR, PamR, da)
    If algaeB(i) = 0 Then
    Comealgae(k, j) = Comealgae(k, j) + 1
    End If

    mossB(i) = bmoss(mossB(i - 1), algaeB(i - 1), rm, km, PumR, PamR, dm)
    If mossB(i) = 0 Then
    Comemoss(k, j) = Comemoss(k, j) + 1
    End If
    Next i

    'calculate equiliburium density
    EndN(k, j) = (soilN(990) + soilN(991) + soilN(992) + soilN(993) + soilN(994) + soilN(995) +
soilN(996) + soilN(997) + soilN(998) + soilN(999)) / 10
    Endcyano(k, j) = (cyanoB(990) + cyanoB(991) + cyanoB(992) + cyanoB(993) + cyanoB(994) +
cyanoB(995) + cyanoB(996) + cyanoB(997) + cyanoB(998) + cyanoB(999)) / 10
    Endalgae(k, j) = (algaeB(990) + algaeB(991) + algaeB(992) + algaeB(993) + algaeB(994) +
algaeB(995) + algaeB(996) + algaeB(997) + algaeB(998) + algaeB(999)) / 10
    Endmoss(k, j) = (mossB(990) + mossB(991) + mossB(992) + mossB(993) + mossB(994) +
mossB(995) + mossB(996) + mossB(997) + mossB(998) + mossB(999)) / 10
Next j
Next k
'print results
For k = 1 To 301
    Cells(k + 1, 19) = WorksheetFunction.Average(WorksheetFunction.Index(Endcyano, k, 0))
    Cells(k + 1, 20) = WorksheetFunction.StDev(WorksheetFunction.Index(Endcyano, k, 0))
    Cells(k + 1, 21) = WorksheetFunction.Average(WorksheetFunction.Index(Endalgae, k, 0))
    Cells(k + 1, 22) = WorksheetFunction.StDev(WorksheetFunction.Index(Endalgae, k, 0))
```

```
    Cells(k + 1, 23) = WorksheetFunction.Average(WorksheetFunction.Index(Endmoss, k, 0))
    Cells(k + 1, 24) = WorksheetFunction.StDev(WorksheetFunction.Index(Endmoss, k, 0))
    Cells(k + 1, 25) = WorksheetFunction.Average(WorksheetFunction.Index(EndN, k, 0))
    Cells(k + 1, 26) = WorksheetFunction.StDev(WorksheetFunction.Index(EndN, k, 0))
    Cells(k + 1, 27) = WorksheetFunction.Average(WorksheetFunction.Index(Comealgae, k, 0))
    Cells(k + 1, 28) = WorksheetFunction.StDev(WorksheetFunction.Index(Comealgae, k, 0))
    Cells(k + 1, 29) = WorksheetFunction.Average(WorksheetFunction.Index(Comemoss, k, 0))
    Cells(k + 1, 30) = WorksheetFunction.StDev(WorksheetFunction.Index(Comemoss, k, 0))
    Cells(k + 1, 31) = WorksheetFunction.Average(WorksheetFunction.Index(Comecyano, k, 0))
    Cells(k + 1, 32) = WorksheetFunction.StDev(WorksheetFunction.Index(Comecyano, k, 0))
Next k
End Sub
```

Code S5-8. Effect of soil surface soil N loss rate (operated in VBA).

```
Sub Macro1()
Dim soilN(999) As Double, cyanoB(999) As Double, algaeB(999) As Double, mossB(999) As Double 'mg/m2
Dim EndN(99, 4999) As Double, Endcyano(99, 4999) As Double, Endalgae(99, 4999) As Double, Endmoss(99, 4999) As Double 'equilibrium density
Dim Comealgae(99, 4999) As Double, Comemoss(99, 4999) As Double
Dim rc As Double, ra As Double, rm As Double, dc As Double, da As Double, dm As Double
Dim kc As Double, ka As Double, km As Double, PucR As Double, PuaR As Double, PumR As Double, PcaR As Double, PamR As Double
Dim i As Long, j As Long, k As Long
'initial state
kc = Cells(8, 4)
For k = 0 To 99
For j = 0 To 4999
Comealgae(k, j) = 2
Comemoss(k, j) = 2
Next j
Next k

For k = 0 To 99
'initial state
rc = Cells(9, 4)
ra = Cells(10, 4)
rm = Cells(11, 4)
dc = Cells(12, 4)
da = Cells(13, 4)
dm = Cells(14, 4)
soilN(0) = Cells(20, 4)
cyanoB(0) = Cells(5, 4)
algaeB(0) = Cells(6, 4)
mossB(0) = Cells(7, 4)

For i = 1 To 999
soilN(i) = 0
cyanoB(i) = 0
algaeB(i) = 0
mossB(i) = 0
Next i
For j = 0 To 4999
For i = 1 To 999 '1000days
'calculate parameters
PucR = Puc(soilN(i - 1))
PuaR = Pua(soilN(i - 1))
```

```
PumR = Pum(soilN(i - 1))
PcaR = Pca(soilN(i - 1), ra)
PamR = Pam(soilN(i - 1), rm)
ka = soilN(i - 1) / 0.06
km = soilN(i - 1) / 0.12

'calculate amounts
soilN(i) = nitrogen(k, cyanoB(i - 1), algaeB(i - 1), mossB(i - 1), rc, ra, rm, kc, ka, km, dc, da, dm,
PucR, PcaR, PamR, soilN(i - 1))
cyanoB(i) = bcyano(cyanoB(i - 1), rc, kc, PcaR, PucR, dc)
algaeB(i) = balgae(algaeB(i - 1), cyanoB(i - 1), ra, ka, PuaR, PcaR, PamR, da)
If algaeB(i) = 0 Then
Comealgae(k, j) = Comealgae(k, j) + 1
End If
mossB(i) = bmoss(mossB(i - 1), algaeB(i - 1), rm, km, PumR, PamR, dm)
If mossB(i) = 0 Then
Comemoss(k, j) = Comemoss(k, j) + 1
End If
Next i

'calculate equiliburium density
EndN(k, j) = (soilN(990) + soilN(991) + soilN(992) + soilN(993) + soilN(994) + soilN(995) +
soilN(996) + soilN(997) + soilN(998) + soilN(999)) / 10
Endcyano(k, j) = (cyanoB(990) + cyanoB(991) + cyanoB(992) + cyanoB(993) + cyanoB(994) +
cyanoB(995) + cyanoB(996) + cyanoB(997) + cyanoB(998) + cyanoB(999)) / 10
Endalgae(k, j) = (algaeB(990) + algaeB(991) + algaeB(992) + algaeB(993) + algaeB(994) +
algaeB(995) + algaeB(996) + algaeB(997) + algaeB(998) + algaeB(999)) / 10
Endmoss(k, j) = (mossB(990) + mossB(991) + mossB(992) + mossB(993) + mossB(994) +
mossB(995) + mossB(996) + mossB(997) + mossB(998) + mossB(999)) / 10

Next j
Next k

'print results
For k = 1 To 100
Cells(k + 1, 19) = WorksheetFunction.Average(WorksheetFunction.Index(Endcyano, k, 0))
Cells(k + 1, 20) = WorksheetFunction.StDev(WorksheetFunction.Index(Endcyano, k, 0))
Cells(k + 1, 21) = WorksheetFunction.Average(WorksheetFunction.Index(Endalgae, k, 0))
Cells(k + 1, 22) = WorksheetFunction.StDev(WorksheetFunction.Index(Endalgae, k, 0))
Cells(k + 1, 23) = WorksheetFunction.Average(WorksheetFunction.Index(Endmoss, k, 0))
Cells(k + 1, 24) = WorksheetFunction.StDev(WorksheetFunction.Index(Endmoss, k, 0))
Cells(k + 1, 25) = WorksheetFunction.Average(WorksheetFunction.Index(EndN, k, 0))
Cells(k + 1, 26) = WorksheetFunction.StDev(WorksheetFunction.Index(EndN, k, 0))
Cells(k + 1, 27) = WorksheetFunction.Average(WorksheetFunction.Index(Comealgae, k, 0))
Cells(k + 1, 28) = WorksheetFunction.StDev(WorksheetFunction.Index(Comealgae, k, 0))
Cells(k + 1, 29) = WorksheetFunction.Average(WorksheetFunction.Index(Comemoss, k, 0))
```

```
Cells(k + 1, 30) = WorksheetFunction.StDev(WorksheetFunction.Index(Comemoss, k, 0))
Next k
End Sub

'calculate nitrogen content
Function nitrogen(k, bcyano, balgae, bmoss, rc, ra, rm, kc, ka, km, dc, da, dm, Puc, Pca, Pam,
preN As Double) As Double
Dim newalgae, newmoss, newcyano, paa, pmm, pcc, R As Double
paa = 1 - da - Pam
pmm = 1 - dm
pcc = 1 - dc - Pca
newcyano = Puc + pcc * rc * bcyano * (1 - bcyano / kc)
If ka > 0 Then
newalgae = Pca * bcyano + paa * ra * balgae * (1 - balgae / ka)
Else: newalgae = 0
End If

If km > 0 Then
newmoss = Pam * balgae + pmm * rm * bmoss * (1 - bmoss / km)
Else: newmoss = 0
End If
If preN > 10 Then
R = 0.77
Else: R = 0
End If

nitrogen = preN + (dc + Pca) * bcyano * 0.087 + (da + Pam) * balgae * 0.06 + dm * bmoss * 0.012
- newalgae * 0.06 - newmoss * 0.012 - newcyano * R * 0.087 - (0.001 + 0.001 * k) * preN
If nitrogen < preN * 0.98 Then 'pure N loss no uptake
nitrogen = preN * 0.98
End If


End Function
```

Code S5-9. Evaluation of net nitrogen contribution and nitrogen contributing effectively (operated in VBA).

```
Sub Macro1() ' add vs N vs N contribution

Dim soilN(99) As Double, cyanoB(99) As Double, algaeB(99) As Double, mossB(99) As Double
'mg/m2
Dim soilN2(99) As Double, cyanoB2(99) As Double, algaeB2(99) As Double, mossB2(99) As
Double 'no inoculum condition
Dim Nadd(4999) As Double  ' net N contribution
Dim rc As Double, ra As Double, rm As Double, dc As Double, da As Double, dm As Double
Dim kc As Double, ka As Double, km As Double, PucR As Double, PuaR As Double, PumR As
Double, PcaR As Double, PamR As Double
Dim i As Long, j As Long, k As Long, kk As Long

'initial state
rc = Cells(9, 4)
ra = Cells(10, 4)
rm = Cells(11, 4)
dc = Cells(12, 4)
da = Cells(13, 4)
dm = Cells(14, 4)
kc = Cells(8, 4)
algaeB(0) = Cells(6, 4)
mossB(0) = Cells(7, 4)
cyanoB2(0) = 0 'no innoculum as comparison
algaeB2(0) = 0
mossB2(0) = 0

For kk = 0 To 100
  soilN(0) = kk * 100
  soilN2(0) = kk * 100

For k = 0 To 100
  cyanoB(0) = k * 50

  For i = 1 To 99
    soilN(i) = 0
    soilN2(i) = 0
    cyanoB(i) = 0
    cyanoB2(i) = 0
    algaeB(i) = 0
    algaeB2(i) = 0
    mossB(i) = 0
    mossB2(i) = 0
  Next i
```

```
For j = 0 To 4999
   For i = 1 To 99                '100days
   'calculate parameters
      PucR = Puc(soilN(i - 1))
      PuaR = Pua(soilN(i - 1))
      PumR = Pum(soilN(i - 1))
      PcaR = Pca(soilN(i - 1), ra)
      PamR = Pam(soilN(i - 1), rm)
      ka = soilN(i - 1) / 0.06
      km = soilN(i - 1) / 0.12

   'calculate amounts
   soilN(i) = nitrogen(cyanoB(i - 1), algaeB(i - 1), mossB(i - 1), rc, ra, rm, kc, ka, km, dc, da, dm,
PucR, PcaR, PamR, soilN(i - 1))
   soilN2(i) = nitrogen(cyanoB2(i - 1), algaeB2(i - 1), mossB2(i - 1), rc, ra, rm, kc, ka, km, dc, da,
dm, PucR, PcaR, PamR, soilN2(i - 1))
   cyanoB(i) = bcyano(cyanoB(i - 1), rc, kc, PcaR, PucR, dc)
   cyanoB2(i) = bcyano(cyanoB2(i - 1), rc, kc, PcaR, PucR, dc)
   algaeB(i) = balgae(algaeB(i - 1), cyanoB(i - 1), ra, ka, PuaR, PcaR, PamR, da)
   algaeB2(i) = balgae(algaeB2(i - 1), cyanoB2(i - 1), ra, ka, PuaR, PcaR, PamR, da)
   mossB(i) = bmoss(mossB(i - 1), algaeB(i - 1), rm, km, PumR, PamR, dm)
   mossB2(i) = bmoss(mossB2(i - 1), algaeB2(i - 1), rm, km, PumR, PamR, dm)
   Next i

  'calculate N contribution
   Nadd(j) = WorksheetFunction.Sum(soilN) - WorksheetFunction.Sum(soilN2)
Next j

'print results
Cells(kk + 2, k + 9) = WorksheetFunction.Average(Nadd)
If k = 0 Then                                  'calculate N per biomass added
Cells(kk + 2, k + 113) = 'NA'
Else
Cells(kk + 2, k + 113) = Cells(kk + 2, k + 9) / (k * 50)
End If

Next k
Next kk
End Sub
```

Code S5-10. Digitize the photographs from field BSC observation (operated in R).

```
library(readbitmap)
fileName<-dir()
N=length(fileName)
Sum<-matrix(0,N,3)
Rlist<-vector("list",N)
Glist<-vector("list",N)
Blist<-vector("list",N)
for (k in 1:N)
{
Rlist[[k]]= read.bitmap(fileName[k],1)
Glist[[k]]= read.bitmap(fileName[k],2)
Blist[[k]]= read.bitmap(fileName[k],3)
r=Rlist[[k]]/255
g= Glist[[k]]/255
b= Blist[[k]]/255
H<-matrix(0,1000,1000)
S<-matrix(0,1000,1000)
V<-matrix(0,1000,1000)

 for(i in 1:1000)
 {
  for(j in 1:1000)
  {
   Cmax<-max(r[i,j],g[i,j],b[i,j])
   Cmin<-min(r[i,j],g[i,j],b[i,j])
   Deta<-Cmax-Cmin
   if (Deta==0) H[i,j]=0
   if (r[i,j]==Cmax) H[i,j]=60*((g[i,j]-b[i,j])/Deta)%%6
   if (g[i,j]== Cmax) H[i,j]=120+60*(b[i,j]-r[i,j])/Deta
   if (b[i,j]== Cmax) H[i,j]=240+60*(r[i,j]-g[i,j])/Deta
   if(Cmax==0) S[i,j]=0
   if(Cmax!=0) S[i,j]=Deta/Cmax
   V[i,j]=Cmax
  }
 }
countAM<-length(which(H>=55&H<85&S>=0.15&V>0.15&V<0.70))/1000000
countB<-length(which(H>=85&H<=195&S>=0.15&V>0.15&V<0.70))/1000000
countT<-countAM+countB
Sum[k,1]<-countAM
Sum[k,2]<-countB
Sum[k,3]<-countT
}
write.table(cbind(fileName,Sum),"E:\\Xin is the Queen of Data Analysis.txt")
```

Code S5-11. Conditional coloring the blue green BSC areas in purple, and other BSC areas in red (operated in Open CV in C++ language, contributed by Dr. Qing Xu).

```
#include <opencv2/opencv.hpp>
#include <fstream>
#include <math.h>
using namespace std;

#pragma comment(linker, "/subsystem:\"windows\" /entry:\"mainCRTStartup\"")

int main()
{
	const char *pstrImageName = "821notill_3_2.bmp";
	const char *pstrWindowsTitle = "OpenCV";

	IplImage *pImage = cvLoadImage(pstrImageName, CV_LOAD_IMAGE_UNCHANGED);

	CvScalar pixel;
	double r,g,b,h,s,v,maxv,minv;
	for(int i=0;i<pImage->height;i++)
	{
		for(int j=0;j<pImage->width;j++)
		{
			b=cvGet2D(pImage,i,j).val[0];
			g=cvGet2D(pImage,i,j).val[1];
			r=cvGet2D(pImage,i,j).val[2];
			r/=255.0;
			g/=255.0;
			b/=255.0;
			maxv=max(max(r,g),b);
			minv=min(min(r,g),b);
			if(maxv==minv){h=0;}
			if(maxv==r&&g>=b){h=60*(g-b)/(maxv-minv);}
			if(maxv==r&&g<b){h=60*(g-b)/(maxv-minv)+360;}
			if(maxv==g){h=60*(b-r)/(maxv-minv)+120;}
			if(maxv==b){h=60*(r-g)/(maxv-minv)+240;}
			if(maxv<0.000001){s=0;}else{s=1-minv/maxv;}
			v=maxv;

			if(h>=55&&h<85&&s>=0.15&&v>0.15&&v<0.70)//red
			{
				pixel.val[0] = 36;
				pixel.val[1] = 28;
				pixel.val[2] = 237;
				cvSet2D(pImage, i, j, pixel);
			}
```

```
                        if(h>=85&&h<=195&&s>=0.15&&v>0.15&&v<0.70)//blue
                        {
                                pixel.val[0] = 204;
                                pixel.val[1] = 72;
                                pixel.val[2] = 63;
                                cvSet2D(pImage, i, j, pixel);
                        }

                }
        }
        //file.close();
        cvNamedWindow(pstrWindowsTitle, CV_WINDOW_AUTOSIZE);
        cvShowImage(pstrWindowsTitle, pImage);
        cvWaitKey();

        cvSaveImage("color notill_3_2.bmp",pImage);
        cvDestroyWindow(pstrWindowsTitle);
        cvReleaseImage(&pImage);
        return 0;
}
```

Chapter 6

General Conclusions

Biological soil crusts (BSCs) have been studied almost exclusively in arid and semi-arid ecosystems, in which the N_2-fixing cyanobacteria play key roles in colonization, nutrient acquisition, and stabilization in BSC succession. Although BSCs are found in diverse ecosystems and make important contributions to biological N fixation and soil formation, the study of BSCs in humid areas, especially in agroecosystems, is very limited. Cyanobacteria applied in rice paddy systems have been reported to reduce fertilizer N use by up to 50%, but they are rarely considered for use in temperate row crop agriculture. Our interest in possible contributions by BSCs to nutrient cycling in agricultural soils has been based on observing annually re-occurring BSCs in diverse agricultural fields at the Pennsylvania State University's Agronomy Research Farm for the past 15 years. Because modern agricultural systems employ large amounts of synthetic N fertilizer that is used inefficiently (losses about 50% N applied), we undertook this study to learn about N contributions by BSCs and how they might be incorporated into agricultural management to improve N use efficiency and soil properties in row crop agriculture.

First, we established a system to screen potential cyanobacterial candidates based on three criteria - reliability of serial transfers in N-free culture media; robust growth in soil microcosms; and resistance to detachment from soil particles by water flushing. Using this selection system, a high-performance cyanobacterial enrichment, named DG1, was efficiently isolated from naturally formed BSCs growing on Hagerstown soil from Penn State's Research Farm. Based on metagenomic analysis, this DG1 cyanobacteria enrichment was a consortium dominated by one or more closely related strains of cyanobacteria in the Nostocaceae family, and contained six other bacterial genotypes. Compared with individual cultures of eight commercially available cyanobacterial strains (*Nostoc spp.* and *Anabaena spp.*), DG1 showed the highest

potential for forming artificial BSCs by meeting all three criteria, whereas commercial cultures satisfied one or at most two criteria. Specifically, DG1 showed robust growth and strong flocculation in N-free liquid medium; formed stable artificial BSCs in soil microcosms (biomass increased 4.5 times within one month); and lost no more than 13% of its biomass after a 100-ml water flushing treatment.

Second, using the $^{15}N_2$ isotopic labeling approach and simulated rainfall treatments, we evaluated DG1's potential benefit in modulating N cycling in soil containing different nitrate-N concentrations. The results indicated that DG1 could potentially improve soil fertility and reduce N fertilizer requirements by both fixing atmospheric N_2 and increasing soil N retention. Based on our experiments, DG1 could fix 0.1 mg N g^{-1} dry biomass day^{-1} under N limited conditions, but it fixed less N_2 in the presence of inorganic N (0.019-0.027 mg N g^{-1} dry biomass day^{-1}). However, when soil mineral N concentration was high, applying a small amount of DG1 (ca. 0.88 g dry biomass m^{-2}) could significantly reduce soil nitrate leaching by 26-30% within a seven-day establishment time after inoculation.

Third, we investigated the most cost-effective application rate and timing of the cyanobacterial enrichment DG1 by combining its capability of soil N retention with three additional criteria: fast growth on soil within a short period after inoculation; BSC stability under simulated rainfall; and ease of soil water infiltration after cyanobacterial application. The results indicated that the application of DG1 to soil had no significant effect on soil water infiltration. Based on our experiments, a seven-day establishment time without significant rain would be highly favorable for DG1's stability on soil subject to subsequent regular rainfall events. Based on observations of DG1's growth in individual petri dishes, applying a small amount of DG1 evenly on soil surfaces (for instance, 0.88 g dry biomass m^{-2}, or about 18% of the environmental carrying capacity in sandy soil microcosms) would be more cost-effective than higher application rates in agricultural management.

Fourth, based on our experimental data of DG1 in Chapter 2, 3, and 4, we built a stochastic Markov model for BSC succession. Model results were compared to one year of field observations of BSCs at the Penn State Agronomy Research Farm to estimate BSC succession and potential N contributions following application of cyanobacteria to agricultural soils. Our model simulations indicated that environmental restrictions on growth rate and local extinction rate are crucial determinants of BSCs' ability to be self-sustaining. On the other hand, soil initial available N was a stronger influence on BSC succession rate and sequence. Integrating field observations with model simulations indicated that the application of cyanobacteria with soil N fertilizer at the beginning of the crop growing season could significantly accelerate BSC growth and succession, and contribute soil N in temperate agroecosystems.

Finally, we performed several additional preliminary experiments to further explore the feasibility of DG1's future field application as a soil amendment. DG1 has been successfully cultured with a photobioreactor (PBR) system at (five photobioreactors × 1.2-L reactor^{-1}), in which the biomass increased 3-5 times within a two-week cultivation period (Appendix A). No cyanotoxin was detected in DG1 liquid cultures grown with either 0 or 124 ppm nitrate-N at the sensitivity levels of test assays that were at least 50% lower than the strictest drinking water safety levels published by EPA (US Environmental Protection Agency). DG1 exhibited good resistance to desiccation. It recovered well after being air dried for eight weeks, and could regrow after being dried on different supporting materials (sand, plastic, paper, etc.) (Appendix B). The fluorescent microscopic observations of DG1 provided evidence of heterocysts (highly specialized cells for N_2-fixation) and the production of mycosporine-like amino acids (MAAs, which function as a sunscreen to protect cells from UV damage) on cell surfaces (Appendix C).

In summary, my dissertation provides proof of concept that N_2-fixing and biofilm forming cyanobacteria, especially those present in naturally formed BSCs on agricultural soils, have great potential to reduce fertilizer N use in agroecosystems by forming self-renewable BSCs

that fix N_2 and increase N retention time in soil, thereby reducing N losses. The cyanobacterial enrichment DG1 is currently deposited in long-term frozen storage in the Department of Plant Pathology and Environmental Microbiology at the Pennsylvania State University. It can be provided to other scientists on request for non-profit purposes. In addition, we have also submitted a provisional patent application as 'Cyanobacteria Soil Amendment' for possible future commercial use of DG1 (provisional patent application No. 62/328,262). More greenhouse and field studies will be needed to fully understand the relationship between cyanobacterial application rates and crop yields, and specifically how much fertilizer N could be substituted for different plants. In addition, the effects of cyanobacterial inocula on BSC succession and dynamics need to be evaluated in larger field trials.

Appendix A

Large Scale Production of Cyanobacterial Biomass

A1 Materials and methods

A1.1 Construction of photobioreactor (PBR)

The completed PBR system allowed for simultaneous growth of cyanobacteria in five cultivation reactors, each with 1.5-L capacity. The system consisted of one multiple-spot magnetic stir plate, five cultivation reactors, five environmental jackets, one light-control panel, one water circulation pump, and one gas-control panel (Figure A1). First, each cultivation reactor was constructed based on Mazowski's patent (Mazowski, 1971) using a 1.5-L volume BELL-FLO Flask (Bellco Glass, Inc., Vineland, NJ) with a thermometer and a gas inlet on one side and a sampling tube and gas outlet on the opposite side (Figure A2-A and B). An additional impeller, constructed from 1-mm thick PVC plastic sheet, was attached to a magnetic rod placed on the bottom of the cultivation reactor (Figure A2-C). The impeller could rotate freely at 80 revolutions per minute (RPM), driven by magnetic stir plates.

Each cultivation reactor was surrounded by an environmental jacket (Figure A3) consisting of a custom glass cylinder lined on the inside with 'natural light' LED light strips (HitLites, Baton Rouge, LA) (Figure A3-C). The glass cylinder was surrounded by a water circulation jacket (Figure A3-D) which was in turn enclosed by a protective sheath. The water circulation jacket and the protective sheath were made from polyethylene plastic film and prepared using the heat sealing technique. Each LED light cylinder was connected to a dimmer on the light-control panel (Figure A4), so that light intensities in individual cultivation reactors could be adjusted separately during cyanobacterial growth (210-260 Lux, measured at the center of the

LED light cylinder). The water jackets were connected to the water circulation pump in parallel (Figure A5-A). Circulating water from the pump was set at about 20℃ to cool the cultivation reactors. The input water flow for each water jacket was controlled by an open-jaw screw compressor clamp (Figure A5-B) to guarantee that the average temperature in all cultivation reactors was maintained at 22.5℃.

Finally, a gas-control panel was built with one gas flow meter (092-04 tube containing a stainless steel ball) (Air Products, Allentown, PA) and seven purge meters (one R-2-15-AAA tube with a glass ball and a stainless steel ball, and six R-2-15-A tubes with a stainless steel ball in each tube) (Sho-Rate, Brooks Instrument, Hatfield, PA) (Figure A6). The meters could be manipulated to support a single seed cultivation reactor or five cultivation reactors at the same time. The gas flow for each cultivation reactor was 400 cm^3 min^{-1} with a mixture of air and 2% CO_2 gas.

A1.2 Strain cultivation and harvesting

In this study, we evaluated the local cyanobacterial enrichment DG1 and two commercial cyanobacterial strains: *A. cylindrica* (UTEX B1611) and *N. muscorum* (UTEX 1037). The cultivation reactor contained 1.2 L liquid medium [MBG11(N-), 62 ppm N, 124 ppm N or MBG11 media (Peng, Chapter 3)] and was sterilized by autoclaving, except for the thermometer. The thermometer probe was treated with the 100× diluted Minncare® Cold Sterilant (Mar Cor Purification, Skippack, PA) for 15 min and rinsed with sterile dH_2O for four times before placing in the cultivation reactor.

To start a new cultivation, 90 ml concentrated cyanobacterial cell suspension (biomass density ~ 2 mg dry biomass ml^{-1}) was added to a cultivation reactor through its sampling tube. The cultivation reactor was then placed within an environmental jacket on the magnetic stir plate and connected to the gas-control panel. Cyanobacteria were cultivated in this PBR system for 14

days, during which the light intensity was initially set at 210 Lux, then increased to 230 Lux after about four to five days' cultivation, and finally increased to 260 Lux on day 12 or 13. In order to monitor cyanobacterial growth during cultivation, samples of well mixed culture media were collected every other day by pulling 8 ml medium through the sampling tube. Samples were oven dried for gravimetric quantification of biomass. Finally, after 14 days' growth, cyanobacterial biomass was harvested by gravitational settling and removal of cleared supernatant.

A2 Results and discussions

Using MBG11(N-) medium, *A. cylindrica*, *N. muscorum* and the DG1 enrichment all showed significant growth in cultivation reactors, which could be visually observed as the culture media turned darker over time (Figure A7). Cell suspensions of *A. cylindrica* were quite uniform during cultivation, while *N. muscorum* and DG1 exhibited flocculated (clumped) growths in the cultivation reactors. The preliminary growth curve experiments in the PBR system indicated that cyanobacterial biomass density could increase 3-5 times in about two weeks (Figure A8). Due to the flocculated nature of the biomass and the small sample volumes, potential sampling error in monitoring biomass densities of *N. muscorum* and DG1 could have been greater in early growth stages than in late stages of cultivation.

We also cultivated *N. muscorum* and DG1 in media with different levels of nitrate-N. Based on several repeated cultivation and observation trials (≥ 3 times for each), *N. muscorum* showed slightly higher biomass density in medium containing 62 ppm N, but it could not grow in MBG11 medium containing 247 ppm N (Figure A9-A). However, DG1 performed well in all three media containing 62, 124 and 247 ppm N (Figure A9-B). In addition, although DG1 grew well in MBG11(N-) medium, it showed slightly better growth in the three media containing nitrate-N.

Most PBRs designed in microalgae research literature have been described to grow well-dispersed and uniformly suspended cells in liquid medium, and cell flocculation has been reported to cause severe growth failures (i.e., crashes) in such cultivation systems (Chen, et al., 2011; Suh and Lee, 2003). However, our studies provide preliminary evidence that flocculating cyanobacteria, especially the DG1 enrichment, have the potential to be cultivated in PBRs at larger scales. In fact, such cyanobacteria also have good potential for cost-effective, large-scale harvesting by gravity sedimentation.

A3 References

Chen, C.Y., Yeh, K.L., Aisyah, R., Lee, D.J., Chang, J.S., 2011. Cultivation, photobioreactor design and harvesting of microalgae for biodiesel production: a critical review. Bioresource technology 102, 71-81.

Mazowski, E., 1971. Magnetic stirrer apparatus. US patent 3622129.

Suh, I.S., Lee, C.G., 2003. Photobioreactor engineering: design and performance. Biotechnology and Bioprocess Engineering 8, 313-321.

A4 Figures

Figure A1. Overview of the PBR system. From left to right, the entire system includes a light-control panel, a water circulation pump, a multiple-spot magnetic stir plate, five cultivation reactors, five environmental jackets, and a gas-control panel.

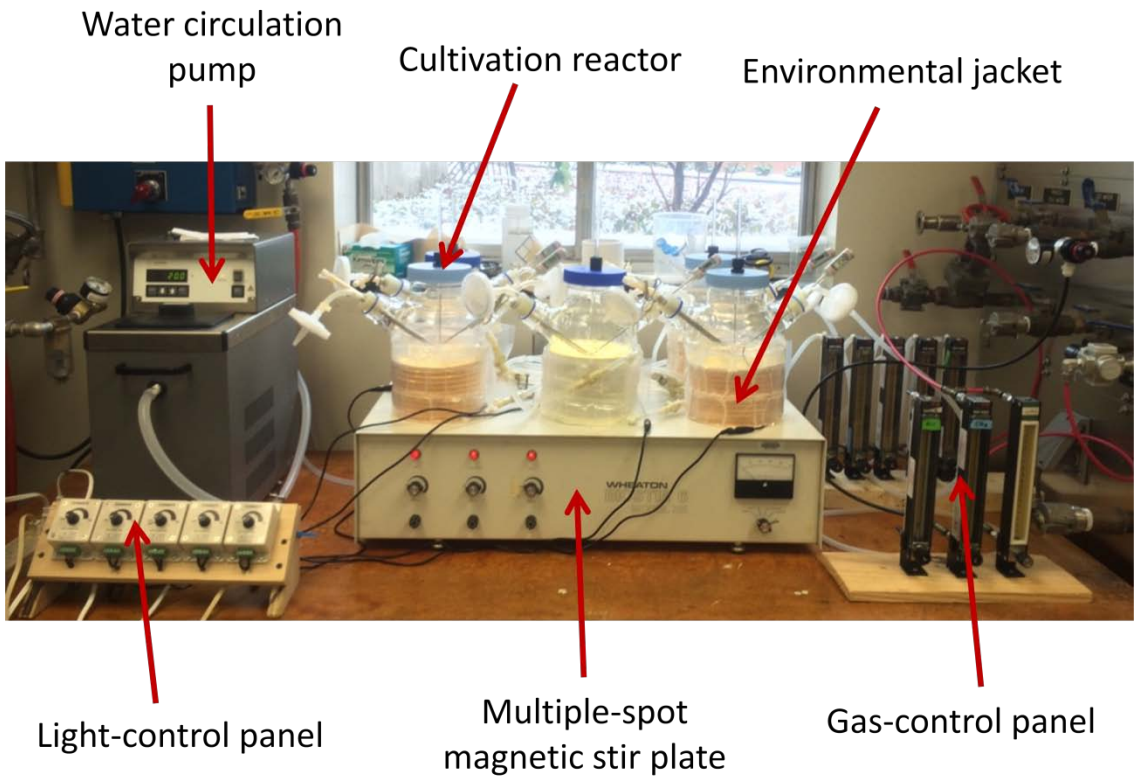

Figure A2. An individual cultivation reactor in the PBR system. (A) Diagram of customized design. (B) Photograph of cultivation reactor. (C) Photograph of the impeller (diameter = 4.8 cm, leaf size = 1.9 cm × 1.6 cm).

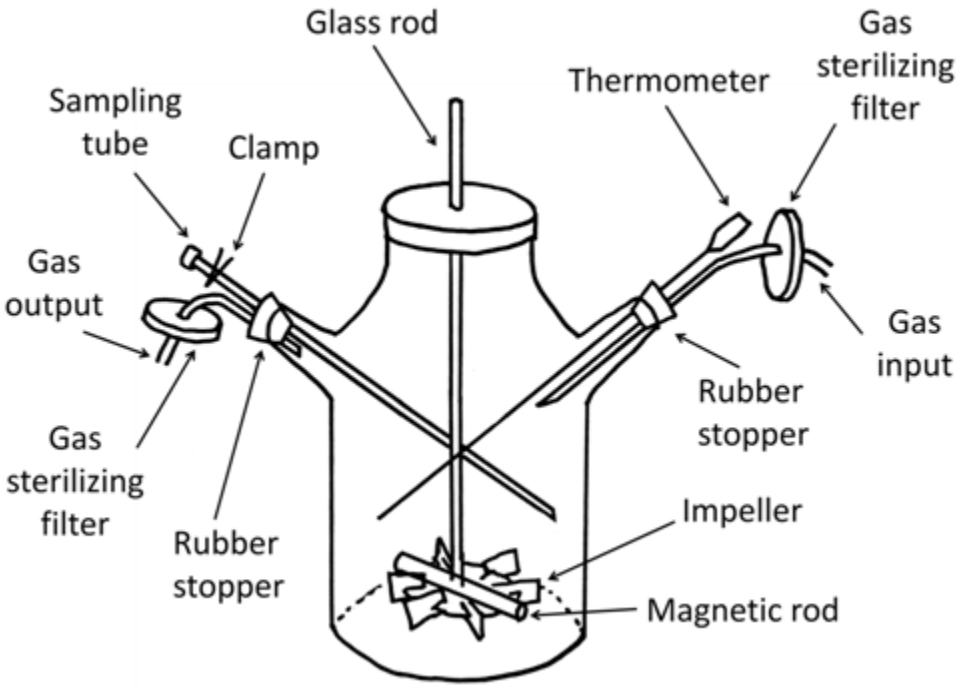

(A)

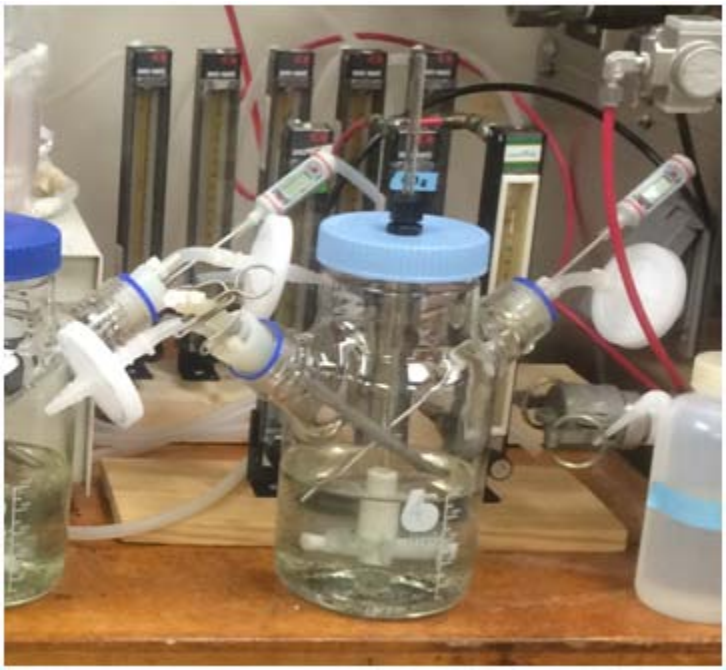

(B)

Figure A2-C. (Continued)

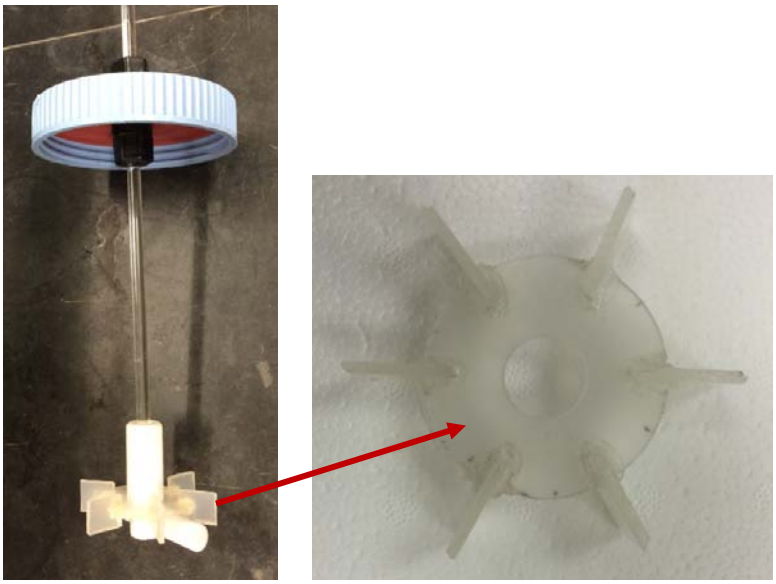

(C)

Figure A3. Environmental jacket for a cultivation reactor. (A) Diagram of design. (B) Photograph of the constructed environmental jacket. (C) Photograph of the LED light cylinder. (D) Photograph of the water jacket (jacket size = 50 cm × 12 cm).

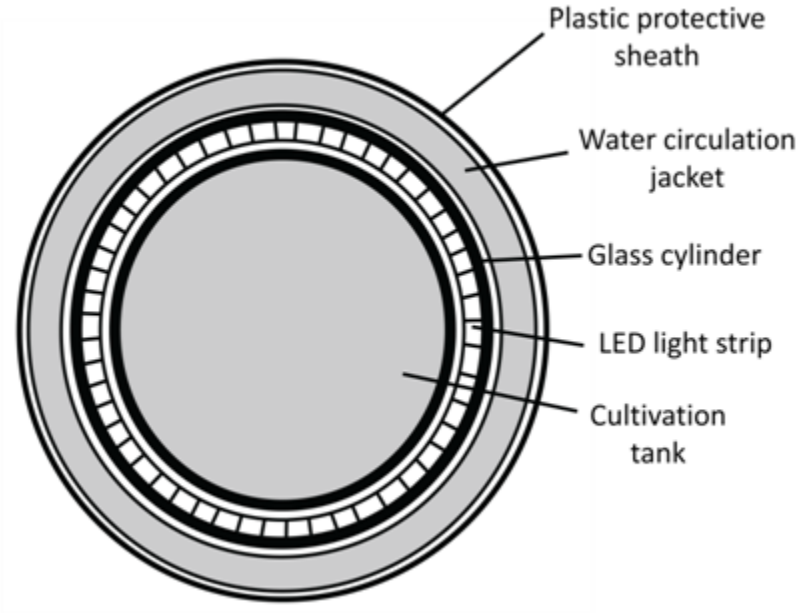

(A)

(B)

(C)

(D)

Figure A4. Light-control panel. (A) Front view. (B) Back view.

(A)

(B)

Figure A5. Water circulation subsystem. (A) Diagram of water circulation design. Red arrows indicate the direction of water flow. (B) Photograph of circulation tubes with open-jaw screw compressor clamps.

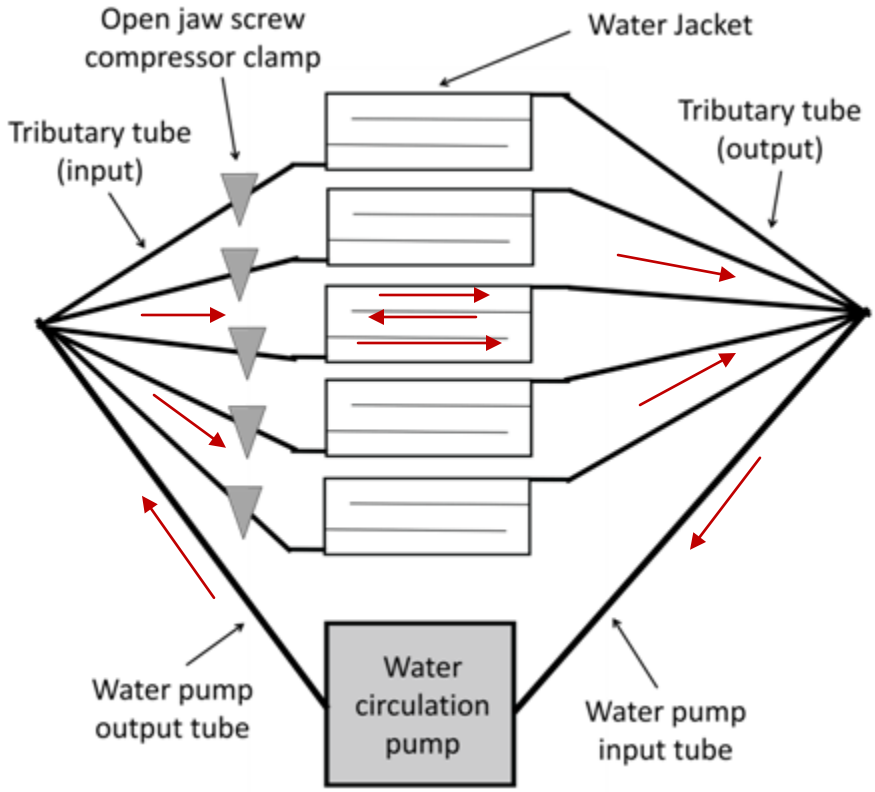

(A)

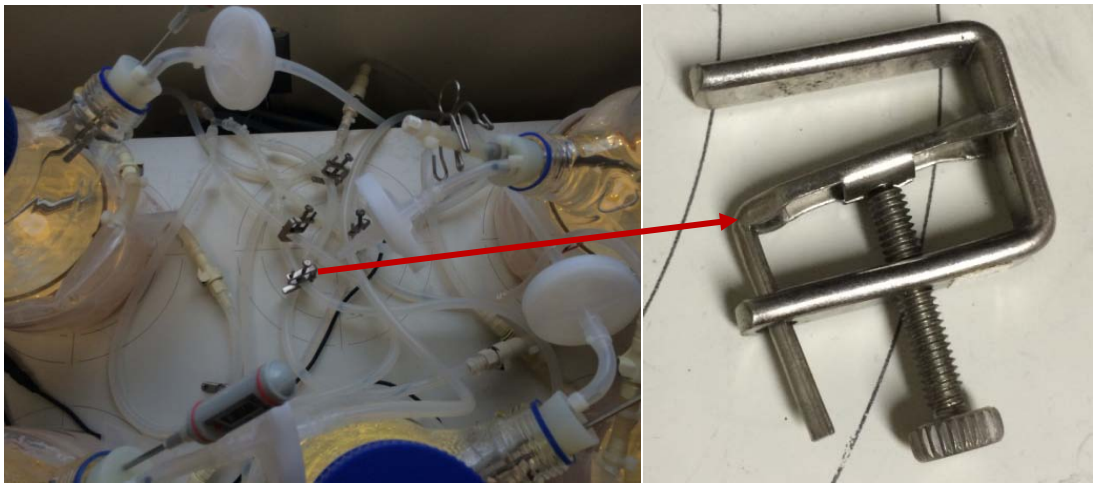

(B)

Figure A6. Gas-control panel. (A) Diagram of gas connection design. The system can support one seed cultivation reactor if the connecting switches are at position (1), and it can also support five cultivation reactors simultaneously if the connecting switches are at position (2). (B) Photograph of the gas-control panel.

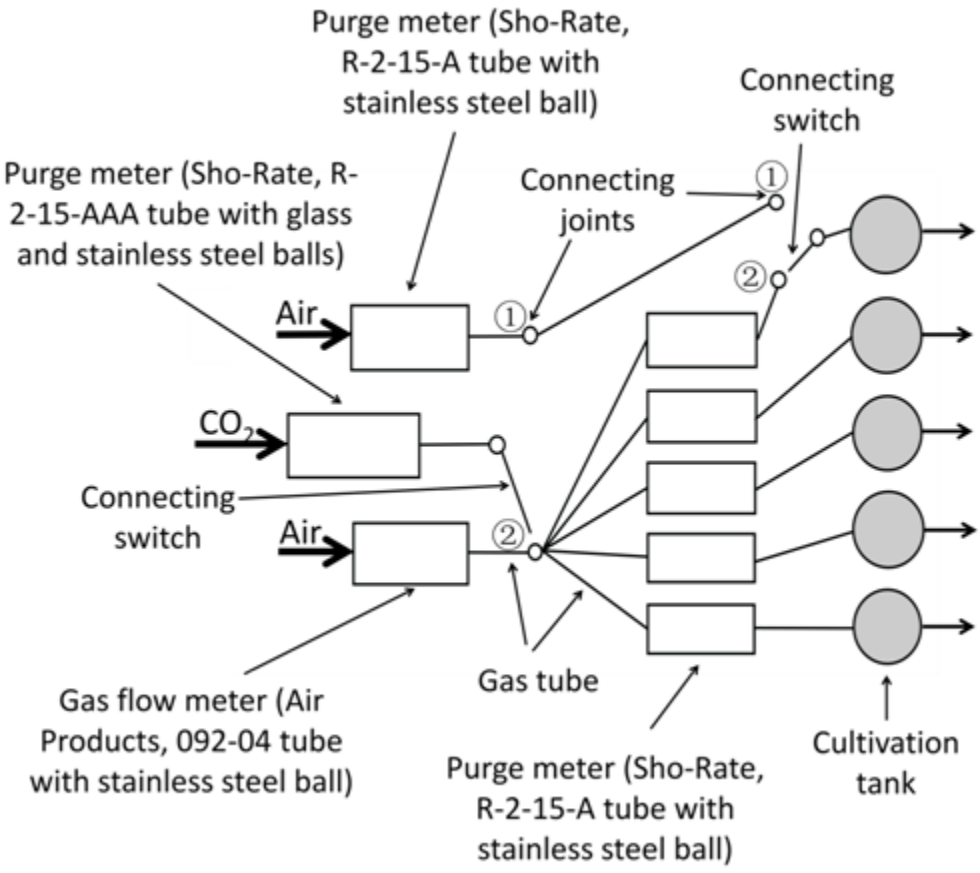

(A)

Figure A6. (Continued)

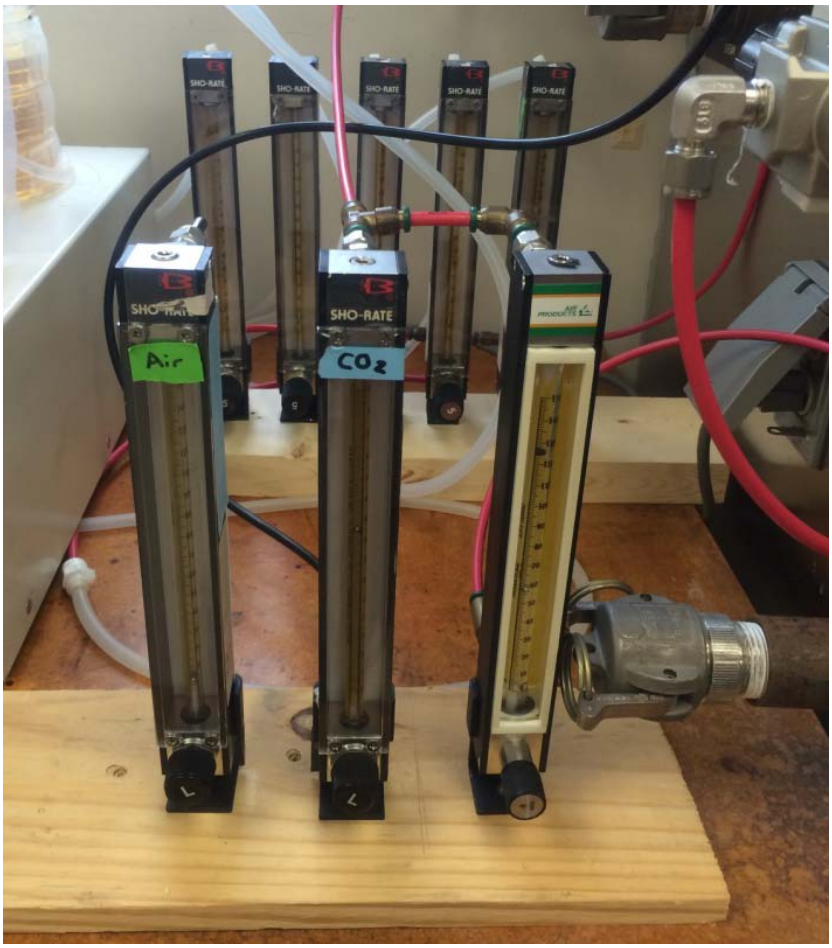

(B)

Figure A7. Photographs of different cyanobacterial cultures after being cultivated for two weeks in MBG11(N-) medium. From left to right are *A. cylindrica*, *N. muscorum* and the DG1 enrichment.

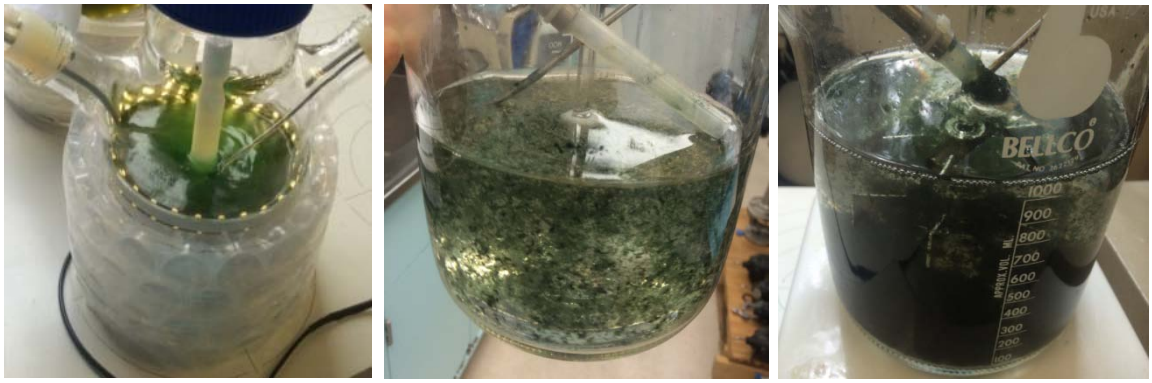

Figure A8. Preliminary growth curves of (A) *A. cylindrica*, and (B) the local enrichment DG1 in MBG11(N-) medium. Arrows indicate the time when light intensity was increased.

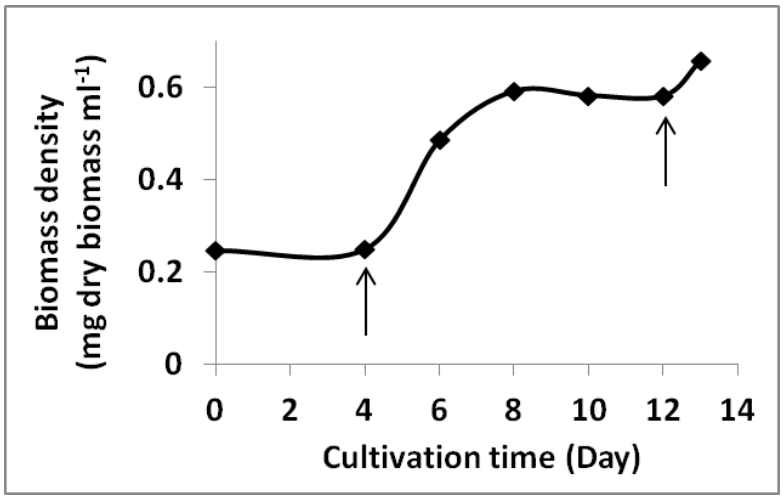

(A)

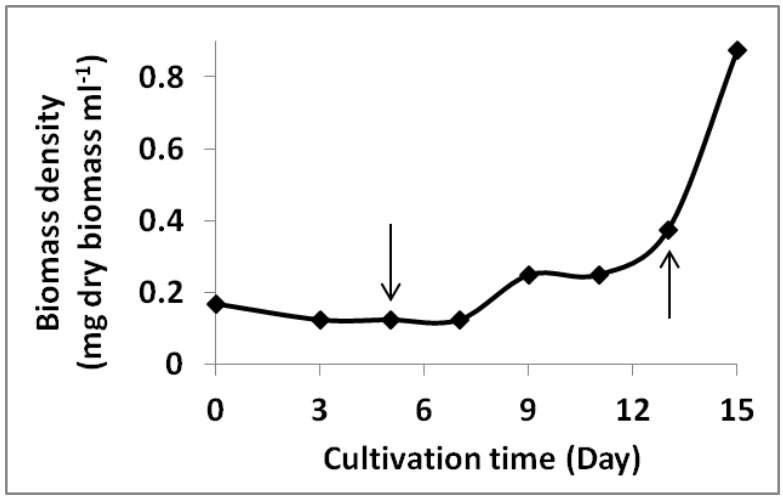

(B)

Figure A9. Photos of (A) *N. muscorum*, and (B) DG1 enrichment after being cultivated for two weeks in media with different nitrate-N. In both photographs, the medium N concentrations in cultivation reactors from left to right were 0, 62, 124 and 247 ppm.

(A)

(B)

Appendix B

Preliminary Study of Cyanobacterial Enrichment DG1's Resistance to Air-Drying

B1 Materials and methods

Cyanobacterial enrichment DG1 was cultured in photobioreactors (described in Appendix A) containing 1.2 L MBG11(N-) medium (Peng, Chapter 2) for two weeks. Biomass was harvested and condensed approximately fourfold by gravitational settling and supernatant removal to about 2 mg dry biomass ml^{-1}. All harvested biomass was pooled and mixed for the following experiments.

Small, disposable petri dishes (d = 5 cm) were used as containers for air-drying of biomass. Half of the petri dishes contained 25 g autoclaved dry sandy soil (Table S2-3), while the other half petri dishs were empty. Five ml of condensed biomass were evenly pipetted into each petri dish, and the dishes were then left open and air dried at room temperature (22.5 ± 1ºC.) A set of two petri dishes, with and without soil, was randomly selected for DG1 recovery after two, four, six and eight week's air drying treatment. From each petri dish, a 1-cm^2 piece of DG1 crust was removed with a sterile forceps and placed in a 125-ml flask containing 25 ml liquid MBG11(N-) medium for two weeks. New visible growth from the flasks was streaked on solid MBG11(N-) medium. Digital images of liquid and solid cultures were obtained media were obtained after two weeks incubation.

We also observed cyanobacterial recovery after spreading and drying the biomass on different support materials. In this preliminary study, sheets of four different support materials were cut to fit exactly on the bottoms of standard-sized petri dishes (d = 8.5 cm). The support materials included filter paper (Whatman Grade 44, Maidstone, UK), paper towel (Georgia-

Pacific, Shippensburg, PA), newspaper (black ink), and linear low-density polyethylene (LLDPE) plastic from a Ziploc bag (Greenville, SC). A volume of 20 ml condensed biomass was evenly pipetted onto each sheet, and then air dried at room temperature (22.5 ± 1ºC). After three weeks, the entire sheet with dried biomass was transferred to 125-ml flasks containing 25 ml liquid MBG11(N-) medium as described previously.

B2 Results and discussions

During the eight weeks of air drying, the color of the biomass on the soil or petri dish surfaces became more purple (Table B1). At all sampling times, dry biomass taken from both soil and petri dish surfaces showed regrowth after transfer and incubation for two weeks in both liquid and solid MBG11 (N-) media. These results demonstrated the resistance of DG1 to air-drying and showed that at least a proportion of its biomass remained viable during air-drying for eight weeks.

After being air dried for three weeks on different support materials, DG1 showed a significant stress response (purple color) immediately after being transferred to liquid MBG11(N-) medium (Figure B1-A). When the cultures were checked again after six days, the cultures again appeared green, which indicated the recovery of viability (Figure B1-B). The type of support material appeared to make no difference in DG1 recovery. These preliminary results showed the potential for rehydration recovery of DG1 after air-drying on support materials at a large-scale. Such support materials containing attached DG1 biomass would be amenable for storage and transportation.

B3 Figures and tables

Figure B1. Cyanobacterial recovery in the liquid MBG11(N-) medium after being dried on sheets of different support materials for three weeks. The photos show the appearance of DG1 at (A) five minutes after the inoculation, and (B) after six-day incubation. The support materials in different flasks from left to right were: filter paper, towel paper, newspaper, and linear low-density polyethylene (LLDPE) plastic sheet.

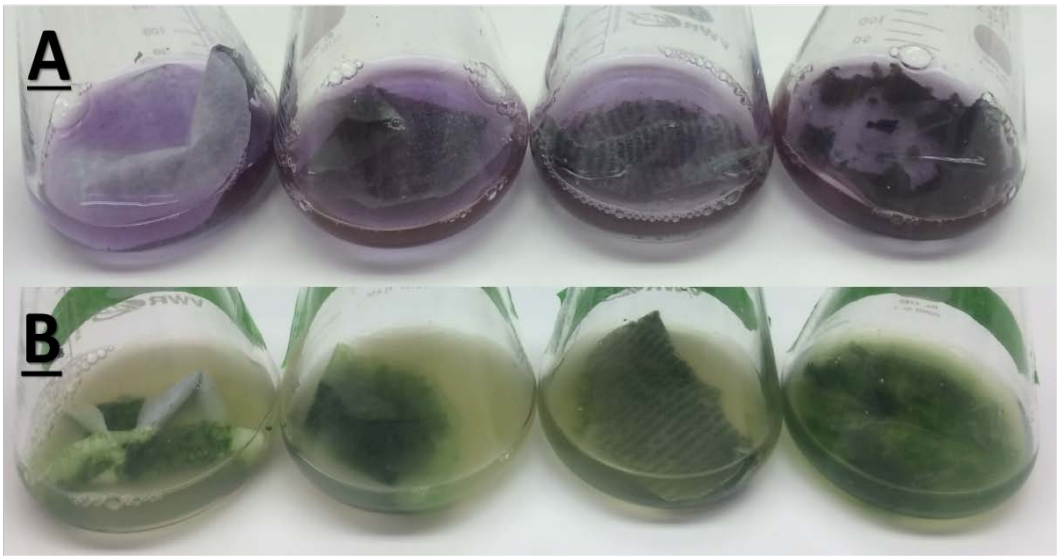

Table B1. Summary of observations of DG1 regrowth during the eight-week air-drying period. The flocs in liquid medium and on solid surfaces were new growth of DG1.

DG1 photos		Air dry duration (week)				
		0	2	4	6	8
Sand surface	Biomass on sand surface					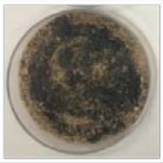
	Recover in liquid MBG11(N-) medium	NA				
	Regrowth on solid MBG11(N-) medium	NA				
Plate surface	Biomass on sand surface	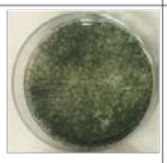	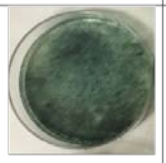	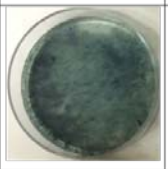	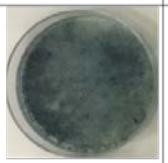	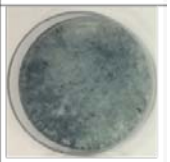
	Recover in liquid MBG11(N-) medium	NA				
	Regrowth on solid MBG11(N-) medium	NA		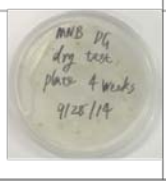	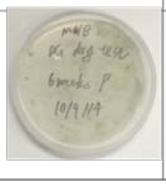	

Appendix C

Additional Microscopic Images of DG1

C1 Methods and results

The DG1 enrichment was observed under 400x magnification with the EVOS® FL Auto Imaging System using three different light sources - white light, Texas Red (585 nm excitation, emission ~ 624 nm), and DAPI (357 nm excitation, emission ~ 447 nm) light cubes. First, a tile scan image was generated from the EVOS® FL Auto software by tiling and stitching multiple images together (Figure C1-A). DG1 had consistent filamentous structure across the whole scanned image, and no significant contamination was observed. Second, distinct heterocysts were distinguished in both white light (Figure C1-B) and red fluorescent micrographs (Figure C2). They had larger cell size and did not produce red biofluorescence due to the lack of chlorophyll (Donze et al., 1972). Finally, DG1 showed blue biofluorescence on cell surfaces under the DAPI light cube (Figure C3). This was evidence of the in vivo production of mycosporine-like amino acids (MAAs), which can protect cyanobacterial cells as UV-sunscreens by absorbing UV radiation (Garcia-Pichel et al., 1993; Rastogi and Incharoensakdi, 2014; Shukla et al., 2016).

C2 References

Donze, M., Haveman, J., Schiereck, P., 1972. Absence of photosystem 2 in heterocysts of the blue-green alga *Anabaena*. Biochimica et Biophysica Acta (BBA)-Bioenergetics 256, 157-161.

Garcia-Pichel, F., Wingard, C.E., Castenholz, R.W., 1993. Evidence regarding the UV sunscreen role of a mycosporine-like compound in the cyanobacterium *Gloeocapsa* sp. Applied and Environmental microbiology 59, 170-176.

Rastogi, R.P., Incharoensakdi, A., 2014. Analysis of UV-absorbing photoprotectant mycosporine-like amino acid (MAA) in the cyanobacterium *Arthrospira sp*. CU2556. Photochemical & Photobiological Sciences 13, 1016-1024.

Shukla, V., Kumari, R., Patel, D.K., Upreti, D.K., 2016. Characterization of the diversity of mycosporine-like amino acids in lichens from high altitude region of Himalaya. Amino acids 48, 129-136.

C3 Figures

Figure C1. Microscopic views of the DG1 enrichment under white light and 400x magnification. A tile scan image (A) was firstly generated by tiling and stitching multiple images together; a zoomed-in image of the square area (outlined in Figure C1-A) is shown in (B) and shows heterocysts marked with arrows.

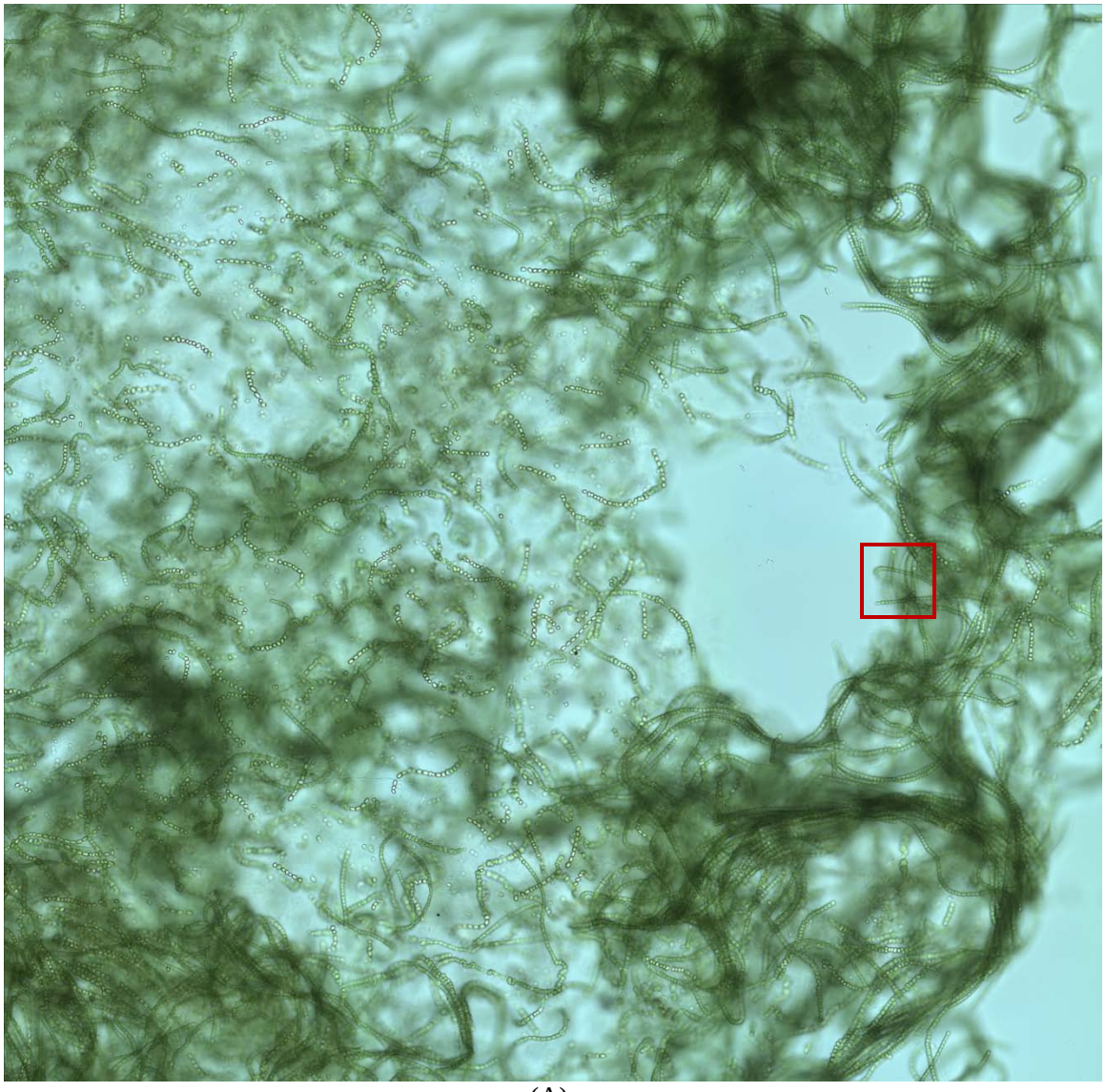

(A)

Figure C1. (Continued)

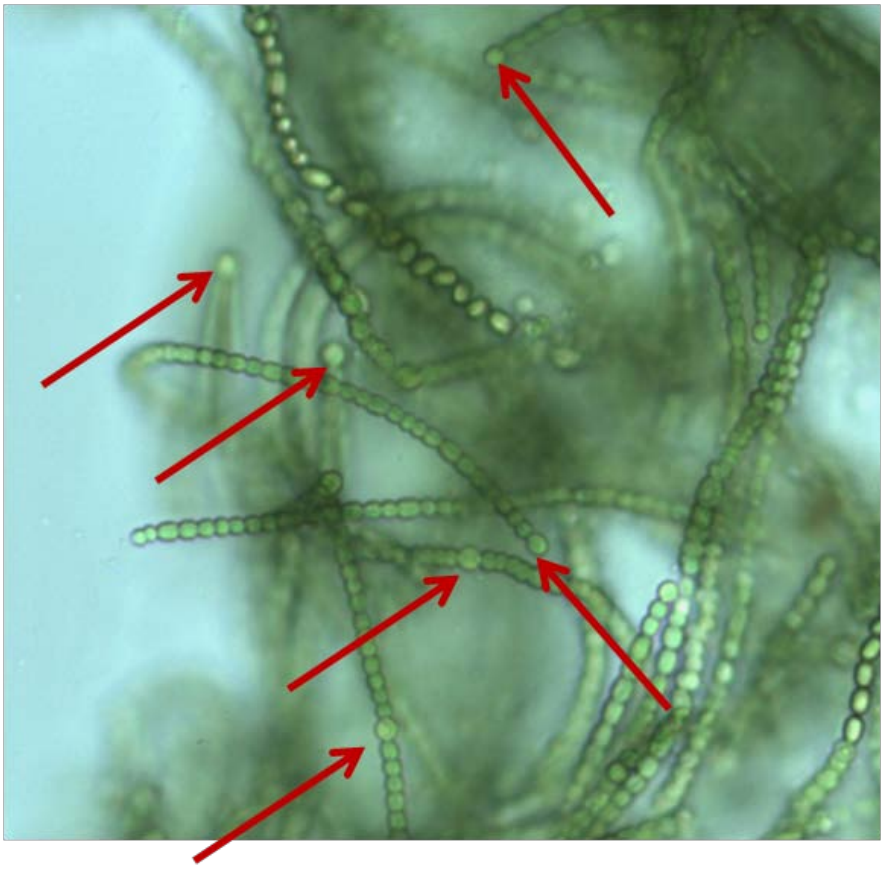

(B)

Figure C2. Auto-biofluorescence produced by chlorophyll a in DG1 vegetative cells examined with the Texas Red light cube (585 nm excitation, emission ~ 624 nm, 400x magnification). The areas showing dark cells (marked by arrows) are heterocysts.

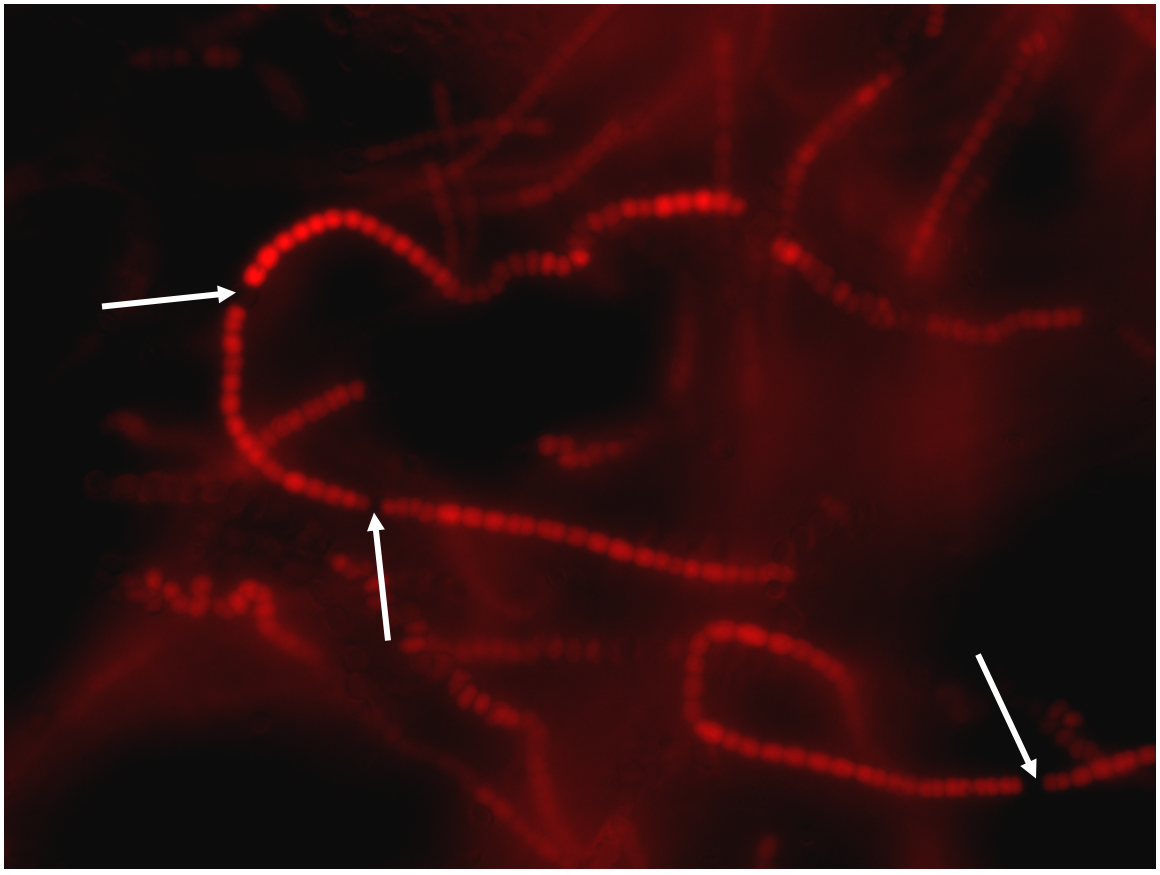

Figure C3. Combined fluorescent micrographs (400x magnification) of the DG1 enrichment from images captured with two separate excitation light cubes (Texas Red and DAPI light cubes). DG1 emitted two auto-biofluorescent colors, red and blue (~ 624 and 447 nm), after being excited under the corresponding wavelengths (585 and 357 nm).

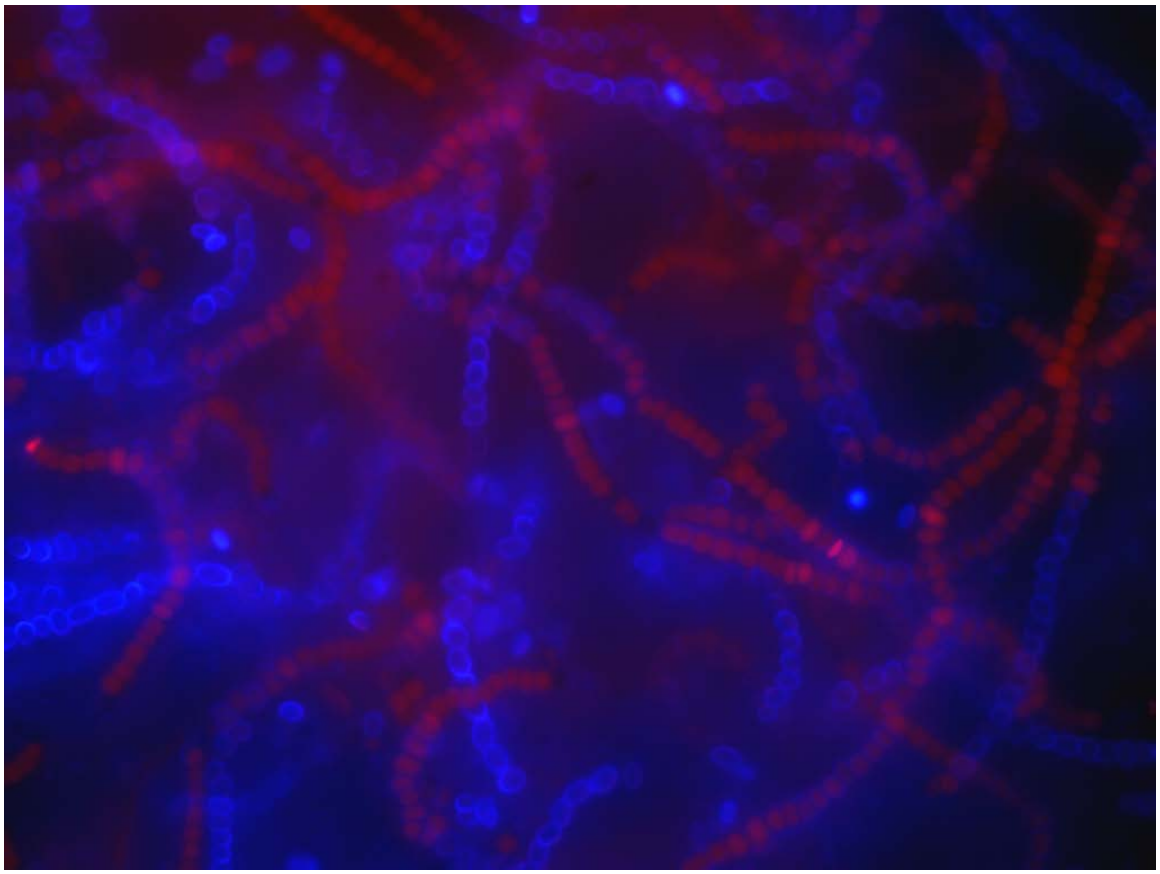

VITA

Xin Peng

Education

Ph.D. 8/2016 Ecology with Graduate Statistcs Minor, The Pennsylvania State University
M.S. 7/2011 Microbiology and Biochemical Pharmacy, Nanjing University
B.S. 7/2008 Biological Science, Nanjing University

Professional Experience

8/2011 - present Research assistant, The Pennsylvania State University
11/2012 - 3/2013 Secretary of the Environmental Chemistry and Microbiology Student Symposium (ECMSS), The Pennsylvania State University
9/2008 - 7/2011 Research assistant, Nanjing University
9/2007 - 7/2008 Assistant academic staff of undergraduate students, Nanjing University
12/2006 - 7/2008 Project leader of National Undergraduate Inovation Program, Nanjing Universiy

Teaching Experience

Spring 2014 & Spring 2015 Instructor, Introductory Soil Science Laboratory, The Pennsylvania State University
Fall 2012 & Fall 2015 Teaching assistant, Soil Ecology, The Pennsylvania State University
Fall 2009 Half-time instructor, Experiment in Genetics, Nanjing University
Spring 2008 & Spring 2009 Teaching assistant, Biostatistics, Nanjing University

Honors and Awards

2015 Huck Institutes travel award
2014 Second place award of oral presentation at ECMSS
2009 Outstanding Red Cross Member
2008 First place Outstanding Undergraduate Thesis
2007 First place People's Scholarship
2006 & 2005 Third place People's Scholarship

Selected Publications

Xin Peng and Mary Ann Bruns, 2015, *Selecting high performance N_2-fixing cyanobacteria for agricultural soil amendment and biological crust formation*, Algae Biomass Summit, Washington DC.

Xin Peng, 2014, *Biologically renewable soil nitrogen: simulation of biological soil crust dynamics after applying cyanobacteria to agricultural soil*, Environmental Chemistry and Microbiology Student Symposium, State College.

Xin Peng and Mary Ann Bruns, 2013, *Potential use of cyanobacteria as soil colonizers to establish biological soil crusts (BSCs) for biofertility*, Environmental Chemistry and Microbiology Student Symposium, State College.

Feng Chen, **Xin Peng**, Xiaomei Hua, Peipei Zhang, HengGui, Jinliang Qi, Deyue Yu,Yonghua Yang, 2012, *Effects of sulfur-rich amino acids transgenic soybeans on soil organic elements and microbial community diversity*, Soybean Science, 2, 250-265.

Xin Peng, Jianwen Yang, Xiaomei Hua, Baolong Zhang, Biao Liu, Shouping Zhao, Rongwu Yang, Yanjun Pang, Wanchao Ni, Jinliang Qi, Yonghua Yang, 2010, *Uncultured bacteria dominate microbial responses in the Bt cotton planted soil*, China National Biosafety Symposium, Guiyang.